Publishing House ASV

begell house, inc. publishers

Scientific coordination is carried out by the Russian Academy of Architecture and Construction Sciences (RAACS)

Volume 15 • Issue 2 • 2019

ISSN 2588-0195 (Online)
ISSN 2587-9618 (Print) Continues ISSN 1524-5845

International Journal for

Computational Civil and Structural Engineering

Международный журнал по расчету гражданских и строительных конструкций

http://raasn.ru/public.php
http://ijccse.iasv.ru/index.php/IJCCSE

DOI: 10.22337/2587-9618
GICID: 71.0000.1500.2830

PUBLISHER

ASV Publishing House
(ООО «Издательство АСВ»)
19/1,12, Yaroslavskoe Shosse, 120338, Moscow, Russia
Tel. +7(925)084-74-24; E-mail: iasv@iasv.ru; Интернет-сайт: http://iasv.ru/

ADVISORY EDITORIAL BOARD

TECHNICAL EDITOR

EDITORIAL TEAM

INVITED REVIEWERS

AIMS AND SCOPE

The aim of the Journal is to advance the research and practice in structural engineering through the application of computational methods. The Journal will publish original papers and educational articles of general value to the field that will bridge the gap between high-performance construction materials, large-scale engineering systems and advanced methods of analysis.

The scope of the Journal includes papers on computer methods in the areas of structural engineering, civil engineering materials and problems concerned with multiple physical processes interacting at multiple spatial and temporal scales. The Journal is intended to be of interest and use to researches and practitioners in academic, governmental and industrial communities.

ОБЩАЯ ИНФОРМАЦИЯ О ЖУРНАЛЕ

International Journal for Computational Civil and Structural Engineering

(Международный журнал по расчету гражданских и строительных конструкций)

Международный научный журнал "International Journal for Computational Civil and Structural Engineering (Международный журнал по расчету гражданских и строительных конструкций)" (IJCCSE) является ведущим научным периодическим изданием по направлению «Инженерные и технические науки», издаваемым, начиная с 1999 года (ISSN 2588-0195 (Online); ISSN 2587-9618 (Print) Continues ISSN 1524-5845). В журнале на высоком научно-техническом уровне рассматриваются проблемы численного и компьютерного моделирования в строительстве, актуальные вопросы разработки, исследования, развития, верификации, апробации и приложений численных, численно-аналитических методов, программно-алгоритмического обеспечения и выполнения автоматизированного проектирования, мониторинга и комплексного наукоемкого расчетно-теоретического и экспериментального обоснования напряженно-деформированного (и иного) состояния, прочности, устойчивости, надежности и безопасности ответственных объектов гражданского и промышленного строительства, энергетики, машиностроения, транспорта, биотехнологий и других высокотехнологичных отраслей.

В редакционный совет журнала входят известные российские и зарубежные деятели науки и техники (в том числе академики, члены-корреспонденты, иностранные члены, почетные члены и советники Российской академии архитектуры и строительных наук). Основной критерий отбора статей для публикации в журнале − их высокий научный уровень, соответствие которому определяется в ходе высококвалифицированного рецензирования и объективной экспертизы, поступающих в редакцию материалов.

Журнал входит в Перечень ВАК РФ ведущих рецензируемых научных изданий, в которых должны быть опубликованы основные научные результаты диссертаций на соискание ученой степени кандидата наук, на соискание ученой степени доктора наук по научным специальностям и соответствующим им отраслям науки:

- 01.02.04 – Механика деформируемого твердого тела (технические науки),
- 05.13.18 – Математическое моделирование численные методы и комплексы программ (технические науки),
- 05.23.01 – Строительные конструкции, здания и сооружения (технические науки),
- 05.23.02 – Основания и фундаменты, подземные сооружения (технические науки),
- 05.23.05 – Строительные материалы и изделия (технические науки),
- 05.23.07 – Гидротехническое строительство (технические науки),
- 05.23.17 – Строительная механика (технические науки).

В Российской Федерации журнал индексируется Российским индексом научного цитирования (РИНЦ).

Журнал входит в базу данных Russian Science Citation Index (RSCI), полностью интегрированную с платформой Web of Science. Журнал имеет международный статус и высылается в ведущие библиотеки и научные организации мира.

Издатели журнала – *Издательство Ассоциации строительных высших учебных заведений /АСВ/* (Россия, г. Москва) и до 2017 года *Издательский дом Begell House Inc.* (США, г. Нью-Йорк). Официальными партнерами издания является *Российская академия архитектуры и строительных наук* (*РААСН*), осуществляющая научное курирование издания, и *Научно-исследовательский центр СтаДиО* (ЗАО НИЦ СтаДиО).

Цели журнала – демонстрировать в публикациях российскому и международному профессиональному сообществу новейшие достижения науки в области вычислительных ме-

тодов решения фундаментальных и прикладных технических задач, прежде всего в области строительства.

Задачи журнала:

- предоставление российским и зарубежным ученым и специалистам возможности публиковать результаты своих исследований;
- привлечение внимания к наиболее актуальным, перспективным, прорывным и интересным направлениям развития и приложений численных и численно-аналитических методов решения фундаментальных и прикладных технических задач, совершенствования технологий математического, компьютерного моделирования, разработки и верификации реализующего программно-алгоритмического обеспечения;
- обеспечение обмена мнениями между исследователями из разных регионов и государств.

Тематика журнала. К рассмотрению и публикации в журнале принимаются аналитические материалы, научные статьи, обзоры, рецензии и отзывы на научные публикации по фундаментальным и прикладным вопросам технических наук, прежде всего в области строительства. В журнале также публикуются информационные материалы, освещающие научные мероприятия и передовые достижения Российской академии архитектуры и строительных наук, научно-образовательных и проектно-конструкторских организаций.

Тематика статей, принимаемых к публикации в журнале, соответствует его названию и охватывает направления научных исследований в области разработки, исследования и приложений численных и численно-аналитических методов, программного обеспечения, технологий компьютерного моделирования в решении прикладных задач в области строительства, а также соответствующие профильные специальности, представленные в диссертационных советах профильных образовательных организациях высшего образования.

Редакционная политика. Политика редакционной коллегии журнала базируется на современных юридических требованиях в отношении авторского права, законности, плагиата и клеветы, изложенных в законодательстве Российской Федерации, и этических принципах, поддерживаемых сообществом ведущих издателей научной периодики.

За публикацию статей плата с авторов не взымается. Публикация статей в журнале бесплатная. На платной основе в журнале могут быть опубликованы материалы рекламного характера, имеющие прямое отношение к тематике журнала.

Журнал предоставляет непосредственный открытый доступ к своему контенту, исходя из следующего принципа: свободный открытый доступ к результатам исследований способствует увеличению глобального обмена знаниями.

Индексирование. Публикации в журнале входят в системы расчетов индексов цитирования авторов и журналов. «Индекс цитирования» — числовой показатель, характеризующий значимость данной статьи и вычисляющийся на основе последующих публикаций, ссылающихся на данную работу.

Авторам. Прежде чем направить статью в редакцию журнала, авторам следует ознакомиться со всеми материалами, размещенными в разделах сайта журнала (интернет-сайт Российской академии архитектуры и строительных наук (http://raasn.ru); подраздел «Издания РААСН» или интернет-сайт Издательства АСВ (http://iasv.ru); подраздел «Журнал IJCCSE»): с основной информацией о журнале, его целями и задачами, составом редакционной коллегии и редакционного совета, редакционной политикой, порядком рецензирования направляемых в журнал статей, сведениями о соблюдении редакционной этики, о политике авторского права и лицензирования, о представлении журнала в информационных системах (индексировании), информацией о подписке на журнал, контактными данными и пр. Журнал рабо-

тает по лицензии Creative Commons типа cc by-nc-sa (Attribution Non-Commercial Share Alike) – Лицензия «С указанием авторства – Некоммерческая – Копилефт».

Рецензирование. Все научные статьи, поступившие в редакцию журнала, проходят обязательное двойное слепое рецензирование (рецензент не знает авторов рукописи, авторы рукописи не знаю рецензентов).

Заимствования и плагиат. Редакционная коллегия журнала при рассмотрении статьи проводит проверку материала с помощью системы «Антиплагиат». В случае обнаружения многочисленных заимствований редакция действует в соответствии с правилами COPE.

Подписка. Журнал зарегистрирован в Федеральном агентстве по средствам массовой информации и охраны культурного наследия Российской Федерации. Индекс в общероссийском каталоге РОСПЕЧАТЬ − 18076.

По вопросам подписки на международный научный журнал “International Journal for Computational Civil and Structural Engineering (Международный журнал по расчету гражданских и строительных конструкций)” обращайтесь в Агентство «Роспечать» (Официальный сайт в сети Интернет: http://www.rosp.ru/) или в издательство Ассоциации строительных вузов (АСВ) в соответствии со следующими контактными данными:

ООО «Издательство АСВ»

Юридический адрес: 129337, Россия, г. Москва, Ярославское ш., д. 26, офис 705;

Фактический адрес: 129337, Россия, г. Москва, Ярославское ш., д. 19, корп. 1, 5 этаж, офис 12 (ТЦ Мебель России);

Телефоны: +7 (925) 084-74-24, +7 (926) 010-91-33

Интернет-сайт: www.iasv.ru. Адрес электронной почты: iasv@iasv.ru.

Контактная информация. По всем вопросам работы редакции, рецензирования, согласования правки текстов и публикации статей следует обращаться к главному редактору журнала члену-корреспонденту РААСН *Сидорову Владимиру Николаевичу* (адреса электронной почты: sidorov.vladimir@gmail.com, sidorov@iasv.ru, iasv@iasv.ru, sidorov@raasn.ru) или к техническому редактору журнала советнику РААСН *Кайтукову Таймуразу Батразовичу* (адреса электронной почты: tkaytukov@gmail.com; Kaytukov@raasn.ru). Кроме того, по указанным вопросам, а также по вопросам размещения в журнале рекламных материалов можно обращаться к генеральному директору ООО «Издательство АСВ» *Никитиной Надежде Сергеевне* (адреса электронной почты: iasv@iasv.ru, nsnikitina@mail.ru, ijccse@iasv.ru).

Журнал становится технологичнее. Издательство АСВ с сентября 2016 года является членом Международной ассоциации издателей научной литературы (Publishers International Linking Association (PILA)), осуществляющей свою деятельность на платформе CrossRef. Оригинальным статьям, публикуемым в журнале, будут присваиваться уникальные номера (индексы DOI – Digital Object Identifier), что значительно облегчит поиск метаданных и местонахождение полнотекстового произведения. DOI – это система определения научного контента в сети Интернет.

С октября 2016 года стал возможен прием статей на рассмотрение и рецензирование через онлайн систему приема статей Open Journal Systems на сайте журнала (электронная редакция): http://ijccse.iasv.ru/index.php/IJCCSE.

Автор имеет возможность следить за продвижением статьи в редакции журнала в личном кабинете Open Journal Systems и получать соответствующие уведомления по электронной почте.

В феврале 2018 года журнал был зарегистрирован в Directory of open access journals (DOAJ) (это один из самых известных поисковых сервисов в мире, который предоставляет открытый доступ к материалам и индексирует не только заголовки журналов, но и научные статьи), в сентябре 2018 года включен в продукты EBSCO Publishing.

International Journal for
Computational Civil and Structural Engineering
(Международный журнал по расчету гражданских и строительных конструкций)
Volume 15, Issue 2 ***2019***

Scientific coordination is carried out by the Russian Academy of Architecture and Construction Sciences (RAACS)

CONTENTS

International Journal for
Computational Civil and Structural Engineering
(Международный журнал по расчету гражданских и строительных конструкций)
Volume 15, Issue 2 ***2019***

Scientific coordination is carried out by the Russian Academy of Architecture and Construction Sciences (RAACS)

СОДЕРЖАНИЕ

DOI:10.22337/2587-9618-2019-15-2-14-23

NUMERICAL SIMULATION OF LAMB WAVE PROPOGATION IN ISOTROPIC LAYER

Anna V. Avershyeva [1, 3], ***Sergey V. Kuznetsov*** [1, 2]
[1] National Research Moscow State University of Civil Engineering, Moscow, RUSSIA
[2] Institute for Problems in Mechanics, Russian Academy of Sciences, Moscow, RUSSIA
[3] S.P. Korolev Rocket and Space Public Corporation Energia (RSC Energia), Korolev, RUSSIA

Abstract: Propagation of Lamb waves in an elastic isotropic layer is studied by analytical and numerical methods. The influence of numerical simulation parameters on the solution stability is analyzed. The results of the finite element modeling and the analytical solution are compared.

Keywords: Numerical simulation, finite element model, Lamb waves, isotropic layer, polarization

ЧИСЛЕННОЕ МОДЕЛИРОВАНИЕ РАСПРОСТРАНЕНИЯ ВОЛН ЛЭМБА В ИЗОТРОПНОМ СЛОЕ

А.В. Авершьева [1, 3], ***С.В. Кузнецов*** [1, 2]
[1] Национальный исследовательский Московский государственный строительный университет, г. Москва, РОССИЯ
[2] Институт проблем механики Российской академии наук, г. Москва, РОССИЯ
[3] Ракетно-космическая корпорация «Энергия» имени С.П. Королёва (РКК «Энергия»), г. Королев, РОССИЯ

Аннотация: С помощью численных методов исследуется распространение волн Лэмба в упругом изотропном слое. Исследуется влияние параметров численного моделирования на устойчивость решения. Сравниваются результаты конечно-элементного моделирования и аналитического решения.

Ключевые слова: численное моделирование, конечно-элементная модель, волны Лэмба, изотропный слой, поляризация

1. INTRODUCTION

Acoustic methods are widely used in the NDT for determining the physical and mechanical properties of materials in aerospace, civil and echanical engineering, and geophysics, to ensure safety, reliability, and precision. These methods allow constructing the dispersion relations that connect the phase velocity of the wave with frequency.

The first theoretical studies described by Rayleigh in [1-4], by Lamb in [5-7]. Later on, theoretical and experimental studies are described in [8-21].

Lamb waves are particular interest. They have an elliptical polarization in the sagittal plane and can penetrate on all thickness of the layer. The three-dimensional formalism [22] and six-dimensional formalisms [13, 23-26] were developed for analysing Lamb waves propagating in anisotropic plates. Experimental studies of Lamb waves propagation are very expensive and it requires the participation of high quality experts. Available theoretical methods for analysis the propagation of Lamb waves in the media are limited. Solution to the problem of Lamb waves propagation with using finite-element modeling is necessary to study.

The finite element method (FEM) used in the algorithms of numerical complexes, such as ABAQUS, ANSYS, NASTRAN and it used in various branches of science and technology.

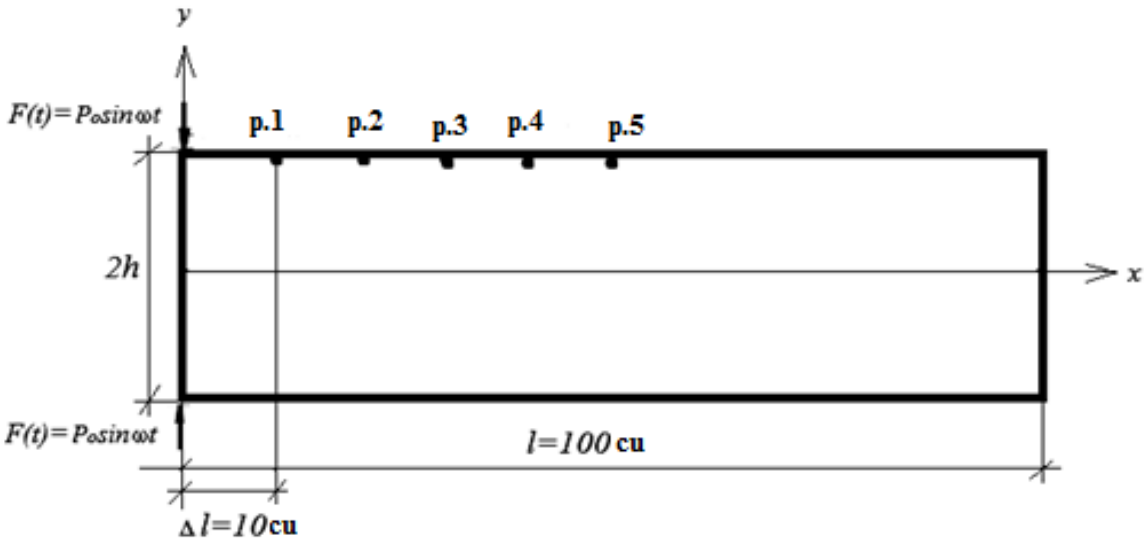

Figure 1. Schematic representation of the problem.

The main ideas of the FEM are given in [27]. FEM in problems of solid mechanics is described in [28, 29].

The use of various finite element complexes for solution problems of Lamb waves propagation will facilitate experimental diagnostics and processing of results. A comparison of the experimental dispersion relations with those found numerically will make to determine the properties of any layer. Of course, numerical modeling cannot replace experimental studies, but it can to help them. FEM integration in experimental diagnostics is an actual scientific technical problem.

Also the problem of Lamb waves polarization is interest since it was not studied in detail before.

The basic concepts of harmonic waves polarization are discussed in [30]. The results of analytical studies of surface waves polarization are given in [31]. In [32] the elastic waves polarization in the layer-elastic half-space system were considered. In this paper, we study the Lamb waves polarization in a layer by the finite element method.

2. FORMULATION OF THE PROBLEM

The isotropic elastic layer thickness in this study is $2h$ with boundaries $\mathbf{x} = \pm h$ (Figure 1). Harmonic in time concentrate force is applied to the layer, as a results longitudinal and transverse waves radiate out from the point of load application. Displacements in the x-direction correspond to longitudinal waves with velocity c_p, and the displacements in the y-direction correspond to vertical shear waves with velocity c_s. Movements in the z-direction is not included.

Finite element modeling and subsequent calculation has been conducted in finite element complex Abaqus®.

Analytical and finite element calculations were performed at density $\rho = 1$, $c_p = 1$, $h = 1$ cu, when the Poisson ratio ranges from 0 to 0.5, where cu is conventional unit (here in after it is assumed that all physical quantities are dimensionless).

The finite element model consists of rectangular 4-node linear elements. Results were obtained for 5 observation points (p.1, p.2, ..., p.5) located at intervals of 10 cu.

3. MESH CONVERGENCE

Finite element modeling of Lamb waves propagation has certain difficulties associated with the stability of difference schemes. So it is a very small amount of work on finite-element modeling of Lamb wave propagation in lay-

er.Finite-element programs use one of two difference schemes: explicit

$$x_{i+1} = x_i + \Delta t \cdot F(x_i, t), \quad (3.1)$$

or implicit

$$x_{i+1} = x_i + \Delta t \cdot F(x_{i+1}, t), \quad (3.2)$$

where x is unknown variable value, Δt is time step, i is integration step number l.
Explicit finite difference schemes used in this study, this scheme allows to analyze all the main effects that occur during the propagation of acoustic waves. For this purpose the module Abaqus/Explicit is used in Abaqus®. To obtain a stable solution we used an approximate method, known as the Courant Criterion [33].
For this criterion time step must satisfy the condition

$$\Delta t < \Delta x_{\min} / c_p, \quad (3.3)$$

where Δt is the time step, Δx is the smallest element dimension, c_p is longitudinal wave velocity.
The magnitude of the amplitude of the impact P_0 is important. For the condition of small deformations it is necessary that the value P_0 satisfies the condition

$$P_0 < 1 \cdot 10^{-4} \cdot E \cdot \Delta x, \quad (3.4)$$

where E – dimensionless modulus of elasticity.
The study of the influence of P_0 and FEM element dimension Δx on the accuracy of the solution was carried out for two values of the dimensionless circular frequency:

$$\omega = 0.397657 \text{ and } \omega = 1.5016813 .$$

Poisson's ratio of the layer was taken to be $\nu = 0.35$.
Results were obtained for 2 observation points spaced 10 cu and 20 cu from the point of load application. The element dimension ranges from 0.005 to 0.5. Results for

$$P_0 > 1 \cdot 10^{-3} \cdot E \cdot \Delta x, \ \omega = 0.397657$$

are shown in the Figures 2-a and 2-b. Results for

$$P_0 < 1 \cdot 10^{-4} \cdot E \cdot \Delta x, \ \omega = 0.397657$$

are shown in the Figures 2-c and 2-d.
From the Figure 2 follows that when

$$\omega = 0.397657$$

accurate solution is achieved when $\Delta x \le 0.05$.
In Figure 3 results are shown for the following cases:

$$P_0 > 1 \cdot 10^{-3} \cdot E \cdot \Delta x,$$
$$P_0 \in \left(1 \cdot 10^{-3} \cdot E \cdot \Delta x; 1 \cdot 10^{-4} \cdot E \cdot \Delta x\right),$$
$$P_0 < 1 \cdot 10^{-4} \cdot E \cdot \Delta x.$$

When $\Delta x = 0.05$ there are

$$P_0 > 3.1154 \cdot 10^{-5},$$
$$P_0 \in \left(3.1154 \cdot 10^{-5}; 3.1154 \cdot 10^{-6}\right),$$
$$P_0 < 3.1154 \cdot 10^{-6}.$$

When $\Delta x = 0.01$ there are

$$P_0 > 6.23 \cdot 10^{-6},$$
$$P_0 \in \left(6.23 \cdot 10^{-6}; 6.23 \cdot 10^{-7}\right),$$
$$P_0 < 6.23 \cdot 10^{-7}.$$

Results for

$$P_0 > 1 \cdot 10^{-3} \cdot E \cdot \Delta x, \ \omega = 1.5016813$$

are shown in the Figure 3-a.
Calculation results with

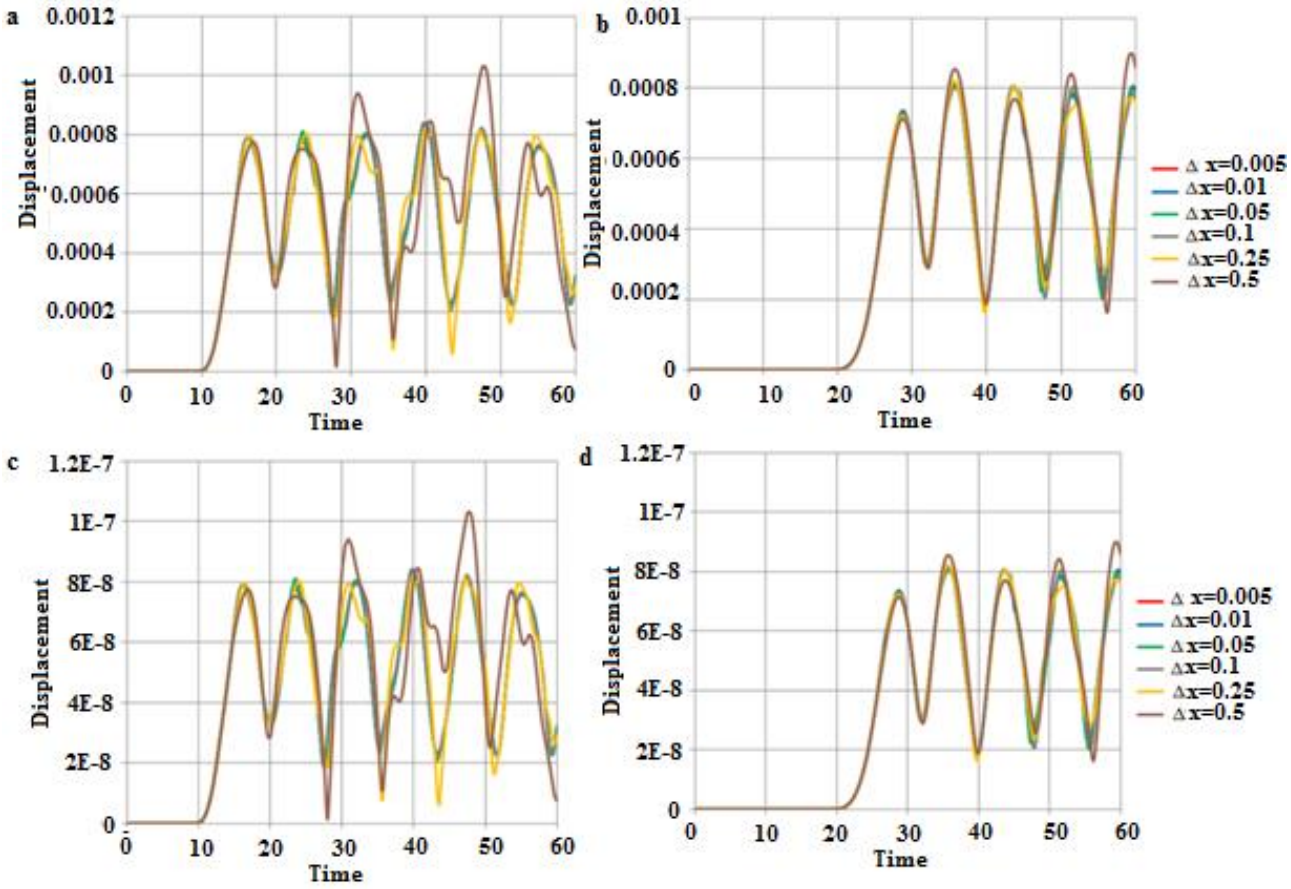

Figure 2. Displacement on the free surface when $\omega = 0.397657$ when the element dimension ranges from 0.005 to 0.5 *a) p.1 when* $P_0 > 1 \cdot 10^{-3} \cdot E \cdot \Delta x$, *b) p.2 when* $P_0 > 1 \cdot 10^{-3} \cdot E \cdot \Delta x$, *c) p.1 when* $P_0 < 1 \cdot 10^{-4} \cdot E \cdot \Delta x$, d) *p.2 when* $P_0 < 1 \cdot 10^{-4} \cdot E \cdot \Delta x$.

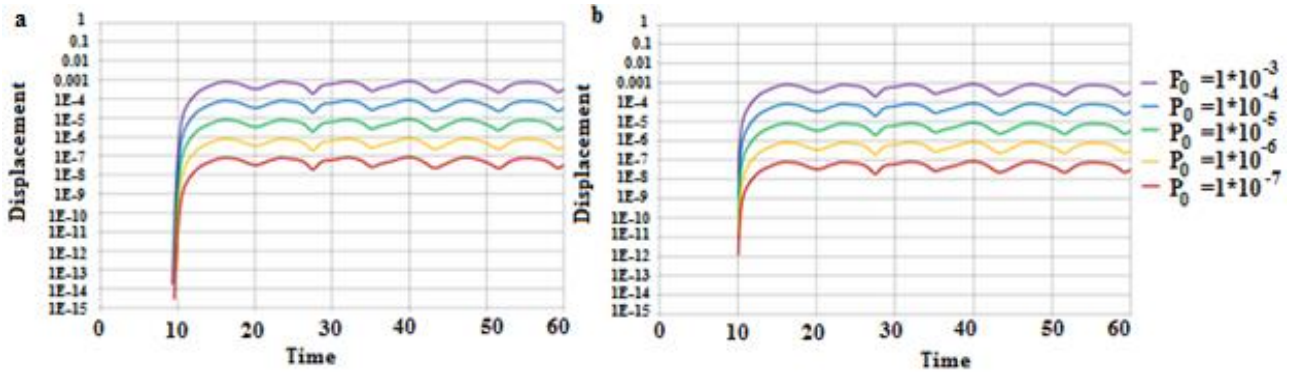

Figure 3. Displacement on the free surface for p.1 when a) $\Delta x = 0.05$, b) $\Delta x = 0.01$.

$$P_0 < 1 \cdot 10^{-4} \cdot E \cdot \Delta x, \omega = 1.5016813$$

are shown in the Figure 3-b.

From the Figure 4 follows that when $\omega = 1{,}5016813$ accurate solution is achieved when $\Delta x \le 0.01$. In Figure 5 results are shown for the following cases:

$$P_0 > 1 \cdot 10^{-3} \cdot E \cdot \Delta x,$$

$$P_0 \in \left(1 \cdot 10^{-3} \cdot E \cdot \Delta x; 1 \cdot 10^{-4} \cdot E \cdot \Delta x\right),$$

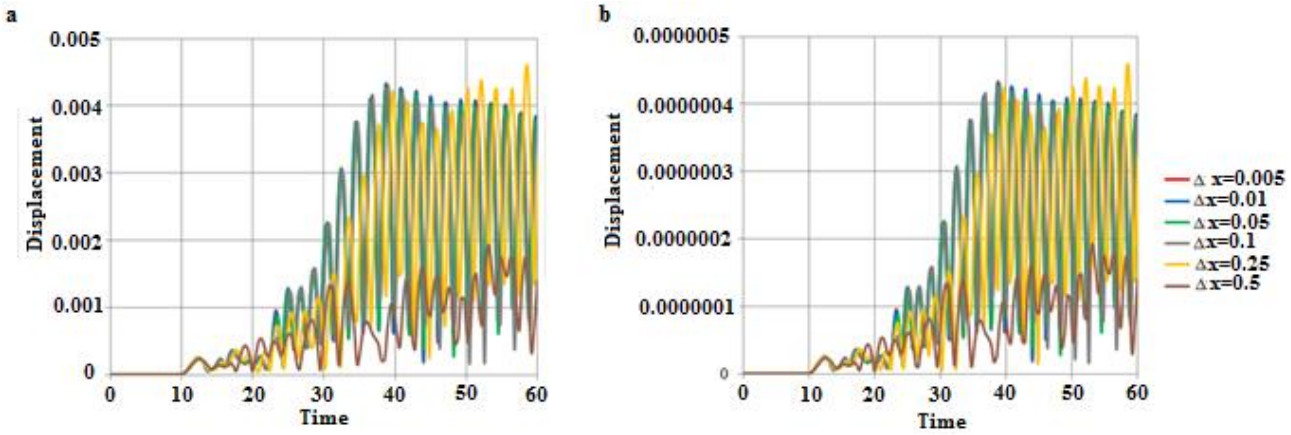

Figure 4. Displacement on the free surface when $\omega = 1.5016813$ *when the element dimension ranges from 0.005 to 0.5 a)* $P_0 > 1 \cdot 10^{-3} \cdot E \cdot \Delta x$, *b)* $P_0 < 1 \cdot 10^{-4} \cdot E \cdot \Delta x$.

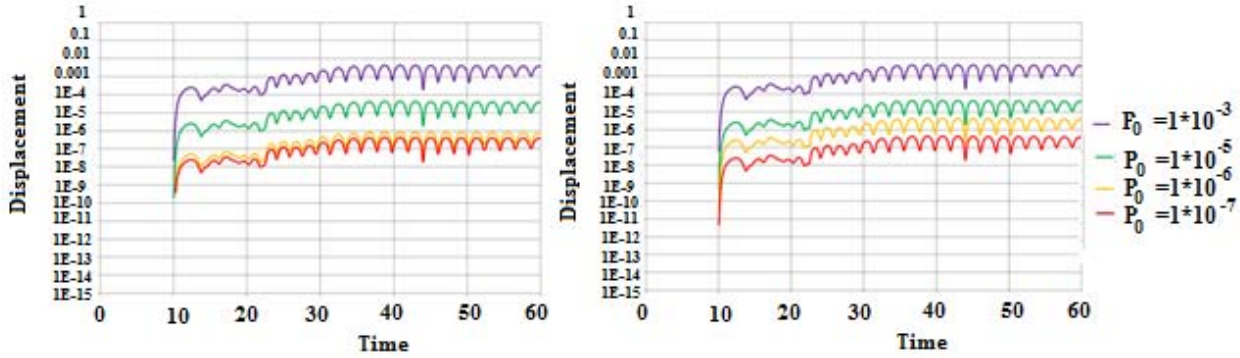

Figure 5. Displacement on the free surface for p.1 when a) $\Delta x = 0.05$, *b)* $\Delta x = 0.01$.

$$P_0 < 1 \cdot 10^{-4} \cdot E \cdot \Delta x.$$

When $\Delta x = 0.05$ there are

$$P_0 > 3.1154 \cdot 10^{-5},$$
$$P_0 \in \left(3.1154 \cdot 10^{-5}; 3.1154 \cdot 10^{-6}\right),$$
$$P_0 < 3.1154 \cdot 10^{-6}.$$

When $\Delta x = 0.01$ there are

$$P_0 > 6.23 \cdot 10^{-6},$$
$$P_0 \in \left(6.23 \cdot 10^{-6}; 6.23 \cdot 10^{-7}\right),$$
$$P_0 < 6.23 \cdot 10^{-7}.$$

It follows from the Figures 3 and 5 that amplitudes P_0 does not have a significant impact on the accuracy and stability of the solution.It means that in the investigated range of changes in external influences, the wave fields are described by linear equations, and the influence of geometrically nonlinear distortions can be neglected.

The dependence of the calculation time on element dimension is given in Table 4.1.

Table 4.1. Dependence of the calculation time on element dimension.

Element dimension Δx, cm	Calculation time, T, h.
0.005	4.4500
0.01	0.5200
0.05	0.0120
0.100	0.0100
0.250	0.0097
0.500	0.0070

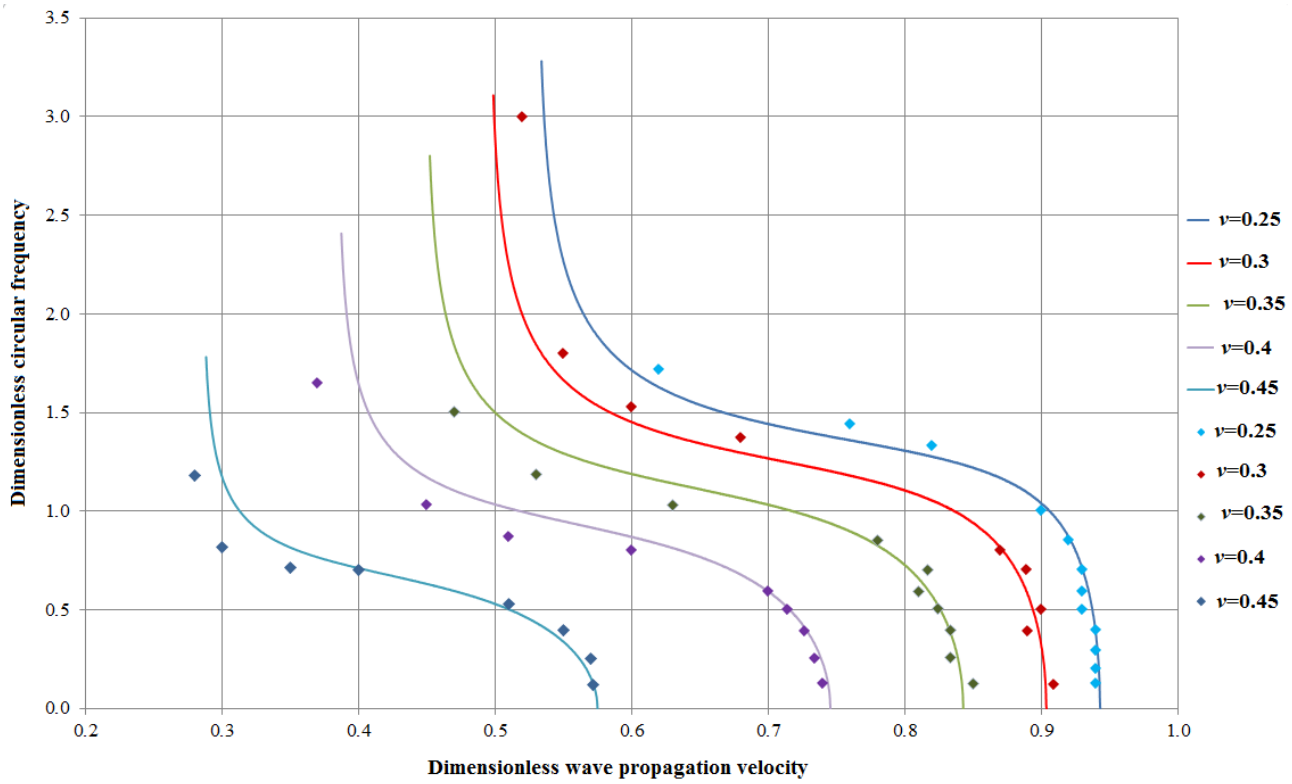

Figure 6. Comparative analysis of analytical (—) and numerical (◆) solutions.

Thus, the optimal size of the element for this study is the size $\Delta x = 0.01$. It should be noted that for calculations with $\omega \to 0$ it is permissible to apply the size of the element $\Delta x = 0.05$. This will not affect the accuracy of the solution, but it will significantly reduce the calculation time.

When the Poisson ratio ranges from 0 to 0.5 comparative analysis of analytical and numerical solutions shown in Figure 6.

Also we studied the effect of element dimension on the Lamb waves polarization. The stability of the difference scheme was also achieved by fulfilling the Courant criterion. (3.3).

Study of the influence of the size of element dimension Δx on the accuracy of calculations and the stability of the difference scheme revealed that with the variation Δx in the interval $[0.005; 0.1]$ item size effect Δx on the accuracy of the solution is observed only at frequencies $\omega > 0.1$ and $\omega < 0.3$. When comparing results for $\Delta x = 0.005$, $\Delta x = 0.5$ and $\Delta x = 1$ item size effect Δx on the accuracy of the solution is observed only at frequencie $\omega > 0.1$ (Figure 7). For this case time, the speed of the solution decreases significantly.

5. CONCLUSIONS

It was first proposed the method of generating of surface waves using the FEM program complex. For the first time, a comparative analysis of the Lamb waves fundamental symmetric mode obtained by analytical methods and the finite element method. It was found stable finite element solution in the vicinity of the second limiting velocities.

Abaqus showed good results for solving problems of propagation of surface waves. We also to determine the range of problems in calculations by the FEM, the solution of which allowed us to minimize the errors caused by:

- the choice of the magnitude of the impact;
- selection of the frequency range;

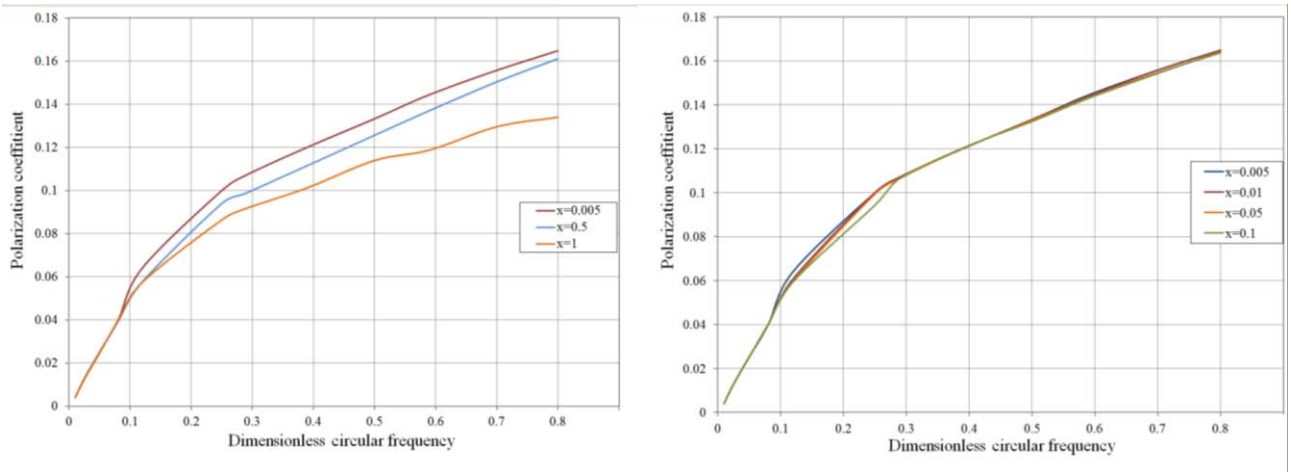

Figure 7. Investigation of mesh convergence forelement dimentions $\Delta x \in [0.005; 1]$.

- optimizing the time step using the finite element dimension.

The results of these studies are necessary for the application of acoustic non-destructive methods for diagnosing plate elements of building structures using Lamb waves.

REFERENCES

1. **Rayleigh J.W.** On Progressive Waves. // *Lond. Math. Soc.*, 1877, Vol. 9, pp. 21-26.
2. **Rayleigh J.W.** On the Free Vibration of an Infinite Plate of Homogeneous Isotropic Elastic Matter. // *Proc. Math. Soc. London*, 1889, Vol. 20, pp. 225-234.
3. **Rayleigh J.W.** On Waves Propagated Along the Plane Surface of an Elastic Solid. // *Proc. Lond. Math. Soc.*, 1885, Vol. 17, pp. 4-11.
4. **Rayleigh J.W.** Theory of Sound. Ulan Press, 2011.
5. **Lamb H.** On the Flexure of an Elastic Plate. // *Proc. Math. Soc. London*, 1889, Vol. 21, pp. 70-90
6. **Lamb H.** On the Propagation of Tremors over the Surface of an Elastic Solid. // *Phil. Trans. Roy. Soc. Lond.*, 1904, A203, pp.1 – 42.
7. **Lamb H.** On Waves in an Elastic Plate. // *Proceedings of the Royal Society of London*, 1917, Series A, Containing Papers of a Mathematical and Physical Character, 93(648), pp. 114-128.
8. **Brekhovskih L.M.** Volni v Sloisti v Sloistyh Sredah [Waves in Layered Media]. Moscow, Nauka, 1973, 343 pages (in Russian).
9. **Viktorov I.A.** Ul'trazvukovye volny Lehmba. Obzor [Ultrasonic Lamb waves. Review]. // *Acoustic journal*, 1965, Vol. 11, pp. 1-18 (in Russian).
10. **Viktorov I.A.** Fizicheskie Osnovy Primeneniya Ul'trazvukovyh Voln Rehleya i Lehmba v Tekhnike. [Physical Basics of Using Ultrasonic Rayleigh and Lamb Waves in Engineering]. Moscow, Nauka, 1966, 168 pages (in Russian).
11. **Viktorov I.A.** Rayleigh and Lamb Waves: Physical Theory and Applications. Plenum, New York (Moscow, Nauka), 1967
12. **Kuznetsov S.V.** Fizicheskie Osnovy Primeneniya Ul'trazvukovyh voln Rehleya i Lehmba v Tekhnike [Lamb Waves in Anisotropic Plates (Review)]. // *Acoustic Journal*, 2014, Vol. 60, No. 1, pp. 90-100 (in Russian).
13. **Kuznetsov S.V.** Cauchy Six-Dimensional Formalism for Lamb Waves in Multilayered Plates. // *ISRN Mechanical Engineering*, 2013, 11 pages, article ID 698706.
14. **Ewing W.M., Jardetzky W.S., Press F.** Elastic Waves in Layered Media. New-

York, Toronto, London, McGraw-hill book company, 1957, 390 pages.
15. **Achenbach D.** Wave Propagation in Elastic Solids. Amsterdam, North Holland, 1975.
16. **Djeran-Maigre I.**, **Kuznetsov S.V.** Soliton-Like Lamb Waves in Layered. // *Waves in Fluids and Solids*, 2011, pp. 53-68.
17. **Rose J.L.** Ultrasonic Guided Waves in Solid Media. Cambridge, Cambridge University Press, 2014, 547 pages.
18. **Hillger W., Pfeiffer U.** Structural Health Monitoring Using Lamb Waves. Germany, Braunschweig, Institute of Composite Structures and Adaptive Systems, ECNDT, Th. 1.7.2, 2006, pp. 1-7.
19. **Soutis C., Diamanti K.** A Lamb Wave Based SHM of Repaired Composite Laminated Structures. // The Second International Symposium on NDT in Aerospace, We.2.B.1, Aerospace Engineering, U.K., The University of Sheffield, 2010.
20. **Alleyne D.N. and Cawley P**. The Excitation of Lamb Waves Using Dry-Coupled Piezoelectric Transdusers. // *Journal of Nondestructive Evaluation*, 1996, Vol. 15, Issue 1, pp. 11-20
21. **Ting T.C.T. and Barnett D. M.** Classifications of Surface Waves in Anisotropic Elastic Materials. // *Wave Motion*, 1997, No. 26, pp. 207-218.
22. **Farnell G.W.** Properties of Elastic Surface Waves. // *Phys. Acoust.*, 1970, No. 6, pp. 109-166.
23. **Chadwick P., Smith G.D.** Foundations of the Theory of Surface Waves in Anisotropic Elastic Materials. // *Adv. Appl. Mech.*, 1977, No. 17, pp. 303-376.
24. **Barnett D.M., Lothe J.** Synthesis of the Sextic and the Integral Formalism for Dislocations, Green's Functions, and Surface Waves in Anisotropic Elastic Solids. // *Phys. Norv*., 1973, No. 7, pp. 13-19.
25. **Stroh A. N.**, Steady State Problems in Anisotropic Elasticity. // *Journal of Mathematical Physics*, 1962, Vol. 41, pp. 77-103.
26. **Kuznetsov S.V.** Subsonic Lamb Waves in Anisotropic Plates. // *Quart. Appl. Math.*, 2002, No. 60, pp. 577-587.
27. **Sigerlind L.** Primenenie Metoda Konechnyh Ehlementov [Application of Finite Element Method]. Moscow, Mir, 1979, 392 pages (in Russian).
28. **Cook R.D.** Concept and Applications of Finite Element Analysis. New-York, Wiley, 1974.
29. **Zienkiewicz O.C.** The Finite Element Method in Engineering Science. New-York, McGraw-Hill, 1971.
30. **Vinogradova M.B., Rudenko O.V., Suhorukij A.P.** Teoriya Voln [Wave Theory]. Moscow, Nauka, 1979, 384 pages (in Russian).
31. **Graff K.F.** Wave Motion in Elastic Solids. New-York, Dover Inc., 1975, 682 pages.
32. **Tolstoy I. Usdin E.** Wave Propagation in Elastic Plates: Low and High Mode Dispersion. // *J. Acoust. Soc. Am.*, 1957, Vol. 29, pp. 37-42.
33. **Kukudzhanov V.N.** Chislennoe Reshenie Neodnomernyh Zadach Rasprostraneniya Voln Napryazhenij v Tverdyh Telah. [Numerical Solution of Non-One-Dimensional Problems of the Propagation of Stress Waves in Solids.]. // *Soobshch. Prikl. Matem*. Moscow, VC AN SSSR, 1976, Vol. 6, pp. 67 (in Russian).

СПИСОК ЛИТЕРАТУРЫ

1. **Rayleigh J.W.** On Progressive Waves. // *Lond. Math. Soc.*, 1877, Vol. 9, pp. 21-26.
2. **Rayleigh J.W.** On the Free Vibration of an Infinite Plate of Homogeneous Isotropic Elastic Matter. // *Proc. Math. Soc. London*, 1889, Vol. 20, pp. 225-234.
3. **Rayleigh J.W.** On Waves Propagated Along the Plane Surface of an Elastic Solid. // *Proc. Lond. Math. Soc.*, 1885, Vol. 17, pp. 4-11.

4. **Rayleigh J.W.** Theory of Sound. Ulan Press, 2011.
5. **Lamb H.** On the Flexure of an Elastic Plate. // *Proc. Math. Soc. London*, 1889, Vol. 21, pp. 70-90
6. **Lamb H.** On the Propagation of Tremors over the Surface of an Elastic Solid. // *Phil. Trans. Roy. Soc. Lond.*, 1904, A203, pp.1 – 42.
7. **Lamb H.** On Waves in an Elastic Plate. // *Proceedings of the Royal Society of London*, 1917, Series A, Containing Papers of a Mathematical and Physical Character, 93(648), pp. 114-128.
8. **Бреховских Л.М.** Волны в слоистых средах. – М.: Наука, 1973. – 343 с.
9. **Викторов И.А.** Ультразвуковые волны Лэмба. Обзор. // *Акуст. журн*, 1965, Том 11, с.1-18.
10. **Викторов И.А.** Физические основы применения ультразвуковых волн Рэлея и Лэмба в технике. – М.: Наука, 1966, 168 с.
11. **Viktorov I.A.** Rayleigh and Lamb Waves: Physical Theory and Applications. Plenum, New York (Moscow, Nauka), 1967.
12. **Кузнецов С.В.** Волны Лэмба в анизотропных пластинах (обзор). // Акустический журнал, 2014, том 60, №1, с.90-100.
13. **Kuznetsov S.V.** Cauchy Six-Dimensional Formalism for Lamb Waves in Multilayered Plates. // *ISRN Mechanical Engineering*, 2013, 11 pages, article ID 698706.
14. **Ewing W.M., Jardetzky W.S., Press F.** Elastic Waves in Layered Media. New-York, Toronto, London, McGraw-hill book company, 1957, 390 pages.
15. **Achenbach D.** Wave Propagation in Elastic Solids. Amsterdam, North Holland, 1975.
16. **Djeran-Maigre I.**, **Kuznetsov S.V.** Soliton-Like Lamb Waves in Layered. // *Waves in Fluids and Solids*, 2011, pp. 53-68.
17. **Rose J.L.** Ultrasonic Guided Waves in Solid Media. Cambridge, Cambridge University Press, 2014, 547 pages.
18. **Hillger W., Pfeiffer U.** Structural Health Monitoring Using Lamb Waves. Germany, Braunschweig, Institute of Composite Structures and Adaptive Systems, ECNDT, Th. 1.7.2, 2006, pp. 1-7.
19. **Soutis C., Diamanti K.** A Lamb Wave Based SHM of Repaired Composite Laminated Structures. // The Second International Symposium on NDT in Aerospace, We.2.B.1, Aerospace Engineering, U.K., The University of Sheffield, 2010.
20. **Alleyne D.N. and Cawley P**. The Excitation of Lamb Waves Using Dry-Coupled Piezoelectric Transdusers. // *Journal of Nondestructive Evaluation*, 1996, Vol. 15, Issue 1, pp. 11-20
21. **Ting T.C.T. and Barnett D. M.** Classifications of Surface Waves in Anisotropic Elastic Materials. // *Wave Motion*, 1997, No. 26, pp. 207-218.
22. **Farnell G.W.** Properties of Elastic Surface Waves. // *Phys. Acoust.*, 1970, No. 6, pp. 109-166.
23. **Chadwick P., Smith G.D.** Foundations of the Theory of Surface Waves in Anisotropic Elastic Materials. // *Adv. Appl. Mech.*, 1977, No. 17, pp. 303-376.
24. **Barnett D.M., Lothe J.** Synthesis of the Sextic and the Integral Formalism for Dislocations, Green's Functions, and Surface Waves in Anisotropic Elastic Solids. // *Phys. Norv*., 1973, No. 7, pp. 13-19.
25. **Stroh A. N.**, Steady State Problems in Anisotropic Elasticity. // *Journal of Mathematical Physics*, 1962, Vol. 41, pp. 77-103.
26. **Kuznetsov S.V.** Subsonic Lamb Waves in Anisotropic Plates. // *Quart. Appl. Math.*, 2002, No. 60, pp. 577-587.
27. **Сигерлинд Л.** Применение метода конечных элементов. – М.: Мир, 1979. – 392 с.
28. **Cook R.D.** Concept and Applications of Finite Element Analysis. New-York, Wiley, 1974.
29. **Zienkiewicz O.C.** The Finite Element Method in Engineering Science. New-York, McGraw-Hill, 1971.

30. **Виноградова М.Б.**, **Руденко О.В., Сухорукий А.П.** Теория волн. – М.: Наука, 1979. – 384 с.
31. **Graff K.F.** Wave Motion in Elastic Solids. New-York, Dover Inc., 1975, 682 pages.
32. **Tolstoy I. Usdin E.** Wave Propagation in Elastic Plates: Low and High Mode Dispersion. // *J. Acoust. Soc. Am.*, 1957, Vol. 29, pp. 37-42.
33. **Kukudzhanov V.N.** Chislennoe Reshenie Neodnomernyh Zadach Rasprostraneniya Voln Napryazhenij v Tverdyh Telah. [Numerical Solution of Non-One-Dimensional Problems of the Propagation of Stress Waves in Solids.]. // *Soobshch. Prikl. Matem*. Moscow, VC AN SSSR, 1976, Vol. 6, pp. 67.
34. **Кукуджанов В.Н.** Численное решение неодномерных задач распространения волн напряжений в твердых телах. // Сообщ. Прикл. Матем. – М.: ВЦ АН СССР, 1976, Вып. 6, с. 67.

Anna V. Avershyeva, PhD Student, Department of Strength of Materials, National Research Moscow State University of Civil Engineering, 26, Yaroslavskoe Shosse, Moscow, 129337, Russia,
phone/fax: +7 (910) 402-35-30;
E-mail: pristanskaia@mail.ru.

Sergey V. Kuznetsov, Professor, Dr.Sc., Department of Strength of Materials, National Research Moscow State University of Civil Engineering; Institute for Problems in Mechanics, Russian Academy of Sciences; 26, Yaroslavskoe Shosse, Moscow, 129337, Russia;
Phones: +7(499)183-85-59, +7(499)183-43-29;
E-mail: sopromat@mgsu.ru.

Авершьева Анна Владимировна, аспирант, кафедра сопротивления материалов, Национальный исследовательский Московский государственный строительный университет»; 129337, Россия, г. Москва, Ярославское шоссе, д. 26; тел/факс: +7 (910) 402-35-30;
E-mail: pristanskaia@mail.ru.

Кузнецов Сергей Владимирович, профессор, доктор физико-математических наук; профессор кафедры сопротивления материалов, Национальный исследовательский Московский государственный строительный университет; Институт проблем механики Российской академии наук; 129337, Россия, г. Москва, Ярославское шоссе, д. 26;
тел. +7(499)183-85-59, +7(499)183-43-29;
E-mail: sopromat@mgsu.ru.

DOI:10.22337/2587-9618-2019-15-2-24-39

ESTIMATION OF PEDESTRIAN COMFORT ON THE BASIS OF NUMERICAL MODELING OF WIND AERODYNAMICS OF BUILDINGS IN THE ENVIRONMENTAL DEVELOPMENT

Alexander M. Belostotsky [1, 2, 3, 4, 5]***, Irina N. Afanasyeva*** [1]***, Irina Yu. Lantsova*** [6]

[1] Scientific Research Center "StaDyO", Moscow, RUSSIA
[2] Tomsk State University of Architecture and Building, Tomsk, RUSSIA
[3] Peoples' Friendship University of Russia, Moscow, RUSSIA
[4] Russian University of Transport (MIIT), Moscow, RUSSIA
[5] Perm National Research Polytechnic University, Perm, RUSSIA
[6] National Research Moscow State University of Civil Engineering, Moscow, RUSSIA

Abstract: The distinctive paper is devoted to the methodology of pedestrian comfort estimation in the nearby area of the object under construction. A verification example of the wind flow simulation around and through a porous object is considered in order to select correct permeability parameters of the computational model of green spaces. The methodology of pedestrian comfort estimation is tested on the example of a real residential complex in Moscow. The results of the numerical simulation of velocity fields are used to calculate the criteria for pedestrian comfort specified in MDS 20-1.2006. Numerical results are obtained and compared for two study cases - without and with green spaces (bushes),to assess their impact on pedestrian comfort and the possibility of its adjustment.

Keywords: numerical simulation, computational fluid dynamics (CFD), pedestrian comfort, porous body, wind chill effect

ОЦЕНКА ПЕШЕХОДНОЙ КОМФОРТНОСТИ НА ОСНОВЕ ЧИСЛЕННОГО МОДЕЛИРОВАНИЯ ВЕТРОВОЙ АЭРОДИНАМИКИ ЗДАНИЙ В ОКРУЖАЮЩЕЙ ЗАСТРОЙКЕ

А.М. Белостоцкий [1, 2, 3, 4, 5]***, И.Н. Афанасьева*** [1]***, И.Ю. Ланцова*** [6]

[1] Научно-исследовательский центр СтаДиО, г. Москва, РОССИЯ
[2] Томский государственный архитектурно-строительный университет, г. Томск, РОССИЯ
[3] Российский университет дружбы народов, г. Москва, РОССИЯ
[4] Российский университет транспорта (МИИТ), г. Москва, РОССИЯ
[5] Пермский национальный исследовательский политехнический университет, г. Пермь, РОССИЯ
[6] Национальный исследовательский Московский государственный строительный университет, г. Москва, РОССИЯ

Аннотация: Настоящая статья посвящена методике оценки пешеходной комфортности в близлежащей территории строящегося объекта. Рассматривается верификационный пример расчета ветрового потока в воздушной среде с пористым объектом для подбора параметров проницаемости расчетной модели зеленых насаждений. Методика оценки пешеходной комфортности апробируется на примере реального жилого комплекса в г. Москва. Результаты численного моделирования ветровых потоков используются для вычисления критериев пешеходной комфортности, указанных в МДС20-1.2006. Численные результаты получены и сопоставлены для двух расчетных случаев – без и с зелеными насаждениями (кустарниками), с целью проведения оценки их влияния на пешеходную комфортность и возможность ее корректировки.

Ключевые слова: численное моделирование, вычислительная гидродинамика и газодинамика (CFD), пешеходная комфортность, пористое тело, ветровое охлаждение

INTRODUCTION

Recently, due to significant growth and compaction of urban buildings in the regions of Russia due to the erection of buildings and complexes of various architectural forms and original design solutions, one of the most important factor to consider during construction of buildings and structures is the type of wind conditions at the construction site. Wind loads and impacts in urban areas are formed taking into account velocity and temperature fields inside and above urban areas due to a wide range of atmospheric processes, which in turn are modified to take into account the topography and configuration of the land surface of the area [1]. The impact of velocity in urban areas can lead to a negative change in the microclimatic conditions of the air environment, and can also be a source of unfavorable situations [1-5]. The lack of a culture and residential practices in designing the wind patterns of residential areas, taking into account the existing and future development, has already led to the emergence of neighborhoods where the velocity does not decrease, as is usually the case in a city, but increases by 20% or more at the end gaps between the buildings, there is a strong narrowing of the air flow, and as a result velocity acceleration zones and/or high turbulence zones are formed, which creates uncomfortable conditions for pedestrians [6]. Wind speeds provided by meteorological stations may differ significantly from the wind conditions on the ground due to the influence of local urban development, unique in its kind for each district of the city. Modeling of aerodynamic conditions (using numerical and /or experimental methods) allows to analyze the occurrence of adverse situations in pedestrian areas, considering the specificity of the landscape and the surrounding buildings, and propose measures to eliminate them or reduce their negative impact.

The aim of this paper is to perform an approbation of the methodology for assessing pedestrian comfort with correct consideration of green spaces using the example of a real construction object, and to determine the design parameters, such as required number of wind angles of attack. As an expected result of an assessment, recommendations on green spaces arrangement that provides pedestrian comfort improvement should be formulated.

1. NORMATIVE AND ANALYTICAL APPROACH TO ASSESS PEDESTRIAN COMFORT

According to SP 20.13330.2016 [7], when developing architectural and planning solutions for urban neighborhoods, as well as when planning the construction of buildings inside existing urban neighborhoods, it is recommended to assess the comfort in pedestrian areas in accordance with the requirements of the standards or technical conditions. However, any criteria for pedestrian comfort in [7] are not formulated. Such criteria are described only in MDS 20-1.2006 [8], according to which the comfort condition for pedestrian areas is as (eq. 1):

$$\forall V < V_{cr} : T_c(V_{cr}) < T_{lim} \qquad (1)$$

where V is the velocity in a gust at the level of 1.5 meters; T_c is the duration of the appearance of velocity V, more than a certain critical value V_{cr}; T_{lim} is T_c limit value.

The V_{cr} and T_{lim} values for the three established comfort levels are listed in table 1.

Usually, when assessing the comfort in pedestrian zones with velocity V at a characteristic height of z_c=1.5 meters, the frequency of its occurrence T_c is determined by the relations (eq. 2):

$$T_c = \Delta T_m P(V > V_{cr}) \qquad (2)$$

where ΔT_m is the interval of measuring velocity V_m at meteorological stations (usually ΔT_m = 3 hours); $P(V>Vcr)$ is the probability that the velocity exceeds the critical value V_{cr}.

Table 1. Critical velocity V_{cr} (m/s) and the maximum duration T_{lim} (hour /year) of their appearance.

Comfort level	I	II	III
V_c, m/s	6	12	20
T_{lim}, hour/year	1000	50	5

2 METHODOLOGY OF PEDESTRIAN COMFORT LEVEL ESTIMATION WITH APPLICATION OF NUMERICAL METHODS

2.1. Basics of the methodology.

In [6, 9], the following method for pedestrian comfort estimation based on numerical modeling of the aerodynamics of buildings in the surrounding buildings is presented. After calculations performed for all wind directions, the results are processed using a special computer module. The values of the wind gusts at the characteristic monitoring points of the urban area are summed with the weight coefficients corresponding to the frequency of occurrence of the wind impact of a given direction and a given speed range. 1.5 m is taken as the estimated height.

After numerical modeling for all wind directions (usually j = 1, ..., 24), the «discomfort time of level l» K_{crl} (l = 1,2,3) for a representative set of points of pedestrian zones is determined by the relations (eq. 3):

$$K_{cr} = \sum S_{ij} T_{ij}, \quad V_{ij} = V_i / V_{10}(1 + \theta \cdot I) \tag{3}$$

where V_i, i=1,2,3 is the velocity in the table of weather data ("wind rose"); T_{ij} is the duration (according to meteorological data, hours per year) of wind influence of direction j and mean velocity V_i; V_j is the mean wind speed at this point according to the calculation for direction j at speed V_{10} at a height of 10 m; $V_{ij}$is the maximum velocity at the point in the gusts at the wind velocity V_i; θ is the assurance coefficient(usually in the range from 1 to 3); S_{ij} is an indicator (0 or 1) that shows the local wind speed exceedance of the critical value V_{crl} for a given comfort level $l$at the point V_{ij}; $I=(\rho \cdot TKE/abs(P)/3)^{1/2}$ is the turbulence intensity (standard of velocity pulsations); $P = \rho V^2/2$ is the mean pressure; $TKE=3/2(I \cdot V)^2$ is the turbulence kinetic energy.

The wind rose is received according to the weather data. To assess the distribution of wind speeds inside the rumba, in practice, as a rule, the Weibull distribution is used [9-12].

Estimation of the standard deviation of the pulsation velocity component is based on the steady state simulation results using calculated values of turbulence kinetic energy TKE and considering the $\theta = 2$ (eq. 4):

$$\sigma = \sqrt{\frac{4}{3} TKE} \tag{4}$$

2.2. Wind chill effect.

In the winter season, due to the cold wind currents and wind gusts, the human body may experience wind chilling, as a result of which the temperature feels completely different than it actually is. Scientists and medical experts of the Joint Action Group on Temperature Indices [13] implemented an index of wind chill. The resulting model can be approximately, with an accuracy of one degree, formulated as equation 5:

$$T_{wc} = 13.12 + 0.6215 \cdot T_a - 11.37 \cdot V^{+0.16} + 0.3965 \cdot T_a \cdot V^{+0.16} \tag{5}$$

where T_{wc} is the wind chill index, T_a is the air temperature in Celsius, V is the velocity in km/h.

2.3. Features of green spaces modeling.

Modeling of the decorative green spaces, both in wind tunnels and numerically, is a very difficult task. This is due, primarily, to the complexity of their form.

When conducting experiments in wind tunnels, trees are modeled simply, or toy models are used [14].

In numerical modeling, it is possible to create a realistic tree model up to the modeling of leaf geometry, but this approach is incredibly resource-demanding and time consuming. It is also possible to set a tree area in a simplified way - as a porous body, and when solving the Navier-Stokes equations, an additional term is added to the equations of motion that characterizes the loss of momentum when air passes through the porous region (eq. 6):

$$\begin{cases} \rho\frac{\partial u}{\partial t}+\rho u\frac{\partial u}{\partial x}+\rho v\frac{\partial u}{\partial y}+\rho w\frac{\partial u}{\partial z}=-\frac{\partial p}{\partial x}+\mu\left(\frac{\partial^2 u}{\partial x^2}+\frac{\partial^2 u}{\partial y^2}+\frac{\partial^2 u}{\partial z^2}\right)+S_{M,x} \\ \rho\frac{\partial v}{\partial t}+\rho u\frac{\partial v}{\partial x}+\rho v\frac{\partial v}{\partial y}+\rho w\frac{\partial v}{\partial z}=-\frac{\partial p}{\partial y}+\mu\left(\frac{\partial^2 v}{\partial x^2}+\frac{\partial^2 v}{\partial y^2}+\frac{\partial^2 v}{\partial z^2}\right)+S_{M,y} \\ \rho\frac{\partial w}{\partial t}+\rho u\frac{\partial w}{\partial x}+\rho v\frac{\partial w}{\partial y}+\rho w\frac{\partial w}{\partial z}=-\frac{\partial p}{\partial z}+\mu\left(\frac{\partial^2 w}{\partial x^2}+\frac{\partial^2 w}{\partial y^2}+\frac{\partial^2 w}{\partial z^2}\right)+S_{M,z} \end{cases} \quad (6)$$

where μ is the coefficient of dynamic viscosity; loss of momentum through the isotropic porous region can be formulated based on permeability and loss coefficients (eq. 7),

$$\begin{cases} S_{M,x}=-K_{loss}\frac{\rho}{2}u\sqrt{u^2+v^2+w^2} \\ S_{M,y}=-K_{loss}\frac{\rho}{2}v\sqrt{u^2+v^2+w^2} \\ S_{M,z}=-K_{loss}\frac{\rho}{2}w\sqrt{u^2+v^2+w^2} \end{cases} \quad (7)$$

K_{loss} is the loss factor associated with inertial losses (m^{-1}).

The model of porosity allows taking into account the Darcy Model [15, 16], which is the continuity equation for flows in porous regions and is characterized by such a parameter as the volume porosity γ.

The volume porosity is the ratio of the volume V' of space in the final volume through which air can flow, to the entire final volume V (eq. 8):

$$V'=\gamma V \quad (8)$$

The Darcy model is summarized as follows (eq. 9):

$$-\frac{\partial p}{\partial x_i}=\frac{\mu}{K_{perm}}U_i+K_{loss}\frac{\rho}{2}|U|U_i \quad (9)$$

where μ is the dynamic viscosity, K_{perm} is the permeability.

When modeling a tree in a simple, porous domain, the difficulty lies in the selection of an adequate loss factor and volume porosity, which will reflect the permeability of the real green planting.

3. VERIFICATION OF THE METHODOLOGY OF NUMERICAL MODELING OF GREEN SPACES AERODYNAMICS

3.1. Problem statement.

For the numerical simulation of the aerodynamics of green spaces, a group of scientists from the Institute of Architecture of Japan (AIJ) [17] proposed a benchmark. A tree with a height of 7 meters in the air flow is considered. At the inlet of the air domain the velocity profile obeys the vertical power law (eq. 10). Sensors (monitoring points) are installed behind the tree, measuring the instantaneous velocity at each height in increments of 1.5 meters. The tree model and flow direction are shown in Figure 1, the layout of the monitoring points is shown in Figure 2.

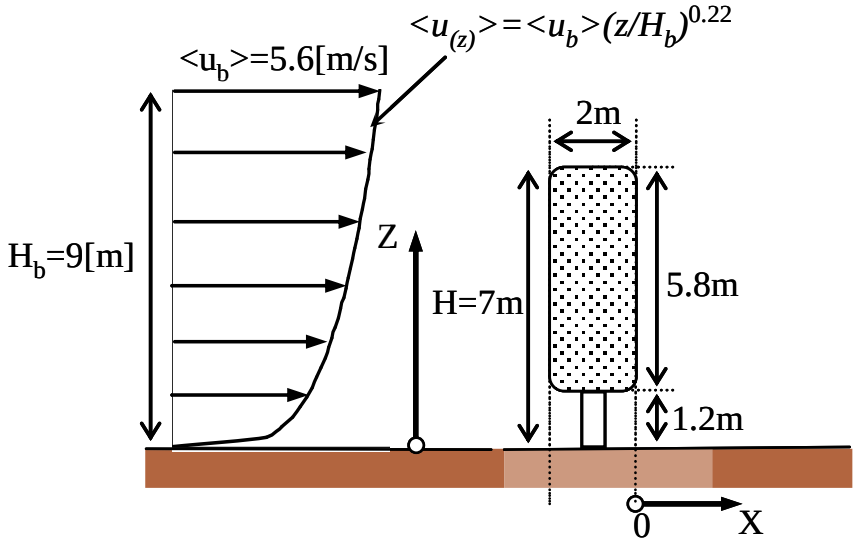

Figure 1. Tree model with indication of characteristic dimensions and wind direction of the inlet flow.

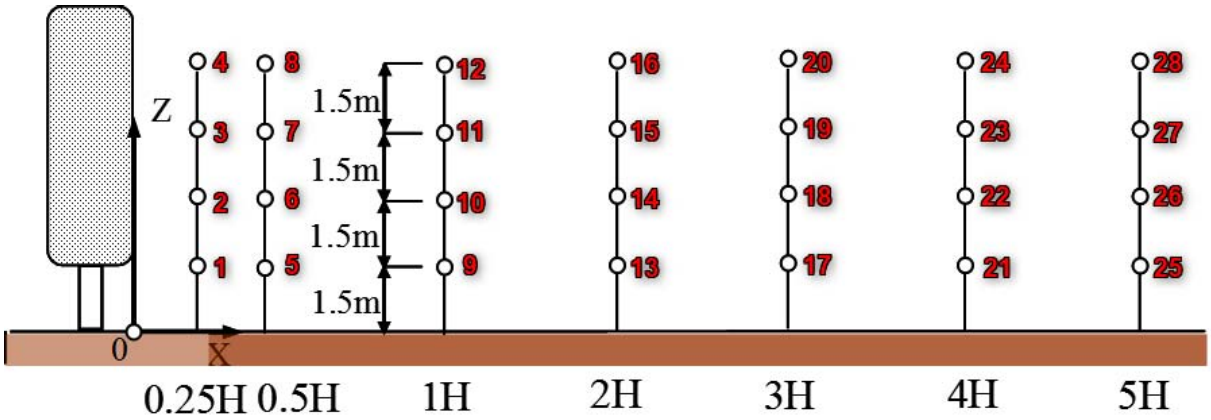

Figure 2. Layout of the monitoring points in a given coordinate system with an indication of the characteristic dimensions.

The tree was modeled as an isotropic porous region. Loss of momentum that occurs when passing through a porous body, are formulated based on permeability and loss coefficients (eq. 7). The loss coefficient K_{loss} was taken equal to 1.75, based on the data obtained [14], which proved to be the most accurate result in comparison with the experimental data.

A comparison of numerical and experimental results (velocities at monitoring points for different values of volume porosity γ (0.3-0.9 with a step of 0.1; 0.99 and 1))was made. Recommendations on the design parameters for modeling the permeability of shrubs crowns (as one of the ways to improve pedestrian comfort) was formulated.

All aerodynamic simulations were performed using ANSYS CFX 17.0 software package [15, 16].

3.2. Simulation Parameters.

The problem was solved in a two-dimensional formulation. As a turbulence closure model, the SST (Shear Stress Transport) model was utilized.

The following basic physical characteristics of the flow for aerodynamic simulations are used:

$$\rho^f = 1.184 \text{ kg/m}^3$$

- air density,

$$\eta = 1.831 \cdot 10^{-5}$$

- the coefficient of dynamic viscosity,

$$\bar{v}_{in}^f = 4.77 \text{ m/s}$$

– the mean velocity at the inlet,

$$Re = 2.1609 \cdot 10^6$$

– the Reynolds number.

The High Resolution advection scheme and the implicit First Order Backward Euler scheme were used. Maximum residuals of 10^{-4} were set as an criterion for convergence and termination ofsteady state solution.The maximum number of iterations was 300.

3.3. Initial and boundary conditions.

The mean flow velocity profile at the inlet obeys the power lawdepending on the tree height and turbulence kinetic energy (eq. 10):

$$u(z) = u_b \left(\frac{z}{H_b}\right)^{0.22} \qquad (10)$$
$$k(z) = 3.02$$

where u_b is velocity at the characteristic height H_b, $k(z)$ is the turbulence kinetic energy.

At the outlet and at the upper boundary of the domain, opening boundary conditions with a relative pressure equal to zero and the same turbulence parameters as at the inlet are assigned. On the «ground», «No Slip Wall» ($U=V=W=0$ m/s) boundarycondition is specified, which excludes penetration of the fluidthrough the surface.

On the surface of the tree crown interface «Fluid-Porous Domain») is set to ensure the penetration of air through the porous body (domain).

As initial conditions, zero velocities

($U=V=W=0$ m/s)

and zero relative pressures areset in the entire domain.

3.4. Simulation results.

Figure 3 and Table 2 demonstrate the main results of the performed computational studies and the comparison of the numerical results with the experiment data.

In the Table 2 the relative errors for real velocity at the monitoring points in comparison with the experiment are presented.

The numerical simulation of hedge aerodynamics showed that the closest to experimental data result was obtained for the values of volume porosity from 0.9 to 1.The maximum discrepancy from the experiment is 29%, and the minimum one is 0.15%.

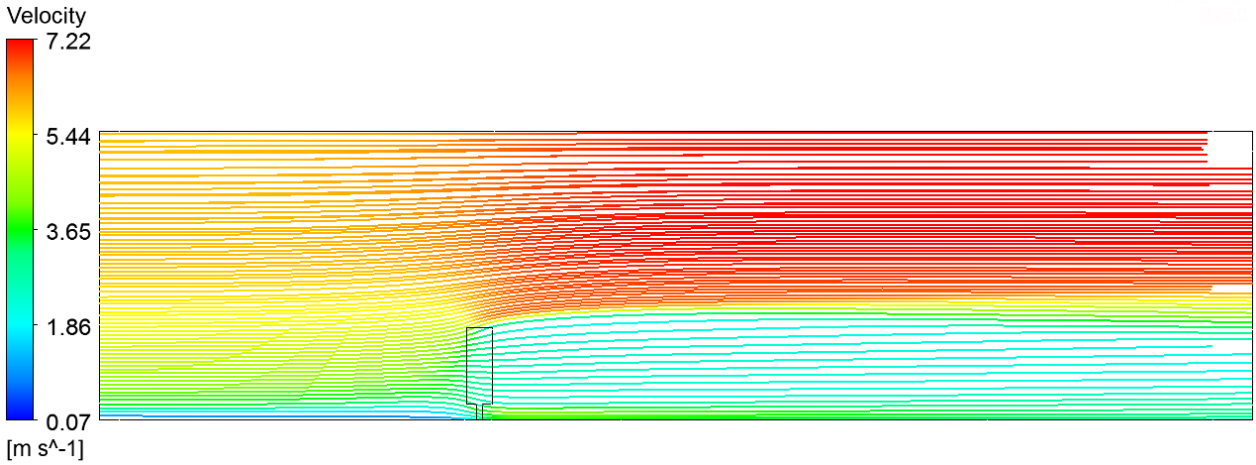

Figure 3. Velocity stream lines, m/s. Volume porosity γ = 1, loss coefficient K_{loss} = 1.75.

Table 2. Comparison of numerical (u) and experimental (u^*_{exp}) velocity simulations at the monitoring points for each considered volume porosity value.

Monitoring points	u^*_{exp} [м/с]	γ=0.3		γ=0.4		γ=0.5		γ=0.6		γ=0.7		γ=0.8		γ=0.9		γ=0.99		γ=1	
		u	ε,%	u	ε,%	u	ε,%	u	ε,%	u	ε,%	u	ε,%	u	ε,%	u	ε,%	u	ε,%
1	2.05	2.20	7.33	3.24	58.11	2.99	45.99	2.77	35.03	2.62	28.15	2.55	24.30	2.50	21.86	2.47	20.49	2.47	20.36
10	2.13	2.60	21.98	2.51	17.45	2.48	16.29	2.48	15.98	2.48	16.00	2.48	16.11	2.48	16.28	2.48	16.44	2.49	16.45
11	2.14	2.39	11.32	2.41	12.35	2.43	13.19	2.44	13.97	2.46	14.61	2.47	15.09	2.47	15.47	2.48	15.73	2.48	15.75
12	2.42	2.75	13.48	2.61	7.59	2.51	3.62	2.45	1.25	2.41	-0.41	2.38	-1.66	2.36	-2.63	2.34	-3.32	2.34	-3.39
13	2.76	2.52	-8.88	2.81	1.84	2.80	1.34	2.70	-2.38	2.63	-4.83	2.60	-5.80	2.59	-6.33	2.58	-6.56	2.58	-6.58
14	2.16	2.52	16.68	2.43	12.58	2.40	11.20	2.39	10.52	2.38	10.20	2.38	10.03	2.38	9.98	2.38	9.96	2.38	9.96
15	2.05	2.27	10.81	2.32	13.35	2.34	14.44	2.36	15.15	2.37	15.67	2.38	16.04	2.38	16.32	2.39	16.51	2.39	16.52
16	2.45	2.52	2.68	2.48	0.88	2.41	-1.61	2.37	-3.37	2.34	-4.70	2.31	-5.75	2.29	-6.57	2.28	-7.16	2.28	-7.22
17	2.83	2.63	-6.91	2.85	0.91	2.86	1.14	2.81	-0.67	2.77	-2.13	2.75	-2.74	2.74	-3.08	2.73	-3.27	2.73	-3.28
18	2.39	2.50	4.67	2.40	0.53	2.37	-0.89	2.35	-1.79	2.33	-2.39	2.32	-2.81	2.31	-3.10	2.31	-3.30	2.31	-3.32
19	2.38	2.23	-6.48	2.28	-4.28	2.30	-3.26	2.31	-2.79	2.32	-2.55	2.32	-2.44	2.32	-2.38	2.32	-2.36	2.32	-2.36
2	2.90	2.72	-6.13	2.62	-9.83	2.61	-10.03	2.62	-9.70	2.63	-9.31	2.64	-8.96	2.65	-8.65	2.66	-8.40	2.66	-8.38
20	2.79	2.44	-12.61	2.41	-13.49	2.37	-15.12	2.33	-16.53	2.30	-17.69	2.27	-18.64	2.25	-19.41	2.23	-19.98	2.23	-20.03
21	2.65	2.69	1.33	2.88	8.64	2.90	9.36	2.86	7.91	2.83	6.67	2.82	6.17	2.81	5.87	2.80	5.67	2.80	5.66
22	2.47	2.49	0.99	2.38	-3.43	2.34	-5.10	2.31	-6.32	2.29	-7.24	2.27	-7.94	2.26	-8.47	2.25	-8.84	2.25	-8.88
23	2.61	2.20	-15.43	2.25	-13.47	2.27	-12.70	2.28	-12.53	2.28	-12.57	2.27	-12.69	2.27	-12.83	2.27	-12.95	2.27	-12.96
24	3.08	2.39	-22.40	2.38	-22.92	2.33	-24.34	2.29	-25.68	2.26	-26.84	2.23	-27.80	2.20	-28.57	2.19	-29.14	2.18	-29.19
25	2.50	2.71	8.24	2.89	15.56	2.92	16.42	2.89	15.23	2.86	14.26	2.85	13.84	2.84	13.55	2.84	13.34	2.84	13.32
26	2.45	2.50	2.00	2.37	-3.18	2.32	-5.22	2.28	-6.84	2.25	-8.11	2.23	-9.10	2.21	-9.86	2.19	-10.39	2.19	-10.45
27	2.62	2.19	-16.72	2.24	-14.76	2.25	-14.24	2.25	-14.37	2.24	-14.67	2.23	-15.01	2.22	-15.31	2.22	-15.55	2.22	-15.57

4. APPROBATION OF THE NUMERICAL METHODOLOGY OF ESTIMATION AND IMPROVEMENT OF PEDESTRIAN COMFORT

4.1. Problem statement.

The application of the developed numerical methodology of pedestrian comfort estimation-was performed on a realresidential building surrounded by existing urban area (Figure 4). As it will be shown below, for the considered group of buildings, it was necessary to improve pedestrian comfort using the above-described methodologyby incorporation of thegreen spaces to particular locationswhere pedestrian comfort criteria were not satisfied.

For the correct shrubs arrangement near the considered buildings, the results of criterion assessments of pedestrian comfortobtained for the model without green spaces were used.Decisions on the location of green space were made based on an analysis of the most unfavorable wind attack angles, a planning scheme for the land plot near the designed building, as well as currently existing planted shrubs (Figure 5).

Figure 4. General view of the building. Project proposal (photo montage).

Figure 5. Construction site (maps.yandex.ru) of the projected residential building (South-West Administrative District, Moscow).

4.2. Geometric model of the building surrounded with nearby buildings with bushes consideration.

The radius of the nearby building area was taken equal to 600 m.The actual location of the buildings relative to the target object, their height and cross section in the plan, as well as the local terrain relief (elevation differences near the target object) were consideredfor the geometric model including surrounding buildings.

Geometric model of the main building surrounded with nearby buildingswas created in ANSYS Mechanical 17.0 [18]. The first-floorlevel was taken as a zero level. The created model of the building, taking into account the development for a certain perspective, is shown in Figure 6-7.

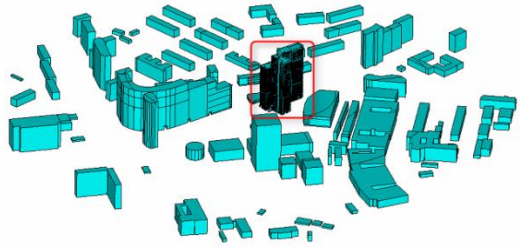

Figure 6. Geometric model of the building surrounded with nearby buildings.

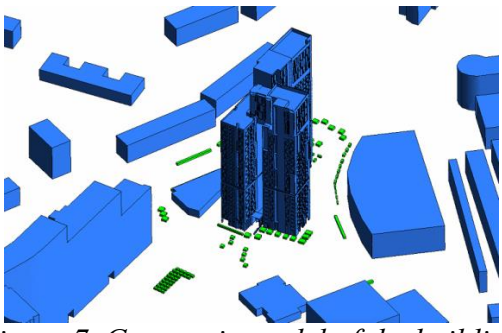

Figure 7. Geometric model of the building surrounded with nearby buildings with bushes consideration.

4.3. Boundary and initial conditions.

The simulated area (Figure 8) is assigned the Air domain with the following physical parameters: incompressible air at a temperature (25°C) and pressure 1 atm.

The boundary conditions at the inlet correspond to the 1st wind region, and the type of terrain B «suburb» in accordance with building codes [7, 19]. The mean pressure and pulsation profiles were converted to theinput data for the ANSYS CFX using the developed macro CFX_PROFIL_SNIP as a vertical profiles (along the height)of mean velocity, turbulence kinetic energy and dissipation energy, corresponding to the loads, taking into account the load reliability factor of 1.4. The integral turbulence length scale is assumed to be 300 m in accordance with the recommendations of Eurocode [20].

At the outlet and at the upper boundary of the domain, opening boundary conditions with a relative pressure equal to zero and the same turbulence parameters as at the inlet are assigned. On the «ground» and on all buildings, «No Slip Wall»

$$(U=V=W=0 \text{ m/s})$$

boundary condition is specified, which excludes penetration of the fluid through the surface.

On the surface of the tree crown interface «Fluid-Porous Domain» is set to ensure the penetration of air through the porous body (domain).

As initial conditions, zero velocities ($U=V=W=0$ m/s) and zero relative pressures are set in the entire domain.

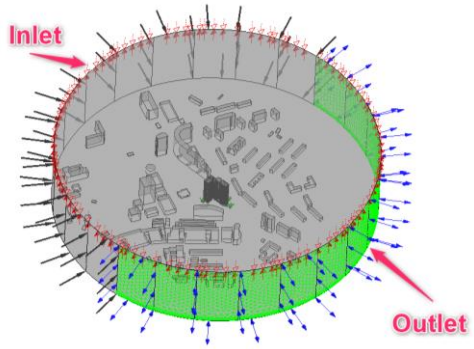

Figure 8. Simulated area (ANSYS CFX) with designated boundary conditions. Wind angle of attack 0°.

4.5. Simulation Parameters.

All aerodynamic calculations were carried out in a three-dimensional steady-stateformulation using the RANS SST turbulence model.

The internal parameters for the shrubs are following: the surface porosity is isotropic; the volume porosity is 1. An isotropic model with a loss coefficient of 1.75 $m^{-1}$was set as the loss model.

Maximum residuals of 10^{-4} were set as a criterion for convergence and termination ofsteady state solution. The maximum number of iterations was 500.

4.6. Results of steady state aerodynamic simulations.

Pedestrian comfort levels (repeatability of meanvelocity, hr/year) according to the 3rd regulatory criteria (K_{cr1}, K_{cr2}, K_{cr3}) were calculated using the data from weather stations named after Michelson [6, 14].

It was necessary to get a set of results for different wind angles of attack was in order to calculate the pedestrian comfort level criteria. The comparisonof the simulation results for 24, 12 and 6 wind directionsevenly distributed in a circle was conductedin order to determine the minimum required number of windangles of attack.

The convergence study resultsfor thepedestrian comfort level criteria depending on the number of wind directions considered, and the determination of the optimal number of simulationcases excluding bushes are presented below (Table 3).

As it can be seen from the results, the difference is insignificant with the number of 12 and 24 wind angles of attack. This allows usto consider only 12 wind attack angles to perform accurate estimation of the pedestrian comfort level.

Table 3. The results of criterion assessments for different number of wind angles of attack.

Number of angles	1st level of pedestrian comfort, exceeding *Vcr1*=6 m/s, not more than *Kcr1*=1000 hours per year in the pedestrian zone at a height of 1.5 m	2nd level of pedestrian comfort, exceeding *Vcr2*=12 m/s, not more than *Kcr2*=50 hours per year in the pedestrian zone at a height of 1.5 m	3st level of pedestrian comfort, exceeding *Vcr3*=20 m/s, not more than *Kcr3*=5 hours per year in the pedestrian zone at a height of 1.5 m
24	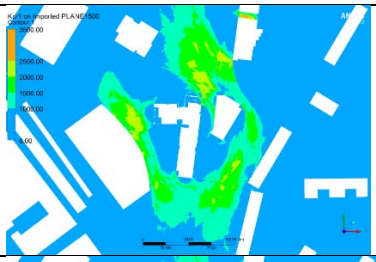	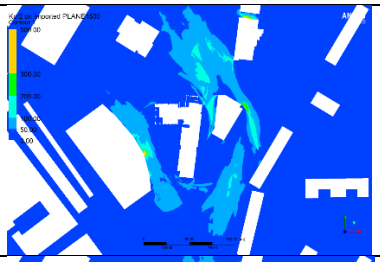	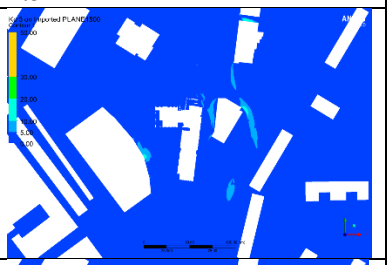
12	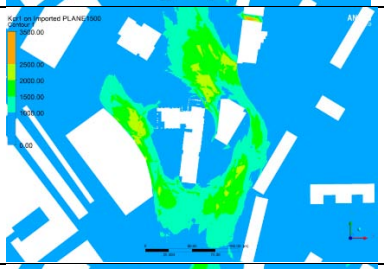	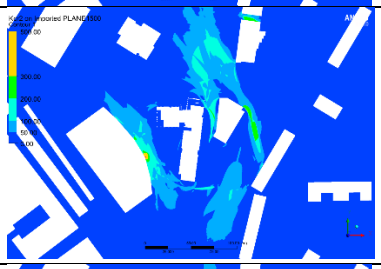	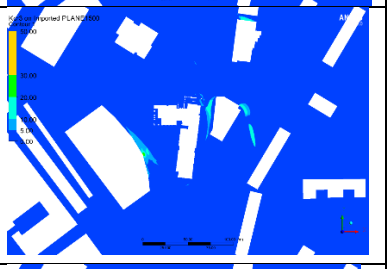
6	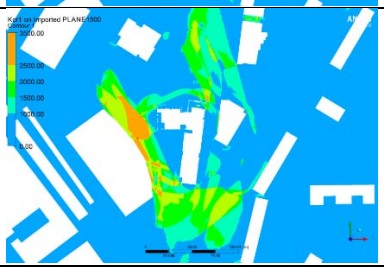	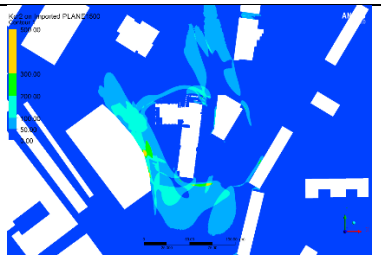	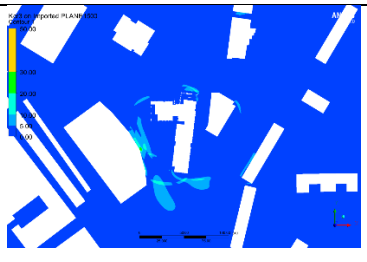

A comparison of the criterion assessment of pedestrian comfort based on numerical modeling of the building surrounded with nearby buildings without bushes consideration and numerical modeling of the building surrounded with nearby buildings and bushes consideration is presented below (Figure 9-11). Results comparison show the significant decrease in the occurrence frequency of winds exceeding 6 m/s for the first criterion, 12 m/s for the second criterion and 20 m/s for the third criterion for the case where bushes were incorporated in to the model.

The results allow us to conclude that bushesplaced near the building help to improve pedestrian comfort.

Pictures of wind speeds amplification at the level of the pedestrian zone of 1.5 m for some wind directions with and without bushes are shown in Figure 12-14. Comparison of the meanvelocity amplification at 1.5 m shows significant improvements in pedestrian zones where highvelocities were observedfor the study cases without bushes.

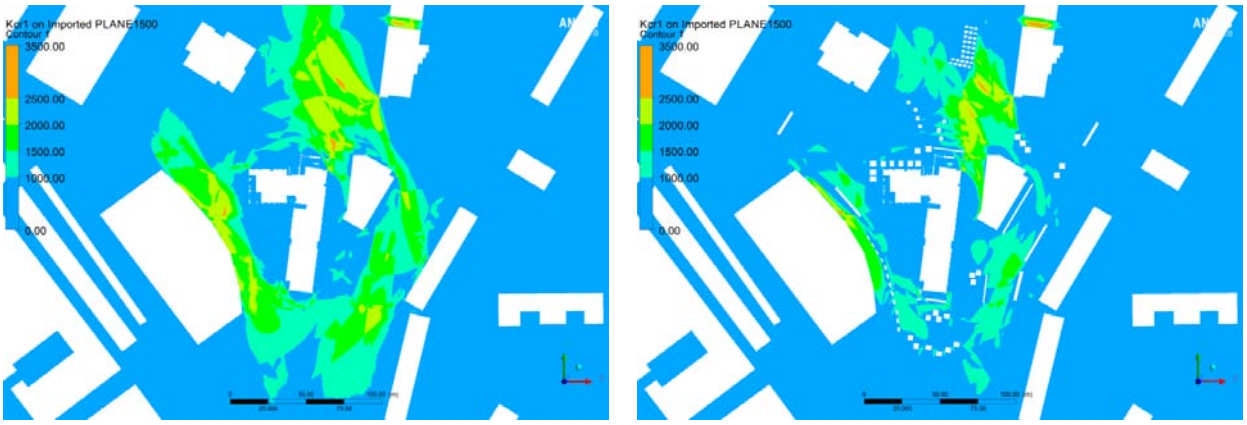

Figure 9. 1st level of pedestrian comfort V_{cr1}=6 m/s exceeding no more K_{cr1}=1000 hours per year in the pedestrian zone at a height of 1.5 m (on the left - without bushes, on the right - with bushes).

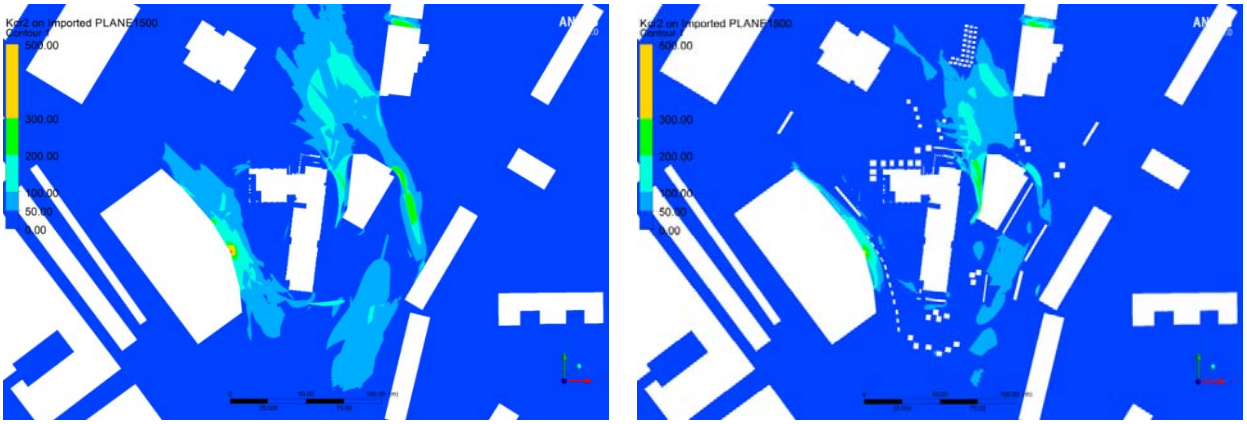

Figure 10. 2nd level of pedestrian comfort V_{cr2}=12 m/s exceeding no more K_{cr2}=50 hours per year in the pedestrian zone at a height of 1.5 m (on the left - without bushes, on the right - with bushes).

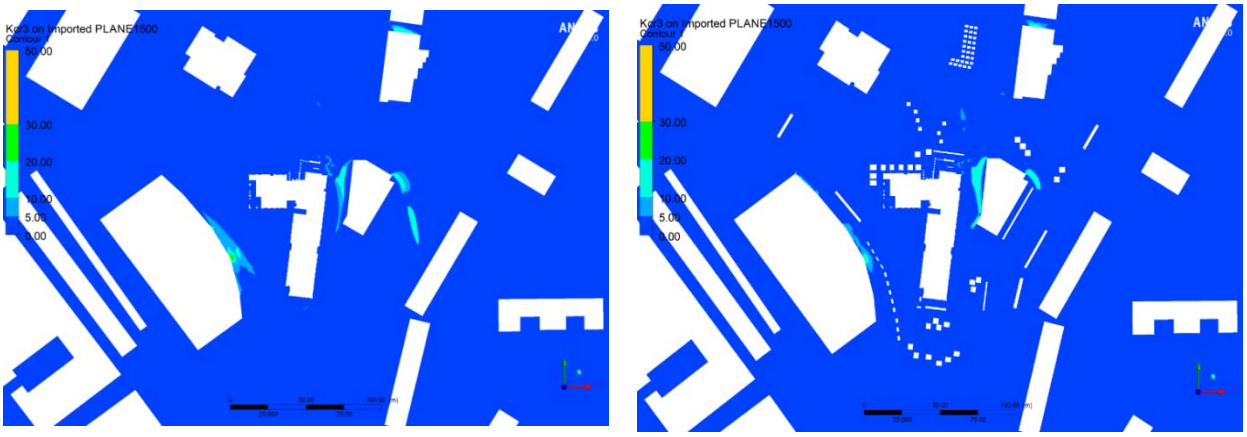

Figure 11. 3st level of pedestrian comfort V_{cr3}=20 m/s exceeding no more K_{cr3}=5 hours per year in the pedestrian zone at a height of 1.5 m (on the left - without bushes, on the right - with bushes).

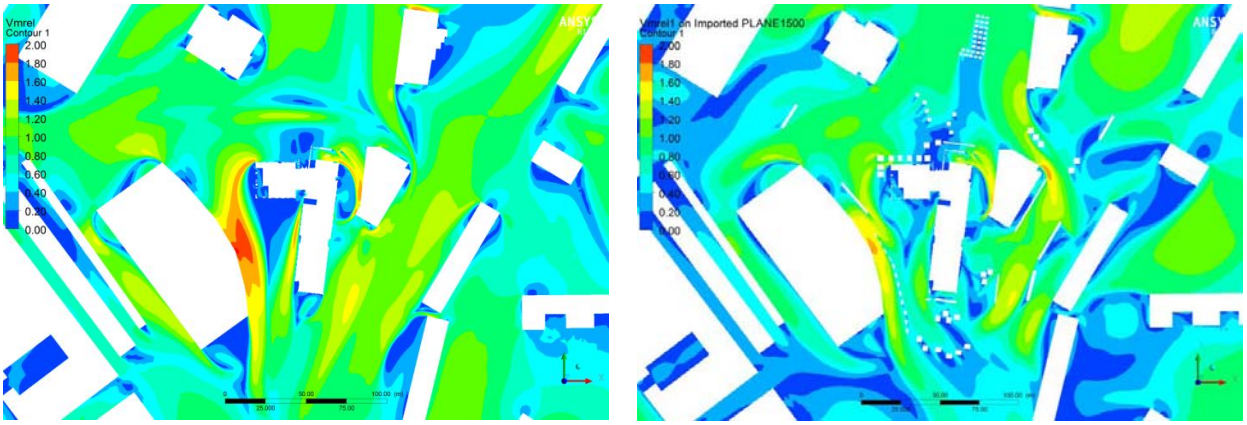

Figure 12. The meanvelocity amplifications in the pedestrian zone at a height of 1.5 m. The wind angle of attack is 0° (on the left - without bushes, on the right - with bushes).

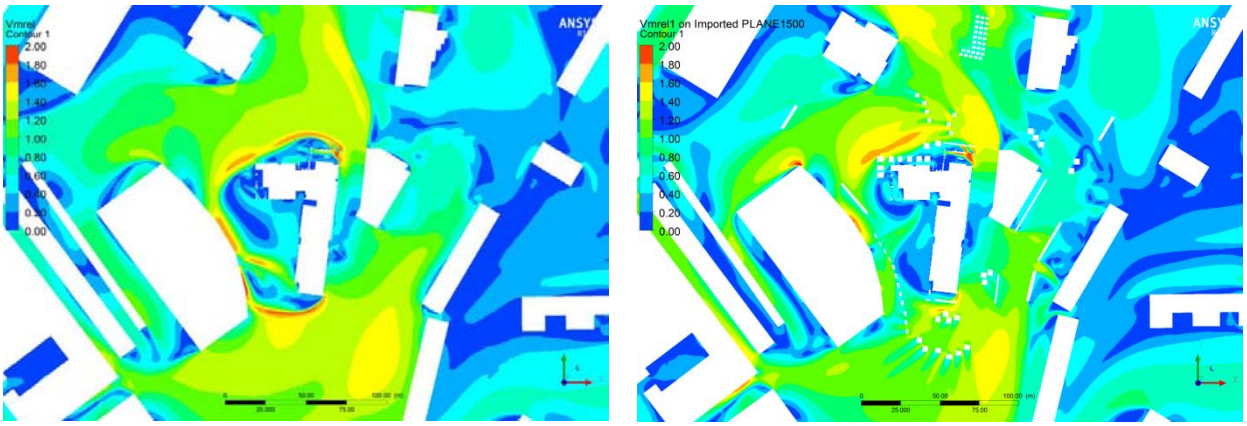

Figure 13. The meanvelocity amplifications in the pedestrian zone at a height of 1.5 m. The wind angle of attack is 90° (on the left - without bushes, on the right - with bushes).

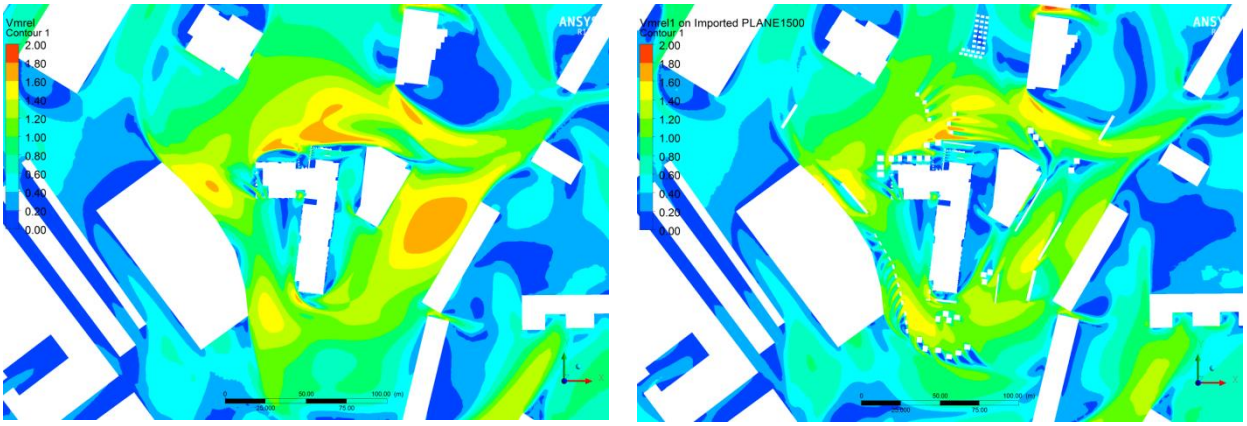

Figure 14. The mean velocity amplifications in the pedestrian zone at a height of 1.5 m. The wind angle of attack is 240° (on the left - without bushes, on the right - with bushes).

Comparison of the results of numerical modeling of the buildings aerodynamics taking into account wind chill effect in the winter season at a temperature of - 20°C for some wind directions with and without shrubs is presented below (Figure 15-18).

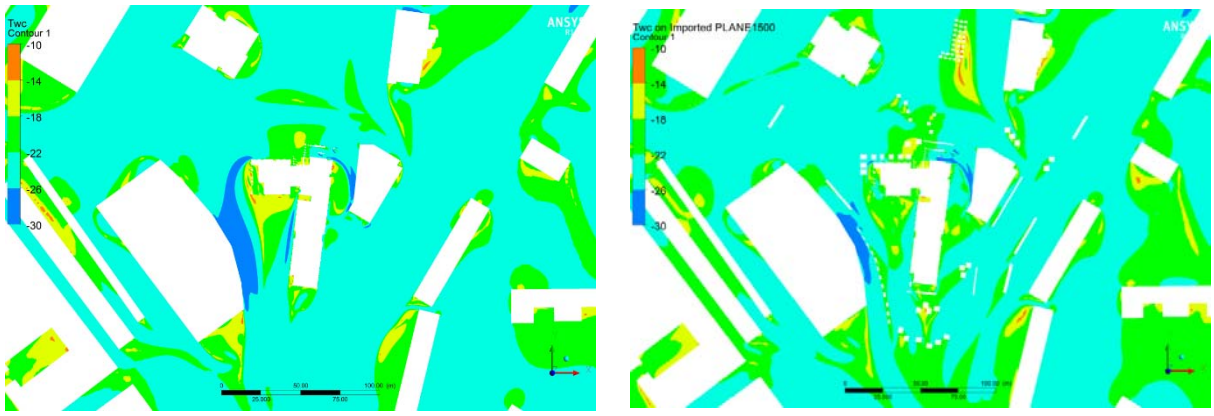

Figure 15. Comparison of the results of numerical modeling of the buildings aerodynamics taking into account wind chill effect in the winter season at a temperature of -20 °C, wind angle of attack 0° (on the left - without bushes, on the right - with bushes).

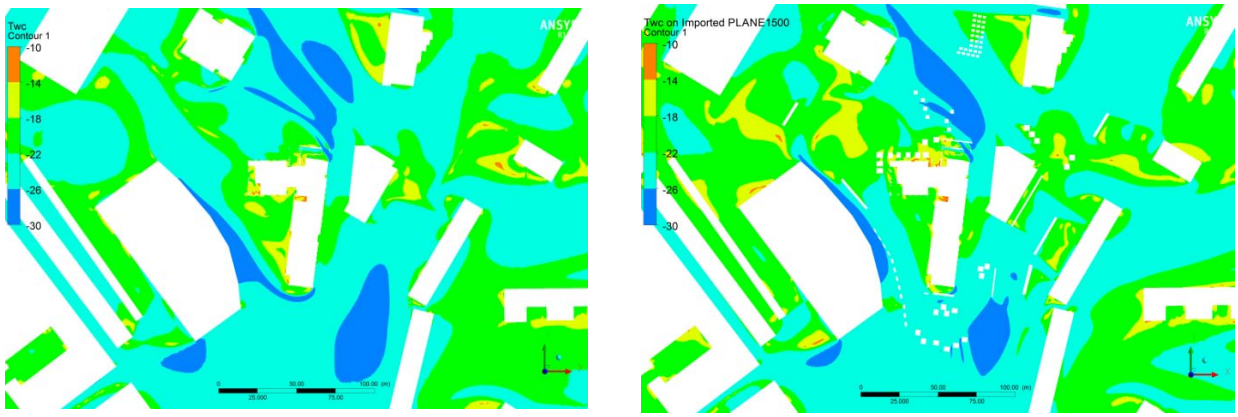

Figure 16. Comparison of the results of numerical modeling of the buildings aerodynamics taking into account wind chill effect n the winter season at a temperature of -20 °C, wind angle of attack 120° (on the left - without bushes, on the right - with bushes).

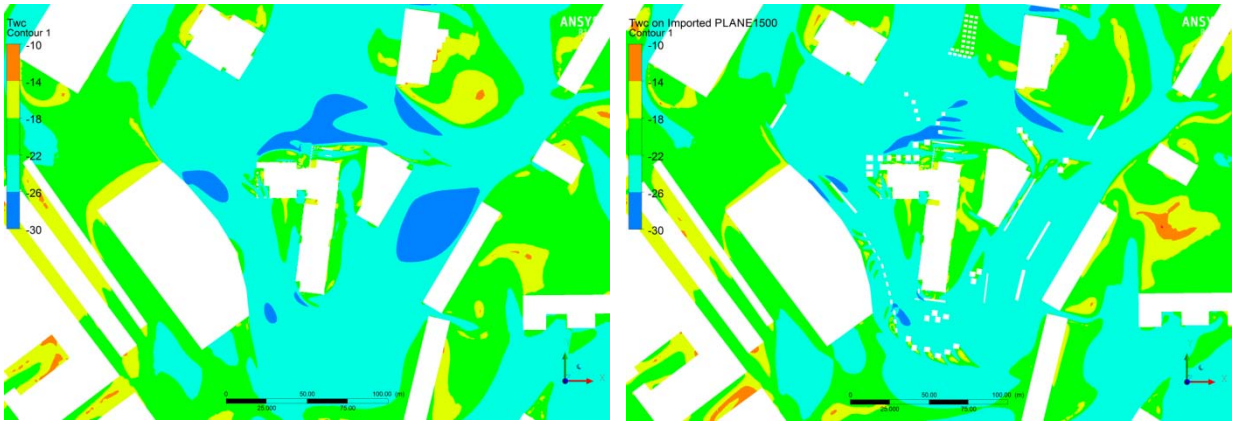

Figure 17. Comparison of the results of numerical modeling of the buildings aerodynamics taking into account wind chill effect in the winter season at a temperature of -20 °C, wind angle of attack 240° (on the left - without bushes, on the right - with bushes).

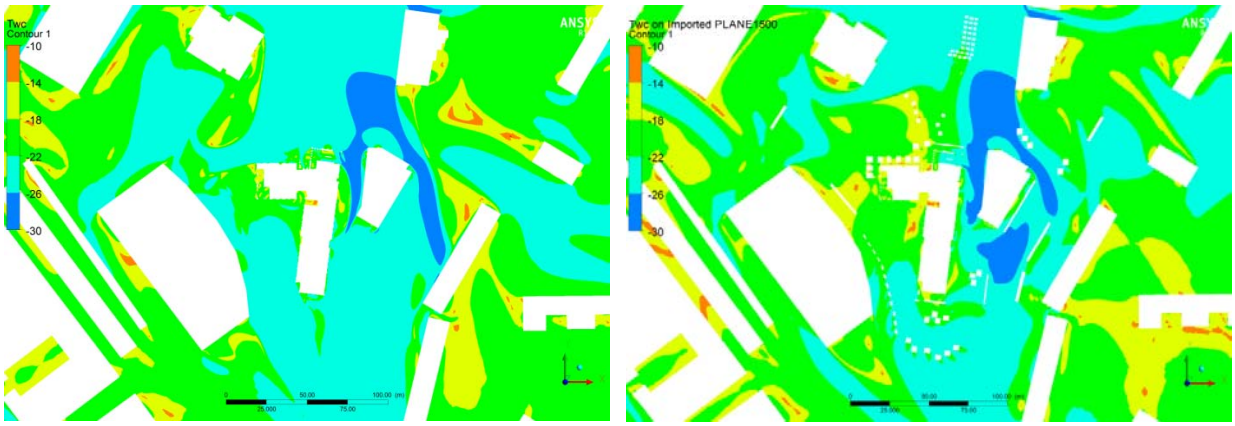

Figure 18. Comparison of the results of numerical modeling of the buildings aerodynamics taking into account wind chill effect in the winter season at a temperature of -20 °C, wind angle of attack 300° (on the left - without bushes, on the right - with bushes).

The results of numerical modeling of the buildings aerodynamics taking into account wind chill allow us to conclude that the human body feels the temperature 1.5 times lower than the actual temperature that equal to – 20 C. Calculations have shown that the temperature reaches the mark - 30 ° C. This gives a tangible contribution to a comfortable stay of people in these areas. The correct location of green spaces in pedestrian areas has contributed to the narrowing of areas where the minimum (minus) temperatures occur.

5. CONCLUSION

The presented results showed a wide applicability of the pedestrian comfort assessment methodology and the possibility of its adjustment by planting green spaces. The solved model problem allowed to findthe right parameters of the tree model. Comparison of the results for different numbers of windangles of attack showed that 12 angles are sufficient for obtaining the required accuracy.Further development of this methodology may include a more detailed analysis of wind flows (especially maximum velocity amplification) for each individual angle of

attack, namely using the results of non-steadysimulationsobtained using more accurate (and also resource-demanding) turbulence models such as DES and LES.The results showed the practical importance of conducting suchkind of research, and therefore there is a need to include amethodology for pedestrian comfort assessment in Russian building codes.

REFERENCES

1. **Valger S.A.** Sozdaniye vychislitel'noy tekhnologii dlya rascheta vetrovykh nagruzok i udarno-volnovykh vozdeystviy na konstruktsii: Diss. na soiskaniye uchenoy stepeni k.f.-m.n. [Creating a computational technology for calculating wind loads and shock-wave effects on structures: thesis for the degree of Ph.D.]. Novosibirsk, NGASU, 2015, 240 pages (in Russian).
2. **Jackson P.S.** The evaluation of windy environments. // *Building and environment*, 1978, vol. 13, pp. 251-260.
3. **Murakami S.** Wind tunnelmodeling applied to pedestrian comfort. In: Reinhold, 1982, pp. 486-503.
4. **Murakami S., Uehara K., Deguchi K.** Wind effects on pedestrians: New criteria based on outdoor observation of over 2000 persons. In: (Germak, 1980), pp. 277-288.
5. **Simiu E., Scanlan R.** Wind Effects on Structures. New-York, Wiley, 1996.
6. **Belostotskiy A.M., Akimov P.A., Afanasyeva I.N.** Vychislitel'naya aerodinamika v zadachakh stroitel'stva. Uchebnoye posobiye [Computational aerodynamics in construction problems]. Moscow, ASV, 2017, 720 pages (in Russian).
7. SP 20.13330.2016 Nagruzki i vozdeystviya [Loads and Impacts]. Moscow, Minregion Rossii, 2016 (in Russian).
8. MDS 20-1.2006. Vremennyye normy po naznacheniyu nagruzok i vozdeystviy, deystvuyushchikh na mnogofunktsional'nyye vysotnyye zdaniya i kompleksy v Moskve [Temporary standards for the appointment of loads and impacts acting on multifunctional high-rise buildings and complexes in Moscow] (in Russian). Moscow, 2006.
9. **Dubinskiy S.I.** Chislennoye modelirovaniye vetrovykh vozdeystviy na vysotnyye zdaniya: Diss. na soiskaniye uchenoy stepeni k.t.n. [Numerical modeling of wind effects on high-rise buildings: thesis for the degree of Ph.D.]. Moscow, MGSU, 2010, 198 pages (in Russian).
10. **Borisenko M.M.** Vertikal'nyye profili vetra i temperatury v nizhnikh sloyakh atmosfery [Vertical profiles of wind and temperature in the lower atmosphere]. // *Trudy GGO*, 1974, Vol. 320 (in Russian).
11. **Nikolayev V.G., Ganaga S.V., Kudryashov Yu.I**. Natsional'nyy Kadastr vetroenergeticheskikh resursov Rossii i metodicheskiye osnovy ikh opredeleniya [The National Cadastre of Wind Energy Resources of Russia and the Methodological Basis of Their Definition]. Moscow, Atmograf, 2008 (in Russian).
12. **Starkov A.N., Bezrukikh P.P., Landberg L., Borisenko M.M.** Atlas vetrov Rossii [Atlas of the winds of Russia]. Mozhaysk-Terra, 2000(in Russian).
13. FCM-R19-2003 Report on Wind Chill Temperature and Extreme Heat Indices: Evaluation and Improvement Projects. U.S. DEPARTEMENT OF COMMERCE, National Oceanic and Atmospheric Administration, 2003, 75 pages.
14. **Doroshenko A.V.** Metodika chislennogo modelirovaniya skorostey vetra i peshekhodnoy komfortnosti v zonakh zhiloy zastroyki: Diss. na soiskaniye uchenoy stepeni k.t.n. [Methods of numerical modeling of wind speeds and pedestrian comfort in residential areas: thesis for the degree of Ph.D.]. Moscow, MGSU, 2013, 169 pages (in Russian).
15. ANSYS CFX-Solver 17.0 Theory Guide. Canonsburg, 2016.
16. ANSYS CFX-Pre 17.0 User's Guide. Canonsburg, 2016.

17. **Tominaga, Y., Mochida, A. et al.**AIJ guidelines for practical applications of CFD to pedestrian wind environment around buildings. // *Journal of Wind Engineering and Industrial Aerodynamics*, 2008, Volume 96, Issues 10-11, pp. 1749-1761.
18. ANSYS Mechanical 17.0 Tutorials. Canonsburg, 2016.
19. SNiP 2.01.07-85*. Nagruzki i vozdeystviya. Gosstroy Rossii vozdeystviya [Loads and Impacts]. Moscow, GUP TSPP, 2001, 44 pages (in Russian).
20. Eurocode 1: Basis design and action on structures. Part 2–4: Wind action. ENV 1991-2-4, CEN, 1994.

СПИСОК ЛИТЕРАТУРЫ

1. **Вальгер С.А.** Создание вычислительной технологии для расчета ветровых нагрузок и ударно-волновых воздействий на конструкции. Диссертация на соискание ученой степени кандидата физико-математических наук по специальности 05.13.18 – «Математическое моделирование, численные методы и комплексы программ». – Новосибирск, НГАСУ, 2015. – 240 с.
2. **Jackson, P.S.** The evaluation of windy environments. // *Building and environment*, 1978, vol. 13, pp. 251-260.
3. **Murakami S.** Wind tunnel modeling applied to pedestrian comfort. In: Reinhold, 1982, pp. 486-503.
4. **Murakami S., Uehara K., Deguchi K.** Wind effects on pedestrians: New criteria based on outdoor observation of over 2000 persons. In: (Germak, 1980), pp. 277-288.
5. **Simiu E., Scanlan R.** Wind Effects on Structures. New-York: Wiley, 1996.
6. **Белостоцкий А.М., Акимов П.А., Афанасьева И.Н.** Вычислительная аэродинамика в задачах строительства. – М.: АСВ, 2017. – 720 с.
7. СП 20.13330.2016 Нагрузки и воздействия. – М.: Минрегион России, 2016.
8. МДС 20-1.2006. Временные нормы по назначению нагрузок и воздействий, действующих на многофункциональные высотные здания и комплексы в Москве. – М., 2006.
9. **Дубинский С.И.** Численное моделирование ветровых воздействий на высотные здания. Диссертация на соискание ученой степени кандидата технических наук по специальности 05.13.18 – «Математическое моделирование, численные методы и комплексы программ» – М.: МГСУ, 2010. – 198 с.
10. **Борисенко М.М.** Вертикальные профили ветра и температуры в нижних слоях атмосферы. // *Труды ГГО*, Вып. 320, 1974.
11. **Николаев В.Г., Ганага С.В., Кудряшов Ю.И.** Национальный Кадастр ветроэнергетических ресурсов России и методические основы их определения. – М.: Атмограф, 2008.
12. **Старков А. Н., Безруких П. П., Ландберг Л., Борисенко М. М.** Атлас ветров России. – Можайск: Можайск-Терра, 2000.
13. FCM-R19-2003 Report on Wind Chill Temperature and Extreme Heat Indices: Evaluation and Improvement Projects. U.S. DEPARTEMENT OF COMMERCE, National Oceanic and Atmospheric Administration, 2003, 75 pages.
14. **Дорошенко А.В.** Методика численного моделирования скоростей ветра и пешеходной комфортности в зонах жилой застройки: Диссертация на соискание ученой степени кандидата технических наук по специальности 05.13.18 – «Математическое моделирование, численные методы и комплексы программ». – М., МГСУ, 2013. – 169 с.
15. ANSYS CFX-Solver 17.0 Theory Guide. Canonsburg, 2016.
16. ANSYS CFX-Pre 17.0 User's Guide. Canonsburg, 2016.
17. **Tominaga, Y., Mochida, A. et al.** AIJ guidelines for practical applications of CFD

to pedestrian wind environment around buildings. // *Journal of Wind Engineering and Industrial Aerodynamics*, 2008, Volume 96, Issues 10-11, pp. 1749-1761.
18. ANSYS Mechanical 17.0 Tutorials. Canonsburg, 2016.
19. СНиП 2.01.07-85*. Нагрузки и воздействия. Госстрой России. – М.: ГУП ЦПП, 2001. – 44 с.
20. Eurocode 1: Basis design and action on structures. Part 2–4: Wind action. ENV 1991-2-4, CEN, 1994.

Alexander M. Belostotsky, Corresponding Member of the Russian Academyof Architecture and Construction Sciences, Professor, Dr.Sc.; Director of Scientific Research Center «StaDyO»; Professor of Department of Structures, Buildings and Facilities, Russian University of Transport» (RUT –MIIT); Professor of Department of Architecture and Construction, Peoples' Friendship University; Professor of Department of Building Structures and Computational Mechanics, Peoples' Friendship University of Russia; office 810, 18, 3ya Ulitsa Yamskogo Polya, Moscow, 125040, Russia; phone +7 (499) 706-88-10;
E-mail: amb@stadyo.ru.

Irina N. Afanasyeva, Ph.D., Senior Engineer of Scientific Research Center «StaDyO»; Master's Degree Student, University of Florida (USA); office 810, 18, 3ya Ulitsa Yamskogo Polya, Moscow, 125040, Russia;
phone +7 (499) 706-88-10,
E-mail: irina.n.afanasyeva@gmail.com.

Irina Yu. Lantsova, Lecturer at the Department of Applied Mathematics, National Research Moscow State University of Civil Engineering; 26, Yaroslavskoe Shosse, Moscow, 129337, Russia; phone: +7 (499) 183-59-94;
E-mail: LantsovaIYu@mgsu.ru.

Белостоцкий Александр Михайлович, член-корреспондент РААСН, профессор, доктор технических наук; генеральный директор ЗАО «Научно-исследовательский центр СтаДиО»; профессор кафедры «Строительные конструкции, здания и сооружения» Российского университета транспорта (МИИТ); профессор Департамента архитектуры и строительства Российского университета дружбы народов; профессор кафедры строительных конструкций и вычислительной механики Пермского национального исследовательского политехнического университета; 125040, Россия, Москва, ул. 3-я Ямского Поля, д.18, офис 810; тел. +7 (499) 706-88-10;
E-mail: amb@stadyo.ru.

Афанасьева Ирина Николаевна, кандидат технических наук, ведущий инженер-расчетчик ЗАО «Научно-исследовательский центр СтаДиО» (ЗАО НИЦ «СтаДиО»); магистрант Университета Флориды (США); 125040, Россия, г. Москва, ул. 3-я Ямского Поля, д.18, 8 этаж, офис 810, тел. +7 (495) 706-88-10,
E-mail: irina.n.afanasyeva@gmail.com.

Ланцова Ирина Юрьевна, преподаватель, аспирант кафедры прикладной математики Национального исследовательского Московского строительного университета, 129337, Россия, г. Москва, Ярославское шоссе, д. 26; тел. +7 (499) 183-59-94;
E-mail: LantsovaIYu@mgsu.ru.

DOI:10.22337/2587-9618-2019-15-2-40-50

INTEGRATED MODELING AND FORECASTING OF THE STABILITY AND STRENGTH OF THE CONSTRUCTION OF THE MOTOR ROAD USING MODERN TECHNOLOGIES

Tatiana L. Dmitrieva, Andrey B. Chernyago
Irkutsk National Research Technical University, Irkutsk, RUSSIA

Abstract: The distinctive paper discusses the possibility of obtaining methods of the highest quality and correct calculations for assessing the transport and operational status of a particular road using corresponding mathematical model.

Keywords: mathematical modeling, highways, CAD, modern technologies for the diagnosis of highways

КОМПЛЕКСНОЕ МОДЕЛИРОВАНИЕ И ПРОГНОЗИРОВАНИЕ УСТОЙЧИВОСТИ И ПРОЧНОСТИ КОНСТРУКЦИИ АВТОМОБИЛЬНОЙ ДОРОГИ С ИСПОЛЬЗОВАНИЕМ СОВРЕМЕННЫХ ТЕХНОЛОГИЙ

Т.Л. Дмитриева, А.Б. Черняго
Иркутский национальный исследовательский технический университет, г. Иркутск, РОССИЯ

Аннотация: В статье рассматривается возможность получения методики наиболее качественных и корректных расчётов, для оценки транспортно-эксплуатационного состояния участка автомобильной дороги с помощью математической модели.

Ключевые слова: математическое моделирование, автомобильные дороги, САПР, современные технологии диагностики автомобильных дорог

INTRODUCTION

The road is a set of structural elements intended for movement with established speeds, loads and dimensions of cars and other land vehicles transporting passengers and (or) cargo, as well as land plots provided for their placement [1].
In order to determine as accurately as possible the stability of the road bed and the strength of the pavement, a complex of calculations is necessary, the outcome of which determines the characteristics and design parameters affecting all the structural elements of the road. The reliability parameters of the pavement determine the security of its working condition during the established service life, which is the basis for determining the period between repairs.

In Russia, the period between repairs was developed by the «Soyuzdornii» in the period 1950-1955. and approved by the Resolution of the Council of Ministers of the RSFSR 7.03.61 No. 210 as standards for capital and medium repair, respectively, of road pavements and coatings. These standards were valid until 1988, regardless of the estimated service life taken in the design of road pavements (Instructions DBC 46-60, DBC 46-72, DBC 46-83). According to these standards, the estimated service lives were approximately 20% less, which could be one of the reasons for poor quality repairs of roads. In 1988, regional and sectoral norms for the period between repairs of non-rigid pavements and coatings, developed by «Giprodornii» with the

participation of research, design and other organizations, were put into effect [2].
Capital and lightweight pavement with an improved coating is designed so that over the period between repairs there are no damage and inadmissible, in terms of the violations of the requirements for flatness of coverage, residual deformations provided by the existing regulatory documents, and that the impact of natural factors does not lead to unacceptable changes in its elements [3].
In all cases, solutions of the theory of elasticity are used to estimate the stress state of a structure [3].
The assessment of the overall stability of the roadbed and slopes is to compare the calculated values of the indicators of sustainability with their normative values. For the standard indicator of overall sustainability should be taken as a generalized sustainability factor, determined taking into account the following factors, taking into account [11]:

- reliability of data on the strength and deformative characteristics of the soils of the considered array;
- road category;
- degree of responsibility of the projected object;
- compliance of the design scheme with natural engineering and geological conditions;
- type of soil and its purpose;
- features of the calculation method.

The roadbed is subject to dynamic and static loads from the rolling stock; own weight of the canvas and the complex of natural factors (climatic, hydrological, hydrogeological).

1. EXPERIMENTAL PART

The purpose of the study is to determine the transport and operational (taking into account the climatic characteristics) and the strength parameters of the road to create a mathematical model that reflects the current state of the structure.
The task of the study is to build a mathematical model for the construction of a highway, its automation, for the operational determination of the transport performance indicators of this road and period between repairs.
The research technique is a complex of models, including calculations of dynamic and static loads from rolling stock, soil mechanics and a complex of natural factors.
The object of study: public road.
The subject of study: transport and operational, strength and climatic parameters of the road.
The graphical user interface of the control program of such a mathematical model will include two working windows: Input and Output.
In the input window (Figure 1) it is required to enter the road data, most of which are determined at the design stage. These data include the prospective traffic intensity, which sets the five-year and ten-year forecasts.

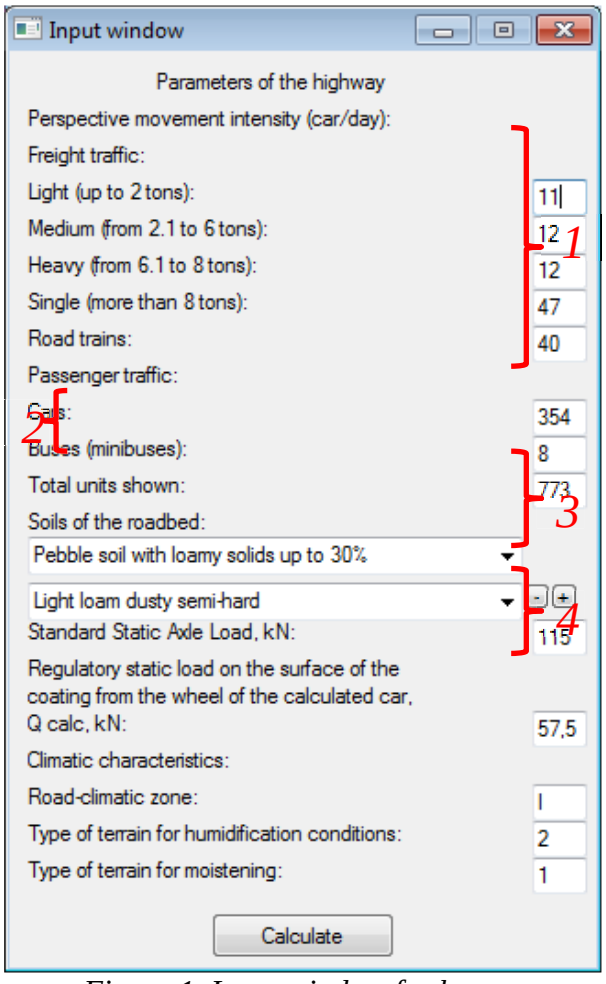

Figure 1. Input window for known road parameters.

Figure 1 presents:

1. Average annual daily perspective traffic intensity, reduced to a passenger car.
The methods used to account for the intensity of traffic flow on roads are intended to obtain and accumulate information on the total number of vehicles and the composition of traffic flow, passing per unit time through the cross section of the road in each of the permitted directions of movement.
Accounting for the intensity of movement is carried out in two ways: automatically or visually. According to the duration, the accounting for the intensity of movement is divided into long-term and short-term [4].
2. Subgrade soil**.** The most commonly used local soils occurring in the upper layers of the earth's surface. In laboratory conditions, check the suitability of certain soils for use in the device of the roadbed.
The soils by nature of structural bonds are divided into the following classes: rock, dispersed and frozen.
The class of rocky soils includes soils with rigid structural bonds (crystallization and cementation) [5]. Such soils are preferred for the construction of roads (provide maximum strength and stability).
The class of dispersed soils are soils with physical, physicochemical, or mechanical structural bonds.
Soils with mechanical structural bonds are distinguished into a subclass of loose (loose) soils, and soils with physical and physico-chemical structural bonds into a subclass of cohesive soils. For road construction, weak soils are distinguished from a cohesive subclass of soils — soils with low mechanical properties: shear strength under natural conditions is less than 0.075 MPa (rotary cut) and / or the slump modulus is more than 50 mm / m with a load of 0.25 MPa (deformation modulus below 5.0 MPa) [5].
The class of frozen soils includes soils that possess, along with structural bonds of non-frozen soils, cryogenic bonds (due to ice).

3. Regulatory loads. The regulatory load from motor vehicles on public roads is shown in Figure 2.
In Figure 2 depicted:
d – base for AK load, m;
c – is the load gauge width, m;
q – uniformly distributed load along the track along the road (structure), kN / m;
D – the base for the load NK, m
The regulatory AK load (Figure 2a) includes one biaxial bogie with an axle load of 10 K (kN) and evenly distributed along the road.
Regulatory load NK (Figure 2b) is presented in the form of a single four-axle truck with a load on each axis of 18 K (kN) [6].
Calculated loading schemes are divided into:

- loading schemes when calculating pavements;
- loading schemes for the calculation of the subgrade;
- loading schemes for the calculation of the structures of bridge structures.

When calculating the stability of the embankment slopes (1), the load from the vehicles is reduced to the equivalent soil layer of the subgrade. The thickness of the equivalent layer of soil Ne, m, is calculated by the formula:

$$N_e = \frac{18K}{(d+0{,}2)(c+0{,}8)\gamma_{zp}} \tag{1}$$

where 18K is the regulatory burden of NC, kN;
d – base of normative load of NC, m;
c – gauge of the standard load of NC, m;
γ_S – specific gravity of the soil, kN / m^3.
When calculating embankment settlement (2), the regulatory load is assumed to be in the form of a standard load that is in a static position (Figure 2a). A uniformly distributed load along the road, imitating the movement of a column of vehicles, is not taken into account in this calculation [6].
The load from vehicles is reduced to an equivalent layer of subgrade soil. The thickness of the equivalent layer of soil he, m, is calculated by the formula:

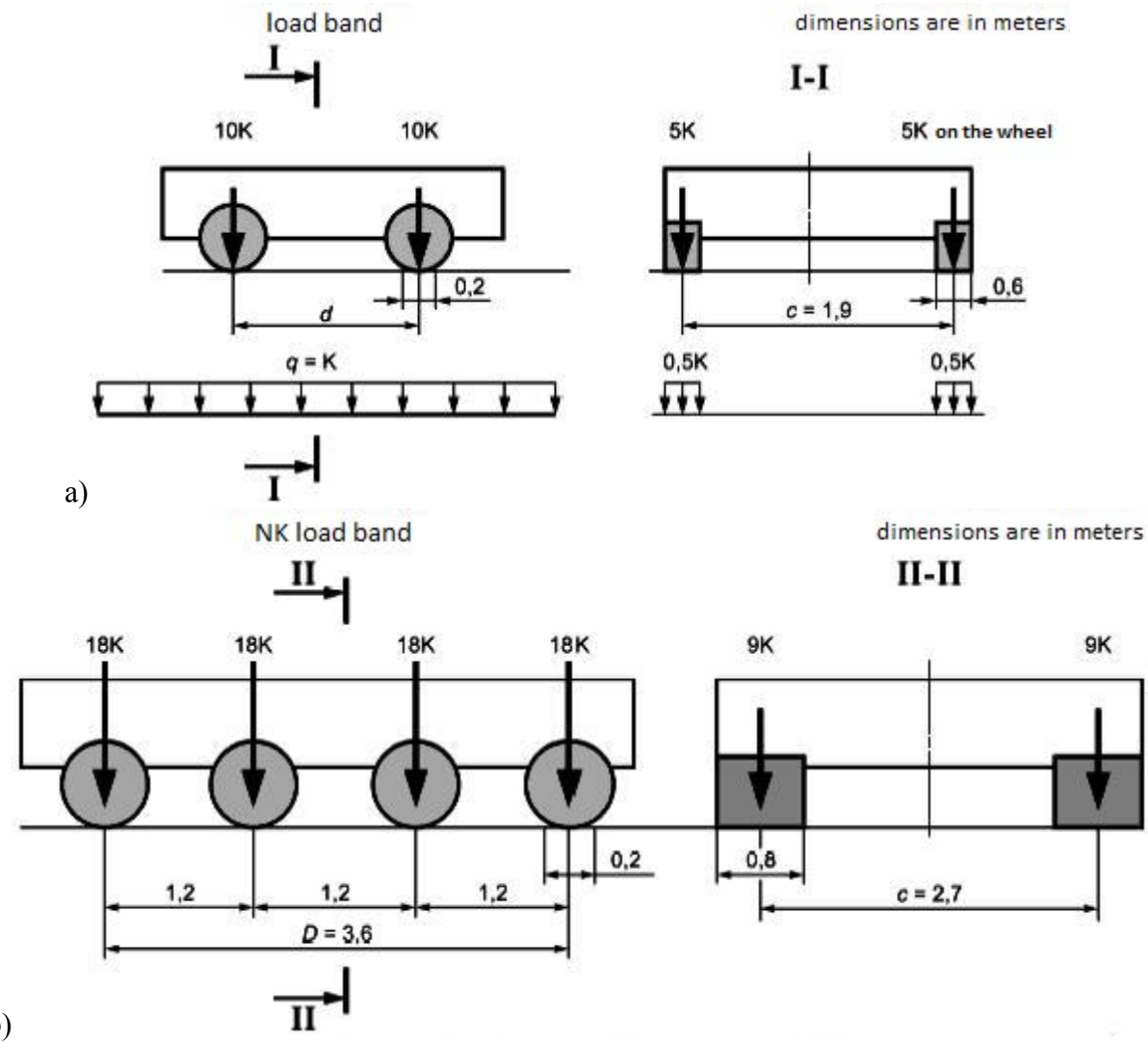

Figure 2. Scheme of the regulatory load for the calculation of pavement, roadbed, retaining walls and bridge structures: a) car wheel load AK; b) heavy single car load NK.

$$h_e = \frac{n}{B_{rb}\gamma_s}\left(\frac{10K}{d+0{,}2}\right) \quad (2)$$

where n is the number of lanes;
B_{rb} – width of the road bed, m;
γ_s – specific gravity of the soil, kN / m3;
10K – AK regulatory load for the calculation of embankment sediments, kN;
d – base of regulatory load AK, m.

4. Climatic, hydrological, hydrogeological conditions of the area.

The terrain, climatic, hydrological and hydrogeological conditions have a significant impact on the construction and operation of roads. These conditions directly affect the main types of deformations of the road structure, the main cause of which is the increase and over moistening of the subgrade soil, i.e. violation of its water-thermal regime (over-wetting of the embankment soils can cause a process of "heaving" (lifting) of the soil, erosion and scouring of the base or the embankments themselves).

The climatic characteristics of the road are determined based on the climatic conditions of the area in which the work will be performed. Our country, as well as the post-Soviet space, is

subdivided in road construction into road-climatic zones (RCZ) [1]. Most of the parameters (in particular, temperature indicators, calculation of the timing of the thaw) are known or can be determined from building climatology (SP 131.13330.2012).

The saturation of the subgrade with moisture is an extremely dangerous phenomenon, in which the strength of the pavement, the stability of the subgrade and the base of the embankments significantly decrease [7].

Sources of moistening of the roadbed are:

- precipitations;
- water inflow from melting snow;
- capillary rise from the groundwater level;
- condensation of water vapor from the air;
- movement of film water.

All of the above parameters maximally affect the quality of both the transport and operational indicators of the road and the road itself as a whole. For a more accurate determination of all key parameters of a highway, it is necessary to track their interdependence as much as possible and to obtain an objective assessment of their condition at the level of accuracy that is now offered by modern diagnostic and examination technologies. This approach will eliminate the development of the situation that exists today, when a lot of calculations are made to assess the transport and operational state, which do not allow to evaluate the current state of the structure, but only in general reflect its suitability for further operation. Considered promising is building, for example, RIM (Road Information Modeling) model [12], which would reflect not only the state of operation, but also the early stages of the road life cycle, which would allow it to be built as quickly and correctly as possible. without departing from the standards, automated to adjust projects and track the entire financial side. Therefore, the construction of a mathematical model that could take into account almost all (affecting the performance) parameters of the road, will be very relevant to the idea of what will happen at the next stage of the life cycle of this design. Based on this model, we can assess the current state and take steps in advance to eliminate construction defects and extend the life of the road.

Such a model (Figure 3) will not only display the existing (actual) situation, but also recommend ways to eliminate various defects that prevent further road operation. This will allow taking measures (according to the current regulatory documents and methodological recommendations), based on the current situation. Further, this model is rebuilt taking into account the already applied recommendations for continuing to conduct assessment of the state of this object.

Figure 3 presents:

1. The entered parameters of the road, which directly affect the construction of a complex of mathematical models of the road. To maximize the assessment of the transport and operational condition of the road, many more other parameters are required, including the geometrical parameters (in Figure 3, are not presented, but conditionally available), affecting:

- width of the carriageway, the main fortified surface of the road and fortifications;
- width of roadsides, incl. fortified; the type and condition of the curb reinforcement;
- longitudinal slopes;
- transverse slopes of the roadway and shoulders;
- the radii of the curves in the plan and the slope of the turn;
- the height of the embankment, the depth of excavation and the slopes of their slopes; condition of the roadbed;

distance of visibility of the road surface in the plan and profile.

2. Time scale. The main function of the technique based on complex mathematical modeling will be the ability to predict the state of the road after some time it is in operational mode. By moving the timeline slider, you can monitor the transport and operational condition of the road a dozen years ahead. When 20% of the selected section of the road does not meet the regulatory requirements, it will become impossible to switch the time scale and the program will offer recommendations on how to increase the period between repairs.

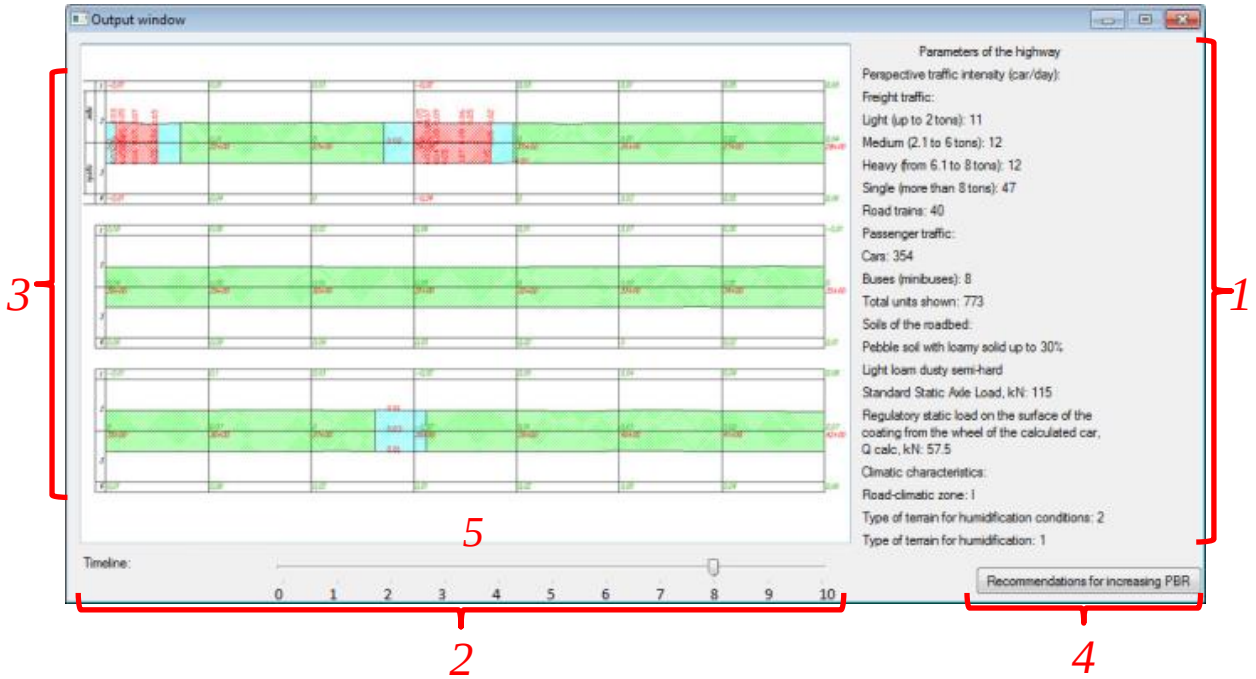

Figure 3. Window for displaying the state of the road with the display of problem areas.

For example, if the thickness of the coating layer became unsatisfactory, options would be offered (at the expense of the maintenance of the selected road section) for surface treatment, patching, and other works to restore the worn out coating layer, and if sources of wetting of the roadbed and / or road pavement, then the optimal longitudinal and transverse slopes of the roadway, the steepness the slopes of the roadbed and the longitudinal slopes of the cuvettes (control of their contamination).

2. Time scale. The main function of the technique based on complex mathematical modeling will be the ability to predict the state of the road after some time it is in operational mode. By moving the timeline slider, you can monitor the transport and operational condition of the road a dozen years ahead. When 20% of the selected section of the road does not meet the regulatory requirements, it will become impossible to switch the time scale and the program will offer recommendations on how to increase the period between repairs. For example, if the thickness of the coating layer became unsatisfactory, options would be offered (at the expense of the maintenance of the selected road section) for surface treatment, patching, and other works to restore the worn out coating layer, and if sources of wetting of the roadbed and / or road pavement, then the optimal longitudinal and transverse slopes of the roadway, the steepness the slopes of the roadbed and the longitudinal slopes of the cuvettes (control of their contamination).

3. Straightened plan of the road section**.** This plan will be the result of calculations of a complex of mathematical models, which will display (visually) all problem areas that do not meet regulatory requirements (highlighted in red). Areas that were restored by the recommendations proposed by this program are highlighted in blue. If the total volume of the restored and unsatisfactory road sections becomes more than 80%, repair will be assigned by the program (time interval, from the beginning of the calculation to its end, and will be the lifetime of the road section).

Building a plan on which geometric parameters are displayed (widths, elevations, longitudinal and transverse slopes, curve radii) is possible in such domestic CAD systems as:

- CAD CREDO;
- CAD AD Robur;
- CAD AD IndorCAD / Road.

In recent years, in connection with the rapid development of geographic information systems

(GIS), the question of their applicability, along with CAD, in computer-aided design of highways is being considered.

With significant external similarities GIS and CAD have fundamental differences.

One of the fundamental differences between GIS and CAD is that a graphic primitive in a GIS is an independent object with its own attributes, and in CAD it is only a graphic tool, i.e. part of the object, and therefore its attributes, as a rule, does not have.

In CAD, objects are usually formed from several graphic primitives, lining up in a hierarchy using grouping. The profound difference between the CAD model and the relational data model does not allow the full preservation of CAD drawings in modern databases and does not allow analyzing the attributes of objects.

In the road industry, the presence of attribute support is the most important in solving problems of diagnostics, certification, inventory, road cadastre. In connection with the scarcity of the capabilities of the attribute description of CAD, it seems most appropriate to create information systems for highways based on GIS [8].

When calculating the pavement design, the most popular (in Russia) is the module of the Topomatic Robur software complex - the Robur Topomatic - Road apparel, where the initial values, in addition to the previously mentioned design, are also such material characteristics as: Elastic moduli (MPa) - on elastic deflection, shear, stretching when bending; Volumetric weight (kg / cubic meter); Characteristics for the calculation of shear - the angle of internal friction, adhesion (MPa) (also, the same characteristics in statics); Characteristics for the calculation of tensile bending and Characteristics of geosynthetics for the reinforcement of the coating (additional parameter). In the CREDO and Indor-CAD / Road software packages, there are also software modules for the calculation of pavements that are not inferior to “Robur Topomatic - Road pant” for most of the key points.

4. Button recommendations to help increase the period between repairs of the road. According to the results of calculations for a certain period of operation, red zones will be allocated - sections of the road that do not meet regulatory requirements. After the appearance of these zones, it will be possible to get recommendations on the elimination of such problem areas.

At the moment, it is not possible to predict as accurately as possible the transport and operational indicators of the road for the years ahead due to the absence of a clear model of the behavior of all the structural elements of such a structure. Today, to assess the quality and condition of highways, inspection and diagnostics are carried out using road laboratories and other engineering equipment. Such checks produce:

- when putting the road into operation after construction in order to determine the initial actual transport and operational condition and comparison with regulatory requirements;
- periodically in the process of operation to monitor the dynamics of changes in the state of the road, to predict this change and to plan repairs and maintenance;
- when developing an action plan or a project for reconstruction, major repair or repair to determine the expected transport and operational status, compare it with regulatory requirements and evaluate the effectiveness of the planned work;
- after the execution of works on the reconstruction, overhaul and repair in the areas where these works are carried out in order to determine the actual change in the transport and operational condition of the roads.

According to the results of diagnostics and assessment of the condition of the roads during operation, they identify sections of roads that do not meet the regulatory requirements for their transport and operational condition and, guided by the "Classification of Works for the Repair and Maintenance of Public Roads", determine the types and composition of the main works and maintenance measures, repair and reconstruction in order to increase their transport and operational status to the required level [9].

In order to accurately assess the situation that occurs over a period of several years and not rely

on additional measures for the seasonal and annual survey and diagnostics, it is necessary to assess the existing situation as thoroughly and objectively as possible, highlighting all key parameters at the post-construction stage, when all executive documents and acts accompanying the commissioning of the object, as well as to conduct a large-scale survey (but only once during the period between repairs). In this case, there is a theoretical possibility to study the erected structure in order to predict its state in the future (implementation in order to predict its state).

One example of obtaining a detailed and objective assessment of the current situation is the technology of the American company Bentley Systems.

To automate the process of managing engineering data, the American company Bentley Systems has created the Bentley ProjectWise platform. After geodetic surveys, the customer uses ProjectWise to get a cloud of laser scanning points for a part of the route.

Streaming uploading did not allow downloading the entire file, which may require a significant amount of electronic memory of significant computational resources, but only the necessary points in a certain area. As you move along the information model, additional points are loaded.

A single engineering data management platform accommodates an infinite number of attribute information about a road object. The evenness of the coating, rutting, cracks, pits, the coefficient of adhesion, the modulus of elasticity of the layers of asphalt concrete and so on - all this information is collected in a convenient form in one place and is automatically updated. That is, all the project participants have a clear picture of the current state of the object, and the data can be used again and again at all stages of its life cycle [10].

5. The rest, calculated by a complex of mathematical models, parameters.

2. MAIN CONCLUSIONS

The article presents a review material, which provides a justification of the relevance of the goal of scientific research by the authors, which is to develop a unified mathematical model reflecting the full state of the linear road object, taking into account the strength and stability of its structural elements, as well as the interaction with the soil foundation.

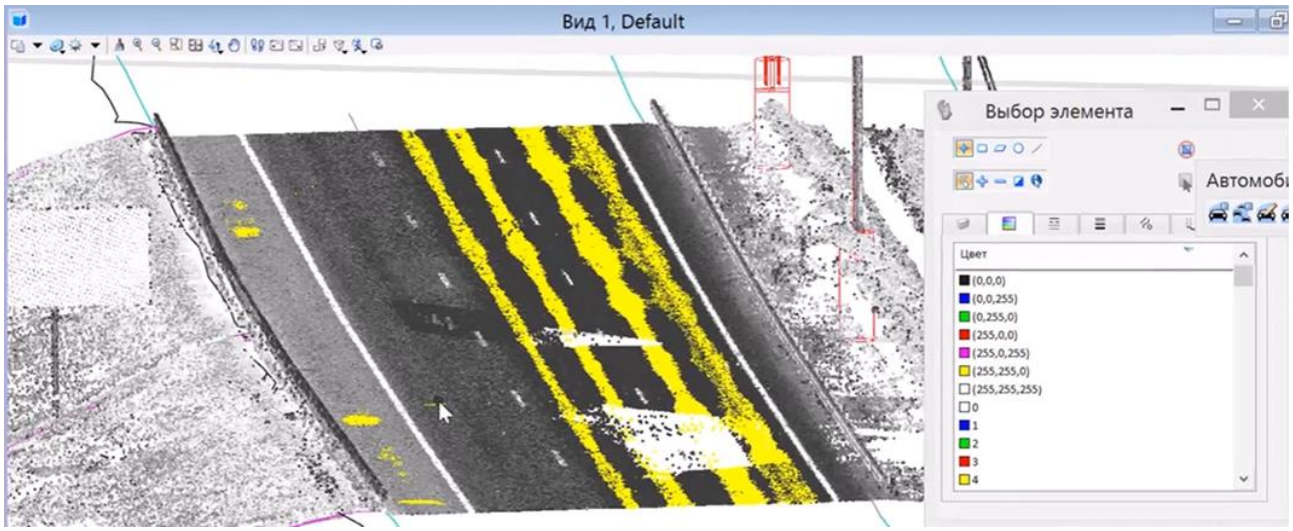

Figure 4. The result of laser scanning with subsequent analysis of the road pavement.

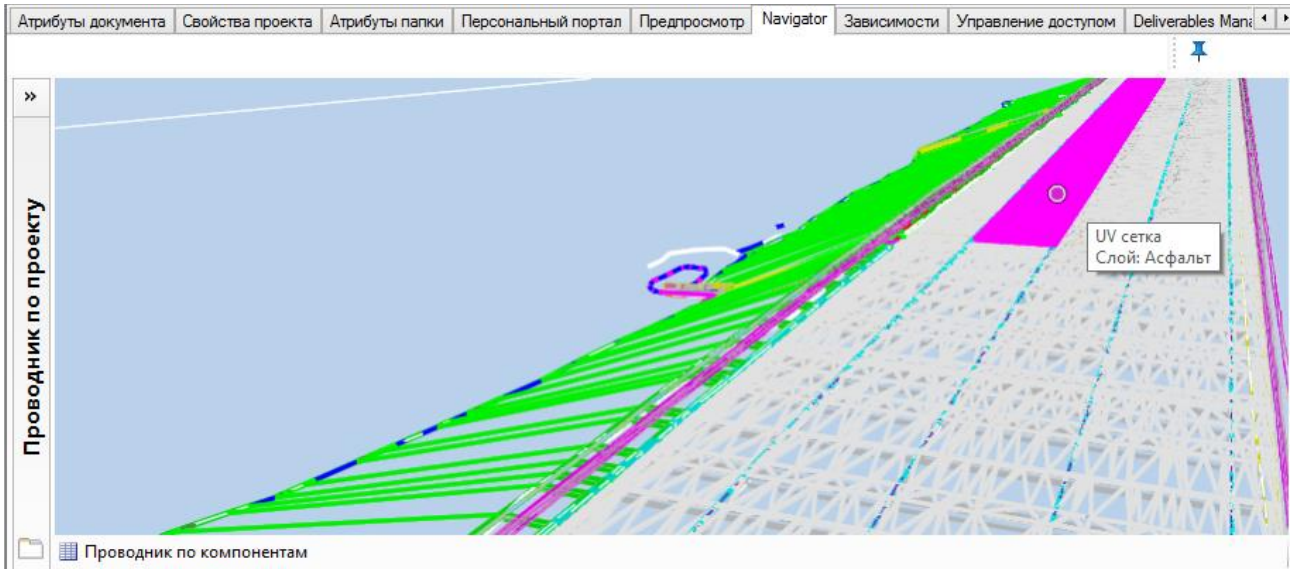

Figure 5. Drawing a digital terrain model from the resulting point cloud using Project Wise.

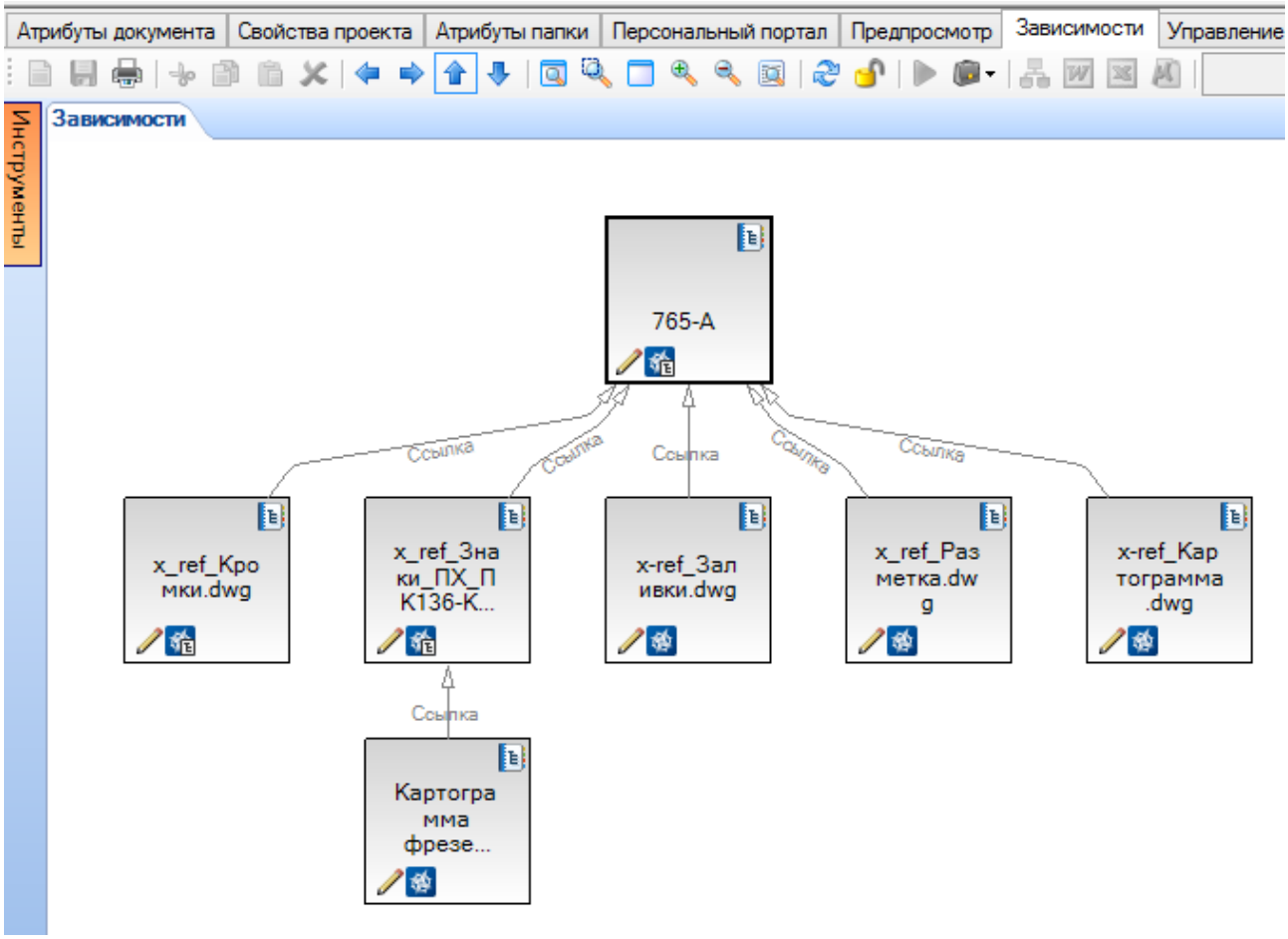

Figure 6. Working with the information model in Bentley Project Wise.

For the practical implementation of this model, it is supposed to create on its basis an automated technology that allows you to manage the preparation of production, road-building equipment (for example, C-V2X, Trimble GCS technologies), time and resources, to produce high-

quality building control, and also to do an executive survey in the framework of the project under consideration.

Thus, using the proposed model, it will be possible to assess the transport and operational status, taking into account all the characteristic causes that affect the destruction of the road. In the promising future, such models will be an integral part of the automation of a global project for the production of roads (design, construction and operation). The implementation of such model is a solvable problem at the present time; however, it requires the study and consideration of a large number of factors.

REFERENCES

1. SP 34.13330.2012 Avtomobil'nye dorogi. Aktualizirovannaya redakciya [SP 34.13330.2012 Motorways. Actual edition]. Moscow, Gosstroy Rossii, 2013 (in Russian).
2. Spravochnaya ehnciklopediya dorozhnika. Tom II. Remont i soderzhanie avtomobil'nyh dorog [Background road encyclopedia. Volume II. Repair and maintenance of roads]. Moscow: Rosavtodor, MADI (GTU), 2004 (in Russian).
3. ODN 218.046-01 Proektirovanie nezhestkih dorozhnyh odezhd [ODN 218.046-01 Design of non-rigid pavement] (in Russian). Moscow, State Service of Road Economy of Ministry of Transport of the Russian Federation, 2001.
4. GOST 32965-2014 Dorogi avtomobil'nye obshchego pol'zovaniya. Metody ucheta intensivnosti dvizheniya transportnogo potoka [GOST 32965-2014 Public roads. Methods of accounting for traffic flow]. Moscow, Standartinform, 2016 (in Russian).
5. GOST 33063-2014 Dorogi avtomobil'nye obshchego pol'zovaniya. Klassifikaciya tipov mestnosti i gruntov [GOST 33063-2014 Public roads. Classification of types of terrain and soils]. Moscow, Standartinform, 2016 (in Russian).
6. GOST R 52748—2007 Normativnye nagruzki, raschetnye skhemy nagruzheniya i gabarity priblizheniya [GOST R 52748-2007 Regulatory loads, design load schemes and approximation dimensions]. Moscow, Standartinform, 2008 (in Russian).
7. **Popov V.G.** Posobie dlya masterov i proizvoditelej rabot dorozhnyh organizacij [Handbook for craftsmen and manufacturers of road organizations]. Moscow, Center for Metrology, Testing and Certification of MADI (GTU), 2001 (in Russian).
8. **Bojkov V.N., Fedotov G.A., Purkin V.I.** Avtomatizirovannoe proektirovanie avtomobil'nyh dorog [Automated road design]. Moscow, MADI (GTU), 2005, 224 pages (in Russian).
9. ODN 218.0.006-2002 Pravila diagnostiki i ocenki sostoyaniya avtomobil'nyh dorog [ODN 218.0.006-2002 Rules for diagnostics and assessment of the condition of roads]. Moscow, Rosavtodor, 2002 (in Russian).
10. Ehffektivnoe upravlenie inzhenernymi dannymi na vsekh ehtapah zhizni dorozhnogo ob"ekta [Effective management of engineering data at all stages of the life of a road object] [Electronic resource] http://dorogniki.com/stati/izyskaniya-i-proektirovanie/effektivnoe-upravlenie-inzhenernymi-dannymi-na-vsex-etapax-zhizni-dorozhnogo-obekta/ (data obrashcheniya: 15.11.2018) (in Russian).
11. GOST 33149-2014 Dorogi avtomobil'nye obshchego pol'zovaniya. Pravila proektirovaniya avtomobil'nyh dorog v slozhnyh usloviyah [GOST 33149-2014 Public roads. Rules for the design of roads in difficult conditions]. Moscow, Standartinform, 2015 (in Russian).
12. **Skvortsov A.V.** BIM for the road industry: something new or are we already doing it? [BIM dlja dorozhnoj otrasli: chto-to novoe

ili my jetim uzhe zanimaemsja?] // *CAD and GIS roads*, 2014, No. 1(2).

СПИСОК ЛИТЕРАТУРЫ

1. СП 34.13330.2012 Автомобильные дороги. Актуализированная редакция. – М.: Госстрой России, 2013.
2. Справочная энциклопедия дорожника. Том II. Ремонт и содержание автомобильных дорог. М: Росавтодор, МАДИ (ГТУ), 2004.
3. ОДН 218.046-01 Проектирование нежестких дорожных одежд. – М.: Государственная служба дорожного хозяйства Министерства транспорта Российской Федерации, 2001
4. ГОСТ 32965-2014 Дороги автомобильные общего пользования. Методы учета интенсивности движения транспортного потока. – М.: Стандартинформ, 2016.
5. ГОСТ 33063-2014 Дороги автомобильные общего пользования. Классификация типов местности и грунтов. – М.: Стандартинформ, 2016.
6. ГОСТ Р 52748-2007 Нормативные нагрузки, расчетные схемы нагружения и габариты приближения. – М.: Стандартинформ, 2008.
7. **Попов В.Г.** Пособие для мастеров и производителей работ дорожных организаций. – М: Центр метрологии, испытаний и сертификации МАДИ (ГТУ), 2001.
8. **Бойков В.Н., Федотов Г.А., Пуркин В.И.** Автоматизированное проектирование автомобильных дорог. – М.: Издательство МАДИ (ГТУ), 2005. – 224 с.
9. ОДН 218.0.006-2002 Правила диагностики и оценки состояния автомобильных дорог. – М.: Росавтодор, 2002.
10. Эффективное управление инженерными данными на всех этапах жизни дорожного объекта [Электронный ресурс] http://dorogniki.com/stati/izyskaniya-i-proektirovanie/effektivnoe-upravlenie-inzhenernymi-dannymi-na-vsex-etapax-zhizni-dorozhnogo-obekta/ (дата обращения: 15.11.18).
11. ГОСТ 33149-2014 Дороги автомобильные общего пользования. Правила проектирования автомобильных дорог в сложных условиях. – М.: Стандартинформ, 2015.
12. **Скворцов А.В.** BIM для дорожной отрасли: что-то новое или мы этим уже занимаемся? // *САПР и ГИС автомобильных дорог*, 2014, №1(2).

Tatiana L. Dmitrieva, Doctor Science of Engineering, Professor, Department of Theoretical Mechanics and Strength of Materials, Irkutsk National Research Technical University, Lermontov street, 83, Irkutsk, 664074, Russia; phone/fax: + 7(914)913612;
E-mail: dmitrievat@list.ru.

Andrey B. Chernyago, Post-Graduate Student, Department of Automated Systems, Irkutsk National Research Technical University, Lermontov street, 83, Irkutsk, 664074, Russia; phone/fax: + 7(904)1155017;
E-mail: abs706080@gmail.com.

Дмитриева Татьяна Львовна, доктор технических наук, профессор, кафедра теоретической механики и сопротивления материалов, Иркутский национальный исследовательский технический университет; 664074, Россия, г. Иркутск, ул. Лермонтова, 83,
тел. + 7(914)9136125, e-mail: dmitrievat@list.ru.

Черняго Андрей Борисович, аспирант, кафедра автоматизированных систем, Иркутский национальный исследовательский технический университет; 664074, Россия, г. Иркутск, ул. Лермонтова, 83, тел. + 7(904)1155017,
E-mail: abs706080@gmail.com.

DOI:10.22337/2587-9618-2019-15-2-51-64

SET OF EQUATIONS OF AFEM AND PROPERTIES OF ADDITIONAL FINITE ELEMENTS

Anna V. Ermakova
South Ural State University, Chelyabinsk, RUSSIA

Abstract: The paper considers the action of additional finite elements on the main set of linear equations when developed Additional Finite Element Method (AFEM) is used for analysis of structures with several nonlinear properties at limit states and failure models. AFEM is a variant of Finite Element Method (FEM), which adds to traditional sequence of solution of problem by FEM the units of two well-known methods of structural analysis: method of additional loads and method of ultimate equilibrium. AFEM suggests the additional finite elements and additional design diagrams for gradually transformation of the main set of equilibrium equations at the first step of loading to this set at the last one according to ideal failure model of structure.

Keywords: additional finite element method, limit state, ideal failure model, additional finite element, additional design diagram, equilibrium equation

СИСТЕМА УРАВНЕНИЙ МЕТОДА ДОПОЛНИТЕЛЬНЫХ КОНЕЧНЫХ ЭЛЕМЕНТОВ И СВОЙСТВА ДОПОЛНИТЕЛЬНЫХ КОНЕЧНЫХ ЭЛЕМЕНТОВ

А.В. Ермакова
Южно-Уральский государственный университет, г. Челябинск, РОССИЯ

Аннотация: Статья рассматривает воздействие дополнительных конечных элементов на основную систему линейных уравнений, когда разрабатываемый метод дополнительных конечных элементов (МДКЭ) используется для расчета конструкций с несколькими нелинейными свойствами по предельным состояниям и моделям разрушения. МДКЭ является вариантом метода конечных элементов (МКЭ), который добавляет к традиционной последовательности решения задачи операции двух широко известных методов расчета конструкций: метода дополнительных нагрузок и метода предельного равновесия. МДКЭ предлагает дополнительные конечные элементы и дополнительные расчетные схемы для постепенного преобразования основной системы уравнений равновесия на первом шаге нагружения в систему на последнем шаге в соответствии с идеальной моделью разрушения конструкции.

Ключевые слова: метод дополнительных конечных элементов, предельное состояние, идеальная модель разрушения, дополнительный конечный элемент, дополнительная расчетная схема, уравнение равновесия

INTRODUCTION

Realization of nonlinear analysis according to method of ultimate equilibrium [1] is impossible without taking account of all physical nonlinear properties exhibited by the structure up to the moment when the ultimate limit state (state of ultimate equilibrium) is reached. The developed Additional Finite Element Method (AFEM) [2, 3, 4] is destined for solving of this problem.

1. GENERAL INFORMATION OF AFEM

Additional finite element method (AFEM) is a variant of finite element method (FEM) destined for nonlinear analysis of plane and space structures at limit state.

This method adds to traditional sequence of solving problem by means of FEM the elements of the method of ultimate equilibrium (limit states) and the method of elastic solutions (method of additional loads).

2. SET OF EQUATIONS OF FEM AND MAIN PROBLEM

The main operation of FEM [5] is the solving of the set of algebraic equation:

$$KV = P \tag{1}$$

where V = matrix of unknown node displacements; P = matrix of external load; K = stiffness matrix of considered structure is formed from coefficients of stiffness matrices of the separate finite elements (FE).
The set of equations (1) solves one time in linear analysis because of matrix $K = const$.
In nonlinear analysis the set of equation (1) looks like this:

$$K_{nonl}V = P \tag{2}$$

where K_{nonl} = stiffness matrix of structure with nonlinear properties which is changed in accordance with the degree of influence of these properties.
In this case the set of equations (2) must be solved by iterative process. In this process matrix K ($K \neq const.$) turns into matrix K_{nonl} gradually.
The transformation of the set of equation (1) into set of equation (2) is connected with difficulties in presence of several of physical nonlinear properties due to its different causes and effects.
Usually the structure has n types of nonlinear properties at the end of its operating period before collapse.
Due to different defects the matrix K_{nonl} gradually decreases from K to K_{min}, where K_{min} = its minimal value:

$$K>K_1>K_2>K>\ldots>K_i>\ldots>K_{n-1}>K_n=K_{min} \tag{3}$$

where K_i = stiffness matrix of structure with i nonlinear properties (i changes from 1 to n).
Each nonlinear property appears under corresponding value of increasing load P. Before collapse the external load P reaches its maximal value P_{max}:

$$P_0<P_1<P_2<P_3<\ldots< P_i<\ldots<P_{n-1}< P_n<P_{max} \tag{4}$$

where P_1, P_2, P_3, P_i, P_{i+1} = values of external load P, when the first, the second, the third, the i-th and the (i+1)-th nonlinear properties appear respectively. Thus the structure reveals i-th nonlinear property under external load $P_i < P < P_{i+1}$.
Therefore the set of equations (2) ought to be created under the conditions (3) and (4) and the must change its form depend on number of nonlinear properties at considered stage and value of load P.
So, the set of equations (2) has view (1) in linear behavior under $P_0 < P < P_1$ and $i = 0$. Then in the beginning and continuing of nonlinear behavior the set of equations changes gradually:
under $P_1 < P < P_2$ and one nonlinear property ($i = 1$):

$$K_1V = P \tag{5}$$

under $P_2 < P < P_3$ and two nonlinear properties ($i = 2$):

$$K_2V = P \tag{6}$$

under $P_3 < P < P_4$ and three nonlinear properties ($i = 3$):

$$K_3V = P \tag{7}$$

and so on
under $P_i < P < P_{i+1}$ and i nonlinear properties:

$$K_i V = P \tag{8}$$

and so on
under $P_{n-1} < P < P_n$ and (n-1) nonlinear properties ($i = n$-1):

$$K_{n-1}V = P \tag{9}$$

under $P_n < P < P_{max}$ and n nonlinear properties ($i = n$):

$$K_n V = P \tag{10}$$

The set of equation must be formed in order to turn matrix K into matrix $K_n = K_{min}$ and external load P into P_{max} due to n nonlinear properties of structures.
It must be realized according to formulas (5)–(10) under conditions (3) and (4).
Such realization is the difficult problem.

3. METHOD ADDITIONAL LOADS (METHOD OF ELASTIC DECISIONS)

This method was suggested for solving of deformation problems of plastic theory by A.A. Ilyushin [6].
This method uses for analysis of structures at plastic behavior when the main of equations has form (2).
Matrix K_{nonl} is stiffness matrix of structure with plastic property which is changed in accordance with the level of influence of this property. The next step is based on separation from this matrix of its linear and nonlinear parts [7]:

$$K_{nonl} = K + \Delta K_{nonl} \tag{11}$$

where K and ΔK_{nonl} = the linear and nonlinear components of matrix K_{nonl} respectively.
If we substitute the formula (11) in the expression (2) we may get the next equation:

$$(K_{nonl} + \Delta K_{nonl})V = P \tag{12}$$

The next step is removing the parentheses and the transferring the second part in right:

$$KV = P - \Delta K_{nonl}V \tag{13}$$

where ($-\Delta K_{nonl}V$) = the value of additional load in carrying out of the iterative process.
This method allows the solving the set of linear equations (2) with constant coefficients in the left hand side and the obtaining of inverse matrix K^{-1} only once.
The simplicity is main advantage of Method of Additional loads (Method of Elastic Decisions).
It is most prevalent and efficient method of nonlinear analysis of structures with plastic properties.

4. IDEAL FAILURE MODEL AND THE SET EQUATIONS OF AFEM

The criterion of collapse of the structure must be determined according to its nonlinear properties. It is necessary to know the limit of operating period of considered structure.
The Theory Ultimate Equilibrium and Ultimate Equilibrium Method (Ultimate Limit State Method) may be used for introduction of such criterion.
According to this method the structure reaches the state of ultimate equilibrium or ultimate limit state before collapse.
In this stage the external load P_{lim} is maximal. Therefore the condition (4) is fulfilled:

$$P_{lim} = P_{max} \tag{14}$$

At ultimate limit state the stiffness matrix of the structure K_{lim} is minimal because all nonlinear properties are manifested.
Thus the condition (3) is fulfilled too:

$$K_{lim} = K_n = K_{min} \tag{15}$$

The definition of this stiffness matrix K_{lim} and its intervening values K_1, K_2, K_3, … , K_i, … K_{n-1}, K_n is difficult problem.
For it decision the ideal failure model is suggested by author [2, 3, 4].
This model is the design diagram of the structure at the ultimate limit state or state of

ultimate equilibrium, i.e. moment previous of collapse.
At one hand the ideal failure model of structure must correspond to possible real failure model and at the other hand to main parameters of initial design diagram.
It helps to solve some problems for analysis of structures with several nonlinear properties [8, 9].
The point is that the initial design diagram must change step-by-step loading in accordance with nonlinear properties appeared as the ultimate limit state is reached.
As a result an initial design diagram transforms into an ideal failure model of the considered structure.
At ultimate limit state the set of equations (1) and (2) ought to have form:

$$K_{lim}\, V = P_{lim} \qquad (16)$$

Thus stiffness matrix K_{lim} of structures with all nonlinear properties at ultimate limit state must form on the basis of ideal failure model. Iterative process must go under condition (3).
Additional Finite Element Method determines that at the moment of limit state the next equation is correct:

$$K_{lim}=K+\Delta K_1+\Delta K_2+\ldots+\Delta K_i+\ldots+\Delta K_n \qquad (17)$$

Here each component ΔK_i is stiffness matrix of the i-th additional design diagram consisting of additional finite elements taking into account the i-th nonlinear property (i changes from 1 to n) and may be solved according to next formula:

$$\Delta K_i = K_i - K_{i-1} \qquad (18)$$

where K_i = stiffness matrix of structure with regard for the i-th nonlinear property; K_{i-1} = stiffness matrix of structure without regard for the i-th nonlinear property.
Introduction of ideal failure model allows realization of step-by-step analysis with gradual taking into account of influence of several (n) nonlinear properties due to determination of criterion of limit state of structure before collapse.
Some examples of ideal failure models of structures are given in [10, 11].
For gradual transformation of the set of equation according to (5) AFEM suggests to develop some operations of Method of Additional loads (Method of Elastic Decision) and use additional design diagrams consisting of additional finite elements (AFE-s) [12, 13].
In this case the sets of equations (5) – (10) are formed according to the formula (13) under conditions (3) and (4):
under $P_1 < P < P_2$ and one nonlinear property ($i = 1$):

$$KV = P - \Delta K_1 V \qquad (19)$$

under $P_2 < P < P_3$ and two nonlinear properties ($i = 2$):

$$KV = P - \Delta K_1 V - \Delta K_2 V \qquad (20)$$

under $P_3 < P < P_4$ and three nonlinear properties ($i = 3$):

$$KV = P - \Delta K_1 V - \Delta K_2 V - \Delta K_3 V \qquad (21)$$

and so on
under $P_i < P < P_{i+1}$ and i nonlinear properties:

$$KV=P-\Delta K_1 V-\Delta K_2 V-\Delta K_3 V-\ldots-\Delta K_i V \qquad (22)$$

and so on
under $P_{n-1} < P < P_n$ and (n-1) nonlinear properties ($i = n$-1):

$$KV=P-\Delta KV-\Delta K_2 V-\Delta K_3 V-\ldots-\Delta K_i V-\ldots -\Delta K_{n-1} V \qquad (23)$$

under $P_n < P < P_{max}$ and n nonlinear properties ($i = n$):

$$KV=P-\Delta K_1 V-\Delta K_2 V-\Delta K_3 V-\ldots-\Delta K_i V-\ldots -\Delta K_{n-1} V-\Delta K_n V \qquad (24)$$

Here ΔK_1 = stiffness matrix of the first additional design diagram consisting of additional finite elements taking into account the first nonlinear property; ΔK_2 = stiffness

matrix of the second additional design diagram consisting of additional finite elements taking into account the second nonlinear property; ΔK_3 = stiffness matrix of the third additional design diagram consisting of additional finite elements taking into account the third nonlinear property; ΔK_i = stiffness matrix of the i-th additional design diagram consisting of additional finite elements taking into account the i-th nonlinear property; ΔK_{n-1} = stiffness matrix of the $(n–1)$-th additional design diagram consisting of additional finite elements taking into account the $(n–1)$-th nonlinear property; ΔK_n = stiffness matrix of the n-th additional design diagram consisting of additional finite elements taking into account the n-th nonlinear property.

Each additional design diagram is a geometrical replica of the initial design diagram but it is destined for gradual transformation of an initial design diagram into design diagram with all n nonlinear properties.

Additional design diagram may be compared with empty space imbedded in the initial design diagram and filled negative stiffness for nonlinear analysis at ultimate limit states.

In relations (19) – (24) every value $(–\Delta K_i V)$ determines the influence of i-th nonlinear property.

For example the term $(–\Delta K_1 V)$ of the left-hand part of these equations is the additional load which with the main load P must be applied to linear structure to reach the displacements corresponding to its displacements with the first nonlinear property under the action of the only external load P.

Thus in nonlinear analysis the sets of algebraic equations (5) – (10) take the forms (19) – (24) and provide taking into account the influence of each nonlinear property.

This way is corresponded to logic of FEM and allows to using of different theoretical data [14,15,16] for nonlinear computer analysis [15, 17] according to normative requirements [18].

5. ADDITIONAL FINITE ELEMENTS AND THREE WAYS FOR CALCULATION OF ADDITIONAL LOADS

Every additional design diagram takes into account only one nonlinear property and consists of corresponding additional finite elements (AFE-s) [19].

Additional finite elements (AFE-s) are recommended for gradual transformation of the initial finite elements with linear properties into the same finite elements but with nonlinear properties which correspond to the reached stage of their limit states.

The scheme of its action of additional finite element (AFE) is

FE with nonlinear property =
= FE without nonlinear property +
+ AFE for taking into account
the nonlinear property.

It is necessary to know mathematical relationships which characterize the properties of additional finite elements for their application in nonlinear analysis of structures at limit state.

These relationships are necessary when the operations of tree numerical methods (elastic decisions (additional loads), additional stresses and additional strains) are used. Such approach is determined by requirements of realization of nonlinear design of the structure at limit state as such design lead to design of physical n-nonlinear systems.

Since the properties of additional finite elements are determined by the properties of a corresponding main finite element then the desired mathematical relationships are determined by analogous relationships of the main finite element:

1) Relationship between node reactions and displacements $\Delta R_e = f(V)$;
2) Formula for determination of stiffness matrices ΔK_e;
3) Formula for determination of node reactions ΔR_e;

4) Relationship between node reactions and stresses $\Delta R_e = f(\sigma)$;
5) Relationship between node reactions and strains $\Delta R_e = f(\Delta\varepsilon)$;
6) Formula for determination of stresses $\Delta\sigma$;
7) Formula for determination of strains $\Delta\varepsilon$;
8) Formula for determination of additional load F_e.
Last formula is necessary when additional load substitutes the action of additional finite element according to next scheme:

FE with nonlinear property =
= FE without nonlinear property +
+ result of action of additional load F_e
for taking into account the nonlinear property.

The appointment of additional finite element is the change of stress-strain state of the main finite element without allowance for nonlinear property to the level of stress-strain state which is appeared in the same finite element with allowance for this property.
Such approach opens the opportunity to use of the two ways of change of properties of the main finite element in view of appearance of the definite nonlinear property: change of its initial stress state and change of its initial strain state.
Since the additional finite element changes the properties of the main finite element then it is recommended to use two types of additional finite elements for realization of each of the two indicated ways:
1) additional finite element of the first type changes a stress state of the main finite element and it does not change its strain state;
2) additional finite element of the second type changes a strain state of the main finite element and it does not change its stress state.
It is known that stiffness matrix of any finite element connects its node forces and displacements.
Thus for the main finite element at definite stage of its behavior at particular limit state for the allowance of the i-th nonlinear property this relation looks like this:

$$K_{nonl,e,i}\, V = R_{nonl,e,i} \qquad (25)$$

where $R_{nonl,e,i}$ = node reactions in the finite element for the allowance of the i-th nonlinear property; V = node displacements; $K_{nonl,e,i}$ = stiffness matrix of finite element for the allowance of the i-th nonlinear property.
In order to further use of operations of the method of elastic decisions let us express the stiffness matrix $K_{nonl,e,i}$ of the finite element with nonlinear properties in the next form:

$$K_{nonl,e,i} = K_{nonl,e,i-1} + \Delta K_{nonl,e,i} \qquad (26)$$

where $K_{nonl,e,i-1}$ = stiffness matrix of the main FE without allowance of the i-th nonlinear property;
$\Delta K_{nonl,e,i}$ = stiffness matrix of additional finite element destined for the allowance of the degree of influence of the i-th nonlinear property on behavior of this element. So that it is determined by means of next formula:

$$\Delta K_{nonl,e,i} = K_{nonl,e,i} - K_{nonl,e,i-1} \qquad (27)$$

In general the stiffness matrix of AFE $\Delta K_{nonl,e,i}$ is not equal to 0, i.e.

$$\Delta K_{nonl,e,i} \neq 0 \qquad (28)$$

If the influence of any i-th nonlinear property on behavior of the main finite element is absent then the stiffness matrix of the corresponding AFE is:

$$\Delta K_{nonle,i} = 0 \qquad (29)$$

In taking account of the first nonlinear property the stiffness matrix of additional FE $\Delta K_{nonl,e,1}$ may be determined by the next formula:

$$\Delta K_{nonl,e,1} = K_{nonl,e,1} - K_{nonl,e,0} = K_{nonl,e,1} - K_e \qquad (30)$$

where K_e = stiffness matrix of the main FE with linear properties.

Node reactions $R_{nonl,i}$ of finite element for the allowance of the i-th nonlinear property may be expressed by reactions $R_{nonl,i-1}$ of the finite element without this i-th nonlinear property:

$$R_{nonl,i} = R_{nonl,i-1} + \Delta R_{nonl,i} \qquad (31)$$

where $\Delta R_{nonl,i}$ = change of node reactions of finite element due to manifestation of the i-th nonlinear property.

The first component of the right-hand part of this expression presents node reactions in the finite element without allowance for the i-th nonlinear property, i.e.

$$K_{nonl,e,i-1}\, V = R_{nonl,i-1} \qquad (32)$$

If we substitute (26) and (31) in (25) with allowance for (32) we obtain:

$$\Delta K_{nonl,e,i}\, V = \Delta R_{nonl,i} \qquad (33)$$

This formula determines the dependence between node reactions and node displacements in additional finite element for the allowance of the i-th nonlinear property.

Its stiffness matrix $\Delta K_{nonl,e,i}$ is determined by formula (27) and for the allowance of the first nonlinear property it is determined by formula (30).

If the influence of any nonlinear property on behavior of the main finite element is absent then the stiffness matrix of the corresponding additional finite element is equal to 0 (29).

The approach to the way of formation of additional load F_e for the allowance of the nonlinear properties for both types of AFE is the same.

Scheme of method of elastic solutions (additional loads) is given at Figure 1. This scheme is used for the allowance of the first nonlinear property (plasticity).

Nevertheless there are special singularities for each type of additional finite element which simplify algorithm of problem solution in comparison with general case.

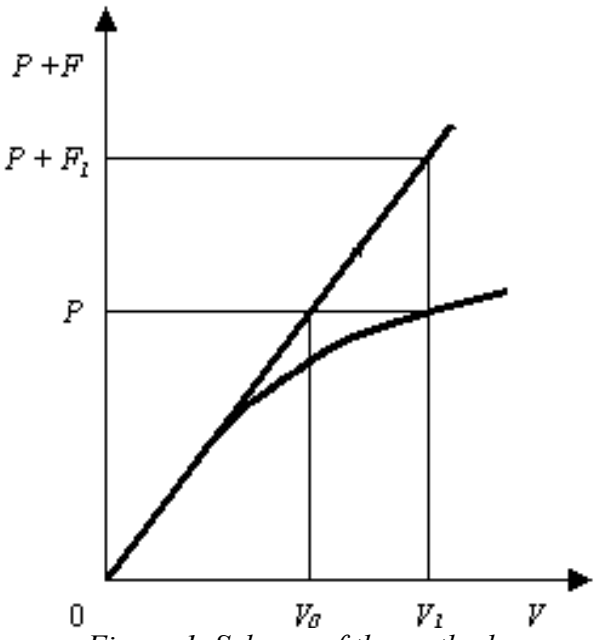

Figure 1. Scheme of the method of elastic decisions which is used by AFEM for the allowance of the first nonlinear property when its additional load is $F_{e,1} = -\Delta R_{nonl,1}$ [20,21].

If we compare formulae (31) and (33), we may make a conclusion that by means of node reactions of additional finite elements it is possible to form the vector of additional load for the main finite element, by means of which it is possible to allow for the considered nonlinear property.

This vector $F_{e,i}$ is determined by means of the next relationship:

$$F_{e,i} = -\Delta K_{nonl,e,i}\, V = -\Delta R_{nonl,i} \qquad (34)$$

Further it follows that we come to a little stop on the case of formation of additional load for collapse of the main finite element after reaching of its ultimate limit state.

In this case let us note the stiffness matrix of additional finite element as ΔK_{lim} and then:

$$\Delta K_{lim} = -\Delta K \qquad (35)$$

where K = stiffness matrix of the main finite element with linear properties.

Node reactions of additional finite element ΔR_{lim} are determined by next formula:

$$\Delta R_{lim} = -\Delta K_e V = -R \quad (36)$$

where R = node reactions of finite element with linear properties. In this connection the additional load for collapse of finite element is equal to:

$$F_e = K_e V = R \quad (37)$$

Actually it means that after collapse the main finite element ceases its existence and does not influence the neighboring elements and additional load guarantees this fact.
On the basis of these vectors $F_{e,i}$ the vector of additional load for the allowance of the i-th nonlinear property of the total structure according its design diagram may be formed. Then on the basis of separate vectors or each considered in analysis nonlinear property the total vector for all considered nonlinear properties may be formed.
The additional finite element of the first type does not change strain state. It changes only the stress state of the main finite element without account of particular nonlinear property up to the level of stress state of the same element with account of the given nonlinear property.

The absence of strains and the presence of stresses are characteristic for the first type of additional finite element, i.e

$$\Delta\varepsilon_{nonl,i} = 0 \quad (38)$$
$$\Delta\sigma_{nonl,i} \neq 0 \quad (39)$$

It means that if the additional finite element of the first type is used for the allowance of the i-th nonlinear property of the main finite element next formulae are correct for determination of stresses and strains:

$$\sigma_{nonl,i} = \sigma_{nonl,i1} + \Delta\sigma_{nonl,i} \quad (40)$$
$$\varepsilon_{nonl,i} = \varepsilon_{nonl,i-1} \quad (41)$$

These relationships for the allowance of the first nonlinear property look like these ones:

$$\sigma_{nonl,1} = \sigma + \Delta\sigma_{nonl,1} \quad (42)$$
$$\varepsilon_{nonl,1} = \varepsilon \quad (43)$$

It should be noted that general formula (34) for calculation of additional load $F_{e,i}$ for the main finite element is correct for both types of additional finite elements.
However besides this general approach there are individual cases of determination of vector of node reactions $\Delta R_{nonl,i}$ and consequently of additional load $F_{e,i}$ for both types of additional finite elements.
These individual cases are based on the relationships between node reactions with stresses and strains.
For additional finite element of the first type this individual case is based on relationship between node reactions and stresses.
So for the main finite element with linear properties the relationship between node reactions R and stresses σ looks like:

$$R = C\,\sigma \quad (44)$$

Where C = matrix connecting elastic node reactions and stresses.
The analogous formula for the main finite element with linear properties looks like:

$$R_{nonl} = C\,\sigma_{nonl} \quad (45)$$

Using the relationships (43) and (44) let us write down the formulae for determinations of node reactions $\Delta R_{nonl,i}$ in additional finite element of the first type for the allowance of the first nonlinear property:

$$\Delta R_{nonl,1} = C\,\Delta\sigma_{nonl,1} \quad (46)$$

and for the allowance of the i-th nonlinear property:

$$\Delta R_{nonl,i} = C\,\Delta\sigma_{nonl,i} \quad (47)$$

Substituting the expression (46) in (34) we obtain the formula for determination of the vector of additional load in general case:

$$F_{e,i} = - C\, \Delta\sigma_{nonl,i} \qquad (48)$$

In elimination of the main finite element after reaching of its ultimate limit state the formula looks like:

$$F_{e,i} = C\, \sigma \qquad (49)$$

where σ = stresses of finite element with linear properties.

This simplified variant of formation of the additional load using stresses $\Delta\sigma_{nonl,i}$ for the allowance of the plastic properties of concrete was developed in research.

It allows to use some operations of the method of additional stresses. Scheme of this process for the allowance of the first nonlinear property by means of additional finite element is shown at Figure 2.

Additional finite element of the second type does not change stress state.

It changes only stain state of the main finite element without allowance of the nonlinear property up to the level of strain state for the allowance of the given nonlinear property.

The dependence (33) connecting node reactions and node displacements as it reflects the main property of any additional finite element is correct for additional finite element of the second type too.

Stiffness matrix of this element may be determined by formula (27) and its additional load for the allowance of the nonlinear property may be determined by formula (34).

These expressions are correct for additional finite element of any type too.

Relating to other formulae describing the properties of additional finite element of the second type that it is necessary to use another approach for their obtaining based on the peculiarities of this element.

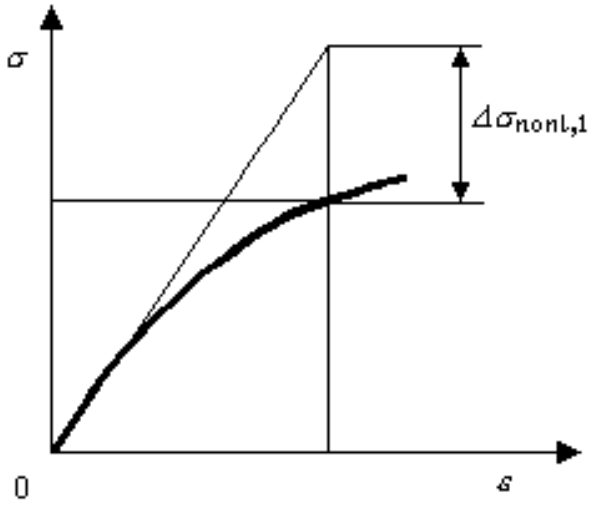

Figure 2. Scheme of the method of additional stresses which is used by AFEM for the allowance of the first nonlinear property by means of AFE of the first type [19, 20]

The absence of stresses and presence of strains is a defining feature of the additional finite element of the second type, i.

$$\Delta\varepsilon_{nonl,i.} \neq 0 \qquad (50)$$

$$\Delta\sigma_{nonl,\,i} = 0 \qquad (51)$$

It means that if the additional finite element of the second type is used for the allowance of the *i*-th nonlinear property of the main finite element the next formulae for determination of stresses and strains are correct:

$$\sigma_{nonl,i} = \sigma_{nonl,i}\, \varepsilon_{nonl,i-1} \qquad (52)$$

$$\varepsilon_{nonl,i} = \varepsilon_{nonl,i-1} + \Delta\varepsilon_{nonl,i} \qquad (53)$$

They are correct for the first nonlinear property:

$$\sigma_{nonl,1} = \sigma(\varepsilon) \qquad (54)$$

$$\varepsilon_{nonl,1} = \varepsilon + \Delta\varepsilon_{nonl,1} \qquad (55)$$

Special case of determination of additional load for additional finite element of the second type is based on the relationship of node reactions and strains of the main finite element.

For the main finite element with linear properties this relationship has next form:

$$R = G\,\varepsilon \qquad (56)$$

where G = matrix connecting elastic node reactions and strains.
For the main finite element with nonlinear properties this relationship looks like:

$$R_{nonl} = G\,\varepsilon_{nonl} \qquad (57)$$

Taking into consideration formulae (56) and (57) the formula for determination of node reaction in additional finite element of the second type for the allowance of the first nonlinear property will be:

$$\Delta R_{nonl,1} = G\,\Delta\,\varepsilon_{nonl,1} \qquad (58)$$

This formula for the allowance of the i-th nonlinear property looks like:

$$\Delta R_{nonl,i} = G\,\Delta\varepsilon_{nonl,i} \qquad (59)$$

Using the formulae (59) and (34) we may obtain the formula for determination of the additional load at any stage:

$$F_{e,i} = -\,G\,\Delta\varepsilon_{nonl,i} \qquad (60)$$

In case of collapse of the main finite element when its ultimate limit state is reached this formula will be of next form:

$$F_e = G\varepsilon \qquad (61)$$

where ε = strains of the finite element with linear properties.
This variant of formation of additional load $F_{e,i}$ using the strains $\Delta\varepsilon_{nonl,i}$ of additional finite element is suitable to take into account residual strains under unloading.
Formula (60) may be used only for additional finite element of the second type as for additional finite element of the first type it is accepted that its strains $\Delta\varepsilon_{nonl,i} = 0$ (38).
The algorithm of the problem solving may be shorted by this formula.
In this case operations of the method of additional strains may be added. Scheme of this process for the allowance of the first nonlinear property is given at Figure 3.

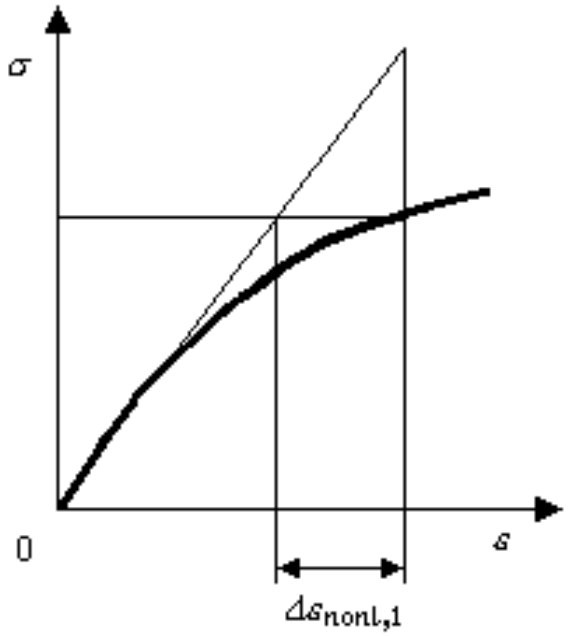

Figure 3. Scheme of the method of additional strains which is used by AFEM for the allowance of the first nonlinear property by means of AFE of the second type [19, 20].

Briefly the main characteristics of the additional finite elements of the first and the second type for the allowance of the any i-th nonlinear property are given in Table 1 [2, 20].
Formula (34) gives the main way for determination of additional load for taking into account of any i-th nonlinear property. Formulae (48) and (60) are suitable for two special cases.
Thus three ways for formation of additional load are possible.

6. FORMATION OF RIGHT HAND PART OF THE SET EQUATIONS OF AFEM

Two ways for changing of the right hand part of the set of equations (19) – (23) may be used for taking into account the i-th nonlinear property.
In the first case stiffness matrix of each additional design diagrams ΔK_i is formed on the base of stiffness matrices $\Delta K_{nonl,e,i}$ of correspon-

Table 1. The main characteristics of additional finite elements for the allowance of the i-th nonlinear property.

N	Type of characteristic	Finite element without the *i*-th nonlinear property	Finite element with the *i*-th nonlinear property	Additional finite element for the allowance of the *i*-th nonlinear property	
				Type 1	Type 2
1	Relationship between node reactions and displacements	$R_{nonl,i-1} = K_{nonl,e,i-1}V$	$R_{nonl,i} = K_{nonl,e,i}V$	$\Delta R_{nonl,i} = \Delta K_{nonl,e,i}V$	
2	Stiffness matrices	$K_{nonl,e,i-1}$	$K_{nonl,e,i}$	$\Delta K_{nonl,e,i} = K_{nonl,e,i} - K_{nonl,e,i-1}$	
3	Node reactions	$R_{nonl,i-1}$	$R_{nonl,i}$	$\Delta R_{nonl,i} = R_{nonl,i} - R_{nonl,i-1}$	
4	Relationship between node reactions and stresses	$R_{nonl,i-1} = C\sigma_{nonl,i-1}$	$R_{nonl,i} = C\,\sigma_{nonl,i}$	$\Delta R_{nonl,i} = C\,\Delta\sigma_{nonl,i}$	–
5	Relationship between node reactions and strains	$R_{nonl,i-1} = G\varepsilon_{nonl,i-1}$	$R_{nonl,i} = G\varepsilon_{nonl,i}$	–	$\Delta R_{nonl,i} = G\Delta\varepsilon_{nonl,i}$
6	Stresses	$\sigma_{nonl,i-1}$	$\sigma_{nonl,i}$	$\Delta\sigma_{nonl,i} = \sigma_{nonl,i} - \sigma_{nonl,i-}$	$\Delta\sigma_{nonl,i} = 0$
7	Strains	$\varepsilon_{nonl,i-1}$	$\varepsilon_{nonl,i}$	$\Delta\varepsilon_{nonl,i} = 0$	$\Delta\varepsilon_{nonl,i} = \varepsilon_{nonl,i} - \varepsilon_{nonl,i-1}$
8	Additional load	$F_{e,i} = -\Delta R_{nonl,i}$	–	–	–

ding additional finite elements taking into account given nonlinear property.
The formula (27) is used for it only.
In the second case every component

$$(-\Delta K_i V)$$

is formed on the base of the values

$$(-\Delta R_{nonl,i})$$

for taking into account the result of action of corresponding additional finite element taking into account this nonlinear property.
Three formulae (33), (47) and (59) may be used for calculation of node reactions $\Delta R_{nonl,i}$.
The choice suitable formula depends on characteristics of considered nonlinear property.

Both of these ways must correspond to real conditions of nonlinear analysis at limit state and failure model.

7. CONCLUSIONS

Suggested by AFEM set of linear equations according to ideal failure model of structure is developed on basis of theory of FEM and theory of ultimate equilibrium. It allows:

1) to take into account each nonlinear property which is appeared at definite stage of operating period of structure;
2) to introduce the criterion of collapse structure according to logic of FEM;
3) to realize nonlinear analysis of structures at limit states according to requirements of Codes;
4) to introduce different theoretical models of behavior of structures according to degree of

reaching of ultimate limit state due to properties of additional finite elements;
5) to use of all advantages of method of elastic decisions (additional loads).

REFERENCES

1. **Gvozdev A.A.** Raschet nesushchei sposobnosti konstruktsii po metodu predel'nogo ravnovesiia. Vyp. 1. Sushchnost' metoda i ego obosnovanie [Analysis of bearing capacity of structures by Limit State Method]. Moscow, Gosstroyisdat, 1949, 280 pages (in Russian).
2. **Ermakova A.V.** Metod dopolnitel'nykh konechnykh elementov dlia rascheta zhelezobetonnykh konstruktsii po predel'nym sostoianiiam [Additional finite element method for analysis of reinforced concrete structures at limit states]. Moscow, ASV, 2007, 128 pages (in Russian).
3. **Ermakova A.V.** Additional finite element method for analysis of reinforced concrete structures at limit states. Moscow, ASV, 2012, 114 pages.
4. **Ermakova A.V.** Additional finite element method for analysis of reinforced concrete structures at limit states. Stockholm, Sweden, ASV Construction, 2016, 116 pages.
5. **Zienkiewicz O.C.** Metod konechnix elementov v texnike [The finite element method in technique]. Moscow, Mir, 1975, 541 pages (in Russian).
6. **Ilyushin A.A.** Plastichnost' [Plasticity]. Moscow, Gostechisdat, 1948, 376 pages (in Russian).
7. **Postnov V.A.** Chislennye metody rascheta sudovykh konstruktsii [Numerical methods of design of ship structures]. Leningrad, Shipbuilding, 1977, 280 pages (in Russian).
8. **Ermakova A.** Actual problems of nonlinear design of reinforced concrete structures. // *International Journal for Computational Civil and Structural Engineering*, 2009, Volume 5, Issue 1&2, pp. 23-34.
9. **Ermakova A.** Solving Some Problems of Nonlinear Analysis of Reinforced Concrete Structures by Additional finite Element. // *Concrete in the Low Carbon Era. Proceedings of the International Conference* held at the University of Dundee, Scotland, UK on 9-11 July 2012. UK, Scotland, Dundee, pp. 1153-1163.
10. **Ermakova A.** Ideal'nye modeli razrusheniia konstruktsii dlia nelineinogo rascheta metodom dopolnitel'nykh konechnykh elementov [Ideal failure models of structures for nonlinear analysis by additional finite element method]. // *Structural mechanics and analysis of constructions*, 2017, No. 6, pp. 46-50.
11. **Ermakova A.** Ideal Failure Models of Structures for Analysis by FEM and AFEM. // Proceedings ICIE – 2017, 2017, Vol. 206, pp. 9-15.
12. **Ermakova A.V.** Reshenie sistemy lineinykh algebraicheskikh uravnenii metoda dopolnitel'nykh konechnykh elementov [The solving of the set of linear algebraic equations of additional finite element method]. // *Concrete and reinforced concrete*, 2010, No. 5, pp. 21-24 (in Russian).
13. **Ermakova A.V.** Dva sposoba postroeniia iteratsionnogo protsessa metoda dopolnitel'nykh konechnykh elementov [Two ways for realization of iterative process at additional finite element method]. // *Structural mechanics and analysis of constructions*, 2018, No. 6, pp. 45-52 (in Russian).
14. **Gorodetsky A.S., Evzerov I.D.** Komp'iuternye modeli konstruktsii [Computer models of structures]. Kiev, Fact, 2007, 394 pages (in Russian).
15. **Karpenko N.I**. Obshchie modeli mekhaniki zhelezobetona [Construction of Schemes of Reinforced Concrete],

Moscow, State Administration of Construction, 1996, 416 pages (in Russian).
16. **Shugaev V.V.** Inzhenernye metody v nelineinoi teorii predel'nogo ravnovesiia obolochek [Engineer Methods of Non-Linear Theory of Limit Equilibrium of the Shells], Moscow, Gotika, 2001, 368 pages (in Russian).
17. **Oatul A.A., Karyakin A.A., Kutin U.F.** Raschet i proektirovanie elementov zhelezobetonnykh konstruktsii na osnove primeneniia EVM. Konspekt lektsii [Computer-aided of reinforced concrete structural elements. Collected lectures]. Part 4 (Edited by Prof. Oatul A.A.), Chelyabinsk, Chelyabinsk Polytechnic Institute, 1980, 67 pages (in Russian).
18. SP 63.13330.2012. Betonnye i zhelezobetonnye konstruktsii. Aktualizirovannaia redaktsiia SNiP 52-01-2003 [SP 63.13330.2012. Concrete and Reinforced Concrete Structures. Actual version SP and C 52-01-2003] (in Russian).
19. **Ermakova A.** Additional Finite Elements and Additional Loads for Analysis of Systems with Several Nonlinear Properties. // Proceedings ICIE – 2016, 2016, Volume 150, pp. 1817-1823.
20. **Ermakova A.V.** Vzaimosviaz' metoda dopolnitel'nykh konechnykh elementov i drugikh chislennykh metodov rascheta konstruktsii [Correlation between additional finite element method and other numerical methods of the structural analysis]. // *Structural mechanics and analysis of constructions*, 2012, Np. No. 5, pp. 28-33 (in Russian).
21. **Ermakova A.V.** Metod dopolnitel'nykh konechnykh elementov dlia nelineinogo rascheta zhelezobetonnykh konstruktsii po predel'nym sostoianiiam. Tekst lektsii [Additional finite element method for nonlinear analysis of reinforced concrete structures at limit states]. Moscow, Publishing house ASV, 2017, 60 pages (in Russian).

СПИСОК ЛИТЕРАТУРЫ

1. **Гвоздев А.А.** Расчет несущей способности конструкций по методу предельного равновесия. Выпуск 1. Сущность метода и его обоснование. – М: Госстройиздат, 1949. – 280 с.
2. **Ермакова А.В.** Метод дополнительных конечных элементов для расчета железобетонных конструкций по предельным состояниям. М., АСВ, 2007. – 128 с.
3. **Ermakova A.V.** Additional finite element method for analysis of reinforced concrete structures at limit states. Moscow, ASV, 2012, 114 pages.
4. **Ermakova A.V**. Additional finite element method for analysis of reinforced concrete structures at limit states. Moscow, ASV Construction, Stockholm, Sweden, 2016, 116 pages.
5. **Зенкевич О.К**. Метод конечных элементов в технике. – М.: Мир, 1975. – 541 с.
6. **Ильюшин А.А**. Пластичность. – М.: Гостехиздат, 1948. – 376 с.
7. **Постнов В.А**. Численные методы расчета судовых конструкций. – Л.: Судостроение, 1977 – 280 с.
8. **Ermakova A.** Actual problems of nonlinear design of reinforced concrete structures. // *International Journal for Computational Civil and Structural Engineering*, 2009, Volume 5, Issue 1&2, pp. 23-34.
9. **Ermakova A.** Solving Some Problems of Nonlinear Analysis of Reinforced Concrete Structures by Additional finite Element. // *Concrete in the Low Carbon Era. Proceedings of the International Conference* held at the University of Dundee, Scotland, UK on 9-11 July 2012. UK, Scotland, Dundee, pp. 1153-1163

10. **Ермакова А.В.** Идеальные модели разрушения конструкций для нелинейного расчета методом дополнительных конечных элементов. // *Строительная механика и расчет сооружений*, 2017, № 6, с. 46 – 50.
11. **Ermakova A.** Ideal Failure Models of Structures for Analysis by FEM and AFEM. // Proceedings ICIE – 2017, 2017, Vol. 206, pp. 9-15.
12. **Ермакова А.В.** Решение системы линейных алгебраических уравнений метода дополнительных конечных элементов. // *Бетон и железобетон*, 2010, №5, с. 21-24.
13. **Ермакова А.В.** Два способа построения итерационного процесса метода дополнительных конечных элементов. // *Строительная механика и расчет сооружений*, 2018, № 6, с. 45-52.
14. **Городецкий А.С., Евзеров И.Д.** Компьютерные модели конструкций. Киев: Факт, 2007. – 394 с.
15. **Карпенко Н.И.** Общие модели механики железобетона. – М.: Стройиздат, 1996. – 416 с.
16. **Шугаев В.В.** Инженерные методы в нелинейной теории предельного равновесия оболочек. – М.: Готика, 2001. – 368 с.
17. **Оатул А.А., Карякин А.А., Кутин Ю.Ф.** Расчет и проектирование элементов железобетонных конструкций на основе применения ЭВМ. Конспект лекций. Часть 4 (под ред. Оатула А.А.). – Челябинск: ЧПИ, 1980. – 67 с.
18. СП 63.13330.2012. Бетонные и железобетонные конструкции. Актуализированная редакция СНиП 52-01-2003. – М., 2012.
19. **Ermakova A**. Additional Finite Elements and Additional Loads for Analysis of Systems with Several Nonlinear Properties. // Proceedings ICIE – 2016, Vol. 150, pp. 1817-1823.
20. **Ермакова А.В.** Взаимосвязь метода дополнительных конечных элементов и других численных методов расчета конструкций. // *Строительная механика и расчет сооружений*, 2012, №5, с. 28-33.
21. **Ермакова А.В.** Метод дополнительных конечных элементов для нелинейного расчета железобетонных конструкций по предельным состояниям. Текст лекций. – М: АСВ, 2017. – 64 с.

Anna V. Ermsakova, PhD, Assistant professor, South Ural State University, 76, Lenina prospekt, Chelyabinsk, Russia, 454080; phone +7(351)722-63-42;
E-mail: annaolga11@gmail.com.

Ермакова Анна Витальевна, кандидат технических наук, доцент; Южно-Уральский государственный университет; 454080, Челябинск, пр. Ленина, 76;
тел. +7(351)722-63-42;
E-mail: annaolga11@gmail.com.

DOI:10.22337/2587-9618-2019-15-2-65-71

ADHESION OF COMPONENTS OF COMPOSITE STEEL AND CONCRETE CROSS SECTION IN ANALYSIS OF BEAMS WITH CONCRETE ENCASED SECTIONS

Alexey S. Krylov
JSC Research Center of Construction, Moscow, RUSSIA

Abstract: A brief overview of the issues of aggregate work of components of the composite steel and concrete section is made. It is presented various options for the layout of the cross-section of beams used in the practice of design. A review of the design of the regulatory documents regarding the issues of adhesion of cross-section elements is performed. The characteristic of experimental models is given. The features of destruction of models are shown. The reasons of the destruction are analyzed. The case of the loss of the bearing capacity of the element due to relaxation (loss) of adhesion at the steel – concrete interaction boundary is considered. Various shear surfaces of the concrete section are given. Calculations of the bearing capacity of the composite steel – concrete beams for each computational surface were performed, the obtained results were evaluated. Conclusions have been made on the question of ensuring aggregate work in case of composite steel – concrete beams with a fully encased steel core.

Keywords: concrete, steel, reinforced concrete, composite steel and concrete structure, shear, adhesion, stud

УЧЕТ СЦЕПЛЕНИЯ КОМПОНЕНТОВ СТАЛЕЖЕЛЕЗОБЕТОННОГО СЕЧЕНИЯ В РАСЧЕТАХ БАЛОК С ПОЛНОСТЬЮ ОБЕТОНИРОВАННЫМ СТАЛЬНЫМ СЕРДЕЧНИКОМ

А.С. Крылов
Научно-исследовательский центр «Строительство», г. Москва, РОССИЯ

Аннотация: Выполнен краткий обзор вопросов совместной работы компонентов сталежелезобетонного сечения. Представлены различные варианты компоновки поперечного сечения балок, используемые в практике современного проектирования. Выполнен обзор расчетных положений нормативных документов касательно вопросов сцепления элементов поперечного сечения. Дана характеристика экспериментальных моделей. Приведены общие картины разрушения моделей, проанализированы причины разрушения. Рассмотрен вариант потери несущей способности элемента в следствии ухудшения (потери) сцепления на границе сталь-бетон. Приведены различные поверхности среза бетонной части сечения. Выполнены расчеты несущей способности сталежелезобетонных балок для каждой расчетной поверхности, дана оценка полученных результатов. Сделаны выводы по вопросу обеспечения совместной работы применительно к случаю сталежелезобетонных балок с полностью обетонированным стальным сердечником.

Ключевые слова: бетон, сталь, железобетон, сталежелезобетонная конструкция, сдвиг, сцепление, анкерное устройство

The late XX – early XXI centuries were marked by the extensive introduction of steel-concrete structures into building practice, the main types of which are columns and beams with stiff reinforcement. The significant development of high-rise construction required an increase in the bearing capacity of structural elements and at the same time a reduction in their dimensions. The columns made of the composite steel-concrete ensure these requirements [1]. The development of transport networks and an increase in the carrying capacity of transport lead to the

widespread use of composite steel – concrete structure in bridge construction. Majority of modern transport overpasses and bridge junctions are implemented using composite steel-concrete structure (beams), where a common design consideration is the combination of steel beams with a slab of concrete along top flange (Figure 1) [2]. Composite steel – concrete beams with a fully encased steel core also find appliance [3], as it is shown in Figure 2.

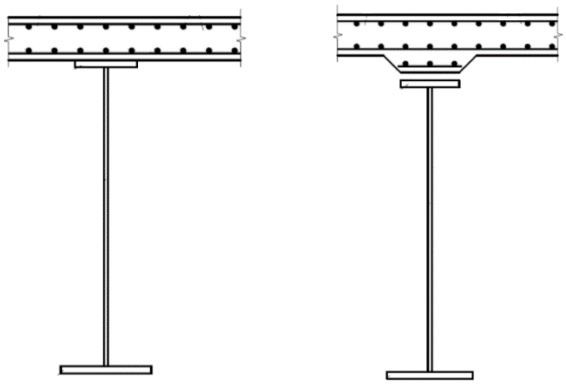

a) slab without thickening b) slab with thickening

Figure 1. Example of composite steel-concrete beam – steel I-beam with reinforced concrete slab along top flange.

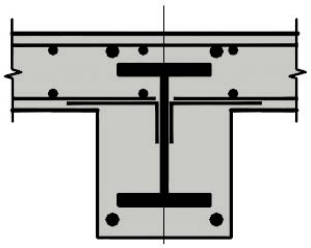

Figure 2. Example of composite steel – concrete beam with a fully encased steel core.

The issues of adhesion of a reinforced concrete slab with a steel beam, as well as the effect of various anchors (flexible, rigid connectors) on the bearing capacity of the composite reinforced concrete elements are studied quite well [2, 4] due to it wide acceptance. The necessity of applying anchors and features of the calculation are governed by the relevant regulatory documents [2, 4, 5, 6] and recommendations [7].

The issues of adhesion with a fully encased steel section to concrete were also investigated by a number of authors [8]. Let us note that regulatory documents [4, 5] regulate placing of anchors for beams with rigid reinforcement (with a fully encased steel core), but the focus is on placing the stud only on the wall of a steel section (Figure 3).

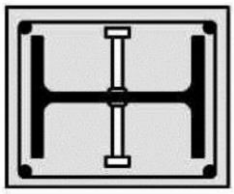

Figure 3. Installation of anchor studs on the wall of the steel profile according to [4].

The special attention is not paid to placing the studs on the shells of the I-beam (in contrast to the case of a steel non-concrete beam with a reinforced concrete slab along the upper shelf). This can be explained by the layout of the composite steel - concrete section, when rigid reinforcement is distributed fairly evenly over the entire cross section and the distance from the top shell of the I-section (Figure 3) to the edge of the beam is small. At the same time, in Eurocode 4 [4], in section 6.7.4.2, there is a note on this issue - it is necessary to check the sufficiency of web reinforcement to resist shear force for zones of the concrete part of the cross section that do not have direct contact with the steel core by anchors (Figure 4 - considered a shear along the lines A-A).

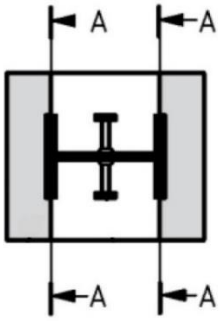

Figure 4. Checking composite steel – concrete element under shear force along line A-A according to [4].

However, such a check is provided only for the composite steel - concrete columns in case when the load is attached either only to the steel or to the concrete part of the section. The need for such checks is not regulated for beams with rigid reinforcement and fully encased steel core, although in some cases it must be performed.
Alternatively, the cross-sectional layout of beams with rigid reinforcement, when all or most of the steel core are located in the tension side, that implies a significant distance from the top shell of steel section to the edge of the cross-section (Figure 5).

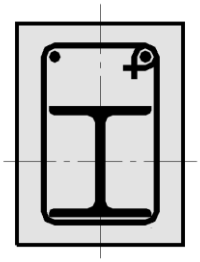

Figure 5. An example of a beam with rigid reinforcement with a non-standard arrangement of an I-beam.

In this case, in addition to strength analysis of the normal section of the element and the corresponding fracture features (chipping of compressed zone of the concrete or breakage of the tensile reinforcement), attention should be paid to the possibility of the component damage as a result of deterioration (loss) of adhesion at the steel-concrete interface and shear of the concrete part of the beam. A choice of line of shear is marked in red in Figure 6.
A series of experiments were performed to study the behavior of the composite steel-concrete beams using high-strength concrete. The described non-standard type of destruction is recorded in the process of testing, although a detailed study of damage of a similar type was not a purpose of these experiments. During the experimental studies, 9 models of composite steel-concrete beams of rectangular cross section 200x150 mm and 1.5 m length were tested. The steel core is made in the form of an I-beam.

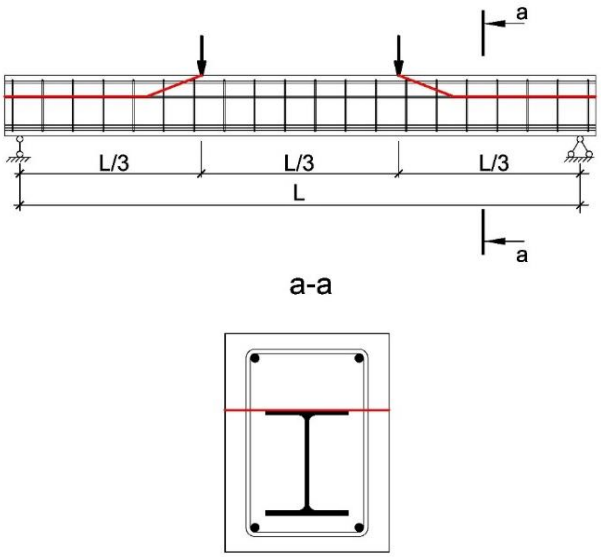

Figure 6. Possible location of the line of concrete shear at the component damage due to deterioration (loss) of adhesion at the steel-concrete interface.

The core material is C255 steel according to National Standard of Russian Federation GOST 27772-2015. The concrete of the models is high-strength of B75 ... B90 compressive strength class. Upper and transverse reinforcement have diameter 10 mm class A400 of steel 35GS. The percent of reinforcement is 7.8 ... 9.2%. The beams were tested for pure bending by attaching concentrated loads in 1/3 and 2/3 of the span of the models. The general view of the models is shown in Figure 7. A detailed description of the experiment is given in [9].

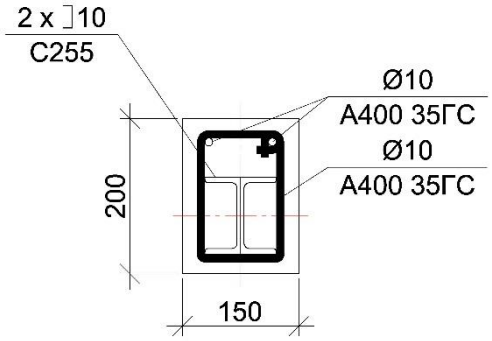

Figure 7. General view of the composite steel – concrete beam model.

Figure 8. Characteristic destruction of models of the composite steel – concrete beams (beam fragment – extreme third part of the span).

The destruction of the models was similar and characterized by the appearance of a large number of vertical and inclined cracks, as well as horizontal cracks on the upper and lower edges of the beam. This led to partial shear of the concrete of the protection cover and uncovering of the reinforcement cage and steel core in the extreme thirds of the beam span - between the point of support and the point of attaching of the load at the last stages of loading (Figure 8). At more detailed observing of the failure models, it is supposed, that a possible reason of the destruction is a violation of the adhesion between the upper shell of the steel I-beam and concrete. In contrary to widespread destruction variant, the shear (Figure 9) occurred on the boundary of steel and concrete parts of section as it is shown in Figure 6. The destruction of a similar type is not considered in the literature before.

Theoretical calculations were performed to evaluate the obtained experimental results. The sequence of checking the shear strength of concrete along the indicated surfaces (Figure 6, 9) is given below. In the presented calculations, the characteristics of materials are assumed to be equal to it actual values.

1. The height of the compressed zone of the cross section was determined and compared with the experimental value. The sequence of calculations is described in detail in regulatory documents [5, 7]. The height of the compressed zone is x = 7.0 cm.

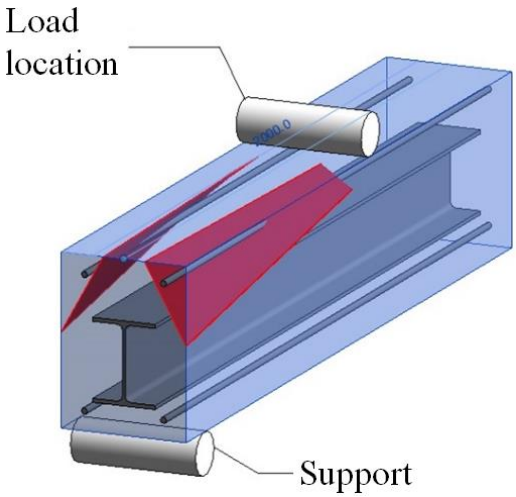

a) overall view

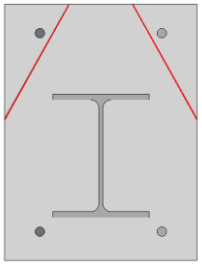

b) front view

Figure 9. Possible location of the shear surface in the concrete during the destruction of the element caused by deterioration (loss) of adhesion at the steel-concrete interface.

2. The shearing force is determined by the formula similar (since the type of the destruction is another) (6.63) [SP 266]:

$$S_i = (\sigma_{b1}A_b + \sigma_{s1}A_s) - (\sigma_{b2}A_b + \sigma_{s2}A_s), \quad (1)$$

Where σ_{b1}, σ_{b2} are compressive stresses in concrete in the right and left sections of the calculated part of the beam

σ_{s1}, σ_{s2} are stresses in the longitudinal reinforcement in the same sections, respectively. In the above formulas, the distance from the point of load attaching to the beam support and, respectively, the stresses σ_{b2} и σ_{s2} at the end of the beam is assumed to be equal to zero. Value of the shear force is:

$$S = (R_b bx + R_{sc} A'_{sc}) = 943{,}9 \cdot 15{,}0 \cdot 7{,}0 + 4440{,}0 \cdot 1{,}57 = 106\,080 \text{ kg}, \quad (2)$$

where $R_b = 943{,}9 \frac{\text{kg}}{\text{cm}^2}$, $R_{sc} = 4444{,}0 \frac{\text{kg}}{\text{cm}^2}$

are compressive strength of concrete and reinforcement rod respectively,
$b = 15$ cm is cross section width,
$x = 7{,}0$ cm is height of the compressed zone of the section,
$A'_{sc} = 1{,}57 \text{ cm}^2$ is area of compressed reinforcement rod.
3. The shear strength R_τ of an element for various computational surfaces is calculated:

$$R_\tau = A_\tau R_{bt}, \quad (3)$$

Where A_τ is area of the calculated shear surface, R_{bt} is tension strength of concrete.
a) for the case shown in Figure 6:

$$R_\tau = (l_1 \cdot l_2 \cdot 2) \cdot R_{bt} = (51{,}5 \cdot 2{,}9 \cdot 2) \cdot 68{,}3 = 20\,401 \text{ kg}, \quad (4)$$

where $R_{bt} = 68{,}3 \frac{\text{kg}}{\text{cm}^2}$,

$l_1 = 51{,}5$ cm is the distance from the point of load attaching to the edge of the beam (length of the shear surface),
$l_2 = 2{,}9$ cm is the distance from the edge of the flange of the I-beam to the edge of the cross section (width of the shear surface).
b) for the case shown in Figure 9.
Here we note that the contour of the calculated surface to determine the shear bearing capacity for concrete is accepted by the results of experimental studies. The specified computational contour accurately reflects the features of the destruction recorded during the experiments performed in this paper.

$$R_\tau = (l_1 \cdot l_2 \cdot 2) \cdot R_{bt} = (51{,}5 \cdot 14{,}75 \cdot 2) \cdot 68{,}3 = 103\,765 \text{ kg}, \quad (5)$$

where $R_{bt} = 68{,}3 \frac{\text{kg}}{\text{cm}^2}$

$l_1 = 51{,}5$ cm is the distance from the point of application of the load to the edge of the beam (length of the shear surface).
$l_2 = 14{,}75$ cm is the average width of the shear surface on the test results.
The obtained value of the shear strength of the element almost completely coincided with the fracture load. The difference is 2.2%.
4. A comparison of the theoretical and experimental bearing capacity of the beam, determined by the shear of concrete, is carried out. The values is quite close.
We also note that the value of the carrying capacity for shear is quite close to the bearing capacity of the element obtained in the calculation for the normal section. At the same time, the limiting state in the cross section is reached at the moment of concrete shearing along the specified calculated surfaces. The concrete stresses in the compressed zone reach the limit values, and in the tensile rigid reinforcement, the stresses correspond to the yield strength.

CONCLUSIONS

A review on the subject of combining of elements of steel-concrete structures is carried out.
The features of steel-concrete beam models' destruction are analyzed for the bending tests. The destruction of the models is similar and characterized by the appearance of a large number of vertical and inclined cracks, as well as horizontal cracks. This leads to partial shear of the concrete of the protection cover and uncovering of the reinforcement cage and steel core in the extreme third of the beam span - between the point of support and the point of load attaching at the last stages of loading. The shear oc-

curs by the surface shown in red in Figure 9, in contrast to the most common type of destruction - by the interface of steel and concrete (Figure 6). The damage of a similar type in the literature has not been considered previously. This type of destruction can be considered as a new type of limit state concerning to the first group of limit states (by strength).

The possible variants of the computational destruction surfaces of the composite steel-concrete beams, caused by relaxation (loss) of adhesion at the steel-concrete interface, are considered.

The surface shown in Figure 6 and, respectively, the strength value determined by formula (4) are the most dangerous cases of destruction for elements with not enough transverse reinforcement or without it. In the case of powerful transverse reinforcement, the destruction surface takes a more complex shape, that is close to the shape shown in Figure 9. In this case, the fracture load should be determined by the relationship (5).

REFERENCES

1. **Travush V.I., Konin D.V., Rozhkova L.S., Krylov A.S., Kaprielov S. S., Chilin I.A., Martirosyan A.S., Fimkin A.I.** Jeksperimental'nye issledovanija stalezhelezobetonnyh konstrukcij, rabotajushhih na vnecentrennoe szhatie [Experimental study of composite structures, working for eccentric compression]. // *Academia. Architecture and Construction*, 2016, No. 3, pp. 127-135 (in Russian).
2. SP 63.13330.2012 Mosty i truby. Aktualizirovannaja redakcija SNiP 2.05.03-84 [Bridges and culverts. The updated edition of SNiP 2.05.03-84]. Moscow, 2011 (in Russian).
3. **Travush V.I., Konin D.V., Krylov A.S., Kaprielov S.S., Chilin I.A.** Jeksperimental'nye issledovanija stalezhelezobetonnyh konstrukcij, rabotajushhih na izgib [Experimental study of composite structures for bending elements]. // *Building and Reconstruction*, 2017, No. 4(72), pp. 63-71 (in Russian).
4. EN 1994-1-1 (2004) (English): Eurocode 4: Design of composite steel and concrete structures – Part 1-1: General rules and rules for buildings [Authority: The European Union Per Regulation 305/2011, Directive 98/34/EC, Directive 2004/18/EC].
5. SP 266.1325800.2016 Konstrukcii stalezhelezobetonnye. Pravila proektirovanija [Composite steel and concrete structures. Rules of design]. Moscow, 2017 (in Russian).
6. SP 63.13330.2012 Betonnye i zhelezobetonnye konstrukcii. Aktualizirovannaja redakcija SNiP 52-01-2003 [Concrete and reinforced concrete structures. The updated edition of SNiP 52-01-2003]. Moscow, 2013 (in Russian).
7. Standard of organization STO SCDA 11251254.001-018-4 Rukovodstvo po proektirovaniju stalezhelezobetonnyh konstrukcij (v razvitie SP 266.1325800.2016 “Konstrukcii stalezhelezobetonnye. Pravila proektirovanija”) [Guidelines for the design of composite steel and concrete structures]. Moscow. 2018 (in Russian).
8. **Travush V.I., Kaprielov S. S., Konin, D. V., Krylov A. S., Kashevarova G.G., Chilin I.A.** Determination of bearing capacity for shear of the contact surface “steel – concrete” in composite steel and concrete structures for concrete of different compressive strength and fiber-reinforced concrete. // *Building and reconstruction*, 2016, No. 4(66), pp. 45-55 (in Russian).
9. **Travush V.I., Konin D.V., Krylov A.S.** Strength of composite steel and concrete beams of high-performance concrete. // *Magazine of Civil Engineering*, 2018, No. 3(79), pp. 36-44.

СПИСОК ЛИТЕРАТУРЫ

1. **Травуш В.И., Конин Д.В., Рожкова Л.С., Крылов А.С., Каприелов С.С.,**

Чилин И.А., Мартиросян А.С., Фимкин А.И. Экспериментальные исследования сталежелезобетонных конструкций, работающих на внецентренное сжатие. // *Academia. Архитектура и строительство*, 2016, №3, с. 127-135.
2. СП 35.13330.2011 Мосты и трубы. Актуализированная редакция СНиП 2.05.03-84. – М.: ОАО «ЦПП», 2011.
3. **Травуш В.И., Конин Д.В., Крылов А.С., Каприелов С.С., Чилин И.А.** Экспериментальные исследования сталежелезобетонных конструкций, работающих на изгиб. // *Строительство и реконструкция*, 2017, №4(72), с. 63-71.
4. EN 1994-1-1 (2004) (English): Eurocode 4: Design of composite steel and concrete structures – Part 1-1: General rules and rules for buildings [Authority: The European Union Per Regulation 305/2011, Directive 98/34/EC, Directive 2004/18/EC].
5. СП 266.1325800.2016 Конструкции сталежелезобетонные. Правила проектирования. – М.: Кодекс, 2017.
6. СП 63.13330.2012 Бетонные и железобетонные конструкции. Актуализированная редакция СНиП 52-01-2003. – М.: Кодекс, 2011.
7. Стандарт организации СТО АРСС 11251254.001-018-4 Руководство по проектированию сталежелезобетонных конструкций (в развитие СП 266.1325800.2016 «Конструкции сталежелезобетонные. Правила проектирования»). – М., 2018.
8. **Травуш В.И., Каприелов С.С., Конин Д.В., Крылов А.С., Кашеварова Г.Г., Чилин И.А.** Определение несущей способности на сдвиг контактной поверхности «сталь – бетон» в сталежелезобетонных конструкциях для бетонов различной прочности на сжатие и фибробетона. // *Строительство и реконструкция*, 2016, №4(66), с. 45-55.
9. **Travush V.I., Konin D.V., Krylov A.S.** Strength of composite steel and concrete beams of high-performance concrete. // *Magazine of Civil Engineering*, 2018, No. 3(79), pp. 36-44.

Alexey S. Krylov, Researcher; Research Center of Construction, Research Institute of Building Constructions (TSNIISK) named after V. A. Koucherenko; b. 6, 2-ja Institutskaja ul., Moscow, 109428, Russia;
phone +7(499)174-79-21; e-mail: kryl07@mail.ru.

Крылов Алексей Сергеевич, научный сотрудник; Научно-исследовательский центр «Строительство», Центральный научно-исследовательский институт строительных конструкций (ЦНИИСК) имени В.А. Кучеренко; 109428, Российская Федерация, г. Москва, ул. 2-я Институтская, д. 6; тел. +7(499)174-79-21;
E-mail: kryl07@mail.ru.

DOI:10.22337/2587-9618-2019-15-2-72-76

DETERMINATION OF THE LIMIT HEIGHT OF THE COMPRESSED ZONE OF STEEL-CONCRETE COMPOSITE SECTIONS

Alexey S. Krylov
Research Center of Construction, Moscow, RUSSIA

Abstract: A brief review of power resistance of cross sections with a complex composition was made using the examples of steel-concrete composite structures. The features and difficulties that appear when calculate steel-concrete composite structures, materials of which have different strength characteristics, are noted. The procedure for calculation the limit height of the compressed zone for steel-concrete composite beam section is given.

Keywords: concrete, steel, reinforced concrete, steel-concrete composite structure, height of compressed zone

ОПРЕДЕЛЕНИЕ ГРАНИЧНОЙ ВЫСОТЫ СЖАТОЙ ЗОНЫ ДЛЯ ЖЕЛЕЗОБЕТОННЫХ СЕЧЕНИЙ С ЖЕСТКОЙ АРМАТУРОЙ

А.С. Крылов
Научно-исследовательский центр «Строительство», г. Москва, РОССИЯ

Аннотация: Выполнен краткой обзор работы поперечных сечений, имеющих сложную внутреннюю компоновку на примере сталежелезобетонных конструкций. Отмечены особенности и трудности расчетов в случае наличия в сечении материалов с различными прочностными характеристиками на примере определения граничной высоты сжатой зоны сталежелезобетонного сечения. Приведена последовательность расчета граничной высоты сжатой зоны поперечного сечения балки, армированной стержневой и жесткой арматурой.

Ключевые слова: бетон, сталь, железобетон, сталежелезобетонная конструкция, высота сжатой зоны

The developing construction industry offers a wide range of building materials and products, which gives the designer the opportunity to implement the most difficult architectural decisions. Often in modern construction practice, even one structural element can have a complex internal composition, including several materials with different strength characteristics. An example is the steel-concrete structures (Figure 1), which have great development in recent times [1, 2, 3, 4, 5].

Considering steel-concrete structures (columns and beams with fully concreted core [4, 5, 6, 7] – Figure 1) a fairly common design solution is a combination of modern flexible rebars (for example, class A500) with a rolled or welded profile of steel C255/C345. Thus, the design characteristics of the steel elements of the cross section may differ by 35 ... 80%. For some stages of strength calculation of normal cross sections of composite elements, the noted feature can cause some difficulties and complicate the calculation process.

In accordance with the current Building Code Russian Federation SP 63.13330 [8], the limit height of the compressed zone should be calculated for the entire cross section, taking into account the all reinforcement in tension. If the reinforcement is laid in several layers, it is assumed that reinforcement is concentrated in the center of its gravity (h_0 is calculated as a distance from the most compressed fiber to the center of gravity of the reinforcement in tension).

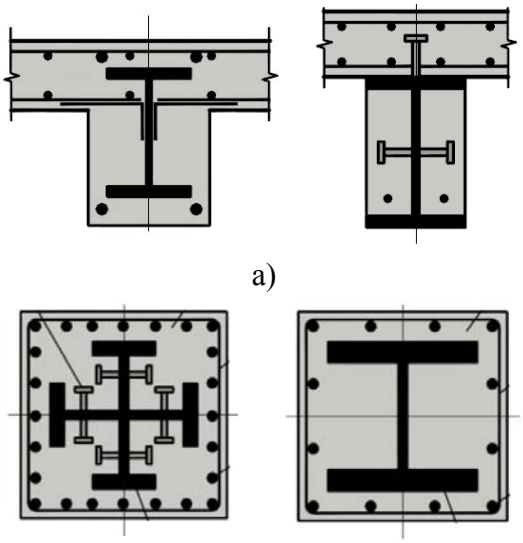

a)

b)

Figure 1. Examples of cross sections of steel-concrete columns [2].

Also the formula for the limit height of the compressed zone, that is contained in SP 63.13330, assumes that the strains of the whole reinforcement in tension has reached a value corresponding to the yield strength of the material or exceed it.

In practice, this approach may cause the following difficulties. If some layer of reinforcement is located close to the boundary of the compressed zone, it is not clear whether the stresses in this reinforcement will have reach the design resistance when the structure is destroyed. It is possible that different layers of reinforcement work with different resistances and the formulas of the current Building Code do not allow describing this case correctly when calculating at the limit values of forces. This becomes especially apparent when calculating steel-concrete composite cross-section with a whole rolling profile. The second difficulty arises when using steels with different strength characteristics in the same section. Then, the reinforcement elements reach the yield point of strain-stress diagram at different deformation values despite the same elastic modules.

Let us consider in more detail the definition of the limit height of the compressed zone of the steel-concrete cross-section of the beam, designed with the use of steels of different strengths (Figure 2).

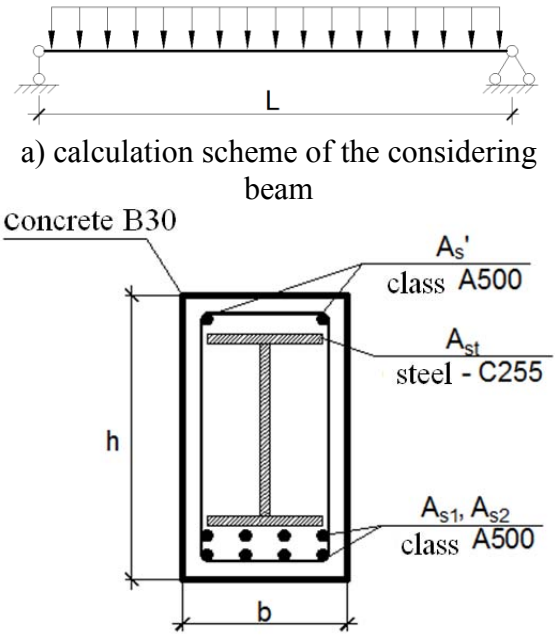

a) calculation scheme of the considering beam

b) cross section

Figure 2. Steel-concrete beam designed with steel elements of different strength.

The section under consideration has dimensions $b \times h$. The beam is reinforced with rebars and rigid steel profiles. The core of cross section is made in the form of an I-beam of C255 steel. Rods of upper and lower reinforcement are made of rebars of A500 class. In the work, it is considered heavy concrete of compressive strength class C30.

According to SP 63.13330 [8] the limit height of the compressed zone is calculated by the following formula

$$x_R = \frac{0.8}{1+\frac{\varepsilon_{s,el}}{\varepsilon_{b2}}} h_0, \qquad (1)$$

where $\varepsilon_{s,el}$ is deformation of reinforcement in tension at stress value R_s ,

$$\varepsilon_{s,el} = \frac{R_s}{E_s},$$

ε_{b2} is deformation of compressed concrete at stress value R_b.

Thus, there are rebar elements of different strength and different deformation characteristics, located at different sites, in the cross section. Respectively, the limit heights of the compressed zone defined for the various steel elements of the section also differ. The schematic arrangement of the limit heights of the compressed zone for different section of the steel core (the section is divided into several parts through the height to obtain a more accurate result) and the reinforcement rods are shown in figure 3. The height of the compressed zone *x* of the cross section is marked with hatching in figure 3. The limit height of the compressed zone for the each steel element indicated as x_{R_i}.

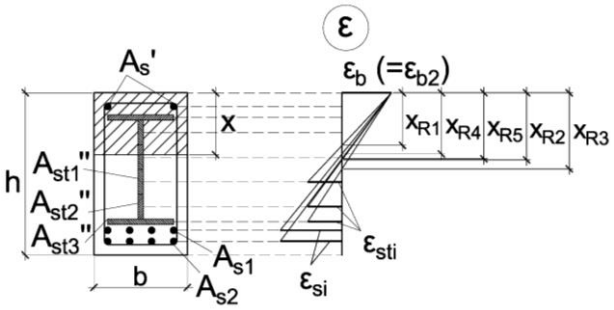

Figure 3. Steel-concrete cross section in bent. Determination of limit height of compressed zone.

When determining the limit height of the compressed zone of a cross section of a steel-concrete element, the following sequence of calculations should be accepted:

- determination of the limit height of the compressed zone x_R by formula (1) for each stretched section of steel reinforcement (steel core and rod reinforcement). At the same time, the profile of rigid reinforcement should be divided into parts through the height of the cross section.
- determination of the height of the compressed zone *x*, assuming that the stresses in the entire stretched reinforcement reached the yield strength of the material ($\sigma_s = R_s$);
- comparison of x and x_R for each stretched steel element of cross section. Selection of rod and rigid reinforcement elements for which $x > x_R$;
- recalculation of the height of the compressed zone excluding the elements for which $x > x_R$ since the stresses in them $\sigma_s < R_s$. In this case, the steel parts of the section should be excluded from the calculation one by one, starting with the element for which the difference between *x* and x_R s greatest. Besides, in the case whether of rigid reinforcement or symmetrical flexible reinforcement, the elements of the core or rod reinforcement should be excluded from the calculation, taking into account their symmetrical placement respectively to the current location of the boundary of the compressed zone at this stage of calculation or iteration.

Further, according to the mentioned technique, several iterations should be performed (if necessary) until the inequality $x < x_R$ is performed taking into account all the elements entered into the calculation. Then the stresses correspond to the yield strength of the material ($\sigma_s = R_s$) for the elements involved in the calculation. Further, when determining the limit moment in the cross section in order to obtain margin of safety, only the elements, in which the stress reach the value $\sigma_s = R_s$, should be entered into the calculation.

In the case when the cross section is strongly over-reinforced, and it is impossible to identify elements that work with full design resistance, it is possible to use the technique of the current SP 63.13330 [8], taking as the limit height of the compressed zone the smallest value ξ_{Ri} from those values that relate to the reinforcement taken into account in the calculation.

In order to obtain more accurate results, the stretched rebars and the stretched sections of the rigid reinforcement for which the $x < x_R$ inequality is true should be taken into account in the expressions for determining the height of the compressed zone and the limit bending moment, taking into account their real stress state. In this case, the stress in the rod and rigid reinforce-

ment should be determined from the conditions of elastic operation of the material:

- plot the relative strain/stress diagram using two points: the ultimate strain/stress of concrete and the zero point (calculated height of the compressed zone);
- guided by the Euler–Bernoulli hypotheses, determine the strain / stress in the series of reinforcing bars (from the diagram);
- take into account the real strain / stress for all elements involved in calculation.

CONCLUSIONS

The problems of determination of limit height of the compressed zone of a cross section of a steel-concrete element are considered in the general form. The complexity of the calculation is that there is a reinforcement (rod and rigid core) of different strength and with different deformation characteristics, located at different levels through the height of cross section.
The sequence of calculation of the limit height of the compressed cross-sectional area of the beam reinforced with rod and rigid reinforcement is presented. Recommendations on possible improvements of calculations are given.

REFERENCES

1. EN 1994-1-1 (2004) (English): Eurocode 4: Design of composite steel and concrete structures – Part 1-1: General rules and rules for buildings [Authority: The European Union Per Regulation 305/2011, Directive 98/34/EC, Directive 2004/18/EC].
2. SP 266.1325800.2016 Konstrukcii stalezhelezobetonnye. Pravila proektirovanija [Composite steel and concrete structures. Rules of design]. Moscow, 2017 (in Russian).
3. Standard of organization STO SCDA 11251254.001-018-4 Rukovodstvo po proektirovaniju stalezhelezobetonnyh konstrukcij (v razvitie SP 266.1325800.2016 “Konstrukcii stalezhelezobetonnye. Pravila proektirovanija”) [Guidelines for the design of composite steel and concrete structures]. Moscow. 2018 (in Russian).
4. **Travush V.I., Konin D.V., Rozhkova L.S., Krylov A.S., Kaprielov S. S., Chilin I.A., Martirosyan A.S., Fimkin A.I.** Jeksperimental'nye issledovanija stalezhelezobetonnyh konstrukcij, rabotajushhih na vnecentrennoe szhatie [Experimental study of composite structures, working for eccentric compression]. // *Academia. Architecture and Construction*, 2016, No. 3, pp. 127-135 (in Russian).
5. **Travush V.I., Konin D.V., Krylov A.S., Kaprielov S.S., Chilin I.A.** Jeksperimental'nye issledovanija stalezhelezobetonnyh konstrukcij, rabotajushhih na izgib [Experimental study of composite structures for bending elements]. // *Building and Reconstruction*, 2017, No. 4(72), pp. 63-71 (in Russian).
6. **Travush V.I., Konin D.V., Krylov A.S.** Strength of composite steel and concrete beams of high-performance concrete. // *Magazine of Civil Engineering*, 2018, No. 3(79), pp. 36-44.
7. **Travush V.I., Kaprielov S. S., Konin, D. V., Krylov A. S., Kashevarova G.G., Chilin I.A.** Opredelenie nesushhej sposobnosti na sdvig kontaktnoj poverhnosti «stal' – beton» v stalezhelezobetonnyh konstrukcijah dlja betonov razlichnoj prochnosti na szhatie i fibrobetona [Determination of bearing capacity for shear of the contact surface “steel – concrete” in composite steel and concrete structures for concrete of different compressive strength and fiber-reinforced concrete]. // *Building and reconstruction*, 2016, No. 4(66), pp. 45-55 (in Russian).
8. SP 63.13330.2012 Betonnye i zhelezobetonnye konstrukcii. Aktualizirovannaja redakcija SNiP 52-01-2003 [Concrete and reinforced concrete structures. The updated edition of SNiP 52-01-2003]. Moscow, 2013 (in Russian).

СПИСОК ЛИТЕРАТУРЫ

1. EN 1994-1-1 (2004) (English): Eurocode 4: Design of composite steel and concrete structures – Part 1-1: General rules and rules for buildings [Authority: The European Union Per Regulation 305/2011, Directive 98/34/EC, Directive 2004/18/EC].
2. СП 266.1325800.2016 Конструкции сталежелезобетонные. Правила проектирования. – М.: Кодекс, 2017.
3. Стандарт организации СТО АРСС 11251254.001-018-4 Руководство по проектированию сталежелезобетонных конструкций (в развитие СП 266.1325800.2016 «Конструкции сталежелезобетонные. Правила проектирования»). – М., 2018.
4. **Травуш В.И., Конин Д.В., Рожкова Л.С., Крылов А.С., Каприелов С.С., Чилин И.А., Мартиросян А.С., Фимкин А.И.** Экспериментальные исследования сталежелезобетонных конструкций, работающих на внецентренное сжатие. // *Academia. Архитектура и строительство*, 2016, No. 3, pp. 127-135.
5. **Травуш В.И., Конин Д.В., Крылов А.С., Каприелов С.С., Чилин И.А.** Экспериментальные исследования сталежелезобетонных конструкций, работающих на изгиб. // *Строительство и реконструкция*, 2017, №4(72), с. 63-71.
6. **Travush V.I., Konin D.V., Krylov A.S.** Strength of composite steel and concrete beams of high-performance concrete. // *Magazine of Civil Engineering*, 2018, No. 3(79), pp. 36-44.
7. **Травуш В.И., Каприелов С.С., Конин Д.В., Крылов А.С., Кашеварова Г.Г., Чилин И.А.** Определение несущей способности на сдвиг контактной поверхности «сталь – бетон» в сталежелезобетонных конструкциях для бетонов различной прочности на сжатие и фибробетона. // *Строительство и реконструкция*, 2016, №4(66), с. 45-55.
8. СП 63.13330.2012 Бетонные и железобетонные конструкции. Актуализированная редакция СНиП 52-01-2003. – М.: Кодекс, 2013.

Alexey S. Krylov, Researcher; Research Center of Construction, Research Institute of Building Constructions (TSNIISK) named after V. A. Koucherenko; b. 6, 2-ja Institutskaja ul., Moscow, 109428, Russia;
phone +7(499)174-79-21; e-mail: kryl07@mail.ru.

Крылов Алексей Сергеевич, научный сотрудник; Научно-исследовательский центр «Строительство», Центральный научно-исследовательский институт строительных конструкций (ЦНИИСК) имени В.А. Кучеренко; 109428, Российская Федерация, г. Москва, ул. 2-я Институтская, д. 6; тел. +7(499)174-79-21;
E-mail: kryl07@mail.ru.

DOI:10.22337/2587-9618-2019-15-2-77-85

GLOBAL ASYMPTOTICS OF THE FILTRATION PROBLEM IN A POROUS MEDIUM

Lyudmila I. Kuzmina [1], Yuri V. Osipov [2], Yulia G. Zheglova [2]
[1] National Research University Higher School of Economics, Moscow, RUSSIA
[2] National Research Moscow State University of Civil Engineering, Moscow, RUSSIA

Abstract: Filtration of the suspension in a porous medium is important when strengthening the soil and creating watertight partitions for the construction of tunnels and underground structures. A model of deep bed filtration with variable porosity and fractional flow, and a size-exclusion mechanism of particle retention are considered. A global asymptotic solution is constructed in the entire domain in which the filtering process takes place. The obtained asymptotics is close to the numerical solution.

Keywords: deep bed filtration, porous medium, suspended and retained particles, mathematical model, global asymptotics

ГЛОБАЛЬНАЯ АСИМПТОТИКА ЗАДАЧИ ФИЛЬТРАЦИИ В ПОРИСТОЙ СРЕДЕ

Л.И. Кузьмина [1], Ю.В. Осипов [2], Ю.Г. Жеглова [2]
[1] Национальный исследовательский университет «Высшая школа экономики», г. Москва, РОССИЯ
[2] Национальный исследовательский Московский государственный строительный университет, г. Москва, РОССИЯ

Аннотация: Задачи фильтрации суспензии в пористой среде важны при укреплении грунта и создании водонепроницаемых перегородок для строительства туннелей и подземных сооружений. Рассматривается модель долговременной глубинной фильтрации с переменной пористостью и доступным потоком, и размерным механизмом задержания частиц. Строится глобальное асимптотическое решение во всей области, в которой происходит процесс фильтрации. Найденная асимптотика всюду близка к численному решению.

Ключевые слова: долговременная глубинная фильтрация, пористая среда, взвешенные и осажденные частицы, математическая модель, глобальная асимптотика

1. INTRODUCTION

Construction of tunnels and underground structures construction requires strengthening the soil and creation of watertight partitions protecting the structures from ground and flood waters. When pumping a liquefied solution of concrete into a porous soil, the grout penetrates into the pores and is filtered by porous rock. After drying and hardening of grout, the soil becomes durable and waterproof [1, 2].

When filtering the suspension in a porous medium, part of the solid particles is transferred from the inlet to the outlet of a porous sample, and some particles get stuck in the pores and form a deposit. Particles retention is influenced by different forces depending on the chemical and physical composition of the porous medium and suspension. There are many different filtration models with various mechanisms for the transport and deposition of particles [3-5]. If the size distribution of particles and pores overlap, then the main reason for particle retention becomes size-exclusion: solid suspended particles freely pass through large pores and get stuck at the inlet of small pores [6].

The classical mathematical model of deep bed filtration includes the mass balance equation for suspended and retained particles and the kinetic equation for deposit growth [7]. With a relative-

ly small number of solid particles in suspension, deposit growth is proportional to the first degree of suspended particles concentration. In the general case the proportionality coefficient between the growth rate of the deposit and the suspended concentration depends nonlinearly on the retained particles concentration and is called the filtration coefficient. The exact solution of this problem was obtained in [8].

More complex filtration models suggest that the porosity and the fractional flow are not constant, but depend on retained particles concentration [9]. For a complicated system of equations, local asymptotic solutions were obtained near the porous medium inlet, on the concentrations front, and for large time [10–12]. However, it is not possible to construct a global asymptotics on the basis of these solutions, since the applicability domains of local asymptotics do not cover the entire zone in which the system of equations is considered.

In this paper, a new method for constructing a global asymptotic solution has been developed. On its basis, the global asymptotics of the deep bed filtration problem of a monodisperse suspension in a homogeneous porous medium is obtained. Coordinate transformation leads to a variable that is small in the entire filtration zone. The global asymptotic solution is constructed as a series in powers of the new variable. The asymptotics is compared with the numerical solution obtained by the finite difference method [13-15]. The calculations show that the asymptotic and numerical solutions are close in the entire filtration zone.

2. MATHEMATICAL MODEL

A one-dimensional model of deep bed filtration of suspensions and colloids in a porous medium with variable porosity and fractional flow in the domain $\Omega = \{0 \le x \le 1,\ t \ge 0\}$ is determined by a quasilinear hyperbolic system of two first-order equations

$$\frac{\partial}{\partial t}\big(\mathrm{g}(S)C\big) + \frac{\partial}{\partial x}\big(f(S)C\big) + \frac{\partial S}{\partial t} = 0; \qquad (1)$$

$$\frac{\partial S}{\partial t} = \Lambda(S)C. \qquad (2)$$

Here $g(S)$, $f(S)$ are smooth positive functions for $S \ge 0$; the blocking filtration coefficient $\Lambda(S)$ is positive for $0 \le S < S_{\max}$ and turns to zero for $S = S_{\max}$; unknown functions $C(x,t)$; $S(x,t)$ are concentrations of suspended and retained particles.

The unique solution to the system (1), (2) is determined by the initial and boundary conditions

$$C\big|_{x=0} = 1; \qquad (3)$$

$$C\big|_{t=0} = 0; \quad S\big|_{t=0} = 0. \qquad (4)$$

Condition (3) means that a suspension of constant concentration is injected at the inlet of the porous medium; condition (4) corresponds to the absence of suspended and retained particles in the porous medium at the initial moment.

The concentrations front of suspended and retained particles moves in a porous medium from the inlet to the outlet at a constant velocity $v = f(0)/g(0)$ and is determined by formula $t = \alpha x,\ \alpha = g(0)/f(0)$.

Before the front in the domain $\Omega_0 = \{0 \le x \le 1,\ 0 \le t \le \alpha x\}$, the porous medium is empty, and the problem has a zero solution. Behind the concentration front in the domain $\Omega_S = \{0 \le x \le 1,\ t \ge \alpha x\}$, the porous medium contains suspended and retained particles, and the solution is positive. Since conditions (3) and (4) are not consistent at the origin, the solution $C(x,t)$ is discontinuous on the concentration front; the solution $S(x,t)$ is continuous in the domain Ω and vanishes on the front

$$S\big|_{t=\alpha x} = 0. \qquad (5)$$

In the domain Ω_S, the solution of the original problem (1) - (4) coincides with the solution of problem (1) - (3), (5).

For constant coefficients $g = g_0,\ f = f_0$ of equation (1) and linear blocking filtration coefficient (Langmuir coefficient)

$$\Lambda(S) = a - bS; \quad a > 0,\ b > 0, \tag{6}$$

the simplified problem (1) - (3), (5) in the domain Ω_S has an exact solution

$$C(x,t) = \frac{e^{b(t-\alpha x)}}{e^{b(t-\alpha x)} + e^{\alpha x/f_0} - 1};$$
$$S(x,t) = \frac{a}{b} \cdot \frac{e^{b(t-\alpha x)} - 1}{e^{b(t-\alpha x)} + e^{\alpha x/f_0} - 1}. \tag{7}$$

In the general case, the exact solution of problem (1) - (3), (5) cannot be written down by explicit formulas [16]; therefore, asymptotics are constructed.

In characteristic variables $\tau = t - \alpha x,\ y = x$, the concentration front is given by the equation $\tau = 0$. In the half-strip $\Omega' = \{0 \le y \le 1,\ \tau \ge 0\}$, problem (1) - (3), (5). takes the form

$$\frac{\partial\left(\left(g(S) - \alpha f(S)\right)C\right)}{\partial\tau} + \frac{\partial\left(f(S)C\right)}{\partial y} + \frac{\partial S}{\partial\tau} = 0; \tag{8}$$

$$\frac{\partial S}{\partial\tau} = \Lambda(S)C; \tag{9}$$

$$C\big|_{y=0} = 1; \quad S\big|_{\tau=0} = 0. \tag{10}$$

Near the concentration front, the local asymptotic solution of the problem (8) - (10) is constructed using the small parameter τ.

3. ASYMPTOTIC SOLUTION

A change of variables in the system (8) - (10)

$$z = 1 - e^{-ay/f_0};\ T = 1 - e^{-b\tau} \tag{11}$$

allows to use z as a small parameter, because for $(y,\tau) \in \Omega'$ the variables z, T belong to the domain $\Omega'' = \{0 \le z \le 1 - e^{a/f_0} < 1,\ 0 \le T < 1\}$.

In the new variables, the solution (7) of the simplified problem takes the form

$$C(z,\tau) = \frac{1-z}{1-zT}; \qquad S(z,\tau) = \frac{a}{b} \cdot \frac{(1-z)T}{1-zT}. \tag{12}$$

Assume that the coefficients of equation (8) are almost constant, and the filtration coefficient differs little from a linear function:

$$g(S) = g_0 + \varepsilon SG(S);$$
$$f(S) = f_0 + \varepsilon SF(S); \tag{13}$$
$$\Lambda(S) = a - bS + \varepsilon S^2\lambda(S)$$

Here $\varepsilon > 0$ is a small parameter.

In the domain Ω'' the problem (8)-(10) takes the form

$$b(1-T)\varepsilon S\left(G(S) - \alpha F(S)\right)\frac{\partial C}{\partial T} + a(1-z)\left(1 + \varepsilon\frac{SF(S)}{f_0}\right)\frac{\partial C}{\partial z} +$$
$$+\left(\varepsilon\left(SG(S) - \alpha SF(S)\right)'\Lambda(S)C + \varepsilon\left(SF(S)\right)'\frac{a}{f_0}(1-z)\frac{\partial S}{\partial z} + \Lambda(S)\right)C = 0; \tag{14}$$

$$b(1-T)\frac{\partial S}{\partial T} = \left(a - bS + \varepsilon S^2\lambda(S)\right)C \tag{15}$$

$$C\big|_{z=0} = 1; \quad S\big|_{T=0} = 0 \tag{16}$$

A solution of equations (8)-(10) is obtained in the form of a double series in powers of ε, z:

$$C(\varepsilon,z,T)=1+\sum_{i=0}^{n}\sum_{j=1}^{m}c_{i,j}(T)\varepsilon^i z^j/j!=1+z(c_{0,1}+\varepsilon c_{1,1}+\varepsilon^2 c_{2,1}+...)+$$
$$+\frac{z^2}{2}(c_{0,2}+\varepsilon c_{1,2}+\varepsilon^2 c_{2,2}+...)+...; \quad (17)$$

$$S(\varepsilon,z,T)=\sum_{i=0}^{n}\sum_{j=0}^{m}s_{i,j}(T)\varepsilon^i z^j/j!=(s_{0,0}+\varepsilon s_{1,0}+\varepsilon^2 s_{2,0}+...)+$$
$$+z(s_{0,1}+\varepsilon s_{1,1}+\varepsilon^2 s_{2,1}+...)+\frac{z^2}{2}(s_{0,2}+\varepsilon s_{1,2}+\varepsilon^2 s_{2,2}+...)+... . \quad (18)$$

The coefficients $c_{i,j}$, $s_{i,j}$ depend only on T.

From conditions (16): $c_{i,0}=0;\quad s_{ij}\big|_{T=0}=0$.

Substituting the expansions (17), (18) into equations (14), (15) and equating the terms with the same degrees of ε, z, implies a recurrent system of differential and algebraic equations

$$\varepsilon^0 z^0:\ b(1-T)s'_{0,0}=(a-bs_{0,0})\cdot 1;$$
$$\varepsilon^0 z^0:\ ac_{0,1}+(a-bs_{0,0})\cdot 1=0;$$
$$\varepsilon^0 z^1:\ b(1-T)s'_{0,1}=-bs_{0,1}\cdot 1+(a-bs_{0,0})c_{0,1};$$
$$\varepsilon^0 z^1:\ ac_{0,2}-ac_{0,1}-bs_{0,1}\cdot 1+(a-bs_{0,0})c_{0,1}=0;$$
$$\varepsilon^1 z^0:\ b(1-T)s'_{1,0}=\left(-bs_{1,0}+s_{0,0}^2\lambda(s_{0,0})\right)\cdot 1+(a-bs_{0,0})\cdot 0;$$
$$\varepsilon^1 z^0:\ ac_{1,1}+a\frac{s_{0,0}F(s_{0,0})}{f_0}c_{0,1}+\left(SG(S)-\alpha SF(S)\right)'\Big|_{S=s_{0,0}}\cdot(a-bs_{0,0})\cdot 1+$$
$$+\left(SF(S)\right)'\Big|_{S=s_{0,0}}\frac{a}{f_0}s_{0,1}+\left(-bs_{1,0}+s_{0,0}^2\lambda(s_{0,0})\right)\cdot 1+(a-bs_{0,0})\cdot 0=0;$$
$$\varepsilon^1 z^1:\ b(1-T)s'_{1,1}=-bs_{1,1}+\left(S^2\lambda(S)\right)'\Big|_{S=s_{0,0}}\cdot s_{0,1}-bs_{1,0}c_{0,1}+(a-bs_{0,0})c_{1,1}+s_{0,0}^2\lambda(s_{0,0})c_{0,1}.$$

Solving equations sequentially, the coefficients of expansions (17), (18) are obtained

$$s_{0,0}=\frac{a}{b}T;\quad c_{0,1}=T-1;\quad s_{0,1}=\frac{a}{b}T(T-1);$$
$$c_{0,2}=2T(T-1);\quad ....$$

Since the parameters ε, z are small in the entire domain Ω'', the expansions (17), (18) determine the global asymptotic solution of problem (14) - (16) in the domain Ω''.

4. NUMERICAL CALCULATION

The calculations were performed for the coefficients calculated in the laboratory of the University of Adelaide (Australia) in the study of deep bed filtration of a monodisperse suspension with particles of radius $r=2.179$ μm in a homogeneous porous medium [10]

$$g(S)=0.9743-8.88\cdot 10^{-14}S+1.27\cdot 10^{-11}S^2-1.24\cdot 10^{-9}S^3;$$
$$f(S)=0.9947+6.27\cdot 10^{-5}S-2.9\cdot 10^{-8}S^2+6.21\cdot 10^{-10}S^3; \quad (19)$$
$$\Lambda(S)=0.51-5.956\cdot 10^{-3}S+2.29\cdot 10^{-6}S^2+1.35\cdot 10^{-8}S^3.$$

In expansions (17), (18) of the nonlinear problem (14) - (16), terms were calculated up to ε^1 and z^5. The asymptotics was compared with a numerical calculation performed by the finite difference method. The equations (1), (2) was approximated by an original second-order scheme using the trapezium method [17]. The obtained solution was compared with the exact solution (7) of the simplified problem with a linear filtration coefficient.

Figures 1-5 show graphs of global asymptotics (red line), numerical solution (blue line), and exact solution (7) (green line). Full graph images are in the center of Fig. 1–4; their enlarged fragments are shown on the left and right.

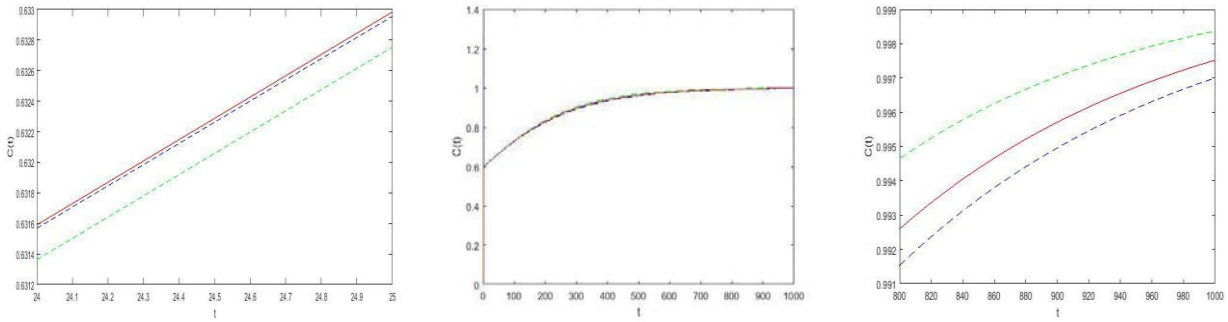

Figure 1. Graphs of suspended particles concentration $C(1,t)$ at the porous medium outlet.

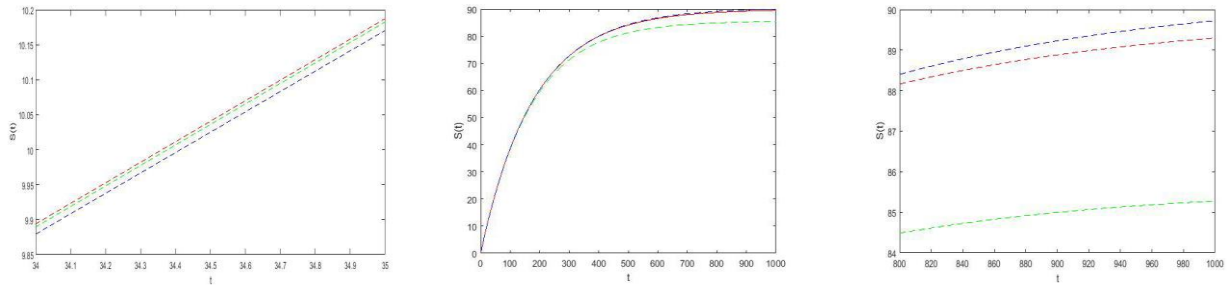

Figure 2. Graphs of retained particles concentration $S(1,t)$ at the porous medium outlet.

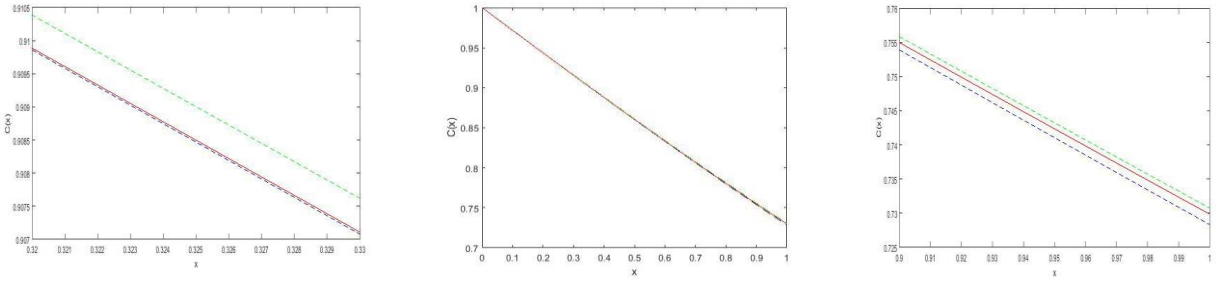

Figure 3. Graphs of suspended particles concentration $C(x,100)$ at the fixed moment $t=100$.

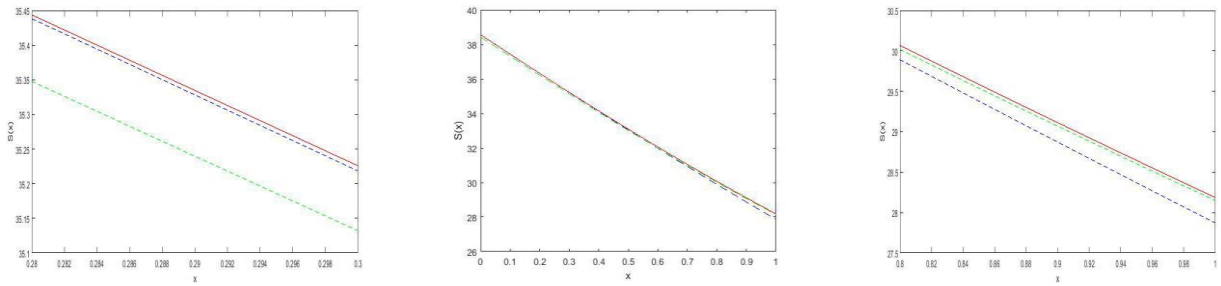

Figure 4. Graphs of retained particles concentration $S(x,100)$ at the fixed moment $t=100$.

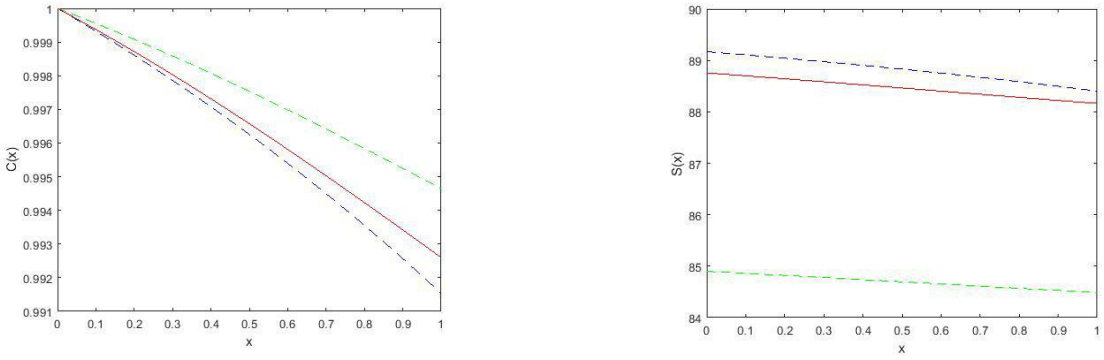

a) $C(x,800)$ b) $S(x,800)$

Figure 5. Graphs of suspended and retained particles concentration at the fixed moment $t = 800$.

Graphs of global asymptotics and numerical solutions are close to each other, the discrepancy increases with increasing coordinate x. The greatest deviation is observed at the outlet $x = 1$ at time $t = 200$: 1,6% for C and 1,1% for S. The graphs of the exact solution (7) for the linear case are further away from the numerical solution than the asymptotic graphs.

5. CONCLUSION

A mathematical model of deep bed filtration with variable porosity and fractional flow does not have an exact solution in explicit form. Asymptotic and numerical methods are used to obtain the solution.

The global asymptotics approximates well the solution in the entire domain in which the suspension or colloid is filtered. Deviation increases with time.

The exact solution (7) of the simplified problem is not suitable for approximating the solution of a complex system.

The global asymptotics extends the possibilities of solving the inverse filtration problem — determining the coefficients (19) of system (1) - (4) from a known suspended particles concentration at the porous medium outlet [18–20].

The obtained asymptotic solutions can be used to fine-tune laboratory experiments [21], which significantly reduces the amount and cost of research.

REFERENCES

1. **Tsuji M., Kobayashi S., Mikake S., Sato T., Matsui H.** Post-Grouting Experiences for Reducing Groundwater Inflow at 500 m Depth of the Mizunami Underground Research Laboratory, Japan. // *Procedia Engineering*, 2017, vol. 191, pp. 543–550.
2. **Lyapidevskaya O.** Grouting mortar for annular injection. // *MATEC Web of Conferences*, 2018, vol. 251, 01004.
3. **Bedrikovetsky P.** Mathematical theory of oil and gas recovery: with applications to ex-USSR oil and gas fields. Springer Science & Business Media, 2013.
4. **Civan F.** Reservoir formation damage, third ed. Gulf Professional Publishing, Burlington, MA, USA, 2014.
5. **Tien C., Ramarao B.V.** Granular filtration of aerosols and hydrosols. Amsterdam, Elsevier, 2007.
6. **Badalyan A., You Z., Aji K., Bedrikovetsky P., Carageorgos T., Zeinijahromi A.** Size exclusion deep bed filtration: Experimental and modelling uncertainties. // *Review of Scientific Instruments*, 2014, vol. 85(1), 015111.
7. **Herzig J.P., Leclerc D.M., Legoff P.** Flow of suspensions through porous media - application to deep filtration. // *Industrial and Engineering Chemistry*, 1970, vol. 62(5), pp. 8-35.
8. **Vyazmina E.A., Bedrikovetskii P.G., Polyanin A.D.** New classes of exact

solutions to nonlinear sets of equations in the theory of filtration and convective mass transfer. // *Theoretical Foundations of Chemical Engineering*, 2007, vol. 41(5), pp. 556-564.
9. **Bedrikovetsky P.** Upscaling of stochastic micro model for suspension transport in porous media. // *Transport in Porous Media*, 2008, vol. 75, pp. 335-369.
10. **You Z., Osipov Y., Bedrikovetsky P., Kuzmina L.** Asymptotic model for deep bed filtration. // *Chemical Engineering Journal*, 2014, vol. 258, pp. 374-385.
11. **Kuzmina L.I., Osipov Yu.V.** Particle transportation at the filter inlet. // *International Journal for Computational Civil and Structural Engineering*, 2014, Volume 10, Issue 3, pp. 17-22.
12. **Kuzmina L.I., Osipov Yu.V.** Asymptotic model of filtration in almost stationary mode. // *International Journal for Computational Civil and Structural Engineering*, 2016, Volume 12, Issue 1, pp. 158-163.
13. **Toro E.F.** Riemann solvers and numerical methods for fluid dynamics. Dordrecht, Springer, 2009.
14. **Galaguz Y.P.** Realization of the TVD-scheme for a numerical solution of the filtration problem. // *International Journal for Computational Civil and Structural Engineering*, 2017, Volume 13, Issue 2, pp. 93-102.
15. **Galaguz Y.P., Safina G.L.** Modeling of fine migration in a porous medium. // *MATEC Web of Conferences*, 2016, vol. 86, 03003.
16. **Bedrikovetsky P., You Z., Badalyan A., Osipov Y., Kuzmina L.** Analytical model for straining-dominant large-retention depth filtration. // *Chemical Engineering Journal*, 2017, vol. 330, pp. 1148-1159.
17. **Osipov Yu., Safina G., Galaguz Yu.** Calculation of the filtration problem by finite differences methods. // *MATEC Web of Conferences*, 2018, vol. 251, 04021.
18. **Alvarez A.C., Bedrikovetsky P.G., Hime G., Marchesin A.O., Marchesin D., Rodrigues J.R.** A fast inverse solver for the filtration function for flow of water with particles in porous media. // *Inverse Problems*, 2006, vol. 22, pp. 69-88.
19. **Alvarez A.C., Hime G., Marchesin D., Bedrikovetsky P.G.** The inverse problem of determining the filtration function and permeability reduction in flow of water with particles in porous media. // Transport in Porous Media, 2007, vol. 70(1), pp. 43-62.
20. **Alvarez A.C., Hime G., Silva J.D., Marchesin D.** Analytic regularization of an inverse filtration problem in porous media. // *Inverse Problems*, 2013, vol. 29, 025006.
21. **Vaz A., Bedrikovetsky P., Fernandes P.D., Badalyan A., Carageorgos T.** Determining model parameters for non-linear deep-bed filtration using laboratory pressure measurements. // *Journal of Petroleum Science and Engineering*, 2017, vol. 151, pp. 421-433.

СПИСОК ЛИТЕРАТУРЫ

1. **Tsuji M., Kobayashi S., Mikake S., Sato T., Matsui H.** Post-Grouting Experiences for Reducing Groundwater Inflow at 500 m Depth of the Mizunami Underground Research Laboratory, Japan. // *Procedia Engineering*, 2017, vol. 191, pp. 543–550.
2. **Lyapidevskaya O.** Grouting mortar for annular injection. // *MATEC Web of Conferences*, 2018, vol. 251, 01004.
3. **Bedrikovetsky P.** Mathematical theory of oil and gas recovery: with applications to ex-USSR oil and gas fields. Springer Science & Business Media, 2013.
4. **Civan F.** Reservoir formation damage, third ed. Gulf Professional Publishing, Burlington, MA, USA, 2014.
5. **Tien C., Ramarao B.V.** Granular filtration of aerosols and hydrosols. Amsterdam, Elsevier, 2007.
6. **Badalyan A., You Z., Aji K., Bedrikovetsky P., Carageorgos T., Zeinijahromi**

A. Size exclusion deep bed filtration: Experimental and modelling uncertainties. // *Review of Scientific Instruments*, 2014, vol. 85(1), 015111.

7. **Herzig J.P., Leclerc D.M., Legoff P.** Flow of suspensions through porous media - application to deep filtration. // *Industrial and Engineering Chemistry*, 1970, vol. 62(5), pp. 8-35.
8. **Vyazmina E.A., Bedrikovetskii P.G., Polyanin A.D.** New classes of exact solutions to nonlinear sets of equations in the theory of filtration and convective mass transfer. // *Theoretical Foundations of Chemical Engineering*, 2007, vol. 41(5), pp. 556-564.
9. **Bedrikovetsky P.** Upscaling of stochastic micro model for suspension transport in porous media. // *Transport in Porous Media*, 2008, vol. 75, pp. 335-369.
10. **You Z., Osipov Y., Bedrikovetsky P., Kuzmina L.** Asymptotic model for deep bed filtration. // *Chemical Engineering Journal*, 2014, vol. 258, pp. 374-385.
11. **Kuzmina L.I., Osipov Yu.V.** Particle transportation at the filter inlet. // *International Journal for Computational Civil and Structural Engineering*, 2014, Volume 10, Issue 3, pp. 17-22.
12. **Kuzmina L.I., Osipov Yu.V.** Asymptotic model of filtration in almost stationary mode. // *International Journal for Computational Civil and Structural Engineering*, 2016, Volume 12, Issue 1, pp. 158-163.
13. **Toro E.F.** Riemann solvers and numerical methods for fluid dynamics. Dordrecht, Springer, 2009.
14. **Galaguz Y.P.** Realization of the TVD-scheme for a numerical solution of the filtration problem. // *International Journal for Computational Civil and Structural Engineering*, 2017, Volume 13, Issue 2, pp. 93-102.
15. **Galaguz Y.P., Safina G.L.** Modeling of fine migration in a porous medium. // *MATEC Web of Conferences*, 2016, vol. 86, 03003.
16. **Bedrikovetsky P., You Z., Badalyan A., Osipov Y., Kuzmina L.** Analytical model for straining-dominant large-retention depth filtration. // *Chemical Engineering Journal*, 2017, vol. 330, pp. 1148-1159.
17. **Osipov Yu., Safina G., Galaguz Yu.** Calculation of the filtration problem by finite differences methods. // *MATEC Web of Conferences*, 2018, vol. 251, 04021.
18. **Alvarez A.C., Bedrikovetsky P.G., Hime G., Marchesin A.O., Marchesin D., Rodrigues J.R.** A fast inverse solver for the filtration function for flow of water with particles in porous media. // *Inverse Problems*, 2006, vol. 22, pp. 69-88.
19. **Alvarez A.C., Hime G., Marchesin D., Bedrikovetsky P.G.** The inverse problem of determining the filtration function and permeability reduction in flow of water with particles in porous media. // Transport in Porous Media, 2007, vol. 70(1), pp. 43-62.
20. **Alvarez A.C., Hime G., Silva J.D., Marchesin D.** Analytic regularization of an inverse filtration problem in porous media. // *Inverse Problems*, 2013, vol. 29, 025006.
21. **Vaz A., Bedrikovetsky P., Fernandes P.D., Badalyan A., Carageorgos T.** Determining model parameters for non-linear deep-bed filtration using laboratory pressure measurements. // *Journal of Petroleum Science and Engineering*, 2017, vol. 151, pp. 421-433.

Lyudmila I. Kuzmina, Candidate of Physical and Mathematical Sciences, Associate Professor, Department of Applied Mathematics, National Research University Higher School of Economics; 20, Myasnitskaya st., Moscow, 101000, Russia; phone +7(495) 7729590 15219;
E-mail: lkuzmina@hse.ru.

Yuri V. Osipov, Candidate of Physical and Mathematical Sciences, Associate Professor, Department of Applied Mathematics, National Research Moscow State University of Civil Engineering; 26, Yaroslavskoe Shosse, Moscow, 129337, Russia; phone +7(499)1835994;
E-mail: yuri-osipov@mail.ru.

Yulia G. Zheglova, Assistant Professor, Department of Applied Mathematics, National Research Moscow State University of Civil Engineering; 26, Yaroslavskoe Shosse, Moscow, 129337, Russia;
phone +7(499)1835994;
E-mail: uliagermanovna@yandex.ru.

Кузьмина Людмила Ивановна, доцент, кандидат физико-математических наук, Департамент прикладной математики, Национальный исследовательский университет «Высшая школа экономики»; 101000, г. Москва, ул. Мясницкая, д. 20, тел. +7(495) 77295 90 *15219; e-mail: lkuzmina@hse.ru.

Осипов Юрий Викторович, доцент, кандидат физико-математических наук; кафедра прикладной математики, Национальный исследовательский Московский государственный строительный университет; 129337, Россия, г. Москва, Ярославское шоссе, д. 26; тел. +7(499)1835994; e-mail: yuri-osipov@mail.ru.

Жеглова Юлия Германовна, преподаватель; кафедра прикладной математики, Национальный исследовательский Московский государственный строительный университет; 129337, Россия, г. Москва, Ярославское шоссе, д. 26; тел. +7(499)1835994;
E-mail: uliagermanovna@yandex.ru.

DOI:10.22337/2587-9618-2019-15-2-86-94

THE DISCRETE-LINEAR AND THE DISCRETE-CONTINUOUS MODELS OF THE NONLINEAR OBJECT MANAGING IN WIDE RANGE OF OPERATING MODES

Roman L. Leibov
Moscow Aviation Institute (National Research University), Moscow, RUSSIA

Abstract: The article deals with the features of calculating the vector and matrix parameters of a discrete-continuous model using the vector and matrix parameters of a discrete-linear model in a wide range of operating modes of a nonlinear object of management. The results of the application of the proposed approach for creating a discrete-continuous model of an aircraft gas-turbine engine are given.

Keywords: nonlinear object of managing, discrete-linear model, discrete-continuous model, wide range of operation modes

КУСОЧНО-ЛИНЕЙНАЯ И КУСОЧНО-НЕПРЕРЫВНАЯ МОДЕЛИ НЕЛИНЕЙНОГО ОБЪЕКТА УПРАВЛЕНИЯ В ШИРОКОМ ДИАПАЗОНЕ РЕЖИМОВ РАБОТЫ

Р.Л. Лейбов
Московский авиационный институт (национальный исследовательский университет),
г. Москва, РОССИЯ

Аннотация: В настоящей статье рассмотрены особенности расчета векторных и матричных параметров кусочно-непрерывной модели с помощью векторных и матричных параметров кусочно-линейной модели в широком диапазоне режимов работы нелинейного объекта управления. Приведены результаты применения предлагаемого подхода при создании кусочно-непрерывной модели авиационного газотурбинного двигателя.

Ключевые слова: нелинейный объект управления, кусочно-линейная модель, кусочно-непрерывная модель, широкий диапазон режимов работы

1. INTRODUCTION

If we develop algorithms for detecting, localizing, specifying, and countering failures of digital automatic control systems (DACS), as well as for evaluating the robustness of these systems and algorithms, it is necessary to use linear models of nonlinear control objects [1]. The matrix parameters of linear and piecewise linear models are estimated by transient processes of nonlinear models of managing objects [1], [2]. The matrix parameters of the discrete-continuous model can also be evaluated by the transition processes of the nonlinear model [3]. In addition, the vector and matrix parameters of the discrete-continuous model can be calculated using the vector and matrix parameters of the original discrete-linear model. The discrete-continuous model, in its turn, makes it possible to construct various new discrete-linear models consisting of an arbitrary number of linear models, which can alternate each other with arbitrary frequency, for example, at each step of DACS operation. This paper describes the features of calculating the vector and matrix parameters of a discrete-continuous model using vector and matrix parameters of the original discrete-linear model in a wide range of operating modes of a nonlinear object of managing.

2. NONLINEAR, LINEAR, DISCRETE-LINEAR AND DISCRETE-CONTINUOUS MODELS OF NONLINEAR OBJECT OF MANAGING

A nonlinear model of managed object takes the following form [1], [2], [3]

$$\dot{\mathbf{x}} = \mathbf{f}\left(\mathbf{x}^{\mathrm{p}}, \mathbf{u}^{\mathrm{p}}, \mathbf{w}^{\mathrm{p}}\right), \tag{1}$$

where $\mathbf{x}^{\mathrm{p}}$ is vector of state, $\mathbf{u}^{\mathrm{p}}$ is vector of managing, $\mathbf{w}^{\mathrm{p}}$ is vector of external impacts, and $\mathbf{f}$ is nonlinear real vector function. The coordinates of the state vector (state variables) of such an object of managing, for example, an aviation gas-turbine engine (GTE), are rotor rotation frequencies, temperatures and pressures in different sections of the flow-through part of the engine. The coordinates of the control vector (control variables) are fuel consumption, variable geometrical characteristics of the flow part of the engine, in particular, the critical area of the jet nozzle and the angles of rotation of the fan directing equipment and the compressor. The coordinates of the vector of external impacts (variable external impacts) is the angle of deviations of the engine control lever (control action), as well as the height and speed of flight (variable external conditions). The constant control action and the external conditions included in the ${}_{\mathrm{s}}\mathbf{w}^{\mathrm{p}}$, vector determining the steady state of engine operation (operating point), which corresponds to the vector of steady-state values of control variables ${}_{\mathrm{s}}\mathbf{u}^{\mathrm{p}}$ and the steady-state vector of state variables ${}_{\mathrm{s}}\mathbf{x}^{\mathrm{p}}$.

In a small neighborhood of an arbitrary steady state, a nonlinear control object can be approximately described [1] using a linear model in the form of normalized deviations from steady values

$$\dot{\mathbf{x}}^{\mathrm{n}} = \mathbf{A}\left(\mathbf{x}^{\mathrm{n}} - {}_{\mathrm{s}}\mathbf{x}^{\mathrm{n}}\right) + \mathbf{B}\left(\mathbf{u}^{\mathrm{n}} - {}_{\mathrm{s}}\mathbf{u}^{\mathrm{n}}\right), \tag{2}$$

where

$$x_i^{\mathrm{n}} - {}_{\mathrm{s}}x_i^{\mathrm{n}} = \frac{x_i^{\mathrm{p}} - {}_{\mathrm{s}}x_i^{\mathrm{p}}}{\max\left|{}_{\mathrm{s}}x_i^{\mathrm{p}}\right|}, \quad i = 1,\ldots,n, \tag{3}$$

$$u_i^{\mathrm{n}} - {}_{\mathrm{s}}u_i^{\mathrm{n}} = \frac{u_i^{\mathrm{p}} - {}_{\mathrm{s}}u_i^{\mathrm{p}}}{\max\left|{}_{\mathrm{s}}u_i^{\mathrm{p}}\right|}, \quad i = 1,\ldots,m, \tag{4}$$

$\mathbf{A}$ and $\mathbf{B}$ are matrixes of dynamic linear model for observed steady mode.

For steady values of normalized deviations it takes the following form

$$\left(\mathbf{x}^{\mathrm{n}} - {}_{\mathrm{s}}\mathbf{x}^{\mathrm{n}}\right) = \mathbf{S}\left(\mathbf{u}^{\mathrm{n}} - {}_{\mathrm{s}}\mathbf{u}^{\mathrm{n}}\right), \tag{5}$$

$$\mathbf{0} = \mathbf{A}\left(\mathbf{x}^{\mathrm{n}} - {}_{\mathrm{s}}\mathbf{x}^{\mathrm{n}}\right) + \mathbf{B}\left(\mathbf{u}^{\mathrm{n}} - {}_{\mathrm{s}}\mathbf{u}^{\mathrm{n}}\right). \tag{6}$$

From where the matrix of static linear model is

$$\mathbf{S} = -\mathbf{A}^{-1}\mathbf{B}, \tag{7}$$

Thus, we have

$$\mathbf{B} = -\mathbf{A}\mathbf{S}. \tag{8}$$

If the discreteness step is small enough, then at discrete points in time we can approximately assume that

$$\mathbf{x}^{\mathrm{n}}\left(t_{k+1}\right) = \mathbf{x}^{\mathrm{n}}\left(t_k\right) + \Delta t\,\mathbf{A}\left[\mathbf{x}^{\mathrm{n}}\left(t_k\right) - {}_{\mathrm{s}}\mathbf{x}^{\mathrm{n}}\right] + \Delta t\,\mathbf{B}\left[\mathbf{u}^{\mathrm{n}}\left(t_k\right) - {}_{\mathrm{s}}\mathbf{u}^{\mathrm{n}}\right], \tag{9}$$

$k = 0, 1, 2,\ldots$ corresponds to discrete moments of time $t_0, t_1, t_2,\ldots$, at that $t_{k+1} = t_k + \Delta t$, where Δt is discreteness step.

The set of linear models for all selected steady-state modes is a discrete-linear model

$$\dot{\mathbf{x}}^{\mathrm{n}} = {}^{r_1\ldots r_m}\mathbf{A}\left(\mathbf{x}^{\mathrm{n}} - {}^{r_1\ldots r_m}_{\mathrm{s}}\mathbf{x}^{\mathrm{n}}\right) + {}^{r_1\ldots r_m}\mathbf{B}\left(\mathbf{u}^{\mathrm{n}} - {}^{r_1\ldots r_m}_{\mathrm{s}}\mathbf{u}^{\mathrm{n}}\right), \tag{10}$$

$$\mathbf{x}^{\mathrm{n}}\left(t_{k+1}\right) = \mathbf{x}^{\mathrm{n}}\left(t_k\right) + \Delta t\ {}^{r_1\ldots r_m}\mathbf{A}\left[\mathbf{x}^{\mathrm{n}}\left(t_k\right) - {}_{\mathrm{s}}\mathbf{x}^{\mathrm{n}}\right] + \Delta t\ {}^{r_1\ldots r_m}\mathbf{B}\left[\mathbf{u}^{\mathrm{n}}\left(t_k\right) - {}^{r_1\ldots r_m}_{\mathrm{s}}\mathbf{u}^{\mathrm{n}}\right], \quad k = 0,1,2,\ldots \tag{11}$$

$${}^{r_1\ldots r_m}\mathbf{B} = {}^{r_1\ldots r_m}\mathbf{A}\ {}^{r_1\ldots r_m}\mathbf{S}, \tag{12}$$

where

$$ {}^{r_1 \dots r_m}_{\mathrm{s}}\mathbf{u}^{\mathrm{n}} = \begin{bmatrix} {}^{r_1}_{\mathrm{s}}u_1^{\mathrm{n}} \\ \cdots \\ {}^{r_m}_{\mathrm{s}}u_m^{\mathrm{n}} \end{bmatrix}, \quad (13) $$

$$ r_1 \in (1,\dots,R_1),\dots,r_m \in (1,\dots,R_m), \quad (14) $$

and $R_1,\dots,R_m$ are equal to quantity of choosen steady values of each from m variables of the equation.

Vectors of normalized steady values of variables of control ${}_{\mathrm{s}}\mathbf{u}^{\mathrm{n}}$ and state variables ${}_{\mathrm{s}}\mathbf{x}^{\mathrm{n}}$, as well as matrixes **A** and **B**, involved into transition matrixes $\mathbf{I} + \Delta t\,\mathbf{A}$ and $\Delta t\,\mathbf{B}$ of discrete-continuous model [3], in this case can be determined as following

$$ {}_{\mathrm{s}}\mathbf{u}^{\mathrm{n}} = {}^{r_1 \dots r_m}_{\mathrm{s}}\mathbf{u}^{\mathrm{n}} + \theta\left({}^{\tilde{r}_1 \dots \tilde{r}_m}_{\mathrm{s}}\mathbf{u}^{\mathrm{n}} - {}^{r_1 \dots r_m}_{\mathrm{s}}\mathbf{u}^{\mathrm{n}}\right), \quad (15) $$

$$ {}_{\mathrm{s}}\mathbf{x}^{\mathrm{n}} = {}^{r_1 \dots r_m}_{\mathrm{s}}\mathbf{x}^{\mathrm{n}} + \theta\left({}^{\tilde{r}_1 \dots \tilde{r}_m}_{\mathrm{s}}\mathbf{x}^{\mathrm{n}} - {}^{r_1 \dots r_m}_{\mathrm{s}}\mathbf{x}^{\mathrm{n}}\right), \quad (16) $$

$$ \mathbf{A} = {}^{r_1 \dots r_m}\mathbf{A} + \theta\left({}^{\tilde{r}_1 \dots \tilde{r}_m}\mathbf{A} - {}^{r_1 \dots r_m}\mathbf{A}\right), \quad (17) $$

$$ \mathbf{B} = {}^{r_1 \dots r_m}\mathbf{B} + \theta\left({}^{\tilde{r}_1 \dots \tilde{r}_m}\mathbf{B} - {}^{r_1 \dots r_m}\mathbf{B}\right), \quad (18) $$

$$ 0 \le \theta = \theta\left(\mathbf{u}^{\mathrm{n}}, {}^{r_1 \dots r_m}_{\mathrm{s}}\mathbf{u}^{\mathrm{n}}, {}^{\tilde{r}_1 \dots \tilde{r}_m}_{\mathrm{s}}\mathbf{u}^{\mathrm{n}}\right) < 1 \;\Big|\; \left\| {}^{r_1 \dots r_m}_{\mathrm{s}}\mathbf{u}^{\mathrm{n}} \right\| \le \left\| \mathbf{u}^{\mathrm{n}} \right\| < \left\| {}^{\tilde{r}_1 \dots \tilde{r}_m}_{\mathrm{s}}\mathbf{u}^{\mathrm{n}} \right\|, $$

$$ \tilde{r}_1 \in (1,\dots,R_1),\dots,\tilde{r}_m \in (1,\dots,R_m). \quad (19) $$

3. CALCULATION EXAMPLE FOR VECTORS AND MATRIXES OF THE DISCRETE-CONTINUOUS MODEL

To determine the vectors and matrices of the discrete-continuous model, the vectors and matrixes of the discrete-linear model of the two-shaft double-circuit turbojet aviation GTE are used [1].

In this example (environmental variables), the altitude and speed (Mach number) of the flight of the aircraft (FA) are equal zero (ALT = 0, MN = 0), the values (control impact) of the deflection angle of the engine control leverage correspond to the operating modes of the GTE from the maximum ($\alpha_{\mathrm{lce}} = 68^\circ$) to the minimum ($\alpha_{\mathrm{lce}} = 15^\circ$). Four control variables ($m = 4$) correspond to the fuel consumption in the main combustion chamber G_{to}, the critical area of the jet nozzle F_{cr}, the angle of rotation of the fan directing equipment φ_{na} and the angle of rotation of the compressor directing equipment φ_{nak}. Five state variables of the control object ($n = 5$) correspond to the engine rotation frequency n_r, the engine compressor frequency n_c, the braking pressure behind the compressor P_c^*, the braking pressure behind the turbine P_t^* and the braking temperature behind the turbine T_t^*.

Let us assume [1] that the normalized control variables u_3^{n} and u_4^{n} change consistently with the control variable u_1^{n}, that is, approximately simultaneously these variables are on the boundaries of the neighboring acting areas of different linear models that are part of the discrete-linear model. Therefore, for all these three variables, let us to considering only $R_1 = 9$ selected steady-state values for the variable u_1^{n}. At the same time, the number of different considered steady-state values for the variables u_3^{n} and u_4^{n} equal to 5 and 7, respectively, since ones remain unchanged at the other working points.

Let us also assume that the control variable u_2^{n} changes in this way so that the number of selected steady-state values $R_2 = 9$.

Thus, the number of steady-state modes of operation of the considered discrete-linear model are $R_1 R_2 = 81$.

Vector and matrix parameters of the discrete-linear model, which is the source for creating a discrete-continuous model, are given in [1].

The vectors of steady-state values of control variables and state variables, as well as matrixes of linear models in the considered example, take the form

$$ {}^{r_1 r_2 r_3 r_4}_{\mathrm{s}}\mathbf{u}^{\mathrm{n}} = {}^{r_1 r_2}_{\mathrm{s}}\mathbf{u}^{\mathrm{n}}, \quad r_1 = r_3 = r_4 = 1,\dots,9, \quad r_2 = 1,\dots,9, $$

$$ {}^{r_1 r_2 r_3 r_4}_{\mathrm{s}}\mathbf{x}^{\mathrm{n}} = {}^{r_1 r_2}_{\mathrm{s}}\mathbf{x}^{\mathrm{n}}, \quad r_1 = r_3 = r_4 = 1,\dots,9, \quad r_2 = 1,\dots,9, $$

$$ {}^{r_1 r_2 r_3 r_4}_{\mathrm{s}}\mathbf{A}^{\mathrm{n}} = {}^{r_1 r_2}_{\mathrm{s}}\mathbf{A}^{\mathrm{n}}, \quad r_1 = r_3 = r_4 = 1,\dots,9, \quad r_2 = 1,\dots,9, $$

$$ {}^{r_1 r_2 r_3 r_4}_{\mathrm{s}}\mathbf{B}^{\mathrm{n}} = {}^{r_1 r_2}_{\mathrm{s}}\mathbf{B}^{\mathrm{n}}, \quad r_1 = r_3 = r_4 = 1,\dots,9, \quad r_2 = 1,\dots,9. $$

The acting areas of linear models, involved into discrete-linear model, is determined as following.

$$r_1 = 1 \quad : \quad u_1^{\mathrm{n}} \le {}_{\mathrm{s}}^{1}u_1^{\mathrm{n}},$$
$$r_1 = 2,...,9 \quad : \quad {}_{\mathrm{s}}^{r_1}u_1^{\mathrm{n}} \ge u_1^{\mathrm{n}} > {}_{\mathrm{s}}^{r_1-1}u_1^{\mathrm{n}},$$
$$r_1 = 9 \quad : \quad u_1^{\mathrm{n}} > {}_{\mathrm{s}}^{9}u_1^{\mathrm{n}},$$
$$r_2 = 1 \quad : \quad u_2^{\mathrm{n}} \ge {}_{\mathrm{s}}^{1}u_2^{\mathrm{n}},$$
$$r_2 = 2,...,9 \quad : \quad {}_{\mathrm{s}}^{r_2}u_2^{\mathrm{n}} \le u_2^{\mathrm{n}} < {}_{\mathrm{s}}^{r_2-1}u_2^{\mathrm{n}},$$
$$r_2 = 9 \quad : \quad u_2^{\mathrm{n}} < {}_{\mathrm{s}}^{9}u_2^{\mathrm{n}}.$$

If at some point in the transition process the control variables are outside the acting areas of the selected linear models, then the linear model, that has been used before, is used. At the same time, the matrixes of dynamic linear models for neighboring areas, where it is possible, are the same or close.

The vector of normalized steady-state values of the control variables ${}_{\mathrm{s}}\mathbf{u}^{\mathrm{n}}$ is assumed to be

$${}_{\mathrm{s}}\mathbf{u}^{\mathrm{n}} = \mathbf{u}^{\mathrm{n}}(t_{k-1}).$$

The vectors of normalized steady state variables ${}_{\mathrm{s}}\mathbf{x}^{\mathrm{n}}$, as well as matrixes $\mathbf{A}$ and $\mathbf{B}$, included in the transition matrixes $\mathbf{I} + \Delta t\,\mathbf{A}$ and $\Delta t\,\mathbf{B}$ of the discrete-continuous model, at the time t_k, $k = 1, 2, ...$ are calculated taking into account that

$$\mathbf{u}^{\mathrm{n}} = \mathbf{u}^{\mathrm{n}}(t_k).$$

Firstly we determine

$$r_1 = 1 \quad : \quad u_1^{\mathrm{n}} \le {}_{\mathrm{s}}^{1}u_1^{\mathrm{n}},$$
$${}_{\mathrm{s}}x_i^{\mathrm{n}}\left(u_1^{\mathrm{n}} \le {}_{\mathrm{s}}^{1}u_1^{\mathrm{n}},\ u_2^{\mathrm{n}} = {}_{\mathrm{s}}^{r_2}u_2^{\mathrm{n}}\right) = {}_{\mathrm{s}}^{1,r_2}x_i^{\mathrm{n}}, \quad i = 1,...,n,$$
$$\mathbf{A}\left(u_1^{\mathrm{n}} \le {}_{\mathrm{s}}^{1}u_1^{\mathrm{n}},\ u_2^{\mathrm{n}} = {}_{\mathrm{s}}^{r_2}u_2^{\mathrm{n}}\right) = {}^{1,r_2}\mathbf{A},$$
$$\mathbf{B}\left(u_1^{\mathrm{n}} \le {}_{\mathrm{s}}^{1}u_1^{\mathrm{n}},\ u_2^{\mathrm{n}} = {}_{\mathrm{s}}^{r_2}u_2^{\mathrm{n}}\right) = {}^{1,r_2}\mathbf{B},$$
$$r_1 = 2,...,9 \quad : \quad {}_{\mathrm{s}}^{r_1}u_1^{\mathrm{n}} \ge u_1^{\mathrm{n}} > {}_{\mathrm{s}}^{r_1-1}u_1^{\mathrm{n}},$$
$${}_{\mathrm{s}}x_i^{\mathrm{n}}\left({}_{\mathrm{s}}^{r_1}u_1^{\mathrm{n}} \ge u_1^{\mathrm{n}} > {}_{\mathrm{s}}^{r_1-1}u_1^{\mathrm{n}},\ u_2^{\mathrm{n}} = {}_{\mathrm{s}}^{r_2}u_2^{\mathrm{n}}\right) = {}^{r_1-1,r_2}{}_{\mathrm{s}}x_i^{\mathrm{n}} +$$
$$\left({}^{r_1 r_2}{}_{\mathrm{s}}x_i^{\mathrm{n}} - {}^{r_1-1,r_2}{}_{\mathrm{s}}x_i^{\mathrm{n}}\right) \Big/ \left({}_{\mathrm{s}}^{r_1}u_1^{\mathrm{n}} - {}_{\mathrm{s}}^{r_1-1}u_1^{\mathrm{n}}\right) \cdot \left(u_1^{\mathrm{n}} - {}_{\mathrm{s}}^{r_1-1}u_1^{\mathrm{n}}\right),$$
$$i = 1,...,n,$$
$$\mathbf{A}\left({}_{\mathrm{s}}^{r_1}u_1^{\mathrm{n}} \ge u_1^{\mathrm{n}} > {}_{\mathrm{s}}^{r_1-1}u_1^{\mathrm{n}},\ u_2^{\mathrm{n}} = {}_{\mathrm{s}}^{r_2}u_2^{\mathrm{n}}\right) = {}^{r_1-1,r_2}\mathbf{A} +$$
$$\left({}^{r_1 r_2}\mathbf{A} - {}^{r_1-1,r_2}\mathbf{A}\right) \Big/ \left({}_{\mathrm{s}}^{r_1}u_1^{\mathrm{n}} - {}_{\mathrm{s}}^{r_1-1}u_1^{\mathrm{n}}\right) \cdot \left(u_1^{\mathrm{n}} - {}_{\mathrm{s}}^{r_1-1}u_1^{\mathrm{n}}\right),$$
$$\mathbf{B}\left({}_{\mathrm{s}}^{r_1}u_1^{\mathrm{n}} \ge u_1^{\mathrm{n}} > {}_{\mathrm{s}}^{r_1-1}u_1^{\mathrm{n}},\ u_2^{\mathrm{n}} = {}_{\mathrm{s}}^{r_2}u_2^{\mathrm{n}}\right) = {}^{r_1-1,r_2}\mathbf{B} +$$
$$\left({}^{r_1 r_2}\mathbf{B} - {}^{r_1-1,r_2}\mathbf{B}\right) \Big/ \left({}_{\mathrm{s}}^{r_1}u_1^{\mathrm{n}} - {}_{\mathrm{s}}^{r_1-1}u_1^{\mathrm{n}}\right) \cdot \left(u_1^{\mathrm{n}} - {}_{\mathrm{s}}^{r_1-1}u_1^{\mathrm{n}}\right),$$
$$r_1 = 9 \quad : \quad u_1^{\mathrm{n}} > {}_{\mathrm{s}}^{9}u_1^{\mathrm{n}},$$
$${}_{\mathrm{s}}x_i^{\mathrm{n}}\left(u_1^{\mathrm{n}} > {}_{\mathrm{s}}^{9}u_1^{\mathrm{n}},\ u_2^{\mathrm{n}} = {}_{\mathrm{s}}^{r_2}u_2^{\mathrm{n}}\right) = {}^{9,r_2}{}_{\mathrm{s}}x_i^{\mathrm{n}}, \quad i = 1,...,n,$$
$$\mathbf{A}\left(u_1^{\mathrm{n}} > {}_{\mathrm{s}}^{9}u_1^{\mathrm{n}},\ u_2^{\mathrm{n}} = {}_{\mathrm{s}}^{r_2}u_2^{\mathrm{n}}\right) = {}^{9,r_2}\mathbf{A},$$
$$\mathbf{B}\left(u_1^{\mathrm{n}} > {}_{\mathrm{s}}^{9}u_1^{\mathrm{n}},\ u_2^{\mathrm{n}} = {}_{\mathrm{s}}^{r_2}u_2^{\mathrm{n}}\right) = {}^{9,r_2}\mathbf{B},$$
$$r_2 = 1,...,9,$$

Further we obtain

$$r_2 = 1 \quad : \quad u_2^{\mathrm{n}} \ge {}_{\mathrm{s}}^{1}u_2^{\mathrm{n}},$$
$$r_1 = 1,$$
$${}_{\mathrm{s}}x_i^{\mathrm{n}} = {}_{\mathrm{s}}x_i^{\mathrm{n}}\left(u_1^{\mathrm{n}} \le {}_{\mathrm{s}}^{1}u_1^{\mathrm{n}},\ u_2^{\mathrm{n}} \ge {}_{\mathrm{s}}^{1}u_2^{\mathrm{n}}\right) = {}^{11}{}_{\mathrm{s}}x_i^{\mathrm{n}}, \quad i = 1,...,n,$$
$$\mathbf{A} = \mathbf{A}\left(u_1^{\mathrm{n}} \le {}_{\mathrm{s}}^{1}u_1^{\mathrm{n}},\ u_2^{\mathrm{n}} \ge {}_{\mathrm{s}}^{1}u_2^{\mathrm{n}}\right) = {}^{11}\mathbf{A},$$
$$\mathbf{B} = \mathbf{B}\left(u_1^{\mathrm{n}} \le {}_{\mathrm{s}}^{1}u_1^{\mathrm{n}},\ u_2^{\mathrm{n}} \ge {}_{\mathrm{s}}^{1}u_2^{\mathrm{n}}\right) = {}^{11}\mathbf{B},$$
$$r_1 = 2,...,9,$$
$${}_{\mathrm{s}}x_i^{\mathrm{n}} = {}_{\mathrm{s}}x_i^{\mathrm{n}}\left({}_{\mathrm{s}}^{r_1}u_1^{\mathrm{n}} \ge u_1^{\mathrm{n}} > {}_{\mathrm{s}}^{r_1-1}u_1^{\mathrm{n}},\ u_2^{\mathrm{n}} = {}_{\mathrm{s}}^{1}u_2^{\mathrm{n}}\right), \quad i = 1,...,n,$$
$$\mathbf{A} = \mathbf{A}\left({}_{\mathrm{s}}^{r_1}u_1^{\mathrm{n}} \ge u_1^{\mathrm{n}} > {}_{\mathrm{s}}^{r_1-1}u_1^{\mathrm{n}},\ u_2^{\mathrm{n}} = {}_{\mathrm{s}}^{1}u_2^{\mathrm{n}}\right),$$
$$\mathbf{B} = \mathbf{B}\left({}_{\mathrm{s}}^{r_1}u_1^{\mathrm{n}} \ge u_1^{\mathrm{n}} > {}_{\mathrm{s}}^{r_1-1}u_1^{\mathrm{n}},\ u_2^{\mathrm{n}} = {}_{\mathrm{s}}^{1}u_2^{\mathrm{n}}\right),$$
$$r_1 = 9,$$
$${}_{\mathrm{s}}x_i^{\mathrm{n}} = {}_{\mathrm{s}}x_i^{\mathrm{n}}\left(u_1^{\mathrm{n}} > {}_{\mathrm{s}}^{9}u_1^{\mathrm{n}},\ u_2^{\mathrm{n}} = {}_{\mathrm{s}}^{1}u_2^{\mathrm{n}}\right) = {}^{91}{}_{\mathrm{s}}x_i^{\mathrm{n}}, \quad i = 1,...,n,$$
$$\mathbf{A} = \mathbf{A}\left(u_1^{\mathrm{n}} > {}_{\mathrm{s}}^{9}u_1^{\mathrm{n}},\ u_2^{\mathrm{n}} = {}_{\mathrm{s}}^{1}u_2^{\mathrm{n}}\right) = {}^{91}\mathbf{A},$$
$$\mathbf{B} = \mathbf{B}\left(u_1^{\mathrm{n}} > {}_{\mathrm{s}}^{9}u_1^{\mathrm{n}},\ u_2^{\mathrm{n}} = {}_{\mathrm{s}}^{1}u_2^{\mathrm{n}}\right) = {}^{91}\mathbf{B},$$
$$r_2 = 2,...,9 \quad : \quad {}_{\mathrm{s}}^{r_2}u_2^{\mathrm{n}} \le u_2^{\mathrm{n}} < {}_{\mathrm{s}}^{r_2-1}u_2^{\mathrm{n}},$$
$$r_1 = 1,$$
$${}_{\mathrm{s}}x_i^{\mathrm{n}} = {}_{\mathrm{s}}x_i^{\mathrm{n}}\left(u_1^{\mathrm{n}} \le {}_{\mathrm{s}}^{1}u_1^{\mathrm{n}},\ {}_{\mathrm{s}}^{r_2}u_2^{\mathrm{n}} \le u_2^{\mathrm{n}} < {}_{\mathrm{s}}^{r_2-1}u_2^{\mathrm{n}}\right) = {}^{1,r_2-1}{}_{\mathrm{s}}x_i^{\mathrm{n}} +$$
$$\left({}^{1,r_2}{}_{\mathrm{s}}x_i^{\mathrm{n}} - {}^{1,r_2-1}{}_{\mathrm{s}}x_i^{\mathrm{n}}\right) \Big/ \left({}_{\mathrm{s}}^{r_2}u_2^{\mathrm{n}} - {}_{\mathrm{s}}^{r_2-1}u_2^{\mathrm{n}}\right) \cdot \left(u_2^{\mathrm{n}} - {}_{\mathrm{s}}^{r_2-1}u_2^{\mathrm{n}}\right),$$
$$i = 1,...,n,$$
$$\mathbf{A} = \mathbf{A}\left(u_1^{\mathrm{n}} \le {}_{\mathrm{s}}^{1}u_1^{\mathrm{n}},\ {}_{\mathrm{s}}^{r_2}u_2^{\mathrm{n}} \le u_2^{\mathrm{n}} < {}_{\mathrm{s}}^{r_2-1}u_2^{\mathrm{n}}\right) = {}^{1,r_2-1}\mathbf{A} +$$
$$\left({}^{1,r_2}\mathbf{A} - {}^{1,r_2-1}\mathbf{A}\right) \Big/ \left({}_{\mathrm{s}}^{r_2}u_2^{\mathrm{n}} - {}_{\mathrm{s}}^{r_2-1}u_2^{\mathrm{n}}\right) \cdot \left(u_2^{\mathrm{n}} - {}_{\mathrm{s}}^{r_2-1}u_2^{\mathrm{n}}\right),$$
$$\mathbf{B} = \mathbf{B}\left(u_1^{\mathrm{n}} \le {}_{\mathrm{s}}^{1}u_1^{\mathrm{n}},\ {}_{\mathrm{s}}^{r_2}u_2^{\mathrm{n}} \le u_2^{\mathrm{n}} < {}_{\mathrm{s}}^{r_2-1}u_2^{\mathrm{n}}\right) = {}^{1,r_2-1}\mathbf{B} +$$
$$\left({}^{1,r_2}\mathbf{B} - {}^{1,r_2-1}\mathbf{B}\right) \Big/ \left({}_{\mathrm{s}}^{r_2}u_2^{\mathrm{n}} - {}_{\mathrm{s}}^{r_2-1}u_2^{\mathrm{n}}\right) \cdot \left(u_2^{\mathrm{n}} - {}_{\mathrm{s}}^{r_2-1}u_2^{\mathrm{n}}\right),$$
$$r_1 = 2,...,9,$$

$$
{}_{\mathrm{s}}x_i^{\mathrm{n}}={}_{\mathrm{s}}x_i^{\mathrm{n}}\left({}_{\mathrm{s}}^{r_1}u_1^{\mathrm{n}}\ge u_1^{\mathrm{n}}>{}_{\mathrm{s}}^{r_1-1}u_1^{\mathrm{n}},\ {}_{\mathrm{s}}^{r_2}u_2^{\mathrm{n}}\le u_2^{\mathrm{n}}<{}_{\mathrm{s}}^{r_2-1}u_2^{\mathrm{n}}\right)=
$$

$$
{}_{\mathrm{s}}x_i^{\mathrm{n}}\left({}_{\mathrm{s}}^{r_1}u_1^{\mathrm{n}}\ge u_1^{\mathrm{n}}>{}_{\mathrm{s}}^{r_1-1}u_1^{\mathrm{n}},\ u_2^{\mathrm{n}}={}_{\mathrm{s}}^{r_2-1}u_2^{\mathrm{n}}\right)+
$$

$$
\left[{}_{\mathrm{s}}x_i^{\mathrm{n}}\left({}_{\mathrm{s}}^{r_1}u_1^{\mathrm{n}}\ge u_1^{\mathrm{n}}>{}_{\mathrm{s}}^{r_1-1}u_1^{\mathrm{n}},\ u_2^{\mathrm{n}}={}_{\mathrm{s}}^{r_2}u_2^{\mathrm{n}}\right)-\right.
$$

$$
\left.{}_{\mathrm{s}}x_i^{\mathrm{n}}\left({}_{\mathrm{s}}^{r_1}u_1^{\mathrm{n}}\ge u_1^{\mathrm{n}}>{}_{\mathrm{s}}^{r_1-1}u_1^{\mathrm{n}},\ u_2^{\mathrm{n}}={}_{\mathrm{s}}^{r_2-1}u_2^{\mathrm{n}}\right)\right]\Big/
$$

$$
\left({}_{\mathrm{s}}^{r_2}u_2^{\mathrm{n}}-{}_{\mathrm{s}}^{r_2-1}u_2^{\mathrm{n}}\right)\cdot\left(u_2^{\mathrm{n}}-{}_{\mathrm{s}}^{r_2-1}u_2^{\mathrm{n}}\right),
$$

$$
i=1,\ldots,n,
$$

$$
\mathbf{A}=\mathbf{A}\left({}_{\mathrm{s}}^{r_1}u_1^{\mathrm{n}}\ge u_1^{\mathrm{n}}>{}_{\mathrm{s}}^{r_1-1}u_1^{\mathrm{n}},\ {}_{\mathrm{s}}^{r_2}u_2^{\mathrm{n}}\le u_2^{\mathrm{n}}<{}_{\mathrm{s}}^{r_2-1}u_2^{\mathrm{n}}\right)=
$$

$$
\mathbf{A}\left({}_{\mathrm{s}}^{r_1}u_1^{\mathrm{n}}\ge u_1^{\mathrm{n}}>{}_{\mathrm{s}}^{r_1-1}u_1^{\mathrm{n}},\ u_2^{\mathrm{n}}={}_{\mathrm{s}}^{r_2-1}u_2^{\mathrm{n}}\right)+
$$

$$
\left[\mathbf{A}\left({}_{\mathrm{s}}^{r_1}u_1^{\mathrm{n}}\ge u_1^{\mathrm{n}}>{}_{\mathrm{s}}^{r_1-1}u_1^{\mathrm{n}},\ u_2^{\mathrm{n}}={}_{\mathrm{s}}^{r_2}u_2^{\mathrm{n}}\right)-\right.
$$

$$
\left.\mathbf{A}\left({}_{\mathrm{s}}^{r_1}u_1^{\mathrm{n}}\ge u_1^{\mathrm{n}}>{}_{\mathrm{s}}^{r_1-1}u_1^{\mathrm{n}},\ u_2^{\mathrm{n}}={}_{\mathrm{s}}^{r_2-1}u_2^{\mathrm{n}}\right)\right]\Big/
$$

$$
\left({}_{\mathrm{s}}^{r_2}u_2^{\mathrm{n}}-{}_{\mathrm{s}}^{r_2-1}u_2^{\mathrm{n}}\right)\cdot\left(u_2^{\mathrm{n}}-{}_{\mathrm{s}}^{r_2-1}u_2^{\mathrm{n}}\right),
$$

$$
\mathbf{B}=\mathbf{B}\left({}_{\mathrm{s}}^{r_1}u_1^{\mathrm{n}}\ge u_1^{\mathrm{n}}>{}_{\mathrm{s}}^{r_1-1}u_1^{\mathrm{n}},\ {}_{\mathrm{s}}^{r_2}u_2^{\mathrm{n}}\le u_2^{\mathrm{n}}<{}_{\mathrm{s}}^{r_2-1}u_2^{\mathrm{n}}\right)=
$$

$$
\mathbf{B}\left({}_{\mathrm{s}}^{r_1}u_1^{\mathrm{n}}\ge u_1^{\mathrm{n}}>{}_{\mathrm{s}}^{r_1-1}u_1^{\mathrm{n}},\ u_2^{\mathrm{n}}={}_{\mathrm{s}}^{r_2-1}u_2^{\mathrm{n}}\right)+
$$

$$
\left[\mathbf{B}\left({}_{\mathrm{s}}^{r_1}u_1^{\mathrm{n}}\ge u_1^{\mathrm{n}}>{}_{\mathrm{s}}^{r_1-1}u_1^{\mathrm{n}},\ u_2^{\mathrm{n}}={}_{\mathrm{s}}^{r_2}u_2^{\mathrm{n}}\right)-\right.
$$

$$
\left.\mathbf{B}\left({}_{\mathrm{s}}^{r_1}u_1^{\mathrm{n}}\ge u_1^{\mathrm{n}}>{}_{\mathrm{s}}^{r_1-1}u_1^{\mathrm{n}},\ u_2^{\mathrm{n}}={}_{\mathrm{s}}^{r_2-1}u_2^{\mathrm{n}}\right)\right]\Big/
$$

$$
\left({}_{\mathrm{s}}^{r_2}u_2^{\mathrm{n}}-{}_{\mathrm{s}}^{r_2-1}u_2^{\mathrm{n}}\right)\cdot\left(u_2^{\mathrm{n}}-{}_{\mathrm{s}}^{r_2-1}u_2^{\mathrm{n}}\right),
$$

$$
r_1=9,
$$

$$
{}_{\mathrm{s}}x_i^{\mathrm{n}}={}_{\mathrm{s}}x_i^{\mathrm{n}}\left(u_1^{\mathrm{n}}>{}_{\mathrm{s}}^{9}u_1^{\mathrm{n}},\ {}_{\mathrm{s}}^{r_2}u_2^{\mathrm{n}}\le u_2^{\mathrm{n}}<{}_{\mathrm{s}}^{r_2-1}u_2^{\mathrm{n}}\right)={}_{\mathrm{s}}^{9,r_2-1}x_i^{\mathrm{n}}+
$$

$$
\left({}_{\mathrm{s}}^{9,r_2}x_i^{\mathrm{n}}-{}_{\mathrm{s}}^{9,r_2-1}x_i^{\mathrm{n}}\right)\Big/\left({}_{\mathrm{s}}^{r_2}u_2^{\mathrm{n}}-{}_{\mathrm{s}}^{r_2-1}u_2^{\mathrm{n}}\right)\cdot\left(u_2^{\mathrm{n}}-{}_{\mathrm{s}}^{r_2-1}u_2^{\mathrm{n}}\right),
$$

$$
i=1,\ldots,n,
$$

$$
\mathbf{A}=\mathbf{A}\left(u_1^{\mathrm{n}}>{}_{\mathrm{s}}^{9}u_1^{\mathrm{n}},\ {}_{\mathrm{s}}^{r_2}u_2^{\mathrm{n}}\le u_2^{\mathrm{n}}<{}_{\mathrm{s}}^{r_2-1}u_2^{\mathrm{n}}\right)={}^{9,r_2-1}\mathbf{A}+
$$

$$
\left({}^{9,r_2}\mathbf{A}-{}^{9,r_2-1}\mathbf{A}\right)\Big/\left({}_{\mathrm{s}}^{r_2}u_2^{\mathrm{n}}-{}_{\mathrm{s}}^{r_2-1}u_2^{\mathrm{n}}\right)\cdot\left(u_2^{\mathrm{n}}-{}_{\mathrm{s}}^{r_2-1}u_2^{\mathrm{n}}\right),
$$

$$
\mathbf{B}=\mathbf{B}\left(u_1^{\mathrm{n}}>{}_{\mathrm{s}}^{9}u_1^{\mathrm{n}},\ {}_{\mathrm{s}}^{r_2}u_2^{\mathrm{n}}\le u_2^{\mathrm{n}}<{}_{\mathrm{s}}^{r_2-1}u_2^{\mathrm{n}}\right)={}^{9,r_2-1}\mathbf{B}+
$$

$$
\left({}^{9,r_2}\mathbf{B}-{}^{9,r_2-1}\mathbf{B}\right)\Big/\left({}_{\mathrm{s}}^{r_2}u_2^{\mathrm{n}}-{}_{\mathrm{s}}^{r_2-1}u_2^{\mathrm{n}}\right)\cdot\left(u_2^{\mathrm{n}}-{}_{\mathrm{s}}^{r_2-1}u_2^{\mathrm{n}}\right),
$$

$$
r_2=9\quad:\quad u_2^{\mathrm{n}}<{}_{\mathrm{s}}^{9}u_2^{\mathrm{n}},
$$

$$
r_1=1,
$$

$$
{}_{\mathrm{s}}x_i^{\mathrm{n}}={}_{\mathrm{s}}x_i^{\mathrm{n}}\left(u_1^{\mathrm{n}}\le{}_{\mathrm{s}}^{1}u_1^{\mathrm{n}},\ u_2^{\mathrm{n}}<{}_{\mathrm{s}}^{9}u_2^{\mathrm{n}}\right)={}_{\mathrm{s}}^{19}x_i^{\mathrm{n}},\quad i=1,\ldots,n,
$$

$$
\mathbf{A}=\mathbf{A}\left(u_1^{\mathrm{n}}\le{}_{\mathrm{s}}^{1}u_1^{\mathrm{n}},\ u_2^{\mathrm{n}}<{}_{\mathrm{s}}^{9}u_2^{\mathrm{n}}\right)={}^{19}\mathbf{A},
$$

$$
\mathbf{B}=\mathbf{B}\left(u_1^{\mathrm{n}}\le{}_{\mathrm{s}}^{1}u_1^{\mathrm{n}},\ u_2^{\mathrm{n}}<{}_{\mathrm{s}}^{9}u_2^{\mathrm{n}}\right)={}^{19}\mathbf{B},
$$

$$
r_1=2,\ldots,9,
$$

$$
{}_{\mathrm{s}}x_i^{\mathrm{n}}={}_{\mathrm{s}}x_i^{\mathrm{n}}\left({}_{\mathrm{s}}^{r_1}u_1^{\mathrm{n}}\ge u_1^{\mathrm{n}}>{}_{\mathrm{s}}^{r_1-1}u_1^{\mathrm{n}},\ u_2^{\mathrm{n}}<{}_{\mathrm{s}}^{9}u_2^{\mathrm{n}}\right)=
$$

$$
{}_{\mathrm{s}}x_i^{\mathrm{n}}\left({}_{\mathrm{s}}^{r_1}u_1^{\mathrm{n}}\ge u_1^{\mathrm{n}}>{}_{\mathrm{s}}^{r_1-1}u_1^{\mathrm{n}},\ u_2^{\mathrm{n}}={}_{\mathrm{s}}^{9}u_2^{\mathrm{n}}\right),\quad i=1,\ldots,n,
$$

$$
\mathbf{A}=\mathbf{A}\left({}_{\mathrm{s}}^{r_1}u_1^{\mathrm{n}}\ge u_1^{\mathrm{n}}>{}_{\mathrm{s}}^{r_1-1}u_1^{\mathrm{n}},\ u_2^{\mathrm{n}}<{}_{\mathrm{s}}^{9}u_2^{\mathrm{n}}\right)=
$$

$$
\mathbf{A}\left({}_{\mathrm{s}}^{r_1}u_1^{\mathrm{n}}\ge u_1^{\mathrm{n}}>{}_{\mathrm{s}}^{r_1-1}u_1^{\mathrm{n}},\ u_2^{\mathrm{n}}={}_{\mathrm{s}}^{9}u_2^{\mathrm{n}}\right),
$$

$$
\mathbf{B}=\mathbf{B}\left({}_{\mathrm{s}}^{r_1}u_1^{\mathrm{n}}\ge u_1^{\mathrm{n}}>{}_{\mathrm{s}}^{r_1-1}u_1^{\mathrm{n}},\ u_2^{\mathrm{n}}<{}_{\mathrm{s}}^{9}u_2^{\mathrm{n}}\right)=
$$

$$
\mathbf{B}\left({}_{\mathrm{s}}^{r_1}u_1^{\mathrm{n}}\ge u_1^{\mathrm{n}}>{}_{\mathrm{s}}^{r_1-1}u_1^{\mathrm{n}},\ u_2^{\mathrm{n}}={}_{\mathrm{s}}^{9}u_2^{\mathrm{n}}\right),
$$

$$
r_1=9,
$$

$$
{}_{\mathrm{s}}x_i^{\mathrm{n}}={}_{\mathrm{s}}x_i^{\mathrm{n}}\left(u_1^{\mathrm{n}}>{}_{\mathrm{s}}^{9}u_1^{\mathrm{n}},\ u_2^{\mathrm{n}}<{}_{\mathrm{s}}^{9}u_2^{\mathrm{n}}\right)={}_{\mathrm{s}}^{99}x_i^{\mathrm{n}},\quad i=1,\ldots,n,
$$

$$
\mathbf{A}=\mathbf{A}\left(u_1^{\mathrm{n}}>{}_{\mathrm{s}}^{9}u_1^{\mathrm{n}},\ u_2^{\mathrm{n}}<{}_{\mathrm{s}}^{9}u_2^{\mathrm{n}}\right)={}^{99}\mathbf{A},
$$

$$
\mathbf{B}=\mathbf{B}\left(u_1^{\mathrm{n}}>{}_{\mathrm{s}}^{9}u_1^{\mathrm{n}},\ u_2^{\mathrm{n}}<{}_{\mathrm{s}}^{9}u_2^{\mathrm{n}}\right)={}^{99}\mathbf{B}.
$$

In figures 1, 2, 3, 4, 5, 6, 7, 8, 9, 10, 11, 12, it is shown the transition processes for normalized control variables u_1^{n}, u_2^{n}, u_3^{n}, u_4^{n}, normalized state variables x_1^{n}, x_2^{n}, x_3^{n}, x_4^{n}, x_5^{n} nonlinear and discrete-continuous models of GTE as well as derivative of normalized state variables for transition processes $\dot{x}_5^{\mathrm{n}}$ for nonlinear, discrete-linear and discrete-continuous models of GTE at changing of values of deviation angle of the engine control leverage from value corresponding to maximum operation mode ($\alpha_{\text{руд}}=68^{\circ}$) to value, corresponding to minimal operation mode ($\alpha_{\text{руд}}=15^{\circ}$), and further in contrary. That is, for example at falling or acceleration into closed-loop DACS. A number of the transition processes' point is $N = 601$, a discreteness step is $\Delta t = 0.025$ C. The deflections form real object (so called "errors") are calculated for each variable using either first or second technique

$$
\sqrt{\frac{\sum\limits_{k=1}^{N}\left[x_i^{\mathrm{n}}(t_k)-{}^{\text{НЛ}}x_i^{\mathrm{n}}(t_k)\right]^2}{\sum\limits_{k=1}^{N}\left[{}^{\text{НЛ}}x_i^{\mathrm{n}}(t_k)-{}^{\text{НЛ}}x_i^{\mathrm{n}}(t_0)\right]^2}},\quad i=1,\ldots,n,
$$

$$
\max_{k=1,\ldots,N}\left|x_i^{\mathrm{n}}(t_k)-{}^{\text{НЛ}}x_i^{\mathrm{n}}(t_k)\right|,\quad i=1,\ldots,n.
$$

4. CONCLUSION

A technique for calculation the vector and matrix parameters of a discrete-continuous model using the vector and matrix parameters of a discrete-linear model of a nonlinear control object is carried out.

The basis of this technique is an approximate representation of the static characteristic of a nonlinear object in the form of a set of $n = 5$ three-dimensional surfaces (in fact, these surfaces are five-dimensional), or rather, a set of n = 5 three-dimensional variety $R_2 = 9$ discrete-linear broken lines, the each of this set corresponds to the selected constant value of one from two considered (from four available) control variables (${}^{r_2}_{s}u_2^{n}$, $r_2 = 1,...,9$).

The errors of the discrete-continuous model for some of the state variables are larger than the errors of the discrete-linear model, but at the boundaries of the acting ereas of different linear models included in the discrete-linear model, the values of the first derivative of the state variable changes much smaller.

The results of this stude can be applied to the development of control algorithms for nonlinear objects, which can be approximately described using linear, discrete-linear and discrete-continuous models, as well as algorithms for detecting failures of sensors and equioment of DACS.

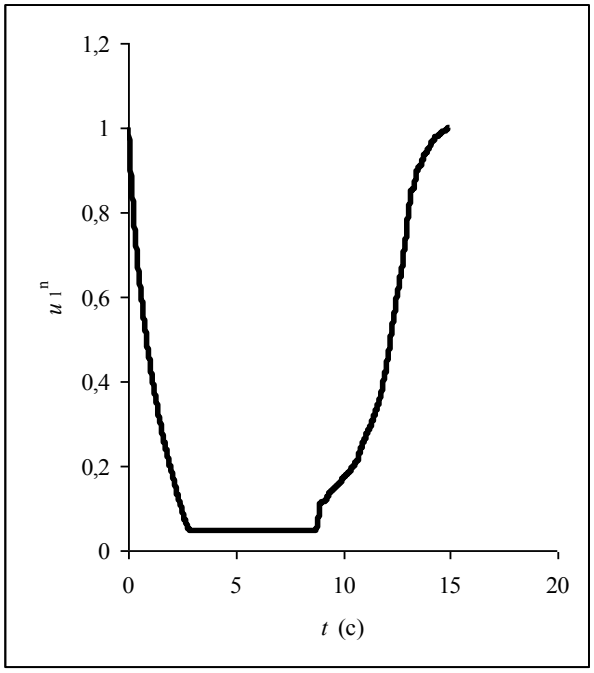

Figure 1. Transition process for normalized control variable u_1^n, corresponding to wide range of operation modes of nonlinear control object.

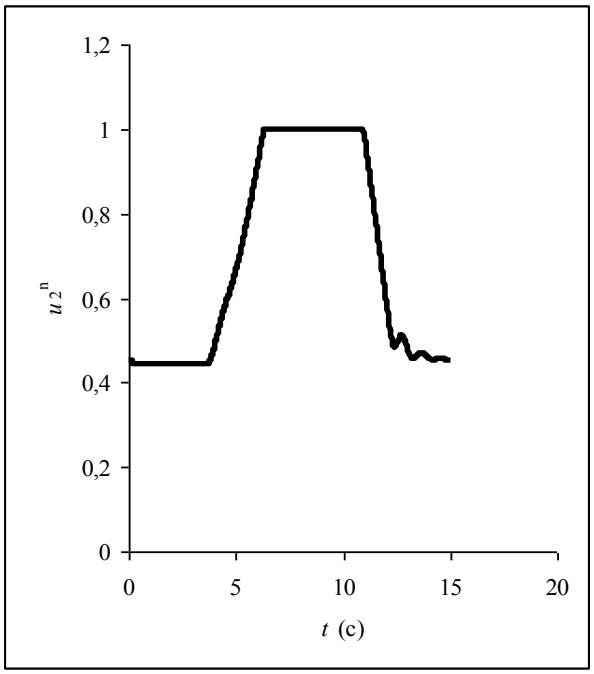

Figure 2. Transition process for normalized control variable u_2^n, corresponding to wide range of operation modes of nonlinear control object.

REFERENCES

1. **Leibov R.L.** Prikladnye Metody Teorii Upravleniya [Applied Methods of Control Theory]. Moscow, ASV, 2014, 192 pages.
2. **Leibov R.L.** Metodika Postroeniya Kusochno-Linejnoj Modeli Nelinejnogo Ob"ekta [Nonlinear Plant Piece-Wise Linear Model Formation Technique]. // *International Journal for Computational Civil and Structural Engineering*, 2013, Volume 9, Issue 4, pp. 186-198.

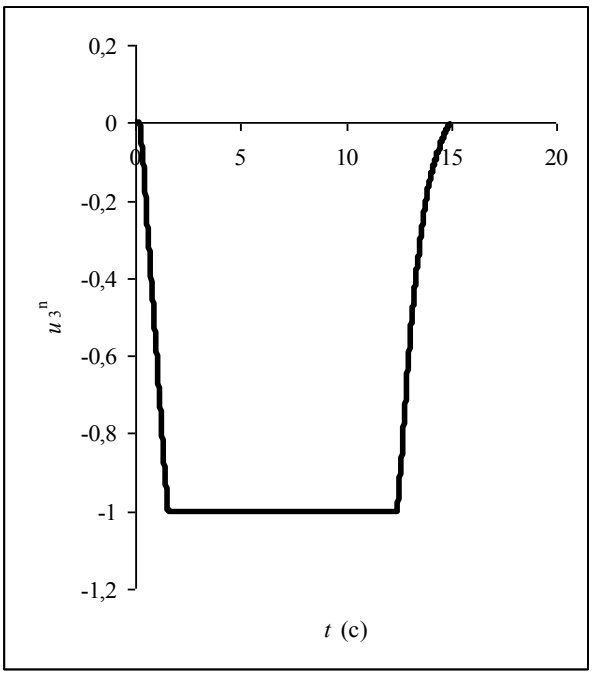

Figure 3. Transition process for normalized control variable u_3^n, corresponding to wide range of operation modes of nonlinear control object.

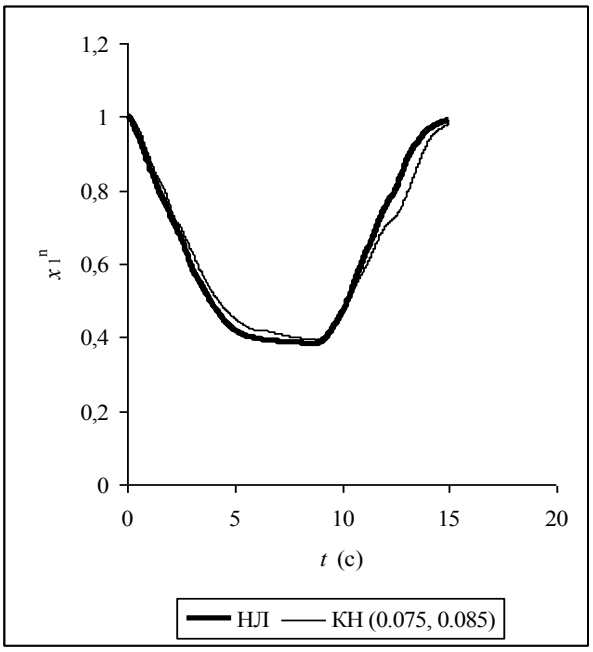

Figure 5. Transition process for normalized control variable x_1^n nonlinear (NL) model and discrete-continuous (DC) model, corresponding to wide range of operation modes of nonlinear control object.

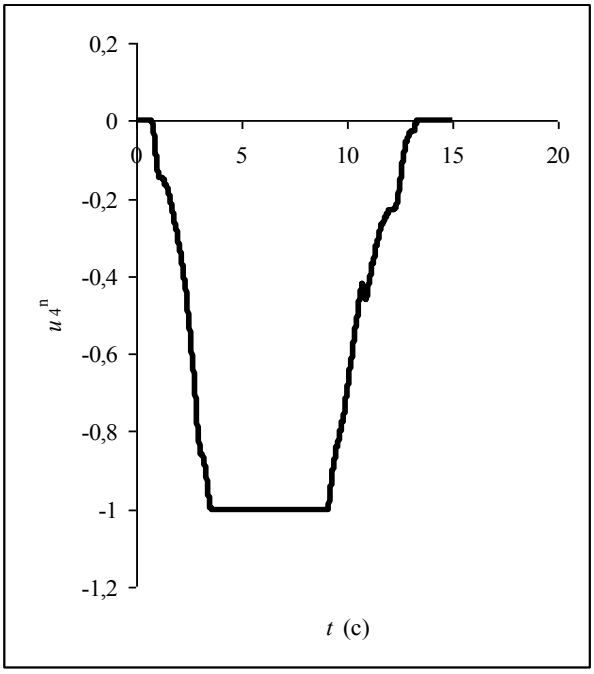

Figure 4. Transition process for normalized control variable u_4^n, corresponding to wide range of operation modes of nonlinear control object.

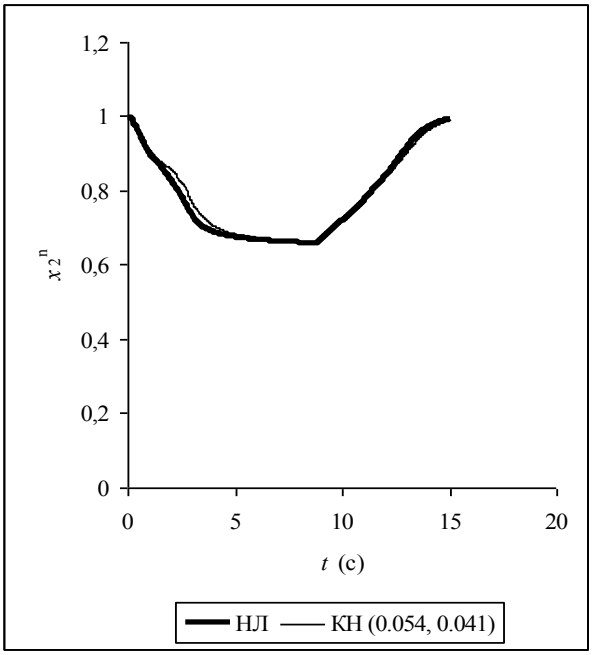

Figure 6. Transition process for normalized control variable x_2^n nonlinear (NL) model and discrete-continuous (DC) model, corresponding to wide range of operation modes of nonlinear control object.

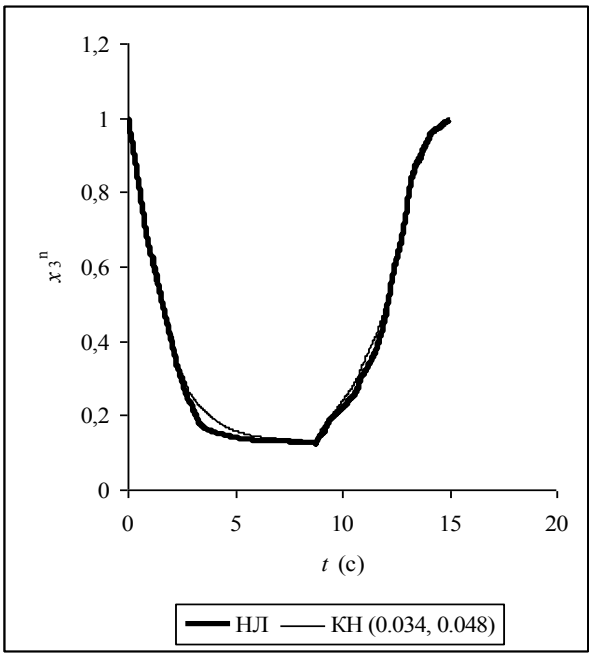

Figure 7. Transition process for normalized control variable x_3^n nonlinear (NL) model and discrete-continuous (DC) model, corresponding to wide range of operation modes of nonlinear control object.

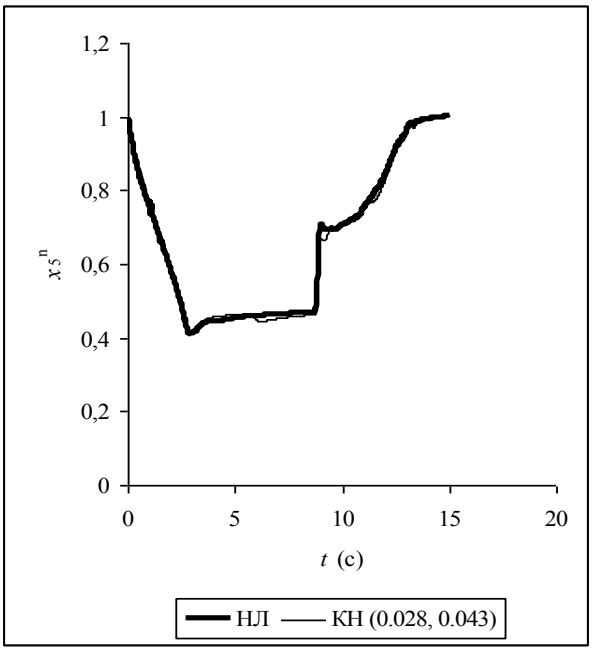

Figure 9. Transition process for normalized control variable x_5^n nonlinear (NL) model and discrete-continuous (DC) model, corresponding to wide range of operation modes of nonlinear control object.

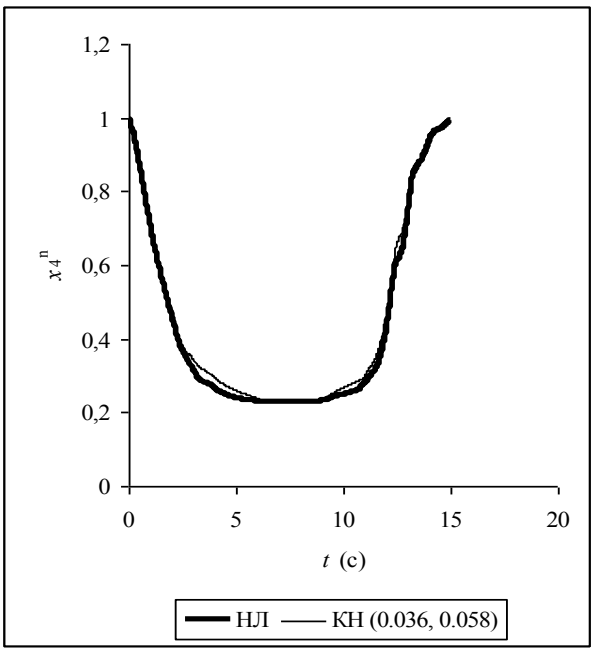

Figure 8. Transition process for normalized control variable x_4^n nonlinear (NL) model and discrete-continuous (DC) model, corresponding to wide range of operation modes of nonlinear control object.

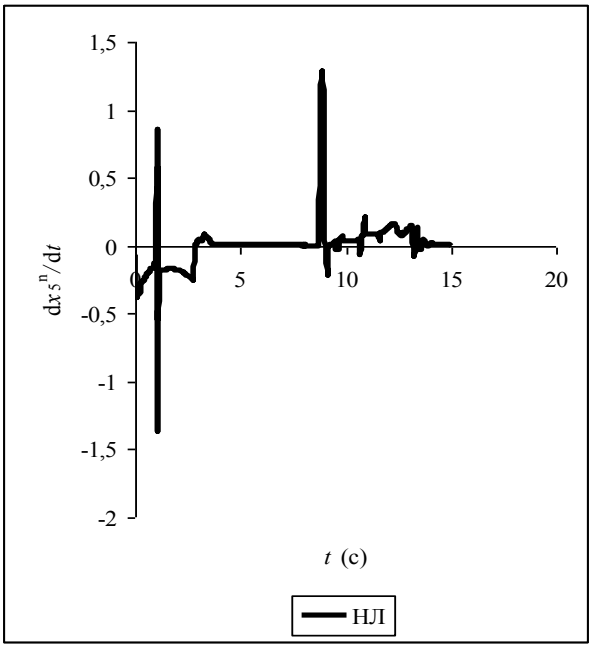

Figure 10. Transition process for derivative of the normalized control variable x_5^n of nonlinear (NL) model , corresponding to wide range of operation modes of nonlinear control object.

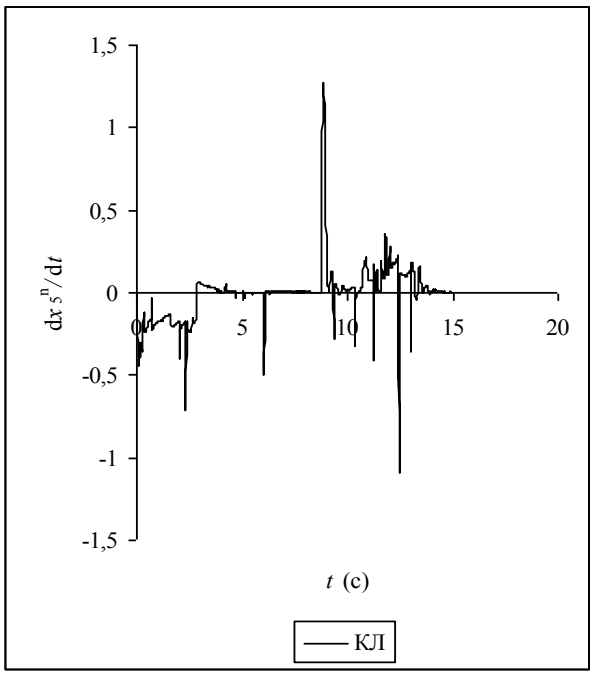

Figure 11. Transition process for derivative of the normalized control variable x_5^n of discrete-linear (DL) model, corresponding to wide range of operation modes of nonlinear control object.

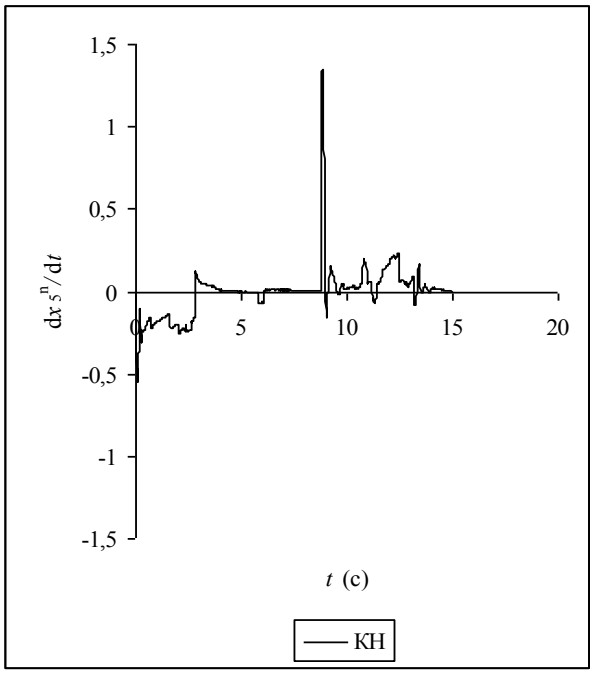

Figure 12. Transition process for derivative of the normalized control variable x_5^n discrete-continuous (DC) model, corresponding to wide range of operation modes of nonlinear control object.

3. **Leibov R.L.** Ocenivanie Matrichnyh Parametrov Kusochno-Nepreryvnoj Modeli Nelinejnogo Ob"ekta Upravleniya [Nonlinear Plant Piecewise Continuous Model Matrix Parameters Estimation]. // *International Journal for Computational Civil and Structural Engineering*, 2017, Volume 13, Issue 3, pp. 77-85.

СПИСОК ЛИТЕРАТУРЫ

1. **Лейбов Р.Л.** Прикладные методы теории управления. – М.: АСВ, 2014. – 192 с.
2. **Лейбов Р.Л.** Методика построения кусочно-линейной модели нелинейного объекта. // *International Journal for Computational Civil and Structural Engineering*, 2013, Volume 9, Issue 4, pp. 186-198.
3. **Лейбов Р.Л.** Оценивание матричных параметров кусочно-непрерывной модели нелинейного объекта управления. // *International Journal for Computational Civil and Structural Engineering*, 2017, Volume 13, Issue 3, pp. 77-85.

Лейбов Роман Львович, доктор технических наук, профессор; Московский авиационный институт (национальный исследовательский университет); 125993, г. Москва, Волоколамское шоссе, д. 4;
тел. +7 499 158-43-33, 158-58-70, 158-00-02;
факс: +7 499 158-29-77;
E-mail: r_leibov@mtu-net.ru, mai@mai.ru.

Roman L. Leibov, Professor, Dr.Sc.; Moscow Aviation Institute (National Research University); 4, Volokolamskoe shosse, Moscow, 125993, Russia;
phones: +7 499 158-43-33, 158-58-70, 158-00-02;
fax: +7 499 158-29-77;
E-mail: r_leibov@mtu-net.ru, mai@mai.ru.

DOI:10.22337/2587-9618-2019-15-2-95-110

ABOUT WAVELET-BASED COMPUTATIONAL BEAM ANALYSIS WITH THE USE OF DAUBECHIES SCALING FUNCTIONS

Marina L. Mozgaleva [1], Pavel A.Akimov [2, 3, 4, 5], Taymuraz B. Kaytukov [2, 6]

[1] National Research Moscow State University of Civil Engineering, Moscow, RUSSIA
[2] Russian Academy of Architecture and Building Sciences, Moscow, RUSSIA
[3] Scientific Research Center "StaDyO", Moscow, RUSSIA
[4] Tomsk State University of Architecture and Civil Engineering, Tomsk, RUSSIA
[5] Peoples' Friendship University of Russia, Moscow, RUSSIA
[6] Central Institute for Research and Design of the Ministry of Construction and Housing and Communal Services of the Russian Federation, Moscow, RUSSIA

Abstract: The first part of the distinctive paper contains brief review of wavelet-based numerical and semianalytical analysis, particularly with the use of Daubechies scaling functions. The second part of the paper is devoted to numerical solution of the problem of static analysis of beam on elastic foundation within Winkler model. Finite element method (FEM) and wavelet analysis (Daubechies scaling functions) are used. Variational formulation and approximation of the problem are under consideration. Numerical sample is presented as well. The third part of the paper is dedicated to wavelet based discrete-continual finite element method of beam analysis with allowance for impulse load. Daubechies scaling functions are used as well.

Keywords: boundary problem, structural analysis, static analysis, dynamic analysis, beam analysis, numerical solution, finite element method, wavelet analysis, Daubechies scaling function, Daubechies wavelet, impulse load, review

О ВЕЙВЛЕТ-РЕАЛИЗАЦИЯХ ВЫЧИСЛИТЕЛЬНЫХ МЕТОДОВ РАСЧЕТА БАЛОЧНЫХ КОНСТРУКЦИЙ С ИСПОЛЬЗОВАНИЕМ МАСШТАБИРУЮЩИХ ФУНКЦИЙ ДОБЕШИ

М.Л. Мозгалева [1], П.А. Акимов [2, 3, 4, 5], Т.Б. Кайтуков [2, 6]

[1] Национальный исследовательский Московский государственный строительный университет, г. Москва, РОССИЯ
[2] Российская академия архитектуры и строительных наук, г. Москва, РОССИЯ
[3] Научно-исследовательский центр СтаДиО, г. Москва, РОССИЯ
[4] Томский государственный архитектурно-строительный университет, г. Томск, РОССИЯ
[5] Российский университет дружбы народов, г. Москва, РОССИЯ
[6] Центральный научно-исследовательский и проектный институт Министерства строительства и жилищно-коммунального хозяйства, г. Москва, РОССИЯ

Аннотация: Настоящая статья в своей первой части содержит относительно краткий обзор вейвлет-реализаций численных и численно-аналитических методов решения краевых задач, в частности с использованием масштабирующих функций Добеши. Вторая часть статьи посвящена численному решению статической задачи об изгибе балки на упругом основании (в рамках модели Винклера). Для построения решения используются метод конечных элементов (МКЭ) в сочетании с аппаратом вейвлет-анализа (масштабирующие функции Добеши). Приведена вариационная (континуальная) формулировка задачи, описаны ее аппроксимация и построение численного решения, представлен пример расчета. В третьей части статьи описан вейвлет-реализация дискретно-континуального метода конечных элементов для расчета балки при ударе на основе использования масштабирующих функций Добеши.

Ключевые слова: краевая задача, расчеты строительных конструкций, статический расчет, динамический расчет, расчет балки, численное решение, метод конечных элементов, вейвлет-анализ, масштабирующая функция Добеши, вейвлет Добеши, ударная нагрузка, обзор

1. INTRODUCTION

As is known, the numerical analysis with wavelet (wavelet-based numerical analysis) received its first attention in 1992, since then (particularly since the corresponding basic work of I. Daubechies [1]) researchers have shown growing interest in it. Various methods including so-called wavelet weighted residual method, wavelet finite element method, wavelet-based numerical methods of local structural analysis [2-6], wavelet boundary method, wavelet meshless method, wavelet-optimized finite difference method, wavelet-based discrete-continual methods of local structural analysis [7-15], wavelet-based multigrid method [16] etc. have acquired an important role in recent years.

First of all, it should be noted that Daubechies scaling functions can be effectively employed within wavelet finite element method or within wavelet-based numerical and semianalytical (discrete-continual) methods of local structural analysis as asapproximate functions in the procedure of construction of so-called wavelet finite element [17].

Corresponding compact support property proves to be more effective in using minimum degrees of freedom over an element to approximate displacement functions. Moreover, sparseness of the matrix is a result of the scaling functions, which have the compactly supported property. Cancellation property allows one to perfectly interpolate polynomials of degree up to N by the scaling function with order N. Corresponding experiments gathered in the wavelet-Galerkin context indicate that orthogonal property satisfies the condition that the matrix is sparse as well as banded if the global nodes are numbered sequentially. Dur to corresponding main properties, Daubechies wavelets can describe the details of the problem conveniently and accurately, and the corresponding Daubechies wavelets-based element has an enormous potential in the analysis of the singularity problem [17].

J. Ko, A.J. Kurdila and M.S. Pillant [18] developed special finite element method based on application of Daubehies wavelet. Corresponding algebraic eigenvalue problem derived from the dyadic refinement equation can be solved by this method. The resulting finite elements could be considered as several generalizations of the connection coefficients employed in the corresponding Daubechies wavelet expansion of periodic differential operators [17].

R.D. Patton and P.C. Marks [19] utilized a Daubechies scaling function as interpolation function of one-dimensional finite element. This element can reduce the computation time and reduce the number of degrees of freedom, which is normally needed for correct solution of vibration and wave propagation problems [17].

J.X. Ma and J.J. Xuee in paper [20] constructed one-dimensional Daubechies wavelet beam element [17].

X.F. Chen, S.J. Yang and J.X. Ma [21] extended such elements to higher dimensions, constructed two-dimensional Daubechies wavelet element, derived the corresponding bending equations for the thin plate based on wavelet finite element, and solved the L-shape plate stress problems. Their results show that wavelet finite element can be effectively used for solution of singularity problems [17].

However, the tensor product space should be constructed firstly [22], which decreases the computational effectiveness [17].

J.M. Jin, P.X. Xue, Y.X. Xu and Y.L. Shu [23] built a two-dimensional Daubechies wavelet directly without tensor product computation and developed corresponding two-dimensional plate element [17].

Nevertheless, the wavelet deflection formulation depends on specific boundary conditions. Besides it is effective only for homogeneous boundary conditions for square plates. In addition, only simple boundary conditions were considered in above mentioned works. Triggered by this motivation, a modified form of wavelet ap-

proximation of deflection solution was proposed for solution of bending problems of beams and square thin plates by Y.H. Zhou and J. Zhou [24]. Boundary rotational degrees of freedom for beams and square plates were explicitly introduced as Daubechies wavelet coefficients in this paper. Thus variation equations were established with the use of corresponding modified approximations and variation principles. Homogeneous and non-homogeneous boundary conditions can betreated in the same way (by analogy with corresponding versions of conventional FEM [17].

M. Mitra and S. Gopalakrishnan presented so-called Daubechies wavelet-based spectral finite element method (WSFEM) for analysis of elastic wave propagation in one-dimensional and two-dimensional connected wave guides [25-27]. First of all, this method transforms the initial partial differential wave equation to corresponding ordinary differential equations (ODEs) with the use of Daubechies wavelet approximation in time domain. Then these ODEs are solved within FEM by deriving the exact interpolating function in the transformed domain. Spectral element can capture the exact mass distribution. Therefor the system size required is very much smaller than the corresponding system size within the conventional FEM. Besides, due to the localized nature of Daubechies wavelet basis functions, the WSFEM proves to be more efficient as it removes the wrap around problem associated with spectral finite element method for time domain analysis.

M. Mitra and S. Gopalakrishnan [28] later extended the method and considered problems of analysis of composite beam with embedded delamination. However, the real-scale structural wave propagation problem requires more different complex spectral elements, interconnections and flexible in flatable components. In accordance with assessments from paper [17], future research work will focus on extending the spectral element method for analysis of damaged structures with more complex geometry [17].

Thus, Daubechies wavelets are used to approximate the displacement and force in the domain, where unknown wavelet coefficients can be determined through imposing the essential boundary condition. The Daubechies wavelet finite elements embodies the properties of locality and adaptivity. However, because Daubechies wavelets lack the explicit function expression, traditional numerical integrals such as Gaussian integrals cannot provide desirable precision. Therefor, the applications of Daubechies wavelets are limited by the this weakness [17].

1. WAVELET-BASED NUMERICAL BEAM ANALYSIS WITH THE USE OF DAUBECHIES SCALING FUNCTIONS

1.1. Mathematical (continual) formulation of the problem of static beam analysis.

The essence of the Winkler model is the assumption that the reaction of the foundation $r(x)$ at an arbitrary point of the beam x is proportional to deflection at this point $r(x) = \beta y$. Therefore, graphically, such a model can be represented by springs that are not connected to each other, each of which has a stiffness proportional to the deflection of the beam at this point (Figure 1.1).

The stress-strain state of such a beam corresponds to the solution of the problem of the minimum of the following functional (energy functional) [29]:

$$\Phi(y) = \frac{1}{2}\int_0^l (EJ(y'')^2 + \beta y^2)dx - \int_0^l q(x)ydx, \quad (1.1)$$

where $EJ(x)$ is bending stiffness of beam; $\beta(x)$ is Winkler coefficient; $q(x)$ is applied load.

1.2. Wavelet-based finite element approximation of the problem of static beam analysis.

Let us divide domain (one-dimensional interval $(0, l)$), occupied by the beam into N_e parts (finite elements);

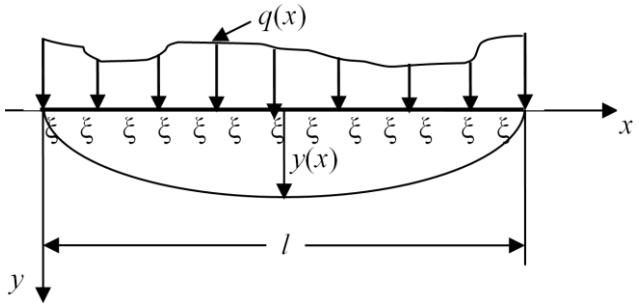

Figure 1.1. Computational scheme of beam.

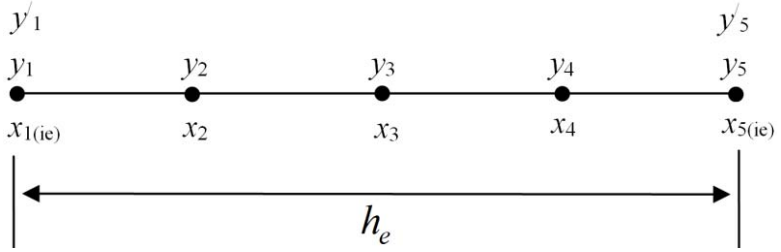

Figure 1.2. Sample of finite element.

$$h_e = l / N_e$$

is the length of the element.

Each element is also divided into N_k parts, for example, $N_k = 4$ (Figure 1.2).

Let us introduce the following notation: i_e is element number; $x_1(i_e)$ is coordinate of the starting point of the i_e-th element; $x_5(i_e)$ is coordinate of the end point of the i_e-th element. At the boundary points (nodes), we can choose unknowns y_i and y_i'; at the inner points we can choose unknowns y_i, $i = 2,3,4$. Thus, the total number of unknowns on an element is equal to

$$N = N_k - 1 + 2 \cdot 2 = N_k + 3 = 7.$$

The number of boundary points for all elements is equal to

$$N_b = N_e + 1.$$

Besides, the number of interior points for all elements is equal to

$$N_p = N_e(N_k - 1).$$

Thus, the total (global) number of unknowns is equal to

$$N_g = N_p + 2N_b.$$

We have

$$\Phi(y) = \sum_{i_e=1}^{N_e} \Phi_{i_e}(y), \qquad (1.2)$$

where

$$\Phi_{i_e}(y) = \frac{1}{2} \int_{x_1(i_e)}^{x_5(i_e)} (EJ(y'')^2 + \beta y^2)\, dx - \int_{x_1(i_e)}^{x_5(i_e)} qy dx. \qquad (1.3)$$

Let us introduce the local coordinates:

$$t = (x - x_{1(i_e)}) / h_e, \quad x_{1(i_e)} \le x \le x_{5(i_e)}. \qquad (1.4)$$

In this case, we have the following relations:

$$\begin{cases} x = x_{1(i_e)} \Rightarrow t = 0 \\ x = x_2 \Rightarrow t = 0.25 \\ x = x_3 \Rightarrow t = 0.5 \\ x = x_4 \Rightarrow t = 0.75 \\ x = x_{5(i_e)} \Rightarrow t = 1; \end{cases} \qquad (1.5)$$

$$\frac{d}{dx}=\frac{d}{dt}\cdot\frac{dt}{dx}=\frac{1}{h_e}\frac{d}{dt};$$
$$\frac{d^p}{dx^p}=\frac{1}{h_e^p}\frac{d^p}{dt^p}; \quad (1.6)$$

$$dx=h_e\cdot dt. \quad (1.7)$$

We can represent displacement (deflection) of beam $y(x)$ in the form

$$y(x)=w(t)=\sum_{k=0}^{N}\alpha_k\varphi(t+k),\ x_{1(i_e)}\le x\le x_{5(i_e)}, \quad (1.8)$$

where $\varphi(s)$ is Daubechies scaling function, $[0,\,N]\subseteq\mathrm{supp}(\varphi)$.

We substitute (1.8) into (1.2), taking into account relations (1.5)-(1.7).

$$\Phi_{i_e}(y)=\frac{1}{2}\int_{x_1(i_e)}^{x_5(i_e)}\left(EJ\left(\frac{d^2y}{dx^2}\right)^2+\beta y^2\right)dx-$$
$$-\int_{x_1(i_e)}^{x_5(i_e)}qy\,dx=\frac{1}{2}\int_0^1\left(\frac{EJ}{h_e^3}(w'')^2+\beta h_e w^2\right)dt-$$
$$-\int_0^1 h_e q w\,dt=\frac{1}{2}\sum_{i=0}^{N}\sum_{j=0}^{N}\alpha_i\alpha_j\times$$
$$\times\int_0^1\left(\frac{EJ}{h_e^3}(\varphi''(t+i)\varphi''(t+j))+\beta h_e(\varphi(t+i)\varphi(t+j))\right)dt-$$
$$-\sum_{i=0}^{N}\alpha_i\int_0^1 h_e q\,\varphi(t+i)dt=$$
$$=\frac{1}{2}(K_\alpha^{i_e}\overline{\alpha},\overline{\alpha})-(\overline{R}_\alpha^{i_e},\overline{\alpha})=\Phi_\alpha(\overline{\alpha})$$

and finally

$$\Phi_{i_e}(y)=\Phi_\alpha(\overline{\alpha})=\frac{1}{2}(K_\alpha^{i_e}\overline{\alpha},\overline{\alpha})-(\overline{R}_\alpha^{i_e},\overline{\alpha}), \quad (1.9)$$

where

$$K_\alpha^{i_e}(i,j)=$$
$$=\int_0^1\left(\frac{EJ}{h_e^3}(\varphi''(t+i)\varphi''(t+j))+\beta h_e(\varphi(t+i)\varphi(t+j))\right)dt; \quad (1.10)$$

$$R_\alpha^{i_e}(i)=\int_0^1(h_e q(t)\varphi(t+i))dt. \quad (1.11)$$

We can define the parameters α_k through the nodal unknowns on the element:

$$\begin{cases}y_1=w(0)=\sum_{k=0}^{N}\alpha_k\varphi(k)\\ \frac{dy_1}{dx}=\frac{1}{h_e}w'(0)=\frac{1}{h_e}\sum_{k=0}^{N}\alpha_k\varphi'(k)\\ y_2=w(0.25)=\sum_{k=0}^{N}\alpha_k\varphi(k+0.25)\\ y_3=w(0.5)=\sum_{k=0}^{N}\alpha_k\varphi(k+0.5)\\ y_4=w(0.75)=\sum_{k=0}^{N}\alpha_k\varphi(k+0.75)\\ y_5=w(1)=\sum_{k=0}^{N}\alpha_k\varphi(k+1)\\ \frac{dy_5}{dx}=\frac{1}{h_e}w'(1)=\frac{1}{h_e}\sum_{k=0}^{N}\alpha_k\varphi'(k+1).\end{cases} \quad (1.12)$$

Thus, we have

$$\overline{y}^{i_e}=T\overline{\alpha}, \quad (1.13)$$

where

$$\overline{y}^{i_e}=[y_1\ \ \frac{dy_1}{dx}\ \ y_2\ \ y_3\ \ y_4\ \ y_5\ \ \frac{dy_5}{dx}]^T; \quad (1.14)$$

$$\overline{\alpha}=[\alpha_0\ \ \alpha_1\ \ \alpha_2\ \ \alpha_3\ \ \alpha_4\ \ \alpha_5\ \ \alpha_6]^T; \quad (1.15)$$

$$D=diag(1\quad 1/h_e\quad 1\quad 1\quad 1\quad 1\quad 1/h_e); \quad (1.16)$$

T is matrix, which is defined in accordance with the following formula:

$$T = D\begin{bmatrix} \varphi(0) & \varphi(1) & \varphi(2) & \varphi(3) & \varphi(4) & \varphi(5) & \varphi(6) \\ \varphi'(0) & \varphi'(1) & \varphi'(2) & \varphi'(3) & \varphi'(4) & \varphi'(5) & \varphi'(6) \\ \varphi(0.25) & \varphi(1.25) & \varphi(2.25) & \varphi(3.25) & \varphi(4.25) & \varphi(5.25) & \varphi(6.25) \\ \varphi(0.5) & \varphi(1.5) & \varphi(2.5) & \varphi(3.5) & \varphi(4.5) & \varphi(5.5) & \varphi(6.5) \\ \varphi(0.75) & \varphi(1.75) & \varphi(2.75) & \varphi(3.75) & \varphi(4.75) & \varphi(5.75) & \varphi(6.75) \\ \varphi(1) & \varphi(2) & \varphi(3) & \varphi(4) & \varphi(5) & \varphi(6) & \varphi(7) \\ \varphi'(1) & \varphi'(2) & \varphi'(3) & \varphi'(4) & \varphi'(5) & \varphi'(6) & \varphi'(7) \end{bmatrix}; \qquad (1.17)$$

Then we have

$$\overline{\alpha} = T^{-1}\overline{y}^{i_e}. \qquad (1.18)$$

Taking into account (1.9) and (1.18) we get

$$\Phi_\alpha(\overline{\alpha}) = \frac{1}{2}(K_\alpha^{i_e} T^{-1}\overline{y}^{i_e}, T^{-1}\overline{y}^{i_e}) - (\overline{R}_\alpha^{i_e}, T^{-1}\overline{y}^{i_e}) =$$
$$= \frac{1}{2}((T^{-1})^{\mathrm{T}} K_\alpha^{i_e} T^{-1}\overline{y}^{i_e}, \overline{y}^{i_e}) - ((T^{-1})^{\mathrm{T}}\overline{R}_\alpha^{i_e}, \overline{y}^{i_e}) =$$
$$= \frac{1}{2}(K^{i_e}\overline{y}^{i_e}, \overline{y}^{i_e}) - (\overline{R}^{i_e}, \overline{y}^{i_e}) = \Phi_{i_e}(\overline{y}^{i_e})$$

and finally

$$\Phi_\alpha(\overline{\alpha}) = \Phi_{i_e}(\overline{y}^{i_e}) = \\ = \frac{1}{2}(K^{i_e}\overline{y}^{i_e}, \overline{y}^{i_e}) - (\overline{R}^{i_e}, \overline{y}^{i_e}), \qquad (1.19)$$

where K^{i_e} is local stiffness matrix; $\overline{R}^{i_e}$ is local load vector;

$$K^{i_e} = (T^{-1})^{\mathrm{T}} K_\alpha^{i_e} T^{-1}; \quad \overline{R}^{i_e} = (T^{-1})^{T}\overline{R}_\alpha^{i_e}. \qquad (1.20)$$

1.3. Numerical implementation and sample of static beam analysis.

The presented algorithm can be implemented using the tools of MATLAB. In particular, the reference to the standard function

```
wavefun('db10',0)
```

allows researcher to get the values of the scaling Daubeshi function φ on the interval $[0,19] = \mathrm{supp}(\varphi)$ with steps $h_t = 1/256 = 2^{-8}$. Let us denote $N_t = 256 = 2^8$. For the considering value $N = 7$ we can use the first $N_l = N_t \cdot N + 1$ values of φ, defined on the segment $[0, N] = [0, 7]$. With such a small step, it will be natural to compute the derivatives in the form of finite differences:

$$\varphi'(t_k) \approx d\varphi_k = \frac{\varphi_{k+1} - \varphi_{k-1}}{2h_t}, \quad k = 1, 2, \ldots, N_l; \qquad (1.21)$$

$$\varphi''(t_k) \approx d2\varphi_k = \frac{\varphi_{k+1} - 2\varphi_k + \varphi_{k-1}}{h_t^2}, \quad k = 1, 2, \ldots, N_l, \qquad (1.22)$$

where $\varphi_k = \varphi(t_k); \quad t_k = k \cdot h_t.$ (1.23)

If $t_k \notin [0,19]$ then $\varphi_k = \varphi(t_k) = 0$.

When computing the coefficients of the local stiffness matrix (formulas (10) and (20)), one can use the simplest quadrature formulas for numerical integration, in particular, midpoint quadrature rule with step $2h_t$.

Let us consider (as a model sample) analysis of beam on an elastic foundation with the following parameters: $q(x) = P\delta(x - L/2)$, $P = 100$ kN is the load specified at the midpoint (Figure 6); $L = 4$ m; $h_b = 1.3$ m; $b_b = 1$ m; $E = 2560 \cdot 10^4$ kN/m^2; $k = 75 \cdot 10^3$ kN/m^3.

In this case, we can consider the following boundary conditions:

$$\begin{cases} y(0) = y''(0) = 0 \\ y(L) = y''(L) = 0. \end{cases} \qquad (1.24)$$

Thus, we consider beam hinged on both sides (simply supported beam).

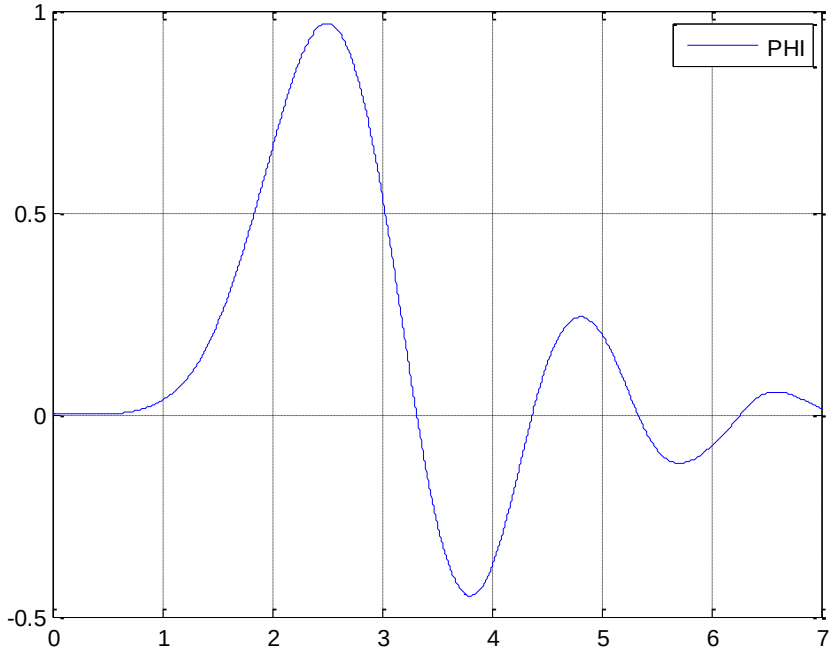

Figure 1.3. Daubechies scaling function.

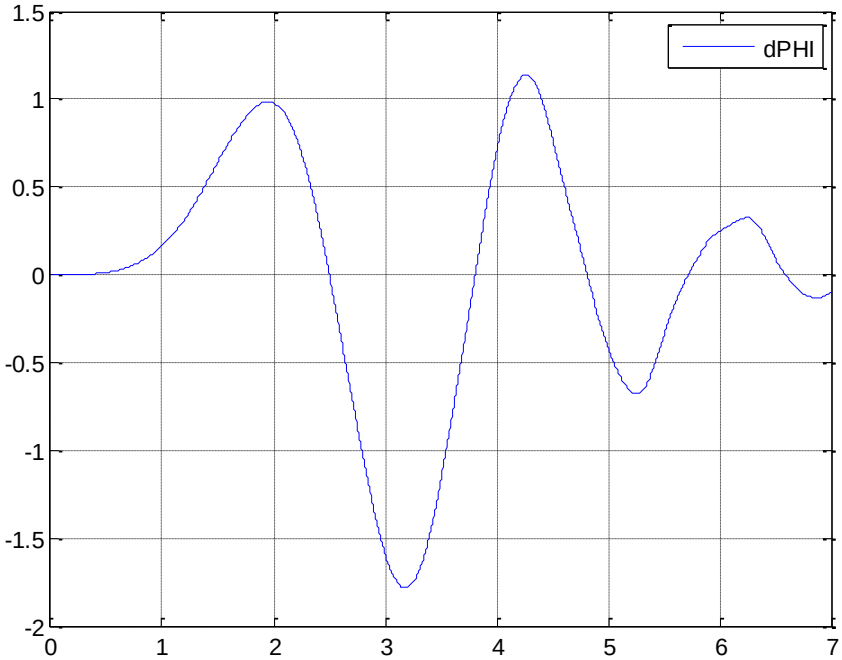

Figure 1.4. The first-order difference derivative of Daubechies scaling function.

Let $N_e = 8$ be a number of elements. Then the total number of unknowns is equal to

$$N_g = N_p + 2N_b = 3 \cdot 8 + 2 \cdot (8+1) = 42 .$$

The length of the element is defined by formula

$$h_e = L / N_e = 4/8 = 0.5 .$$

Distance between coordinates of nodes (step) is equal to

$$h_p = h_e / 4 = 1/8 = 0.125 .$$

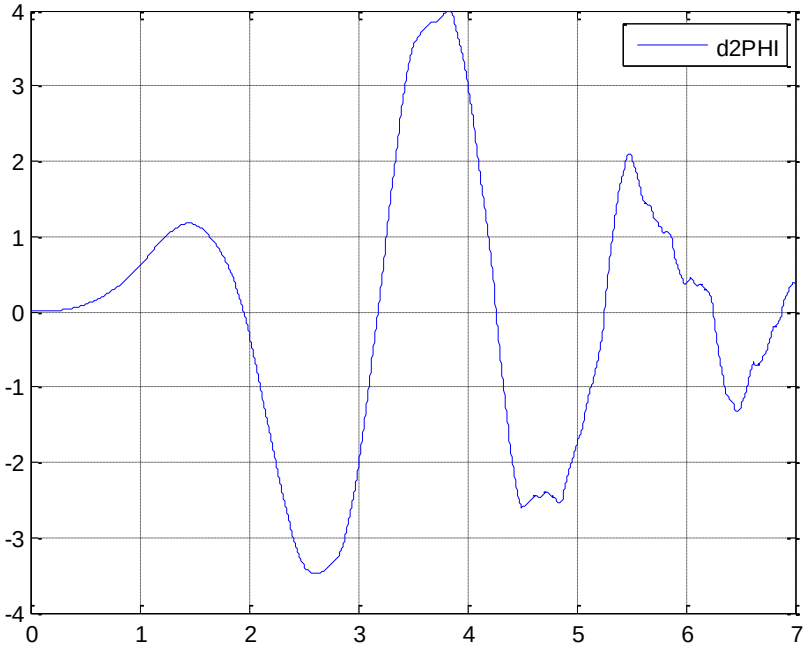

Figure 1.5. The second-order difference derivative of Daubechies scaling function.

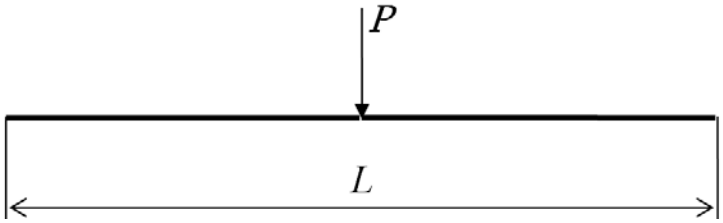

Figure 1.6. Considering beam.

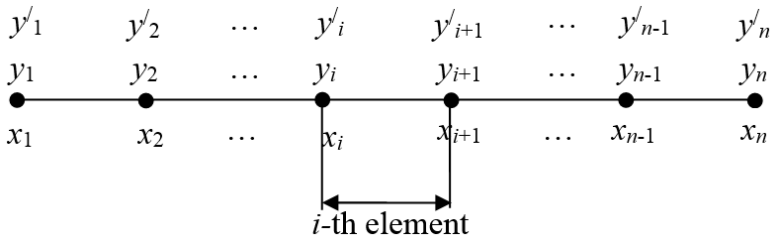

Figure 1.7. Finite element discretization of beam (based on cubic parabola).

As is known, for comparison, we can use the conventional finite element method, where the unknown function of the deflection on the element is represented as a cubic parabola. In this case, the finite element discretization is shown in Figure 7.

Adequate beam approximation requires 32 elements. In this case, the total number of unknowns is equal to

$$N_g = 2 \cdot (32 + 1) = 66 .$$

Graphical comparison of results of analysis is shown in Figure 8. The following notation is used: `Ydb` is the result obtained using Daubechies scaling function; `Yfem` is the result obtained on the basis of a cubic parabola.

As is obvious, the results obtained are almost the same. However, the wavelet-based algorithm of the finite element method based on the Daubechies scaling function leads to a decrease in the number of unknowns.

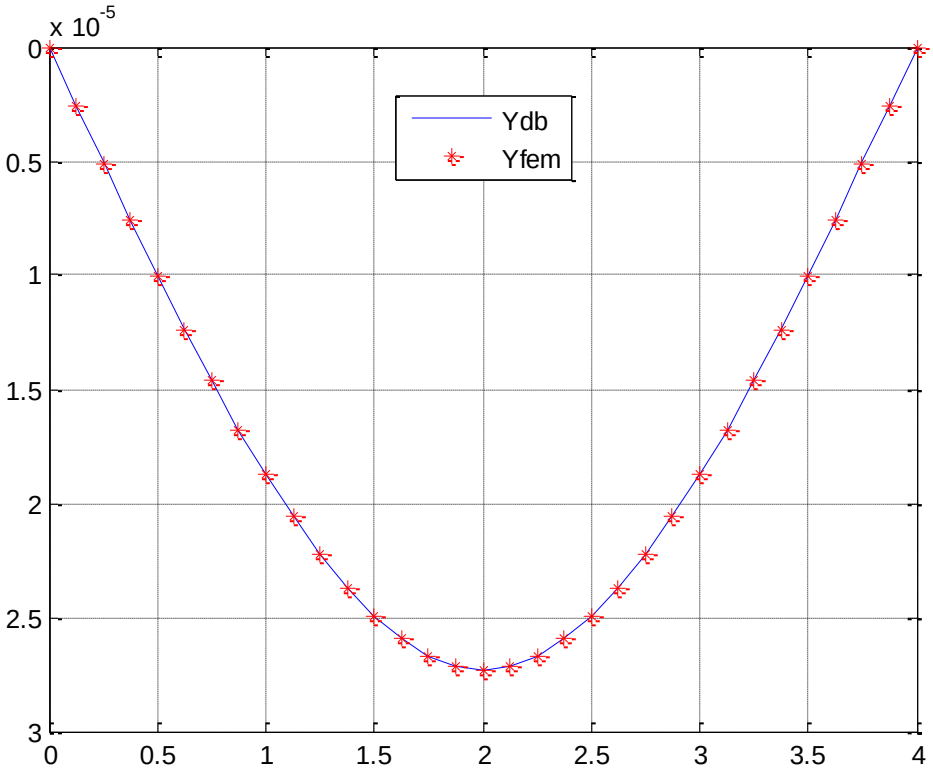

Figure 1.8. Comparison of results of analysis.

2. WAVELET-BASED SEMIANALYTICAL BEAM ANALYSIS WITH THE USE OF DAUBECHIES SCALING FUNCTIONS

2.1. Mathematical (continual) formulation of the problem of dynamic beam analysis.

Let us consider the problem of dynamic beam analysis (Figure 2.1). Corresponding impulse load is applied in the middle of the beam. Mathematical formulation of the problem has the form:

$$\begin{cases} \dfrac{\partial^2 y}{\partial t^2} = -\beta_0 \dfrac{\partial^4 y}{\partial x^4} + F(x,t), \\ 0 < x < \ell, \quad t > 0, \\ \left.\begin{array}{l} y(0,t) = y(\ell,t) = 0 \\ y''(0,t) = y''(\ell,t) = 0 \end{array}\right\}, \ t \geq 0 \\ \left.\begin{array}{l} y(x,0) = y_0(x) = 0 \\ \dfrac{\partial y}{\partial t}(x,0) = y_t'(x) = 0 \end{array}\right\}, \ 0 \leq x \leq \ell, \end{cases} \qquad (2.1)$$

where $y(x,t)$ is the deflection of a beam at a point x at a time t; x is the coordinate along the length of the beam, $0 \leq x \leq \ell$; t is time coordinate, $t \geq 0$; $\beta_0 = EJ/\rho$; EJ is bending stiffness of beam; ρ is density of the beam material; $F(x,t) = P \cdot \delta(x - \ell/2)\delta(t)$ is function simulating the transverse impact of the impact on the beam at a point; $\delta(x - \ell/2)$ and $\delta(t)$ are Dirac delta functions.

2.2. Wavelet-based discrete-continual approximation of the problem of dynamic beam analysis.

Discere-continual finite element method (discrete-analytical approach) is used for solution of the considering problem. Within this method we use finite element approximation along the x axis, and a continual problem is considered along the time axis t.

Let us divide domain (one-dimensional interval $(0, l)$), occupied by the beam into N_e parts (finite elements);

$$h_e = l / N_e$$

is the length of the element.

Each element is also divided into N_k parts, for example, $N_k = 4$.

Once again we can use the following notation: i_e is element number; $x_1(i_e)$ is coordinate of the starting point of the i_e-th element; $x_5(i_e)$ is coordinate of the end point of the i_e-th element. At the boundary points (nodes), we can choose unknowns y_i and y_i'; at the inner points we can choose unknowns y_i, $i = 2,3,4$. Thus, the total number of unknowns on an element is equal to

$$N = N_k - 1 + 2 \cdot 2 = N_k + 3 = 7 .$$

The number of boundary points for all elements, the number of interior points for all elements and the total number of unknowns are equal to

$$N_b = N_e + 1; \quad N_p = N_e(N_k - 1);$$
$$N_g = N_p + 2N_b .$$

We can also introduce the local coordinates

$$t = \frac{x - x_{1(i_e)}}{h_e}, \quad x_{1(i_e)} \le x \le x_{5(i_e)} \tag{2.2}$$

with corresoinding relations

$$\begin{cases} x = x_{1(i_e)} \Rightarrow t = 0 \\ x = x_2 \Rightarrow t = 0.25 \\ x = x_3 \Rightarrow t = 0.5 \\ x = x_4 \Rightarrow t = 0.75 \\ x = x_{5(i_e)} \Rightarrow t = 1; \end{cases} \tag{2.3}$$

$$\frac{d}{dx} = \frac{d}{dt} \cdot \frac{dt}{dx} = \frac{1}{h_e} \frac{d}{dt};$$
$$\frac{d^p}{dx^p} = \frac{1}{h_e^p} \frac{d^p}{dt^p}; \tag{2.4}$$

$$dx = h_e \cdot dt . \tag{2.5}$$

We can represent displacement (deflection) of beam $y(x,t)$ for a given t in the form

$$y(x,\cdot) = w(q) = \sum_{k=0}^{N-1} \alpha_k \varphi(q+k), \; x_{1(i_e)} \le x \le x_{5(i_e)}, \tag{2.6}$$

where $\varphi(s)$ is Daubechies scaling function, $[0, N] \subseteq \mathrm{supp}(\varphi)$.

We substitute (2.6) into the quadratic part of the corresponding energy functional, taking into account relations (2.3)-(2.5). Then we have

$$\int_{x_1(i_e)}^{x_5(i_e)} \left(\frac{d^2 y}{dx^2} \right)^2 dx = \frac{1}{h_e^3} \int_0^1 (w'')^2 dq =$$
$$= \sum_{i=0}^{N-1} \sum_{j=0}^{N-1} \frac{1}{h_e^3} \alpha_i \alpha_j \int_0^1 (\varphi''(q+i)\varphi''(q+j)) dq = \tag{2.7}$$
$$= (K_\alpha^{i_e} \overline{\alpha}, \overline{\alpha})$$

We can define the parameters α_k through the corresponding nodal unknowns on the element $y_i = y_i(t) = y(x_i, t)$:

$$\begin{cases} y_1 = w(0) = \sum_{k=0}^{N} \alpha_k \varphi(k) \\ \frac{dy_1}{dx} = \frac{1}{h_e} w'(0) = \frac{1}{h_e} \sum_{k=0}^{N} \alpha_k \varphi'(k) \\ y_2 = w(0.25) = \sum_{k=0}^{N} \alpha_k \varphi(k+0.25) \\ y_3 = w(0.5) = \sum_{k=0}^{N} \alpha_k \varphi(k+0.5) \\ y_4 = w(0.75) = \sum_{k=0}^{N} \alpha_k \varphi(k+0.75) \\ y_5 = w(1) = \sum_{k=0}^{N} \alpha_k \varphi(k+1) \\ \frac{dy_5}{dx} = \frac{1}{h_e} w'(1) = \frac{1}{h_e} \sum_{k=0}^{N} \alpha_k \varphi'(k+1). \end{cases} \tag{2.8}$$

Thus, we have

$$\overline{y}^{i_e} = T\overline{\alpha}, \tag{2.9}$$

$$T = D\begin{bmatrix} \varphi(0) & \varphi(1) & \varphi(2) & \varphi(3) & \varphi(4) & \varphi(5) & \varphi(6) \\ \varphi'(0) & \varphi'(1) & \varphi'(2) & \varphi'(3) & \varphi'(4) & \varphi'(5) & \varphi'(6) \\ \varphi(0.25) & \varphi(1.25) & \varphi(2.25) & \varphi(3.25) & \varphi(4.25) & \varphi(5.25) & \varphi(6.25) \\ \varphi(0.5) & \varphi(1.5) & \varphi(2.5) & \varphi(3.5) & \varphi(4.5) & \varphi(5.5) & \varphi(6.5) \\ \varphi(0.75) & \varphi(1.75) & \varphi(2.75) & \varphi(3.75) & \varphi(4.75) & \varphi(5.75) & \varphi(6.75) \\ \varphi(1) & \varphi(2) & \varphi(3) & \varphi(4) & \varphi(5) & \varphi(6) & \varphi(7) \\ \varphi'(1) & \varphi'(2) & \varphi'(3) & \varphi'(4) & \varphi'(5) & \varphi'(6) & \varphi'(7) \end{bmatrix}; \quad (2.10)$$

$$\bar{y}^{i_e} = [y_1 \ \frac{dy_1}{dx} \ y_2 \ y_3 \ y_4 \ y_5 \ \frac{dy_5}{dx}]^T; \quad (2.11)$$

$$\bar{\alpha} = [\alpha_0 \ \alpha_1 \ \alpha_2 \ \alpha_3 \ \alpha_4 \ \alpha_5 \ \alpha_6]^T; \quad (2.12)$$

$$D = diag(1 \quad 1/h_e \quad 1 \quad 1 \quad 1 \quad 1 \quad 1/h_e). \quad (2.13)$$

Then we have

$$\bar{\alpha} = T^{-1}\bar{y}^{i_e}. \quad (2.14)$$

Substituting (2.14) into (2.9), we get

$$(K_\alpha^{i_e} T^{-1}\bar{y}^{i_e}, T^{-1}\bar{y}^{i_e}) = (K^{i_e}\bar{y}^{i_e}, \bar{y}^{i_e}), \quad (2.15)$$

where $$K^{i_e} = (T^{-1})^{\mathrm{T}} K_\alpha^{i_e} T^{-1} \quad (2.16)$$

is local stiffness matrix.

We can use the simplest quadrature formulas of numerical integration for computing of coefficients of the local stiffness matrix.

Let us denote

$$\bar{y}(t) = [\, y_1(t) \quad y_2(t) \quad \ldots \quad y_{N_g}(t) \,]^T. \quad (2.17)$$

We can obtain the resultant system of finite element equations in the matrix form

$$\left\{ \begin{array}{l} \bar{y}''(t) = -A\bar{y} + \bar{F} \\ \bar{y}(0) = \bar{y}_0 \\ y'(0) = \bar{y}_0' \end{array} \right\}, \quad (2.18)$$

where A is global stiffness matrix.

The matrix A is positive definite. The general solution of the problem (2.18) has the form:

$$\begin{aligned} \bar{y}(t) = {} & \cos(\sqrt{A}\,t)\bar{y}_0 + \\ & + \sqrt{A^{-1}}\sin(\sqrt{A}\,t)\bar{y}_0' + \\ & + \sqrt{A^{-1}}\int_0^t \sin\sqrt{A}(t-\tau)\bar{F}(\tau)d\tau. \end{aligned} \quad (2.19)$$

In accordance with formulation of the considering problem we have

$$F(x,t) = P\cdot\delta(x-\ell/2)\,\delta(t) \quad (2.20)$$

and consequently

$$\bar{F}(t) = \delta(t)\cdot\bar{F}_0; \quad (2.21)$$

$$\bar{F}_0(i) = P\cdot\begin{cases} 1, & i = (N_g+1)/2 \\ 0, & i \neq (N_g+1)/2. \end{cases} \quad (2.22)$$

Substituting (2.22) into (2.19) and taking into account the initial conditions, we obtain the final form of the solution of the problem:

$$\bar{y}(t) = \sqrt{A^{-1}}\sin(\sqrt{A}\,t)\,\bar{F}_0. \quad (2.23)$$

ACKNOWLEDGMENTS

The distinctive research work was carried out at the expense of the State program of the Russian Federation “Scientific and technological development of the Russian Federation”, State program of the Russian Federation “Development of science and technology” for 2013-2020 and the Program for Fundamental Research of State Academies of Science for 2013–2020, as part of the Plan for Fundamental Scientific Research of the Ministry of Construction and Housing and Communal Services of the Russian Federation

and the Russian Academy of Architecture and Construction Sciences for 2018, within science topic 7.4.2 “Development and numerical implementation of methods for determining the stress-strain state of spatial slab-shell reinforced concrete structures, taking into account physical non-linearity, cracking and acquired anisotropy” and science topic 7.4.17 “Research and development of adaptive mathematical models, numerical and numerical-analytical methods as the basis and component of monitoring systems of bearing structures of unique buildings and constructions”.

REFERENCES

1. **Daubechies I.** Orthonormal bases of compactly supported wavelets. // Commun. Pure Appl. Math., 1988, vol. 41, pp. 909-996.
2. **Akimov P.A., Aslami M.** About Verification of Correct Wavelet-Based Approach to Local Static Analysis of Bernoulli Beam. // *Applied Mechanics and Materials*, 2014, Vols. 580-583, pp. 3013-3016.
3. **Akimov P.A., Aslami M.** Theoretical Foundations of Correct Wavelet-Based Approach to Local Static Analysis of Bernoulli Beam. // *Applied Mechanics and Materials*, 2014, Vols. 580-583, pp. 2924-2927.
4. **Akimov P.A., Belostotsky A.M., Kaytukov T.B., Mozgaleva M.L., Aslami M.** About several numerical and semianalytical methods of local structural analysis. // *International Journal for Computational Civil and Structural Engineering*, 2018, Vol. 14, Issue 4, pp. 59-69.
5. **Akimov P.A., Mozgaleva M.L.** Correct Wavelet-based Multilevel Numerical Method of Local Solution of Boundary Problems of Structural Analysis. // *Applied Mechanics and Materials*, 2012, Vols. 166-169, pp. 3155-3158.
6. **Aslami M., Akimov P.A.** Wavelet-based finite element method for multilevel local plate analysis. // *Thin-Walled Structures*, 2015-2016, Vol. 98, Part B, pp. 392-402.
7. **Akimov P.A., Belostotsky A.M., Mozgaleva M.L., Aslami M., Negrozov O.A.** Correct Multilevel Discrete-Continual Finite Element Method of Structural Analysis. // *Advanced Materials Research*, 2014, Vol. 1040, pp. 664-669.
8. **Akimov P.A., Belostotsky A.M., Sidorov V.N., Mozgaleva M.L., Negrozov O.A.** Application of discrete-continual finite element method for global and local analysis of multilevel systems. // *Applied Mechanics and Materials; AIP Conference Proceedings*, 2014, Vol. 1623(3), pp. 3-6.
9. **Akimov P.A., Mozgaleva M.L.** Correct Wavelet-based Multilevel Discrete-Continual Methods for Local Solution of Boundary Problems of Structural Analysis. // *Applied Mechanics and Materials*, 2013, Vols. 353-356, pp. 3224-3227.
10. **Akimov P.A., Mozgaleva M.L.** Wavelet-based Multilevel Discrete-Continual Finite Element Method for Local Deep Beam Analysis. // *Applied Mechanics and Materials*, 2013, Vols. 405-408, pp. 3165-3168.
11. **Akimov P.A., Mozgaleva M.L.** Wavelet-based Multilevel Discrete-Continual Finite Element Method for Local Plate Analysis. // *Applied Mechanics and Materials*, 2013, Vols. 351-352, pp. 13-16.
12. **Akimov P.A., Mozgaleva M.L., Aslami M., Negrozov O.A.** Modified Wavelet-based Multilevel Discrete-Continual Finite Element. Part 1: Continual and Discrete-Continual Formulations of the Problems Method for Local Structural Analysis. // *Applied Mechanics and Materials*, 2014, Vols. 670-671, pp. 720-723.
13. **Akimov P.A., Mozgaleva M.L., Aslami M., Negrozov O.A.** Modified Wavelet-based Multilevel Discrete-Continual Finite Element. Part 2: Reduced Formulations of the Problems in Haar Basis Method for Local Structural Analysis. // *Applied Mechanics and Materials*, 2014, Vols. 670-671, pp. 724-727.
14. **Mozgaleva M.L., Akimov P.A.** About Verification of Wavelet-Based Discrete-

Continual Finite Element Method for Three-Dimensional Problems. Part 1: Structures with Constant Physical and Geometrical of Structural Analysis Parameters Along Basic Direction. // *Applied Mechanics & Materials*, 2015, Vol. 709, pp. 105-108.

15. **Mozgaleva M.L., Akimov P.A.** About Verification of Wavelet-Based Discrete-Continual Finite Element Method for Three-Dimensional Problems. Part 2: Structures with Piecewise Constant Physical and Geometrical Parameters Along Basic Direction of Structural Analysis. // *Applied Mechanics & Materials*, 2015, Vol. 709, pp. 109-112.
16. **Mozgaleva M.L., Akimov P.A., Kaytukov T.B.** About wavelet-based multigrid numerical method of structural analysis with the use of discrete Haar basis. // *International Journal for Computational Civil and Structural Engineering*, 2018, Vol. 14, Issue 3, pp. 83-102.
17. **Li B., Chen X.** Wavelet-based numerical analysis: A review and classification. // *Finite Elements in Analysis and Design*, 2014, vol. 81, pp. 14-31.
18. **Ko J., Kurdila A.J., Pilant M.S.** A class of finite element methods based on orthonormal, compactly supported wavelets. // *Comput. Mech.*, 1995, Vol. 16, pp. 235-244.
19. **Patton R.D., Marks P.C.** One-dimensional finite elements based on the Daubechies family of wavelets. // *AIAAJ*, 1996, Vol. 34, pp. 1696-1698.
20. **Ma J.X., Xue J.J.** A study of the construction and application of a Daubechies wavelet-based beam element. // *Finite Elem. Anal. Des.*, 2003, vol. 39, pp. 965-975.
21. **Chen X.F., Yang S.J., Ma J.X.** The construction of wavelet finite element and its application. // *Finite Elem. Anal. Des.*, 2004, vol. 40, pp. 541-554.
22. **Li B., Cao H.R., He Z.J.** The construction of one-dimensional Daubechies wavelet-based finite elements for structural response analysis. // *J. Vibroeng*, 2011, vol. 13, pp. 729-738.
23. **Jin J.M., Xue P.X., Xu Y.X., Zhu Y.L.** Compactly supported non-tensor product form two-dimension wavelet finite element. // *Appl. Math. Mech.*, 2006, Vol. 27, pp. 1673-1686.
24. **Zhou Y.H., Zhou J.** A modified wavelet approximation of deflections for solving PDEs of beams and square thin plates. // *Finite Elements in Analysis and Design*, 2008, vol. 44, pp. 773-783.
25. **Mitra M., Gopalakrishnan S.** Extraction of wave characteristics from wavelet-based spectral finite element formulation. // Mech. Syst. Signal Process, 2006, vol. 20, pp. 2046–2079.
26. **Mitra M., Gopalakrishnan S.** Wavelet Spectral element for wave propagation studies in pressure loaded axisymmetric cylinders. // J. Mech. Mater. Struct., 2007, vol. 4, pp. 753-772.
27. **Mitra M., Gopalakrishnan S.** Wave propagationan alysis in anisotropic plate using wavelet spectral element approach. // J. Appl. Mech., 2008, vol. 75, pp. 1-6.
28. **Mitra M., Gopalakrishnan S.** Wavelet-based spectral finite element modelling and detection of delamination in composite beams. // *Proceed. R. Soc. A*, 2006, vol. 462, pp. 1721-1740.
29. **Aslami M., Akimov P.A.** Analytical solution for beams with multipoint boundary conditions on two-parameter elastic foundations. // *Archives of Civil and Mechanical Engineering*, 2016, Vol. 16, Issue 4, pp. 668-677.

СПИСОК ЛИТЕРАТУРЫ

1. **Daubechies I.** Orthonormal bases of compactly supported wavelets. // Commun. Pure Appl. Math., 1988, vol. 41, pp. 909-996.
2. **Akimov P.A., Aslami M.** About Verification of Correct Wavelet-Based Approach to

Local Static Analysis of Bernoulli Beam. // *Applied Mechanics and Materials*, 2014, Vols. 580-583, pp. 3013-3016.

3. **Akimov P.A., Aslami M.** Theoretical Foundations of Correct Wavelet-Based Approach to Local Static Analysis of Bernoulli Beam. // *Applied Mechanics and Materials*, 2014, Vols. 580-583, pp. 2924-2927.
4. **Akimov P.A., Belostotsky A.M., Kaytukov T.B., Mozgaleva M.L., Aslami M.** About several numerical and semianalytical methods of local structural analysis. // *International Journal for Computational Civil and Structural Engineering*, 2018, Vol. 14, Issue 4, pp. 59-69.
5. **Akimov P.A., Mozgaleva M.L.** Correct Wavelet-based Multilevel Numerical Method of Local Solution of Boundary Problems of Structural Analysis. // *Applied Mechanics and Materials*, 2012, Vols. 166-169, pp. 3155-3158.
6. **Aslami M., Akimov P.A.** Wavelet-based finite element method for multilevel local plate analysis. // *Thin-Walled Structures*, 2015-2016, Vol. 98, Part B, pp. 392-402.
7. **Akimov P.A., Belostotsky A.M., Mozgaleva M.L., Aslami M., Negrozov O.A.** Correct Multilevel Discrete-Continual Finite Element Method of Structural Analysis. // *Advanced Materials Research*, 2014, Vol. 1040, pp. 664-669.
8. **Akimov P.A., Belostotsky A.M., Sidorov V.N., Mozgaleva M.L., Negrozov O.A.** Application of discrete-continual finite element method for global and local analysis of multilevel systems. // *Applied Mechanics and Materials; AIP Conference Proceedings*, 2014, Vol. 1623(3), pp. 3-6.
9. **Akimov P.A., Mozgaleva M.L.** Correct Wavelet-based Multilevel Discrete-Continual Methods for Local Solution of Boundary Problems of Structural Analysis. // *Applied Mechanics and Materials*, 2013, Vols. 353-356, pp. 3224-3227.
10. **Akimov P.A., Mozgaleva M.L.** Wavelet-based Multilevel Discrete-Continual Finite Element Method for Local Deep Beam Analysis. // *Applied Mechanics and Materials*, 2013, Vols. 405-408, pp. 3165-3168.
11. **Akimov P.A., Mozgaleva M.L.** Wavelet-based Multilevel Discrete-Continual Finite Element Method for Local Plate Analysis. // *Applied Mechanics and Materials*, 2013, Vols. 351-352, pp. 13-16.
12. **Akimov P.A., Mozgaleva M.L., Aslami M., Negrozov O.A.** Modified Wavelet-based Multilevel Discrete-Continual Finite Element. Part 1: Continual and Discrete-Continual Formulations of the Problems Method for Local Structural Analysis. // *Applied Mechanics and Materials*, 2014, Vols. 670-671, pp. 720-723.
13. **Akimov P.A., Mozgaleva M.L., Aslami M., Negrozov O.A.** Modified Wavelet-based Multilevel Discrete-Continual Finite Element. Part 2: Reduced Formulations of the Problems in Haar Basis Method for Local Structural Analysis. // *Applied Mechanics and Materials*, 2014, Vols. 670-671, pp. 724-727.
14. **Mozgaleva M.L., Akimov P.A.** About Verification of Wavelet-Based Discrete-Continual Finite Element Method for Three-Dimensional Problems. Part 1: Structures with Constant Physical and Geometrical of Structural Analysis Parameters Along Basic Direction. // *Applied Mechanics & Materials*, 2015, Vol. 709, pp. 105-108.
15. **Mozgaleva M.L., Akimov P.A.** About Verification of Wavelet-Based Discrete-Continual Finite Element Method for Three-Dimensional Problems. Part 2: Structures with Piecewise Constant Physical and Geometrical Parameters Along Basic Direction of Structural Analysis. // *Applied Mechanics & Materials*, 2015, Vol. 709, pp. 109-112.
16. **Mozgaleva M.L., Akimov P.A., Kaytukov T.B.** About wavelet-based multigrid numerical method of structural analysis with the use of discrete Haar basis. // *International Journal for Computational Civil and Struc-*

tural Engineering, 2018, Vol. 14, Issue 3, pp. 83-102.
17. **Li B., Chen X.** Wavelet-based numerical analysis: A review and classification. // *Finite Elements in Analysis and Design*, 2014, vol. 81, pp. 14-31.
18. **Ko J., Kurdila A.J., Pilant M.S.** A class of finite element methods based on orthonormal, compactly supported wavelets. // *Comput. Mech.*, 1995, Vol. 16, pp. 235-244.
19. **Patton R.D., Marks P.C.** One-dimensional finite elements based on the Daubechies family of wavelets. // *AIAAJ*, 1996, Vol. 34, pp. 1696-1698.
20. **Ma J.X., Xue J.J.** A study of the construction and application of a Daubechies wavelet-based beam element. // *Finite Elements in Analysis and Design*, 2003, vol. 39, pp. 965-975.
21. **Chen X.F., Yang S.J., Ma J.X.** The construction of wavelet finite element and its application. // *Finite Elements in Analysis and Design*, 2004, vol. 40, pp. 541-554.
22. **Li B., Cao H.R., He Z.J.** The construction of one-dimensional Daubechies wavelet-based finite elements for structural response analysis. // *J. Vibroeng*, 2011, vol. 13, pp. 729-738.
23. **Jin J.M., Xue P.X., Xu Y.X., Zhu Y.L.** Compactly supported non-tensor product form two-dimension wavelet finite element. // *Appl. Math. Mech.*, 2006, Vol. 27, pp. 1673-1686.
24. **Zhou Y.H., Zhou J.** A modified wavelet approximation of deflections for solving PDEs of beams and square thin plates. // *Finite Elements in Analysis and Design*, 2008, vol. 44, pp. 773-783.
25. **Mitra M., Gopalakrishnan S.** Extraction of wave characteristics from wavelet-based spectral finite element formulation. // Mech. Syst. Signal Process, 2006, vol. 20, pp. 2046–2079.
26. **Mitra M., Gopalakrishnan S.** Wavelet Spectral element for wave propagation studies in pressure loaded axisymmetric cylinders. // J. Mech. Mater. Struct., 2007, vol. 4, pp. 753-772.
27. **Mitra M., Gopalakrishnan S.** Wave propagationan alysis in anisotropic plate using wavelet spectral element approach. // J. Appl. Mech., 2008, vol. 75, pp. 1-6.
28. **Mitra M., Gopalakrishnan S.** Wavelet-based spectral finite element modelling and detection of delamination in composite beams. // *Proceed. R. Soc. A*, 2006, vol. 462, pp. 1721-1740.
29. **Aslami M., Akimov P.A.** Analytical solution for beams with multipoint boundary conditions on two-parameter elastic foundations. // *Archives of Civil and Mechanical Engineering*, 2016, Vol. 16, Issue 4, pp. 668-677.

Marina L. Mozgaleva, Dr.Sc., Professor, Department of Applied Mathematics, National Research Moscow State University of Civil Engineering, 26, Yaroslavskoe Shosse, Moscow, 129337, Russia;
phone/fax: +7(499) 183-59-94;
E-mail: marina.mozgaleva@gmail.com.

Pavel A. Akimov, Full Member of the Russian Academy of Architecture and Construction Sciences (RAACS), Professor, Dr.Sc.; Executive Scientific Secretary of Russian Academy of Architecture and Construction Sciences; Vice-Director for Science Activities, Scientific Research Center "StaDyO"; Professor of Department of Architecture and Construction, Peoples' Friendship University of Russia; Professor of Department of Structural Mechanics, Tomsk State University of Architecture and Building; 24, Ul. Bolshaya Dmitrovka, 107031, Moscow, Russia;
phone +7(495) 625-71-63; fax: +7 (495) 650-27-31;
E-mail: akimov@raasn.ru, pavel.akimov@gmail.com.

Taymuraz B. Kaytukov, Advisor of the Russian Academy of Architecture and Construction Sciences, Associated Professor, Ph.D.; Deputy Executive Scientific Secretary of Russian Academy of Architecture and Construction Sciences; Central Institute for Research and Design of the Ministry of Construction and Housing and Communal Services of the Russian Federation; 24, Ul. Bolshaya Dmitrovka, 107031, Moscow, Russia;
phone +7(495) 625-81-53; fax: +7 (495) 650-27-31;
Email: kaytukov@raasn.ru, tkaytukov@gmail.com.

Мозгалева Марина Леонидовна, доцент, доктор технических наук, профессор кафедры прикладной математики, Национальный исследовательский Москов-

ский государственный строительный университет (НИУ МГСУ), Россия, 129337, Москва, Ярославское шоссе, д.26, тел./факс: +7(499) 183-59-94,
E-mail: marina.mozgaleva@gmail.com.

Акимов Павел Алексеевич, академик Российской академии архитектуры и строительных наук (РААСН), профессор, доктор технических наук; главный ученый секретарь Российской академии архитектуры и строительных наук; заместитель генерального директора по науке ЗАО «Научно-исследовательский центр СтаДиО»; профессор Департамента архитектуры и строительства Российского университета дружбы народов; профессор кафедры строительной механики Томского государственного архитектурно-строительного университета; 107031, г. Москва, ул. Большая Дмитровка, д. 24, стр. 1; тел. +7(495) 625-71-63;
факс +7 (495) 650-27-31; Email: akimov@raasn.ru, pavel.akimov@gmail.com.

Кайтуков Таймураз Батразович, советник РААСН, доцент, кандидат технических наук, заместитель главного ученого секретаря Российской академии архитектуры и строительных наук; Центральный научно-исследовательский и проектный институт Министерства строительства и жилищно-коммунального хозяйства Российской Федерации; 107031, г. Москва, ул. Большая Дмитровка, д. 24, стр. 1;
тел. +7(495) 625-81-53; факс +7 (495) 650-27-31;
E-mail: kaytukov@raasn.ru, tkaytukov@gmail.com.

DOI:10.22337/2587-9618-2019-15-2-111-124

MATHEMATICAL MODELING OF NON-STATIONARY ELASTIC WAVES STRESSES UNDER A CONCENTRATED VERTICAL EXPOSURE IN THE FORM OF DELTA FUNCTIONS ON THE SURFACE OF THE HALF-PLANE (LAMB PROBLEM)

Vyacheslav K. Musayev
Russian University of Transport (MIIT), Moscow, RUSSIA
Moscow Polytechnic University, Moscow, RUSSIA
Mingachevir state University, Mingachevir, AZERBAIJAN

Abstract: The problem of numerical simulation of longitudinal, transverse and surface waves on the free surface of an elastic half-plane is considered. The change of the elastic contour stress on the free surface of the half-plane is given. To solve the two-dimensional unsteady dynamic problem of the mathematical theory of elasticity with initial and boundary conditions, we use the finite element method in displacements. Using the finite element method in displacements, a linear problem with initial and boundary conditions resulted in a linear Cauchy problem. Some information on the numerical simulation of elastic stress waves in an elastic half-plane under concentrated wave action in the form of a Delta function is given. The amplitude of the surface Rayleigh waves is significantly greater than the amplitudes of longitudinal, transverse and other waves with concentrated vertical action in the form of a triangular pulse on the surface of the elastic half-plane. After the surface Rayleigh waves there is a dynamic process in the form of standing waves.

Keywords: waves of stress, non-stationary process, computational mechanics, focused effects, a Delta function, leading edge of a disturbance, the falling edge of the perturbation, the direction of wave action, longitudinal wave, transverse wave, free surface, Rayleigh wave, surface wave, lamb problem, elastic half-plane, stress on the free surface

МАТЕМАТИЧЕСКОЕ МОДЕЛИРОВАНИЕ НЕСТАЦИОНАРНЫХ УПРУГИХ ВОЛН НАПРЯЖЕНИЙ ПРИ СОСРЕДОТОЧЕННОМ ВЕРТИКАЛЬНОМ ВОЗДЕЙСТВИИ В ВИДЕ ДЕЛЬТА ФУНКЦИИ НА ПОВЕРХНОСТИ ПОЛУПЛОСКОСТИ (ЗАДАЧА ЛЭМБА)

В.К. Мусаев
Российский университет транспорта (МИИТ), Москва, РОССИЯ
Московский политехнический университет, Москва, РОССИЯ
Мингячевирский государственный университет, Мингячевир, АЗЕРБАЙДЖАН

Аннотация: Рассматривается задача о численном моделировании продольных, поперечных и поверхностных волн на свободной поверхности упругой полуплоскости. Приводится изменение упругого контурного напряжения на свободной поверхности полуплоскости. Для решения двумерной нестационарной динамической задачи математической теории упругости с начальными и граничными условиями используем метод конечных элементов в перемещениях. С помощью метода конечных элементов в перемещениях, линейную задачу с начальными и граничными условиями привели к линейной задаче Коши. Приводится некоторая информация о численном моделировании упругих волн напряжений в упругой полуплоскости при сосредоточенном волновом воздействии в виде дельта функции. Амплитуда поверхностных волн Релея существенно больше амплитуд продольных, поперечных и других волн при сосредоточенном вертикальном воздействии в виде треугольного импульса на поверхности упругой полуплоскости. После поверхностных волн Релея наблюдается динамический процесс в виде стоячих волн.

Ключевые слова: волны напряжений, нестационарный процесс, вычислительная механика, сосредоточенное воздействие, дельта функция, передний фронт возмущения, задний фронт возмущения, направление волнового воздействия, продольная волна, поперечная волна, свободная поверхность, волна Релея, поверхностная волна, задача Лэмба, упругая полуплоскость, напряжения на свободной поверхности

1. STATEMENT OF THE PROBLEM ABOUT NON-STATIONARY WAVE INFLUENCES

Waves of stresses of different nature, spreading, in the deformable body interact with each other, this leads to the formation of new perturbation regions, redistribution of stresses and strains.
After three or four times the passage and reflection of stress waves in the body the process of propagation of disturbances becomes established, stresses and strains are averaged, the body is in oscillatory motion.
The formulation of dynamic problems of solid mechanics is given in the following works [1-5].
Application of the considered numerical method, algorithm and complex of programs in extreme problems of mechanics of deformable bodies is given in the works [6-30].
The estimation of reliability and accuracy of the considered numerical method, algorithm and complex of programs is given in the following works [6-12, 16-29].

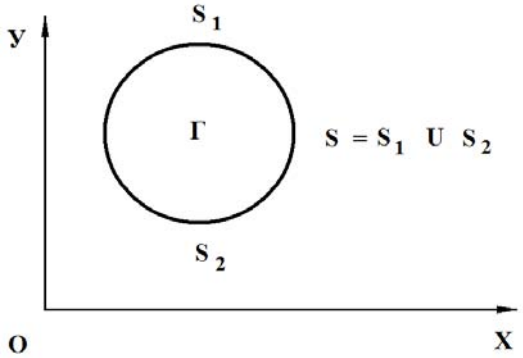

Figure 1. Some body Γ in a rectangular cartesian coordinate system XOY .

To solve the problem the modeling of transient elastic stress waves in deformable areas of the complex form consider some body Γ in a rectangular Cartesian coordinate system XOY (Figure 1), which at the initial time $t = 0$ reported mechanical non-stationary impulsive effects.
Suggest, the body Γ made of homogeneous isotropic material, obeying Hooke's elastic law at small elastic deformations.
Exact two-dimensional equations (flat stress state) the dynamic theory of elasticity have the form

$$\frac{\partial \sigma_x}{\partial X} + \frac{\partial \tau_{xy}}{\partial Y} = \rho \frac{\partial^2 u}{\partial t^2},$$

$$\frac{\partial \tau_{yx}}{\partial X} + \frac{\partial \sigma_y}{\partial Y} = \rho \frac{\partial^2 v}{\partial t^2}, \ (x,y) \in \Gamma,$$

$$\sigma_x = \rho C_p^2 \varepsilon_x + \rho (C_p^2 - 2C_s^2) \varepsilon_y,$$

$$\sigma_y = \rho C_p^2 \varepsilon_y + \rho (C_p^2 - 2C_s^2) \varepsilon_x,$$

$$\tau_{xy} = \rho C_s^2 \gamma_{xy},$$

$$\varepsilon_x = \frac{\partial u}{\partial X}, \ \varepsilon_y = \frac{\partial v}{\partial Y},$$

$$\gamma_{xy} = \frac{\partial u}{\partial Y} + \frac{\partial v}{\partial X}, \quad (x,y) \in (\Gamma \cup S), \quad (1)$$

where: σ_x, σ_y and τ_{xy} – components of elastic stress tensor; ε_x, ε_y и γ_{xy} – components of elastic strain tensor; u and v – the components of the vector of elastic displacements along the axes OX and OY respectively; ρ – material density;

$$C_p = \sqrt{\frac{E}{\rho(1-\nu^2)}}$$

– the speed of longitudinal elastic waves;

$$C_s = \sqrt{\frac{E}{2\rho(1+\nu)}}$$

– the speed of the transverse elastic waves; ν – Poisson ratio; E – elastic modulus; $S\ (S_1 \cup S_2)$ - body boundary contour Γ.

System (1) in the area occupied by the body Γ, it should be integrated under initial and boundary conditions.

2. DEVELOPMENT OF METHODOLOGY AND ALGORITHM

To solve the two-dimensional plane dynamic problem of elasticity theory with initial and boundary conditions (1) we use the finite element method in displacements.

The problem is solved by a method of through computation, without allocation of breaks.

The main relations of the finite element method are obtained using the principle of possible displacements.

Taking into account the definition of the stiffness matrix, the inertia vector and the external force vector for the body Γ, we write the approximate value of the equation of motion in the theory of elasticity

$$\overline{H}\ddot{\vec{\Phi}} + \overline{K}\vec{\Phi} = \vec{R},$$
$$\vec{\Phi}\big|_{t=0} = \vec{\Phi}_0, \quad \dot{\vec{\Phi}}\big|_{t=0} = \dot{\vec{\Phi}}_0, \qquad (2)$$

где: $\overline{H}$ - diagonal inertia matrix; $\overline{K}$ - stiffness matrix; $\vec{\Phi}$ - vector of nodal elastic displacements; $\dot{\vec{\Phi}}$ - vector of nodal elastic velocities of displacements; $\ddot{\vec{\Phi}}$ - the vector of elastic nodal accelerations; $\vec{R}$ - vector of external nodal elastic forces.

Relation (2) a system of linear ordinary differential equations of the second order in displacements with initial conditions.

Thus, using the finite element method in displacements, linear problem with initial and boundary conditions (1) led to the linear Cauchy problem (2).

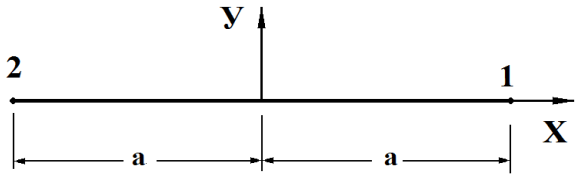

Figure 2. Contour finite element with two nodal points.

We determine the elastic contour stress at the boundary of the area free from loads.

By degenerating a rectangular finite element with four nodal points, we obtain a contour finite element with two nodal points (Figure 2).

When axis is rotated x by an angle α counterclockwise, we obtain an elastic contour stress σ_k at the center of gravity of a contour finite element with two nodal points

$$\sigma_k = (E/(2a(1-\nu^2)))((u_1 - u_2)\cos\alpha + (v_1 - v_2)\sin\alpha). \qquad (3)$$

To integrate the equation (2) with the finite element version of the Galerkin method, we give it to the following form

$$\overline{H}\frac{d}{dt}\dot{\vec{\Phi}} + \overline{K}\vec{\Phi} = \vec{R},\ \frac{d}{dt}\vec{\Phi} = \dot{\vec{\Phi}}. \qquad (4)$$

Integrating the time coordinate ratio (4) using the finite element version of the Galerkin method, we obtain a two-dimensional explicit two-layer finite element linear scheme in displacements for internal and boundary nodal points

$$\dot{\vec{\Phi}}_{i+1} = \dot{\vec{\Phi}}_i + \Delta t\overline{H}^{-1}(-\overline{K}\vec{\Phi}_i + \vec{R}_i),$$
$$\vec{\Phi}_{i+1} = \vec{\Phi}_i + \Delta t\dot{\vec{\Phi}}_{i+1}. \qquad (5)$$

The main relations of the finite element method in displacements are obtained using the principle of possible displacements and the finite element version of the Galerkin method.

The General theory of numerical equations of mathematical physics requires the imposition of certain conditions on the ratio of steps in the

time coordinate Δt and on spatial coordinates, namely

$$\Delta t = k \frac{min\ \Delta l_i}{C_p} \quad (i = 1,\ 2,\ 3,...), \qquad (6)$$

where: Δl – the length of the end element side.
The results of the numerical experiment showed that at k = 0,5 the stability of a two-dimensional explicit two-layer finite element linear scheme in displacements for internal and boundary nodal points on quasi-regular grids is ensured.
For the study area consisting of materials with different physical properties, the minimum step in the time coordinate (6) is selected.
On the basis of the finite element method in displacements the technique is developed, the algorithm is developed and compiled a set of programs to solve two-dimensional wave problems of dynamic elasticity theory.

DETERMINATION OF UNSTEADY WAVE STRESSES IN AN ELASTIC HALF-PLANE

Consider the problem of the action of a concentrated wave in the form of Delta functions (fig. 4) perpendicular to the free surface of the elastic half-plane (Figure 3).
Calculations were carried out in the following units: kilogram-force (kgf); centimeter (cm); second (s). The following assumptions were made for conversion to other units: 1 kgf/cm^2 ≈ 0,1 MPa.
At the point B perpendicular to the free surface ABC elastic normal stress is applied σ_y (fig. 3), which, when $0 \le n \le 11$ ($n = t/\Delta t$) changes linearly against 0 until P, and when $11 \le n \le 21$ against P until 0 ($P = \sigma_0$, σ_0 = -0,1 MPa (-1 kgf/cm^2)).
Boundary conditions for the contour $CDEA$ by $t > 0$ $u = v = \dot{u} = \dot{v} = 0$. Reflected waves from the circuit $CDEA$ do not reach to the point when $0 \le n \le 500$.

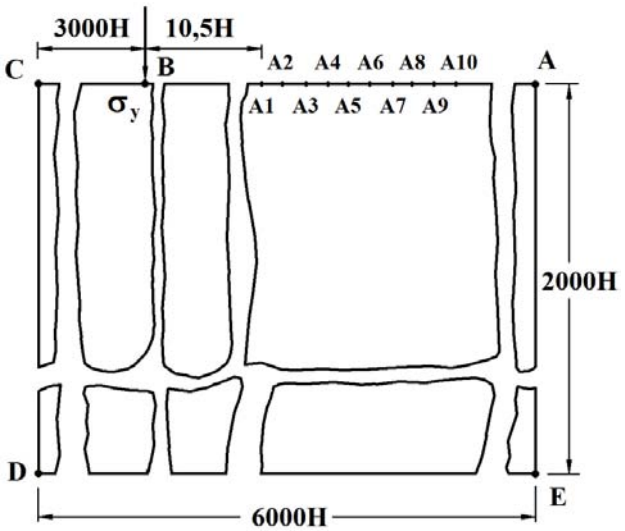

Figure 3. Formulation of the problem of the effect of a concentrated wave in the form of Delta functions on the free surface of the elastic half-plane.

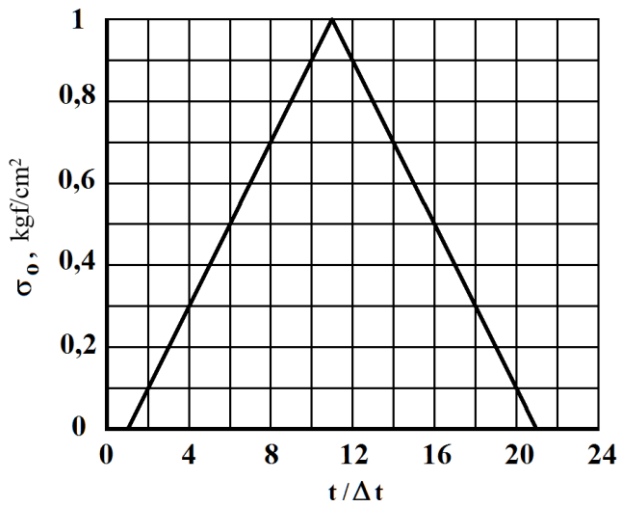

Figure 4. Impact in the form of Delta function.

Circuit ABC free from loads, besides the point B, where concentrated elastic normal stress is applied σ_y.

The calculations are carried out with the following initial data: $H = \Delta x = \Delta y$; Δt = 1,393·10^{-6} s; E = 3,15·10 ^{4} MPa (3,15·10 ^{5} kgf/cm^2); v = 0,2; ρ = 0,255·10^4 kg/m^3 (0,255·10^{-5} kgf·s^2/cm^4); C_p = 3587 m/s; C_s = 2269 m/s.

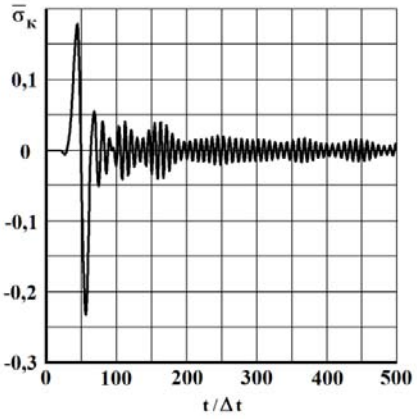

Figure 5. Change of elastic contour stress $\bar{\sigma}_k$ *in time* $t/\Delta t$ *at the point* $A1$.

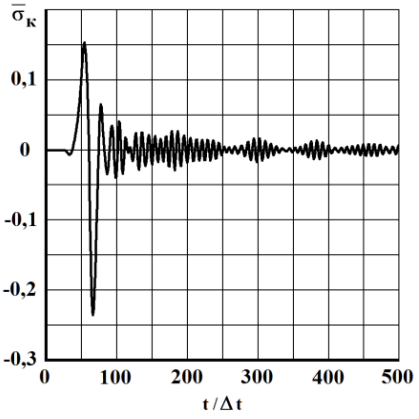

Figure 8. Change of elastic contour stress $\bar{\sigma}_k$ *in time* $t/\Delta t$ *at the point* $A4$.

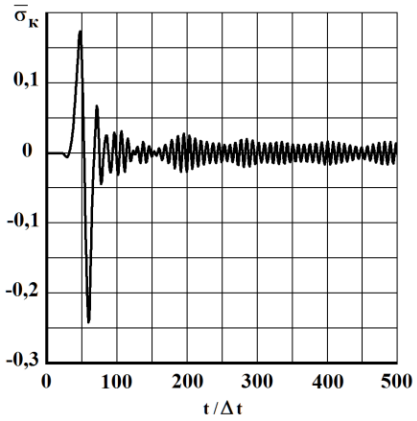

Figure 6. Change of elastic contour stress $\bar{\sigma}_k$ *in time* $t/\Delta t$ *at the point* $A2$.

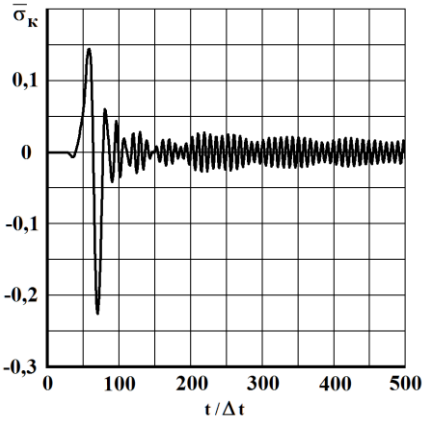

Figure 9. Change of elastic contour stress $\bar{\sigma}_k$ *in time* $t/\Delta t$ *at the point* $A5$.

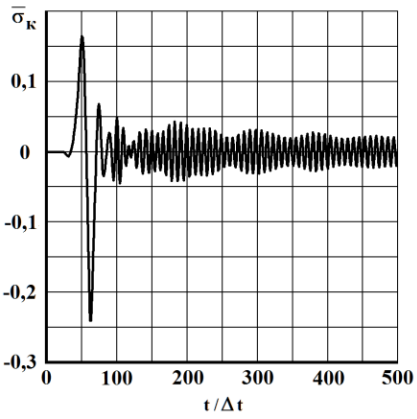

Figure 7. Change of elastic contour stress $\bar{\sigma}_k$ *in time* $t/\Delta t$ *at the point* $A3$.

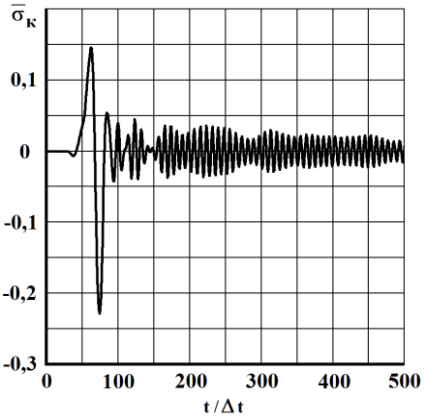

Figure 10. Change of elastic contour stress $\bar{\sigma}_k$ *in time* $t/\Delta t$ *at the point* $A6$.

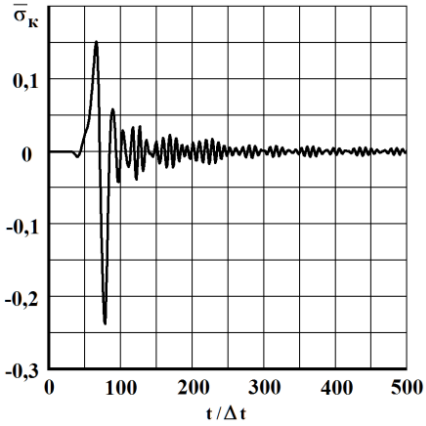

Figure 11. Change of elastic contour stress $\bar{\sigma}_k$ *in time* $t/\Delta t$ *at the point* $A7$.

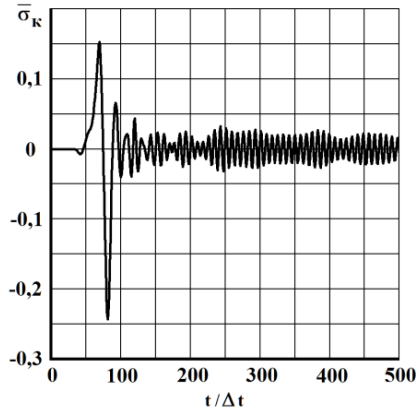

Figure 12. Change of elastic contour stress $\bar{\sigma}_k$ *in time* $t/\Delta t$ *at the point* $A8$.

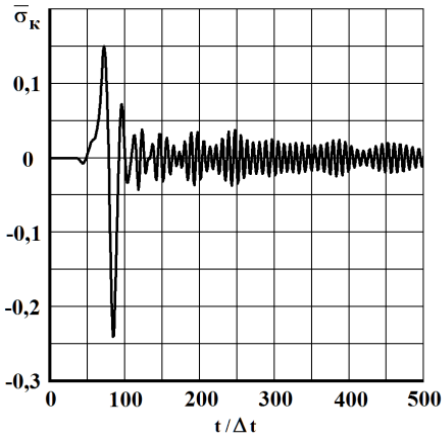

Figure 13. Change of elastic contour stress $\bar{\sigma}_k$ *in time* $t/\Delta t$ *at the point* $A9$.

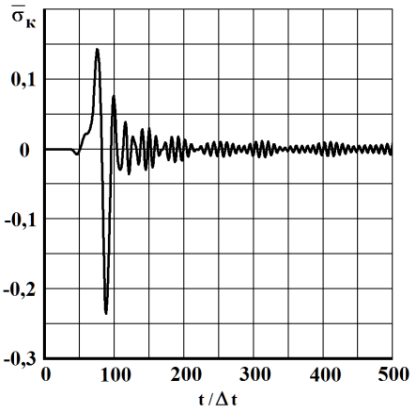

Figure 14. Change of elastic contour stress $\bar{\sigma}_k$ *in time* $t/\Delta t$ *at the point* $A10$.

The studied computational domain has 12008001 nodal point. The system of equations is solved from 48032004 unknown.

Upon fig. 5-14 the change of elastic contour stress is shown $\bar{\sigma}_k$ ($\bar{\sigma}_k = \sigma_k / |\sigma_0|$) in time n in points $A1$ - $A10$ (fig. 3), on the free surface of the elastic half-plane (distance between points: $A1$ and $A2$ equally H; $A2$ and $A3$ equally H; $A3$ and $A4$ equally H; $A4$ and $A5$ equally H; $A5$ and $A6$ equally H; $A6$ and $A7$ equally H; $A7$ and $A8$ equally H; $A8$ and $A9$ equally H; A9 and A10 equally H).

SUMMARY

1. On the basis of the finite element method the technique is developed, algorithm and software for solving linear two-dimensional plane problems, which allow you to solve complex problems in case of unsteady wave effects on complex objects. The main relations of the finite element method are obtained using the principle of possible displacements. The elasticity matrix is expressed in terms of longitudinal wave velocity, transverse wave velocity, and density.
2. Linear dynamic problem with initial and boundary conditions in the form of partial differential equations, to solve problems under wave influences, with the help of the

finite element method in displacements is reduced to a system of linear ordinary differential equations with initial conditions, which is solved by an explicit two-layer scheme.

3. The problem of mathematical modeling of unsteady elastic stress waves with concentrated vertical action in the form of a Delta function on the half-plane surface is solved. The studied computational domain has 12008001 nodal points. Solve the system of equations of 48032004 unknown. Tensile elastic contour stress $\bar{\sigma}_k$ has the following maximum value $\bar{\sigma}_k = 0{,}18$. Compressive elastic contour stress $\bar{\sigma}_k$ has the following maximum value $\bar{\sigma}_k = -0{,}24$.
4. Amplitude of surface Rayleigh waves significantly larger than the amplitudes of the longitudinal, transverse and other waves with concentrated vertical action in the form of a triangular pulse on the surface of an elastic half-plane.
5. After Rayleigh surface waves dynamic process observed in the form of standing waves.

REFERENCES

1. **Kolsky G.** Volny napryazhenij v tverdyh telah [Stress waves in solids]. Moscow, Inostrannaya literatura, 1955. 192 pages.
2. **Ionov V.I., Ogibalov P.M.** Napryazheniya v telah pri impul'sivnom nagruzhenii [Stresses in bodies under impulsive loading]. Moscow, Vysshaya shkola, 1975, 464 pages.
2. **Zenkevich O.** Metod konechnyh ehlementov v tekhnike [Finite element method in engineering]. Moscow, Mir, 1975, 543 pages.
3. **Timoshenko S.P., Gudyer D.** Teoriya uprugosti [Theory of elasticity]. Moscow, Nauka, 1975, 576 pages.
4. **Tikhonov A.N., Samarsky A.A.** Uravneniya matematicheskoj fiziki [Equations of mathematical physics]. Moscow, Nauka, 1977, 736 pages.
5. **Musayev V.K.** O dostovernosti rezul'tatov chislennogo metoda resheniya slozhnyh zadach volnovoj teorii uprugosti pri udarnyh, vzryvnyh i sejsmicheskih vozdejstviyah [On the reliability of the results of the numerical method for solving complex problems of the wave theory of elasticity in shock, explosion and seismic effects]. // *Uchenye zapiski Rossijskogo gosudarstvennogo social'nogo universiteta*. 2009. No. 5, pp. 21-33.
6. **Kurantsov V.A., Denisyuk D.A., Denisenkov A.N., Savichev V.A., Akatyev S.V.** Reshenie zadachi ob interferencii ploskih prodol'nyh uprugih voln napryazhenij v vide funkcii Hevisajda s pomoshch'yu chislennogo metoda Musaeva V.K. v peremeshcheniyah [Solving the problem of interference of plane longitudinal elastic stress waves in the form of the Heaviside function using the numerical method of Musayev V.K. in displacements]. // *Bezopasnost' i ehkologiya tekhnologicheskih processov i proizvodstv. Materialy Vserossijskoj nauchno-prakticheskoj konferencii*. The village Persianovka, Rostov region, Donskoj gosudarstvennyj agrarnyj universitet, 2012, pp. 216-221.
7. **Sazonov K.B., Fedorov A.L., Yuzbekov N.S., Shepelina P.V., Akatyev D.V.** Komp'yuternoe modelirovanie vozdejstviya ploskoj prodol'noj volny v vide pryamougol'nogo impul'sa na upruguyu poluploskost' s pomoshch'yu chislennogo metoda Musaeva V.K. v peremeshcheniyah [Computer simulation of the impact of a plane longitudinal wave in the form of a rectangular pulse on an elastic half-plane using the numerical method Musayev V.K. in displacements]. // *Tekhnosfernaya bezopasnost', nadezhnost', kachestvo, ehnergo i resursosberezhenie*: T38. Materialy Mezhdunarodnoj nauchno-prakticheskoj konferencii. Vypusk XIV. V 3 t. Tom 2. Rostov-on-don, Rostovskij gosudarstvennyj stroitel'nyj universitet, 2012, pp. 368-376.

8. **Starodubtsev V.V., Samoylov S.N., Shepelina P.V., Shiyanov S.M., Sergunov A.B.** Modelirovanie difrakcii voln napryazhenij v svobodnom i podkreplennom kruglom otverstiyah s pomoshch'yu chislennogo metoda Musaeva V.K. v peremeshcheniyah [Simulation of diffraction of stress waves in free and reinforced round holes using the numerical method of Musayev V.K. in displacements]. // *Tekhnosfernaya bezopasnost', nadezhnost', kachestvo, ehnergo i resursosberezhenie*: T38. Materialy Mezhdunarodnoj nauchno-prakticheskoj konferencii. Vypusk XVI. V 2 t. Tom 2. Rostov-on-don, Rostovskij gosudarstvennyj stroitel'nyj universitet, 2014, pp. 303-312.
9. **Starodubtsev V.V., Samoylov S.N., Shepelina P.V., Shiyanov S.M., Sergunov A.B.** Reshenie zadachi o difrakcii voln davleniya v svobodnom i podkreplennom kvadratnom otverstiyah s pomoshch'yu chislennogo metoda Musaeva V.K. v peremeshcheniyah [Solution of the problem of diffraction of pressure waves in free and reinforced square holes using the numerical method of Musayev V.K. in displacements]. // *Tekhnosfernaya bezopasnost', nadezhnost', kachestvo, ehnergo i resursosberezhenie*: T38. Materialy Mezhdunarodnoj nauchno-prakticheskoj konferencii. Vypusk XVI. V 2 t. Tom 2. Rostov-on-don, Rostovskij gosudarstvennyj stroitel'nyj universitet, 2014, pp. 312-321.
10. **Musayev V.K.** Estimation of accuracy of the results of numerical simulation of unsteady vave of the stress in deformable objects of complex shape // *International Journal for Computational Civil and Structural Engineering*, 2015, Volume 11, Issue 1, pp. 135-146.
11. **Musayev V.K.** On the mathematical modeling of nonstationary elastic vaves stresses in corroborated by the round hole // *International Journal for Computational Civil and Structural Engineering*, 2015, Volume 11, Issue 1, pp. 147-156.
12. **Sushchev T.S., Akatyev S.V., Musayev A.V., Samoylov S.N., Starodubtsev V.V.** Modelirovanie nestacionarnyh uprugih voln napryazhenij v deformiruemyh oblastyah s pomoshch'yu chislennogo metoda, algoritma i kompleksa programm Musaeva V.K. [Simulation of unsteady elastic stress waves in deformable areas using the numerical method, the algorithm and the Musayev V.K. program complex]. // *Tekhnosfernaya bezopasnost', nadezhnost', kachestvo, ehnergo i resursosberezhenie*: T38. Materialy Mezhdunarodnoj nauchno-prakticheskoj konferencii. Vypusk XVII. V 2 t. Tom 2. Rostov-on-don, Rostovskij gosudarstvennyj stroitel'nyj universitet, 2015, pp. 333-342.
13. **Spiridonov V.P.** Opredelenie nekotoryh zakonomernostej volnovogo napryazhennogo sostoyaniya v geoob"ektah s pomoshch'yu chislennogo metoda, algoritma i kompleksa programm Musaeva V.K. [The definition of some patterns of wave stress in geoobject using numerical method, algorithm and program complex Musayeva V. K.]. // *Sovremennye naukoemkie tekhnologii*, 2015, No. 12-5, pp. 832-835.
14. **Fedorov A.L., Starodubtsev V.V., Musayev A.V., Kuznetsov M.E., Idelson Ye.V.** Opredelenie zakonomernostej nestacionarnogo volnovogo napryazhennogo sostoyaniya v geoob"ektah s pomoshch'yu chislennogo metoda, algoritma i kompleksa programm Musaeva V.K. [Determination of the regularities of the unsteady wave stress state in geoobjects using the numerical method, algorithm and software complex Musayev V.K.]. // *Tekhnosfernaya bezopasnost', nadezhnost', kachestvo, ehnergo i resursosberezhenie*: T38. Materialy Mezhdunarodnoj nauchno-prakticheskoj konferencii. Vypusk XVIII. V 2 t. Tom 2. Rostov-on-don, Rostovskij gosudarstvennyj stroitel'nyj universitet, 2016, pp. 289-297.
15. **Dikova Ye.V.** Dostovernost' chislennogo metoda, algoritma i kompleksa programm Musaeva V.K. pri reshenii zadachi o rasprostranenii ploskih prodol'nyh uprugih

voln (voskhodyashchaya chast' - linejnaya, niskhodyashchaya chast' - chetvert' kruga) v poluploskosti [Reliability of the numerical method, algorithm and software complex of V.K. Musayev in solving the problem of propagation of plane longitudinal elastic waves (the ascending part is linear, the descending part is a quarter of a circle) in a half-plane]. // *Mezhdunarodnyj zhurnal ehksperimental'nogo obrazovaniya*, 2016. No. 12-3, pp. 354-357.

16. **Starodubtsev V.V., Musayev A.V., Kurantsov V.A., Musayeva S.V., Kulagina N.V.** Ocenka tochnosti i dostovernosti modelirovaniya ploskih nestacionarnyh uprugih voln napryazhenij (treugol'nyj impul's) v poluploskosti s pomoshch'yu chislennogo metoda, algoritma i kompleksa programm Musaeva V.K. [Estimation of accuracy and reliability of simulation of plane unsteady elastic waves of stresses (triangular momentum) in the half-plane using the numerical method, algorithm and software complex Musayev V.K.]. // *Problemy upravleniya bezopasnost'yu slozhnyh sistem. Materialy XXIV Mezhdunarodnoj konferencii*, Moscow, RGGU, 2016, pp. 352-355.
17. **Salikov L.M., Musayev A.V., Idelson Ye.V., Samoylov S.N., Blinnikov V.V.** Ocenka fizicheskoj dostovernosti modelirovaniya ploskih nestacionarnyh uprugih voln napryazhenij v vide impul'snogo vozdejstviya (funkciya Hevisajda) v poluploskosti s pomoshch'yu chislennogo metoda, algoritma i kompleksa programm Musaeva V.K. [Estimation of the physical reliability of modeling plane unsteady elastic waves of stresses in the form of pulse action (Heaviside function) in the half-plane using the numerical method, algorithm and software complex Musayev V.K.]. // *Problemy upravleniya bezopasnost'yu slozhnyh sistem. Materialy XXIV Mezhdunarodnoj konferencii*, Moscow, RGGU, 2016, pp. 356-359.
18. **Akatyev S.V., Kuznetsov M.E., Sushchev T.S., Kurantsov O.V., Kurantsov V.V.** Ocenka tochnosti modelirovaniya ploskih nestacionarnyh uprugih voln napryazhenij (pryamougol'nyj impul's) v poluploskosti s pomoshch'yu chislennogo metoda, algoritma i kompleksa programm Musaeva V.K. [Estimation of the accuracy of simulation of plane unsteady elastic waves of stresses (rectangular pulse) in the half-plane using the numerical method, algorithm and software complex Musayev V.K.]. // *Problemy upravleniya bezopasnost'yu slozhnyh sistem. Materialy XXIV Mezhdunarodnoj konferencii*, Moscow, RGGU, 2016, pp. 371-374.
19. **Starodubtsev V.V., Musayev A.V., Dikova Ye.V., Krylov A.I.** Modelirovanie dostovernosti i tochnosti impul'snogo vozdejstviya v uprugoj poluploskosti s pomoshch'yu chislennogo metoda, algoritma i kompleksa programm Musaeva V.K. [Simulation of the reliability and accuracy of the impulse action in the elastic half-plane using the numerical method, algorithm and software complex Musayev V.K.]. // *Informacionno-telekommunikacionnye tekhnologii i matematicheskoe modelirovanie vysokotekhnologichnyh sistem. Materialy Vserossijskoj konferencii s mezhdunarodnym uchastiem*, Moscow, RUDN, 2017, pp. 339-341.
20. **Fedorov A.L., Shiyanov S.M., Salikov L.M., Blinnikov V.V.** Modelirovanie ploskih voln pri rasprostranenii impul'sa (voskhodyashchaya chast' – linejnaya, niskhodyashchaya chast' – chetvert' kruga) v uprugoj poluploskosti s pomoshch'yu chislennogo metoda, algoritma i kompleksa programm Musaeva V.K. [Simulation of plane waves at momentum propagation (ascending part – linear, descending part – quarter of a circle) in an elastic half-plane by means of the numerical method, algorithm and program complex Musayev V.K.]. // *Informacionno-telekommunikacionnye tekhnologii i matematicheskoe modelirovanie vysokotekhnologichnyh sistem. Materialy Vserossijskoj konferencii s mezhdunarodnym uchastiem*, Moscow, RUDN, 2017, pp. 353-355.
21. **Starodubtsev V.V., Akatyev S.V., Musayev A.V., Shiyanov S.M., Kurantsov O.V.**

Modelirovanie uprugih voln v vide impul'snogo vozdejstviya (voskhodyashchaya chast' – chetvert' kruga, niskhodyashchaya chast' – chetvert' kruga) v poluploskosti s pomoshch'yu chislennogo metoda Musaeva V.K. [Modeling of elastic waves in the form of impulse action (ascending part - a quarter of a circle, descending part – a quarter of a circle) in a half-plane by means of the numerical method Musayev V.K.]. // *Problemy bezopasnosti rossijskogo obshchestva*, 2017, No. 1, pp. 36-40.

22. **Starodubtsev V.V., Akatyev S.V., Musayev A.V., Shiyanov S.M., Kurantsov O.V.** Modelirovanie s pomoshch'yu chislennogo metoda Musaeva V.K. nestacionarnyh uprugih voln v vide impul'snogo vozdejstviya (voskhodyashchaya chast' - chetvert' kruga, srednyaya – gorizontal'naya, niskhodyashchaya chast' – linejnaya) v sploshnoj deformiruemoj srede [Modeling of unsteady elastic waves in the form of pulse action (ascending part – a quarter of a circle, the middle part – horizontal, the descending part – linear) in a continuous deformable medium using the Musayev V.K. numerical method] // *Problemy bezopasnosti rossijskogo obshchestva*, 2017, No. 1, pp. 63-68.
23. **Kurantsov V.A., Starodubtsev V.V., Musayev A.V., Samoylov S.N., Kuznetsov M.E.** Modelirovanie impul'sa (pervaya vetv': voskhodyashchaya chast' – chetvert' kruga, niskhodyashchaya chast' – linejnaya; vtoraya vetv': treugol'nik) v uprugoj poluploskosti s pomoshch'yu chislennogo metoda Musaeva V.K. [Modeling of momentum (the first branch: the ascending part – a quarter of a circle, the descending part - linear; the second branch: a triangle) in an elastic half-plane using the numerical method of Musayev V.K.]. // *Problemy bezopasnosti rossijskogo obshchestva*, 2017, No. 2, pp. 51-55.
24. **Kurantsov V.A., Musayev A.V., Kurantsov O.V., Mikhedova Ye.E., Chernykh Yu.K.** Modelirovanie rasprostraneniya impul'sa (voskhodyashchaya chast' - chetvert' kruga, niskhodyashchaya chast' - linejnaya) v poluploskosti s pomoshch'yu chislennogo metoda, algoritma i kompleksa programm Musaeva V.K. [Modeling of the propagation of the pulse (rising - a quarter of a circle, the descending part of the - linear) in the half-plane using a numerical method, algorithm and program complex Musayev V.K.]. // *Novye tekhnologii nauki, tekhniki, pedagogiki vysshej shkoly: materialy Mezhdunarodnoj nauchno-prakticheskoj konferencii "Nauka – Obshchestvo – Tekhnologii – 2017"*, Moscow, Moskovskij politekh, 2017, pp. 23-28.
25. **Kurantsov V.V., Musayev A.V., Samoylov S.N., Musayeva S.V., Shiyanov S.M.** Modelirovanie impul'sa (voskhodyashchaya chast' - chetvert' kruga, srednyaya - gorizontal'naya, niskhodyashchaya - linejnaya) v uprugoj poluploskosti s pomoshch'yu chislennogo metoda, algoritma i kompleksa programm Musaeva V.K. [Modeling of momentum (ascending part - a quarter of a circle, middle - horizontal, descending - linear) in an elastic half-plane by means of the numerical method, algorithm and program complex Musayev V.K.]. // *Novye tekhnologii nauki, tekhniki, pedagogiki vysshej shkoly: materialy Mezhdunarodnoj nauchno-prakticheskoj konferencii "Nauka – Obshchestvo – Tekhnologii – 2017"*, Moscow, Moskovskij politekh, 2017, pp. 29-35.
26. **Starodubtsev V.V., Akatyev S.V., Dikova Ye.V., Musayev A.V., Krylov A.I.** Modelirovanie impul'snogo vozdejstviya (voskhodyashchaya chast' - chetvert' kruga, niskhodyashchaya chast' - chetvert' kruga) v poluploskosti s pomoshch'yu chislennogo metoda, algoritma i kompleksa programm Musaeva V.K. [Simulation of impulse action (ascending part - quarter of a circle, descending part - quarter of a circle) in a half-plane using the numerical method, algorithm and software complex Musayev V.K.]. // *Novye tekhnologii nauki, tekhniki, pedagogiki vysshej shkoly: materialy*

Mezhdunarodnoj nauchno-prakticheskoj konferencii "Nauka – Obshchestvo – Tekhnologii – 2017", Moscow, Moskovskij politekh, 2017, pp. 82-87.

27. **Starodubtsev V.V., Dikova Ye.V., Denisenkov A.N., Kormilitsin A.I., Shepelina P.V.** Modelirovanie vozdejstviya v vide dvuh impul'sov (pervyj: voskhodyashchaya chast' - chetvert' kruga, niskhodyashchaya chast' – linejnaya; vtoroj - treugol'nik) v uprugoj poluploskosti s pomoshch'yu chislennogo metoda, algoritma i kompleksa programm Musaeva V.K. [Modeling of the impact in the form of two pulses (the first: the ascending part – a quarter of a circle, the descending part – a linear; the second – a triangle) in the elastic half-plane using the numerical method, algorithm and software complex Musayev V. K.]. // *Novye tekhnologii nauki, tekhniki, pedagogiki vysshej shkoly: materialy Mezhdunarodnoj nauchno-prakticheskoj konferencii "Nauka – Obshchestvo – Tekhnologii – 2017"*, Moscow, Moskovskij politekh, 2017, pp. 88-94.
28. **Starodubtsev V.V., Musayev A.V., Dikova Ye.V., Kuznetsov M.E., Fedorov A.L.** Primenenie chislennogo metoda Musaeva V.K. dlya modelirovaniya vozdejstviya v vide dvuh impul'sov (pervyj – polukrug, vtoroj – treugol'nik) v uprugoj poluploskosti [Application of the numerical method Musayev V.K. to simulate the impact of two pulses (the first – a semicircle, the second - a triangle) in the elastic half-plane]. // *Novye tekhnologii nauki, tekhniki, pedagogiki vysshej shkoly: materialy Mezhdunarodnoj nauchno-prakticheskoj konferencii "Nauka – Obshchestvo – Tekhnologii – 2017"*, Moscow, Moskovskij politekh, 2017, pp. 94-100.
29. **Derevyashkin I.V., Popadeykin V.V., Salikov L.M., Blinnikov V.V., Doronin F.L.** Modelirovanie bezopasnosti unikal'nyh sooruzhenij ehnergetiki s pomoshch'yu chislennogo metoda, algoritma i kompleksa programm Musaeva V.K. [Modeling the safety of unique energy facilities using the numerical method, algorithm and software complex Musayev V.K.]. // *Novye tekhnologii nauki, tekhniki, pedagogiki vysshej shkoly: materialy Mezhdunarodnoj nauchno-prakticheskoj konferencii "Nauka – Obshchestvo – Tekhnologii – 2017"*, Moscow, Moskovskij politekh, 2017, pp. 178-184.

СПИСОК ЛИТЕРАТУРЫ

1. **Кольский Г.** Волны напряжений в твердых телах. – М.: Иностранная литература, 1955. – 192 с.
2. **Ионов В.И., Огибалов П.М.** Напряжения в телах при импульсивном нагружении. – М.: Высшая школа, 1975. – 464 с.
3. **Зенкевич О.** Метод конечных элементов в технике. – М: Мир, 1975. – 543 с.
4. **Тимошенко С.П., Гудьер Д.** Теория упругости. – М.: Наука, 1975. – 576 с.
5. **Тихонов А.Н., Самарский А.А.** Уравнения математической физики. – М.: Наука, 1977. – 736 с.
6. **Мусаев В.К.** О достоверности результатов численного метода решения сложных задач волновой теории упругости при ударных, взрывных и сейсмических воздействиях // *Ученые записки Российского государственного социального университета*, 2009, №5, с. 21-33.
7. **Куранцов В.А., Денисюк Д.А., Денисенков А.Н., Савичев В.А., Акатьев С.В.** Решение задачи об интерференции плоских продольных упругих волн напряжений в виде функции Хевисайда с помощью численного метода Мусаева В.К. в перемещениях // *Безопасность и экология технологических процессов и производств. Материалы Всероссийской научно-практической конференции*. Поселок Персиановский Ростовской области: Донской государственный аграрный университет, 2012. С. 216-221.
8. **Сазонов К.Б., Федоров А.Л., Юзбеков Н.С., Шепелина П.В., Акатьев Д.В.** Компьютерное моделирование воздей-

ствия плоской продольной волны в виде прямоугольного импульса на упругую полуплоскость с помощью численного метода Мусаева В.К. в перемещениях // *Техносферная безопасность, надежность, качество, энерго и ресурсосбережение*: Т38. Материалы Международной научно-практической конференции. Выпуск XIV. В 3 т. Том 2. Ростов-на-Дону: Ростовский государственный строительный университет, 2012. С. 368-376.

9. **Стародубцев В.В., Самойлов С.Н., Шепелина П.В., Шиянов С.М., Сергунов А.Б.** Моделирование дифракции волн напряжений в свободном и подкрепленном круглом отверстиях с помощью численного метода Мусаева В.К. в перемещениях // *Техносферная безопасность, надежность, качество, энерго и ресурсосбережение*: Т38. Материалы Международной научно-практической конференции. Выпуск XVI. В 2 т. Том 2. Ростов-на-Дону: Ростовский государственный строительный университет, 2014. С. 303-312.
10. **Стародубцев В.В., Самойлов С.Н., Шепелина П.В., Шиянов С.М., Сергунов А.Б.** Решение задачи о дифракции волн давления в свободном и подкрепленном квадратном отверстиях с помощью численного метода Мусаева В.К. в перемещениях // *Техносферная безопасность, надежность, качество, энерго и ресурсосбережение*: Т38. Материалы Международной научно-практической конференции. Выпуск XVI. В 2 т. Том 2. Ростов-на-Дону: Ростовский государственный строительный университет, 2014. С. 312-321.
11. **Musayev V.K.** Estimation of accuracy of the results of numerical simulation of unsteady wave of the stress in deformable objects of complex shape // *International Journal for Computational Civil and Structural Engineering*, 2015, Volume 11, Issue 1, pp. 135-146.
12. **Musayev V.K.** On the mathematical modeling of nonstationary elastic waves stresses in corroborated by the round hole // *International Journal for Computational Civil and Structural Engineering*, 2015, Volume 11, Issue 1, pp. 147-156.
13. **Сущев Т.С., Акатьев С.В., Мусаев А.В., Самойлов С.Н., Стародубцев В.В**. Моделирование нестационарных упругих волн напряжений в деформируемых областях с помощью численного метода, алгоритма и комплекса программ Мусаева В.К. // *Техносферная безопасность, надежность, качество, энерго и ресурсосбережение*: Т38. Материалы Международной научно-практической конференции. Выпуск XVII. В 2 т. Том 2. Ростов-на-Дону: Ростовский государственный строительный университет, 2015. С. 333-342.
14. **Спиридонов В.П.** Определение некоторых закономерностей волнового напряженного состояния в геообъектах с помощью численного метода, алгоритма и комплекса программ Мусаева В.К. // *Современные наукоемкие технологии*, 2015. №12-5, с. 832-835.
15. **Федоров А.Л., Стародубцев В.В., Мусаев А.В., Кузнецов М.Е., Идельсон Е.В.** Определение закономерностей нестационарного волнового напряженного состояния в геообъектах с помощью численного метода, алгоритма и комплекса программ Мусаева В.К. // *Техносферная безопасность, надежность, качество, энерго и ресурсосбережение*: Т38. Материалы Международной научно-практической конференции. Выпуск XVIII. В 2 т. Том 2. Ростов-на-Дону: Ростовский государственный строительный университет, 2016, с. 289-297.
16. **Дикова Е.В.** Достоверность численного метода, алгоритма и комплекса программ Мусаева В.К. при решении задачи о распространении плоских продольных упругих волн (восходящая часть – линейная, нисходящая часть – четверть круга) в полуплоскости // *Международный журнал экспериментального образования*, 2016, №12-3, с. 354-357.

17. **Стародубцев В.В., Мусаев А.В., Куранцов В.А., Мусаева С.В., Кулагина Н.В.** Оценка точности и достоверности моделирования плоских нестационарных упругих волн напряжений (треугольный импульс) в полуплоскости с помощью численного метода, алгоритма и комплекса программ Мусаева В.К. // *Проблемы управления безопасностью сложных систем. Материалы XXIV Международной конференции*. – М.: РГГУ, 2016, с. 352-355.
18. **Саликов Л.М., Мусаев А.В., Идельсон Е.В., Самойлов С.Н., Блинников В.В.** Оценка физической достоверности моделирования плоских нестационарных упругих волн напряжений в виде импульсного воздействия (функция Хевисайда) в полуплоскости с помощью численного метода, алгоритма и комплекса программ Мусаева В.К. // *Проблемы управления безопасностью сложных систем. Материалы XXIV Международной конференции*. – М.: РГГУ, 2016, с. 356-359.
19. **Акатьев С.В., Кузнецов М.Е., Сущев Т.С., Куранцов О.В., Куранцов В.В.** Оценка точности моделирования плоских нестационарных упругих волн напряжений (прямоугольный импульс) в полуплоскости с помощью численного метода, алгоритма и комплекса программ Мусаева В.К. // *Проблемы управления безопасностью сложных систем. Материалы XXIV Международной конференции*. – М.: РГГУ, 2016, с. 371-374.
20. **Стародубцев В.В., Мусаев А.В., Дикова Е.В., Крылов А.И.** Моделирование достоверности и точности импульсного воздействия в упругой полуплоскости с помощью численного метода, алгоритма и комплекса программ Мусаева В.К. // *Информационно-телекоммуникационные технологии и математическое моделирование высокотехнологичных систем. Материалы Всероссийской конференции с международным участием*. – М.: РУДН, 2017, с. 339-341.
21. **Федоров А.Л., Шиянов С.М., Саликов Л.М., Блинников В.В.** Моделирование плоских волн при распространении импульса (восходящая часть - линейная, нисходящая часть - четверть круга) в упругой полуплоскости с помощью численного метода, алгоритма и комплекса программ Мусаева В.К. // *Информационно-телекоммуникационные технологии и математическое моделирование высокотехнологичных систем. Материалы Всероссийской конференции с международным участием*. – М.: РУДН, 2017, с. 353-355.
22. **Стародубцев В.В., Акатьев С.В., Мусаев А.В., Шиянов С.М., Куранцов О.В.** Моделирование упругих волн в виде импульсного воздействия (восходящая часть – четверть круга, нисходящая часть – четверть круга) в полуплоскости с помощью численного метода Мусаева В.К. // *Проблемы безопасности российского общества*, 2017, №1, с. 36-40.
23. **Стародубцев В.В., Акатьев С.В., Мусаев А.В., Шиянов С.М., Куранцов О.В.** Моделирование с помощью численного метода Мусаева В.К. нестационарных упругих волн в виде импульсного воздействия (восходящая часть – четверть круга, средняя – горизонтальная, нисходящая часть – линейная) в сплошной деформируемой среде // *Проблемы безопасности российского общества*, 2017, №1, с. 63-68.
24. **Куранцов В.А., Стародубцев В.В., Мусаев А.В., Самойлов С.Н., Кузнецов М.Е.** Моделирование импульса (первая ветвь: восходящая часть – четверть круга, нисходящая часть – линейная; вторая ветвь: треугольник) в упругой полуплоскости с помощью численного метода Мусаева В.К. // *Проблемы безопасности российского общества*, 2017, №2, с. 51-55.
25. **Куранцов В.А., Мусаев А.В., Куранцов О.В., Михедова Е.Е., Черных Ю.К.** Моделирование распространения импульса (восходящая часть – четверть круга, нисходящая часть – линейная) в полуплоско-

сти с помощью численного метода, алгоритма и комплекса программ Мусаева В.К. // Новые технологии науки, техники, педагогики высшей школы: материалы Международной научно-практической конференции «Наука – Общество – Технологии - 2017». – М.: Московский политех, 2017, с. 23-28.

26. **Куранцов В.В., Мусаев А.В., Самойлов С.Н., Мусаева С.В., Шиянов С.М.** Моделирование импульса (восходящая часть – четверть круга, средняя – горизонтальная, нисходящая – линейная) в упругой полуплоскости с помощью численного метода, алгоритма и комплекса программ Мусаева В.К. // *Новые технологии науки, техники, педагогики высшей школы: материалы Международной научно-практической конференции «Наука – Общество – Технологии – 2017»*. – М.: Московский политех, 2017, с. 29-35.
27. **Стародубцев В.В., Акатьев С.В., Дикова Е.В., Мусаев А.В., Крылов А.И.** Моделирование импульсного воздействия (восходящая часть – четверть круга, нисходящая часть – четверть круга) в полуплоскости с помощью численного метода, алгоритма и комплекса программ Мусаева В.К. // Новые технологии науки, техники, педагогики высшей школы: материалы Международной научно-практической конференции «Наука – Общество – Технологии – 2017». – М.: Московский политех, 2017, с. 82-87.
28. **Стародубцев В.В., Дикова Е.В., Денисенков А.Н., Кормилицин А.И., Шепелина П.В.** Моделирование воздействия в виде двух импульсов (первый: восходящая часть – четверть круга, нисходящая часть – линейная; второй - треугольник) в упругой полуплоскости с помощью численного метода, алгоритма и комплекса программ Мусаева В.К. // *Новые технологии науки, техники, педагогики высшей школы: материалы Международной научно-практической конференции «Наука – Общество – Технологии - 2017»*. – М.: Московский политех, 2017, с. 88-94.
29. **Стародубцев В.В., Мусаев А.В., Дикова Е.В., Кузнецов М.Е., Федоров А.Л.** Применение численного метода Мусаева В.К. для моделирования воздействия в виде двух импульсов (первый – полукруг, второй – треугольник) в упругой полуплоскости // *Новые технологии науки, техники, педагогики высшей школы: материалы Международной научно-практической конференции «Наука – Общество – Технологии – 2017»*. – М.: Московский политех, 2017. С. 94-100.
30. **Деревяшкин И.В., Попадейкин В.В., Саликов Л.М., Блинников В.В., Доронин Ф.Л.** Моделирование безопасности уникальных сооружений энергетики с помощью численного метода, алгоритма и комплекса программ Мусаева В.К. // *Новые технологии науки, техники, педагогики высшей школы: материалы Международной научно-практической конференции «Наука – Общество – Технологии – 2017»*. – М.: Московский политех, 2017, с. 178-184.

Musayev Vyacheslav Kadyr ogly, Honorary worker of higher professional education of the Russian Federation, doctor of technical Sciences, Professor, Professor of Technosphere safety Department, Russian University of transport, Professor of engineering and technology of mining and oil and gas production Department, Moscow Polytechnic University; 127994, Moscow, 9b9 Obrazcova str., Russia; 107023, Moscow, B. Semenovskaya str., 38, Russia; tel. +7(926)5670558.
E-mail: musayev-vk@yandex.ru.

Мусаев Вячеслав Кадыр оглы, Почетный работник высшего профессионального образования Российской Федерации, доктор технических наук, профессор, профессор кафедры Техносферная безопасность Российского университета транспорта, профессор кафедры Техника и технология горного и нефтегазового производства Московского политехнического университета; 127994, Россия, г. Москва, ул. Образцова, 9, стр. 9; 107023, Россия, г. Москва, ул. Б. Семеновская, 38; тел. +7(926) 5670558.
E-mail: musayev-vk@yandex.ru.

DOI:10.22337/2587-9618-2019-15-2-125-134

PASSIVE VIBRATION SUPPRESSION OF STRUCTURES IN THE VICINITY OF NATURAL FREQUENCIES USING PIEZOEFFECT

Nelly N. Rogacheva
National Research Moscow State University of Civil Engineering, Moscow, RUSSIA

Abstract: The proposed method of passive vibration suppression of structures is based on the use of the piezoelectric effect, which consists in the ability of the piezoelectric material to convert electrical energy into mechanical energy, and conversely. As it is known if the frequency of forced vibrations tends to the resonant frequency, all the desired quantities (forcers, moments, displacements and deformations) grow indefinitely. A new idea is that as we approach the resonant frequency, we change the electrical conditions on the electrodes of piezoelectric layers, thereby obtaining a different boundary value problem and a different spectrum of natural frequencies. Thus, we manage to get away from the resonant vibrations of the structure. Using the example of a laminated beam with elastic and piezoelectric layers the possibility of damping vibrations caused by mechanical load is studied. In this paper, a mathematically based model is used to solve the problem in question. The calculations are performed and the results are presented in the form of graphs. It is shown that forcers, moments, displacements and deformations of beam in the vicinity of the natural frequency can be significantly reduced by as a result of changes in the electrical conditions on the electrodes of the piezoelectric layers.

Keywords: passive vibration suppression, natural frequencies, piezoeffect, laminated electroelastic beam

ПАССИВНОЕ ГАШЕНИЕ ВИБРАЦИЙ КОНСТРУКЦИИ В ОКРЕСТНОСТИ РЕЗОНАНСНЫХ ЧАСТОТ С ИСПОЛЬЗОВАНИЕМ ПЬЕЗОЭФФЕКТА

Н.Н. Рогачева
Национальный исследовательский Московский государственный строительный университет,
г. Москва, РОССИЯ

Аннотация: Предлагаемый метод пассивного гашения вибраций конструкции основывается на использовании пьезоэффекта, который заключается в способности пьезоэлектрического материала преобразовывать электрическую энергию в механическую и наоборот. Известно, что если частота вынужденных колебаний стремится к резонансной частоте, то все искомые величины (усилия, моменты, перемещения и деформации) неограниченно растут. Идея гашения заключается в том, что при приближении к резонансной частоте мы изменяем электрические условия на электродах пьезоэлектрических слоев в результате чего получаем другую краевую задачу с другими резонансными частотами. Таким образом, удается избежать резонанса конструкции. Возможность гашения вибрации, вызванной механической нагрузкой, исследуется на примере слоистой балки с упругими и пьезоэлектрическими слоями. Для решения проблемы используется математически обоснованная модель. Выполнены расчеты, результаты которых представлены в виде графиков. Показано, что усилия, моменты, перемещения и деформации балки могут существенно уменьшаться в результате изменения электрических условий на электродах пьезоэлектрических слоев.

Ключевые слова: пассивное гашение вибраций, собственные частоты, пьезоэффект, слоистая электроупругая балка

1. INTRODUCTION

Operation of structures and equipment in dynamic conditions led to the problems of vibration isolation and vibration suppression. For vibration isolation and vibration suppression passive, active systems and their combinations are used. Active vibration isolation and vibration

damping systems use external energy sources. These are pneumatic, hydropneumatic and hydromechanical devices and so on. Recently, electro-elastic and magneto-elastic systems [1] - [4] began to be used for vibration isolation and active vibration suppression. As a rule, the analysis of the work of such systems consists in the development of an experimental layout and a schematic diagram. Passive vibration isolation usually consists in the fact that the protected object relies on extremely dimensional springs and vibration isolators. Vibration isolation systems containing only passive elastic and damping elements are called passive. Passive vibration isolation and vibration damping systems do not use external energy sources. So, for effective passive vibration damping and vibration isolation, complex and massive equipment is required. Here, another quench route is proposed using the piezoelectric effect. The method is based on the fact that with changing electrical conditions on the surfaces of the piezoelectric elements, the natural frequencies of the structure are changed. We encounter a similar situation in the dynamics of elastic structures: it is known that if we change the mechanical boundary conditions, for example, if we replace the free from fixation edge on the rigidly fixed edge, then the natural frequencies of the structure will change. Of course, in a working structure, nobody changes the mechanical boundary conditions. Another thing is the electrical boundary conditions: it is easy to short or break the electrodes. Structures with different electrical conditions are described by different boundary value problems, which correspond to different spectrum of natural frequencies. Our goal is to find the optimal way to change the natural vibration frequencies and, by changing the boundary value problem, escape from resonance. On this way, many questions arise: what piezoelements to choose from which material (properties, characteristics, electromechanical coupling coefficient, and so on), what form, what direction of pre-polarization, where and how to place them on the structure, how many electrodes to use, where to place them on the piezoelectric elements, and so on. The paper is the first step of our research of the problem under discussion.

2. BASIC EQUATIONS

A three-layer beam with one elastic layer and two piezoelectric layers located symmetrically with respect to the elastic layer is considered. The middle layer is elastic, the outer layers are made of a piezoelectric material. The number of the elastic layer is 1, the numbers of the upper and lower layers are ± 2, respectively. The thickness of the elastic layer is equal $2h_1$, the thickness of each piezoelectric layer is equal h_2, the length of the rod is l, the width of the beam is g (Fig. 1).

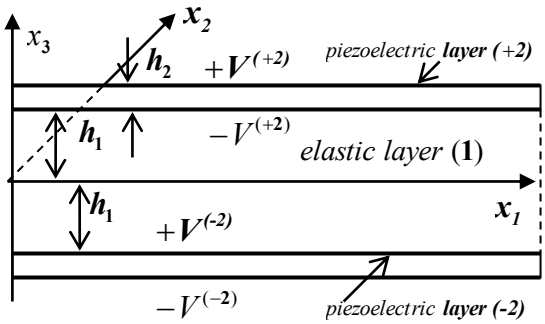

Figure 1. Schematic representation of the structure of the layered beam.

The axis x_1 is directed along the length of the beam, the axis x_2 is directed along the width of the beam, the axis x_3 is orthogonal to them. It is assumed that the piezoelectric layers are prepolarized in the direction x_3 [5] - [8].

In [8], we constructed the theory of the multilayer electroelastic beams. Here we briefly present these results for a particular case - a three-layer beam.

In the case of thin-walled beams in the equations of state, the stresses σ_{22} and σ_{33} can be neglected compared to the stress σ_{11}. In addition, it is assumed that the electroelastic state does not depend on the coordinate x_2.

Taking into account the assumptions made, the equations for the elastic and electroelastic layers will be written as
Equilibrium equations

$$\frac{\partial \sigma_{ii}^{(k)}}{\partial x_i} + \frac{\partial \sigma_{ij}^{(k)}}{\partial x_j} = \rho \frac{\partial^2 u_i^{(k)}}{\partial t^2}, \quad i \neq j = 1,3 \tag{1}$$

Strain - displacement formulas

$$e_1^{(k)} = \frac{\partial u_1^{(k)}}{\partial x_1}, \ \boldsymbol{k = -2,1,2} \tag{2}$$

Equation of state (Hooke's law) for the elastic layer

$$\sigma_{11}^{(1)} = E_1 e_1^{(1)} \tag{3}$$

Equations of state for piezoelectric layers

$$\sigma_{11}^{(\pm 2)} = \frac{1}{s_{11}^E} e_1^{(\pm 2)} - \frac{d_{31}}{s_{11}^E} E_3^{(\pm 2)} \tag{4}$$

$$D_3^{(\pm 2)} = \varepsilon_{33}^T E_3^{(\pm 2)} + d_{31} \sigma_{11}^{(\pm 2)} \tag{5}$$

where $$E_3^{(\pm 2)} = -\frac{\partial \varphi^{(\pm 2)}}{\partial x_3} \tag{6}$$

In formulas (1)-(6) u_1 and e_1 are the displacement and deformation in the direction x_1, respectively, E_3 and D_3 are the components of the electric field vector and electric induction vector in the direction x_3, φ is the electric potential, s_{11}^E is the elastic compliance at zero electric field, d_{31} is the piezoelectric constant, ε_{33}^T is the dielectric constant at zero voltages. The notation used is the same as that used in [8].
For our purposes, we will consider piezoelectric layers, in which the faces $x_3 = \text{const}$ are completely covered with electrodes. Here we will consider only two kinds of conditions on the electrodes:

- the electrodes are short-circuited (the electric potential is zero on the electrodes) and
- the electrodes are open.

On short-circuited electrodes, the electric potential is zero

$$\varphi^{(\pm 2)}\Big|_{x_3 = \pm \boldsymbol{h}} = \varphi^{(\pm 2)}\Big|_{x_3 = \pm h_1} = \boldsymbol{0} \tag{7}$$

On open electrodes the electric potential is not zero. It is equal to

$$\varphi^{(\pm 2)}\Big|_{x_3 = \pm \boldsymbol{h}} = \pm V^{(\pm 2)}, \ \varphi^{(\pm 2)}\Big|_{x_3 = \pm h_1} = \mp V^{(\pm 2)} \tag{8}$$

where the values $V^{(\pm 2)}$ are determined from following integral condition:

$$I = \int_\Omega \frac{\partial D_3}{\partial t} d\Omega = 0 \tag{9}$$

Here the integral is evaluated over the surface Ω of one of the electrodes and t denotes the time.
On the surfaces of the beam, the mechanical surface load is usually specified as

$$\sigma_{13}^{(\pm 2)}\Big|_{x_3 = \pm h} = \pm q_1^{\pm}, \quad \sigma_{33}^{(\pm 2)}\Big|_{x_3 = \pm h} = \pm q_3^{\pm} \tag{10}$$

The superscript in parentheses indicates the layer number. Hereinafter, each formula with double signs $\pm, \mp$ contains two formulas. To get one formula, one should take only the upper signs, to get the second formula one need to leave only the lower signs.

2. DERIVATION OF EQUATIONS FOR ELECTROELASTIC BEAM THEORY

In order to construct the theory of electroelastic beams, one should accept some assumptions regarding electrical quantities. As in the construction of the theory of piezoelectric plates and shells [7], the content of accepted hypotheses depends on the electrical conditions on the surfaces of the piezoelectric layers. For piezoelectric layers, we accept assumptions that were

substantiated by the asymptotic method electro-elastic plates and shells [7].

The mechanical quantities of any layer for which the Kirchhoff hypotheses are valid can be written as the following linear functions of the coordinate x_3

$$\begin{aligned} &u_1 = u_{1,0} + x_3 u_{1,1}, \quad e_1 = \varepsilon + x_3 \kappa \\ &\sigma_{11}^{(k)} = \sigma_{11,0}^{(k)} + x_3 \sigma_{11,1}^{(k)}, \quad k = \text{-2,1,2} \end{aligned} \tag{11}$$

where ε and κ are the components of the tangential and bending deformations of the midline of the beam, respectively, k is the number of the layer

$$\varepsilon = \frac{\partial u}{\partial x_1}, \ \kappa = \frac{\partial^2 w}{\partial x_1^{\,2}}, \ u = u_1\big|_{x_3=0}, \ w = -u_3\big|_{x_3=0} \tag{12}$$

It was shown in the work [7] that the electric potential is a quadratic function of the thickness coordinate x_3

$$\varphi^{(\pm 2)} = \varphi_{,0}^{(\pm 2)} + x_3 \varphi_{,1}^{(\pm 2)} + x_3^2 \varphi_{,2}^{(\pm 2)} \tag{13}$$

We write out the basic formulas for the beam with open electrodes. On open electrodes, the electric potential is non-zero. It is constant at each electrode. This value is determined from the condition (9).

If the electric potential is set on the electrodes (8), then formula (13) can be converted to

$$\begin{aligned} \varphi^{(\pm 2)} = \mp V^{(\pm 2)} &+ (x_3 \mp \boldsymbol{h}_1)\left(\frac{2V^{(\pm 2)}}{h_2} \mp h_2 \varphi_{,2}^{(\pm)} \right) \\ &+ (x_3 \mp h_1)^2 \varphi_{,2}^{(\pm 2)} \end{aligned} \tag{14}$$

Taking into account formulas (14) and (6), we get

$$\begin{aligned} E_{3,0}^{(\pm 2)} &= -\frac{2V^{(\pm 2)}}{h_2} \pm (\boldsymbol{h} + h_1)\varphi_{,2}^{(\pm 2)} \\ E_{3,1}^{(\pm 2)} &= -2\varphi_{,2}^{(\pm 2)} \end{aligned} \tag{15}$$

where

$$E_3^{(\pm 2)} = E_{3,0}^{(\pm 2)} + x_3 E_{3,1}^{(\pm 2)} \tag{16}$$

As a result of the simple transformations the equations of state for the piezoelectric layers with open electrodes can be rewritten as

$$\begin{aligned} \sigma_{11,0}^{(\pm 2)} &= \frac{1}{s_{11}^E}\varepsilon + \frac{2d_{31}}{h_2 s_{11}^E} V^{(\pm 2)} \mp \frac{(h + h_1)k_{31}^{\,2}}{2s_{11}^E(1 - k_{31}^{\,2})}\kappa \\ \sigma_{11,1}^{(\pm 2)} &= \frac{1}{s_{11}^E(1 - k_{31}^{\,2})}\kappa \\ \sigma_{11}^{(\pm 2)} &= \sigma_{11,0}^{(\pm 2)} + x_3 \sigma_{11,1}^{(\pm 2)} \\ \varphi_{,2}^{(\pm)} &= \frac{d_{31}}{2\varepsilon_{33}^T}\sigma_{11,1}^{(\pm 2)} = \frac{k_{31}^{\,2}}{2d_{31}(1 - k_{31}^{\,2})}\kappa \\ E_{3,0}^{(\pm 2)} &= -\frac{2V^{(\pm 2)}}{h_2} \pm \frac{(h + h_1)k_{31}^{\,2}}{2d_{31}(1 - k_{31}^{\,2})}\kappa \\ E_{3,1}^{(\pm 2)} &= -\frac{k_{31}^{\,2}}{d_{31}(1 - k_{31}^{\,2})}\kappa \\ D_{3,0}^{(\pm 2)} &= \varepsilon_{33}^T (1 - k_{31}^{\,2}) E_{3,0}^{(\pm 2)} + \frac{d_{31}}{s_{11}^E}\varepsilon \end{aligned} \tag{17}$$

$$\begin{aligned} &\int_\Omega \frac{\partial D_{3,0}}{\partial t} d\Omega \\ &= \frac{\partial}{\partial t}\int_\Omega \left(\varepsilon_{33}^T (1 - k_{31}^{\,2}) \boldsymbol{E}_{3,0}^{(\pm 2)} + \frac{d_{31}}{s_{11}^E}\varepsilon \right) d\Omega = \boldsymbol{0} \end{aligned} \tag{18}$$

We write out the basic formulas for the beam with short-circuited electrodes taking into account formulas (7) ($V^{(\pm 2)} = \boldsymbol{0}$) in equations (17)

$$\begin{aligned} \sigma_{11,0}^{(\pm 2)} &= \frac{1}{s_{11}^E}\varepsilon \mp \frac{(\boldsymbol{h} + h_1)k_{31}^{\,2}}{2s_{11}^E(1 - k_{31}^{\,2})}\kappa \\ \sigma_{11,1}^{(\pm 2)} &= \frac{1}{s_{11}^E(1 - k_{31}^{\,2})}\kappa \\ E_{3,0}^{(\pm 2)} &= \pm(\boldsymbol{h} + h_1)\varphi_{,2}^{(\pm 2)} \\ D_{3,0}^{(\pm 2)} &= \pm \frac{\varepsilon_{33}^T}{2d_{31}}((\boldsymbol{h} + h_1)k_{31}^{\,2}\kappa \pm 2k_{31}^{\,2}\varepsilon) \end{aligned} \tag{19}$$

We apply the notations of beam theory to our equations. Integrating the stresses in thickness of the beam, we find the resulting tangential force T and bending moment G

$$T = \int_{-h}^{+h} \sigma_{11} dx_3, \; G = -\int_{-h}^{+h} \sigma_{11} x_3 dx_3 \qquad (20)$$

Having integrated the equations of motion and the equations of state for each layer, we obtain one-dimensional equations for a three-layer electroelastic beam. As an example, we consider the damping of harmonic vibrations of a three-layer beam (all values vary according to the variable *t* by the law $e^{-i\omega t}$, where the variable *t* is the time, ω is the circular frequency of vibrations). In the future, we will write down all the equations and boundary conditions with respect to the amplitude values of the unknown quantities.

The equations of the theory of layered electroelastic beams of a symmetric structure have exactly the same form as in the case of elastic beams. The problem in question, as in the theory of elasticity, is divided into two problems - a plane problem and a bending problem.

Note that the electric potential is odd function in plane problem

$$V^{(2)} = V^{(-2)} = \boldsymbol{V_p}$$

Plane problem for beam with shot-circuited electrodes ($\boldsymbol{V_p} = \boldsymbol{0}$,)

$$\frac{\mathrm{d}T}{dx_1} + X + 2h\rho\omega^2 \mathrm{u} = 0, \; T = A\varepsilon, \; \varepsilon = \frac{du}{dx_1} \qquad (21)$$

$$\sigma_{11,0}^{(\pm 2)} = \frac{1}{s_{11}^E}\varepsilon, \; E_{3,0}^{(\pm 2)} = 0, \; D_{3,0}^{(\pm 2)} = \frac{d_{31}}{s_{11}^E}\varepsilon \qquad (22)$$

$$X = q_1^+ + q_1^-, \; A = 2h_1 E + \frac{2h_2}{s_{11}^E}, \; \rho = \frac{1}{h}(\rho_1 h_1 + \rho_2 h_2)$$

Plane problem for beam with open-electrodes

$$\begin{gathered} \frac{\mathrm{d}T}{dx_1} + X + 2h\rho\omega^2 \mathrm{u} = 0 \\ T = A\varepsilon + P^{(\mathrm{d})}, \; \varepsilon = \frac{du}{dx_1} \\ P^{(\mathrm{d})} = \frac{2}{s_{11}^E}\frac{h_2}{l}\frac{\mathrm{k}_{31}^2}{1-\mathrm{k}_{31}^2}\left(u\big|_{x_1=l} - u\big|_{x_1=0}\right) \end{gathered} \qquad (23)$$

$$\begin{gathered} \sigma_{11,0}^{(\pm 2)} = \frac{\boldsymbol{1}}{s_{11}^E}\varepsilon + \frac{\boldsymbol{2}d_{31}}{h_2 s_{11}^E}V_p, \; E_{3,0} = -\frac{\boldsymbol{2}V_p}{h_2} \\ D_{3,0}^{(\pm 2)} = \varepsilon_{33}^T(\boldsymbol{1} - k_{31}{}^2)E_{3,0}^{(\pm 2)} + \frac{d_{31}}{s_{11}^E}\varepsilon \\ V_p = \frac{h_2}{\boldsymbol{2}ld_{31}}\frac{\boldsymbol{k}_{31}^2}{\boldsymbol{1}-\boldsymbol{k}_{31}^2}\left(u\big|_{x_1=l} - u\big|_{x_1=0}\right) \end{gathered} \qquad (24)$$

We determine the value $\boldsymbol{V_p}$ by equation (18).

The electric potential is an even function of the variable x_3 in bending problem

$$V^{(2)} = -V^{(-2)} = \boldsymbol{V_b}$$

Bending problem for beam with shot-circuited electrodes ($V_b = \boldsymbol{0}$)

$$\begin{gathered} \frac{dN}{dx_1} + Z + \boldsymbol{2}h\rho\omega^2\boldsymbol{w} = \boldsymbol{0}, \; N = \frac{dG}{dx_1} \\ G = M\kappa, \; \kappa = \frac{d^2 w}{dx_1^2} \\ Z = -(q_3^+ + q_3^-) \\ M = -\frac{\boldsymbol{2}h_1{}^3 E}{\boldsymbol{3}} - \frac{\boldsymbol{2}(h^3 - h_1{}^3)\kappa}{\boldsymbol{3}s_{11}^E(\boldsymbol{1}-k_{31}^2)}\left(\boldsymbol{1} - \frac{\boldsymbol{3}h_2(h^2 - h_1^2)k_{31}^2}{\boldsymbol{4}(h^3 - h_1^3)}\right) \end{gathered} \qquad (25)$$

$$\begin{gathered} \sigma_{11,0}^{(\pm 2)} = \mp\frac{(\boldsymbol{h} + h_1)k_{31}{}^2}{\boldsymbol{2}s_{11}^E(\boldsymbol{1} - k_{31}{}^2)}\kappa \\ \sigma_{11,1}^{(\pm 2)} = \frac{\boldsymbol{1}}{s_{11}^E(\boldsymbol{1} - k_{31}{}^2)}\kappa \\ E_{3,0}^{(\pm 2)} = \pm\frac{(\boldsymbol{h} + h_1)k_{31}{}^2}{\boldsymbol{2}d_{31}(\boldsymbol{1} - k_{31}{}^2)}\kappa \\ E_{3,1}^{(\pm 2)} = \frac{-k_{31}{}^2}{d_{31}(\boldsymbol{1} - k_{31}{}^2)}\kappa \\ D_{3,0}^{(\pm 2)} = \varepsilon_{33}^T(\boldsymbol{1} - k_{31}{}^2)E_{3,0}^{(\pm 2)} \end{gathered} \qquad (26)$$

Here *N* is the shear force

$$N = -\int_{-h}^{+h} \sigma_{13} dx_3$$

Bending problem for beam with open-electrodes

$$\frac{dN}{dx_1} + Z + 2h\rho\omega^2 w = 0,\ N = \frac{dG}{dx_1},$$
$$G = M\kappa + Q,\ \ \kappa = \frac{d^2 w}{dx_1^2}$$
$$Q = -\frac{h_2(h+h_1)^2}{2l}\frac{k_{31}^{\ 2}}{s_{11}^E(1-k_{31}^{\ 2})} \cdot\left(\left.\frac{dw}{dx}\right|_{x=l} - \left.\frac{dw}{dx}\right|_{x=0}\right) \tag{27}$$
$$Q = -\frac{d_{31}}{s_{11}^E}\frac{h^2 - h_1^2}{h_2}2V_b$$
$$\sigma_{11,0}^{(\pm 2)} = \pm\frac{2d_{31}}{h_2 s_{11}^E}V_b \mp \frac{(h+h_1)k_{31}^{\ 2}}{2s_{11}^E(1-k_{31}^{\ 2})}\kappa \tag{28}$$
$$E_{3,0}^{(\pm 2)} = \mp\frac{2V_b}{h_2} \pm \frac{(h+h_1)k_{31}^{\ 2}}{2d_{31}(1-k_{31}^{\ 2})}\kappa$$

The quantities $\boldsymbol{Z}$, $\boldsymbol{M}$, $\sigma_{11,1}^{(\pm 2)}$, $D_{3,0}^{(\pm 2)}$, $E_{3,1}^{(\pm 2)}$ are determined by formulas (26).

3. DYNAMIC PLANE PROBLEM

We will consider the forced harmonic vibrations of the beam under the action of a constant distributed load with the following boundary conditions:

$$u\big|_{x_1=0} = 0,\ T\big|_{x_1=l} = 0 \tag{29}$$

For numerical examples, we introduce dimensionless coordinates and dimensionless sought quantities

$$\xi = \frac{x}{l},\ u_* = \frac{u}{l},\ \varepsilon = \varepsilon_*,\ T_* = \frac{T}{A}$$
$$X_* = \frac{Xl}{A},\ E_{3*} = d_{31}E_3,\ D_{3*} = \frac{s_{11}^E}{d_{31}}D_3 \tag{30}$$

Let the beam electrodes be short-circuited. Submitting the formulas (30) in the equations (21), we obtain the following system of equations

$$\frac{dT_*}{d\xi} + X_* + \lambda_1^2 u_* = 0,\ T_* = \varepsilon_*,\ \ \varepsilon_* = \frac{du_*}{d\xi}$$
$$\lambda_1^2 = \frac{2h\rho\rho^{\,2}l^2}{A} \tag{31}$$

where λ_1^2 is the dimensionless frequency parameter.

The resolving equation is

$$\frac{d^2 u_*}{d\xi^2} + \lambda_1^2 u_* + \boldsymbol{X}_* = 0 \tag{32}$$

Its solution is

$$u_* = c_1 \sin\lambda_1\xi + c_2\cos\lambda_1\xi - \frac{1}{\lambda_1^2}\boldsymbol{X}_*$$
$$T_* = \lambda_1(c_1\cos\lambda_1\xi - c_2\sin\lambda_1\xi) \tag{33}$$

Arbitrary integration constants c_1 and c_2 are determined from the conditions at the ends of the beam

$$u_*\big|_{\xi=0} = 0,\ T_*\big|_{\xi=1} = 0 \tag{34}$$

Satisfying conditions (34), we get

$$c_1 = \frac{\sin\lambda_1}{\lambda_1^{\ 2}\cos\lambda_1}\boldsymbol{X}_*,\ \ c_2 = \frac{1}{\lambda_1^{\ 2}}\boldsymbol{X}_* \tag{35}$$

The natural frequencies are determined from the equation $\cos\lambda_1 = 0$ and they are equal to

$$n\pi + \pi/2,\ n = 0,1,2,3,... \tag{36}$$

Consider the plane problem for beam with open-electrodes. The system of equations according to the sought quantities has the form

$$\frac{dT_*}{d\xi} + X_* + \lambda_1^2 u_* = 0,\ T_* = \varepsilon_* + P_*,\ \ \varepsilon_* = \frac{du_*}{d\xi}$$
$$P_* = ru_*\big|_{\xi=1},\ \ r = \frac{2h_2}{As_{11}^E}\frac{k_{31}^2}{1-k_{31}^2},\ \ k_{31}^2 = \frac{d_{31}^2}{s_{11}^E\varepsilon_{33}^T} \tag{37}$$

After solving the problem (37), (34), the following desired quantities can be calculated by the formulas:

$$\sigma_{11,0}^{(\pm 2)} = \frac{1}{s_{11}^E}\varepsilon + \frac{2d_{31}}{h_2 s_{11}^E}V_p,\ P = 4\frac{d_{31}}{s_{11}^E}V_p$$
$$V_p = \frac{h_2}{2ld_{31}}\frac{k_{31}^2}{1-k_{31}^2}u\big|_{x_1=l},\ E_{3,0} = -\frac{2V_p}{h_2} \qquad (38)$$
$$D_{3,0}^{(\pm 2)} = \varepsilon_{33}^T(1-k_{31}{}^2)E_{3,0}^{(\pm 2)} + \frac{d_{31}}{s_{11}^E}\varepsilon$$

The solution resolving equation has the form (33). The force T_* is determined by formula

$$T_* = \lambda_1(c_1\cos\lambda_1\xi - c_2\sin\lambda_1\xi) + P_* \qquad (39)$$

Arbitrary integration constants c_1 and c_2 are determined from the conditions at the ends of the beam (34)

$$c_1 = \frac{X_*}{\lambda_1{}^2}\frac{\lambda_1\sin\lambda_1 - r(\cos\lambda_1 - 1)}{\lambda_1\cos\lambda_1 + r\sin\lambda_1},\ c_2 = \frac{X_*}{\lambda_1{}^2} \qquad (40)$$

The natural frequencies are determined from the equation

$$\lambda_1\cos\lambda_1 + r\sin\lambda_1 = 0 \qquad (41)$$

The first natural frequency for different values r is 1.602 (r=0.05), 1.630 (r=0.1), and 1.689 (r=0.2).

Let a beam with short-circuited electrodes vibrates with a frequency close to the first resonant frequency $\lambda_1 = 1.56$. In order to reduce the amplitudes of vibrations of the desired quantities, we will open the electrodes of the piezoelectric layers. Perform a numerical calculation using formulas (33), (35), (39), (40). Figs. 2, 3 show the displacement u_* and the force T_* as function of the longitudinal coordinate ξ. The dashed line represents the same values for a beam with short-circuited electrodes. Thick (thin) line represents the same values for a beam with open electrodes at r = 0.05 (r = 0.1).

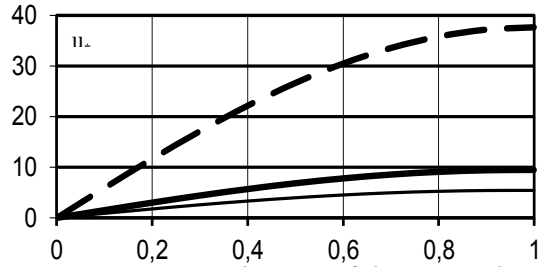

Figure 2. Distribution of dimensionless displacement u_* along the length of a beam.

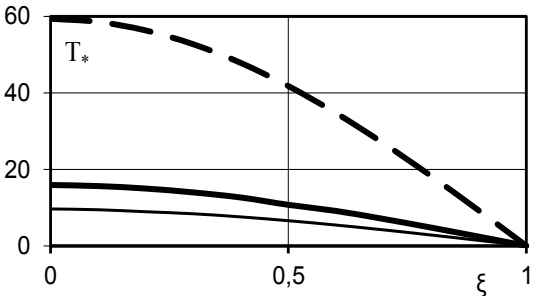

Figure 3. Distribution of dimensionless force T_* along the length of a beam.

From the graphs it can be seen that the vibration amplitudes for a beam with open electrodes are substantially less than for a beam with short-circuited electrodes.

4. DYNAMIC BENDING PROBLEM

Consider the case when only constant distributed load Z_* acts on the beam. We assume that the edge $x_1 = 0$ rigidly fixed, and the edge $x_1 = l$ is free from fixings

$$w\big|_{x_1=0} = 0,\ \left.\frac{dw}{dx_1}\right|_{x_1=0} = 0,\ G\big|_{x_1=l} = 0,\ N\big|_{x_1=l} = 0$$

We introduce the dimensionless sought values

$$\xi = \frac{\mathrm{x}}{\mathrm{l}},\ \mathrm{w}_* = \frac{\mathrm{w}}{\mathrm{l}},\ \kappa_* = \mathrm{l}\kappa = \frac{d^2 w_*}{d\xi^2}$$
$$N_* = \frac{l^2}{M} N,\ G_* = \frac{l}{M} G, \tag{42}$$
$$\mathrm{Z}_* = \frac{l^3}{M} Z, \mathrm{Q}_* = \mathrm{Q}\frac{l}{M}$$

Let the beam electrodes be short-circuited. Taking into account the formulas (42), the system of equations (25) will be rewritten as ($V_b = \mathbf{0},\ \boldsymbol{Q} = \mathbf{0}$)

$$\frac{dN_*}{d\xi} + Z_* - \lambda_2^4 w_* = 0,\ \ \mathrm{N}_* = \frac{dG_*}{d\xi}$$
$$G_* = \kappa_*,\ \ \kappa_* = \frac{d^2 w_*}{d\xi^2} \tag{43}$$

The resolving equation for the bending problem is written as

$$\frac{d^4 w_*}{d\xi^4} - \lambda_2^4 w_* + Z_* = \mathbf{0},\ \lambda_2^4 = -\frac{\mathbf{2}h\rho\omega^2 l^4}{M} \tag{44}$$

The solution of equation (44) is

$$w_* = c_1 ch\lambda_2\xi + c_2 sh\lambda_2\xi + c_3 cos\lambda_2\xi$$
$$+ c_4 \sin\lambda_2\xi + \frac{1}{\lambda_2^4} Z_* \tag{45}$$

Arbitrary integration constants c_1 and c_2 are determined from the conditions at the ends of the beam

$$w_*\big|_{\xi=0} = 0,\ \left.\frac{dw_*}{d\xi}\right|_{\xi=0} = 0,\ G_*\big|_{\xi=1} = 0,\ N_*\big|_{\xi=1} = 0$$

Find arbitrary integration constants c_1, c_2, c_3, c_4

$$c_1 = -c_3 - \frac{\mathbf{1}}{\lambda_2^4} Z_* = -\frac{Z_*}{\mathbf{2}\lambda_2^4\delta}(\boldsymbol{cc} + \boldsymbol{ss} + \mathbf{1})$$
$$c_2 = -c_4 = \frac{Z_*}{\mathbf{2}\lambda_2^4\delta}(\boldsymbol{cs} + sc) \tag{46}$$

$$\delta = cc + \mathbf{1} \tag{47}$$

The new notations are introduced in formulas (46)

$$\boldsymbol{cc} = ch\lambda_2\cos\lambda_2,\ \ ss = sh\lambda_2\sin\lambda_2$$
$$sc = sh\lambda_2\cos\lambda_2,\ \ cs = ch\lambda_2\sin\lambda_2 \tag{48}$$

We calculate the natural frequencies of the beam using the equation (47). The first three natural frequencies are 1.875, 4.694, 7.855.

Consider the bending problem for beam with open-electrodes $V^{(2)} = -V^{(-2)} = \boldsymbol{V_b}$. The system of equations according to the dimensionless sought quantities has the form

$$\frac{dN_*}{d\xi} + Z_* - \lambda_2^4 w_* = 0,\ \ N_* = \frac{dG_*}{d\xi}$$
$$G_* = \kappa_* + \mathrm{Q}_*,\ \ \kappa_* = \frac{d^2 w_*}{d\xi^2}$$
$$Q_* = t\left.\frac{dw_*}{d\xi}\right|_{\xi=1},\ t = -\frac{h_2(h+h_1)^2}{2s_{11}^E M}\frac{{k_{31}}^2}{1-{k_{31}}^2}$$

Satisfying the boundary conditions, we obtain arbitrary integration constants and the equation for determining the resonant frequencies

$$c_1 = -c_3 - \frac{Z_*}{\lambda_2^4} = -\frac{Z_*}{2\lambda_2^4\delta}\left(\lambda_2(cc + ss + 1) + 2t\cdot cs\right)$$
$$c_2 = -c_4 = -\frac{Z_*}{2\lambda_2^4\delta}\left(\lambda_2(\mathrm{cs} + sc + 1) + 2t\cdot ss\right) \tag{49}$$

$$\delta = \lambda_2(cc + \mathbf{1}) + t(\boldsymbol{cs} + sc) \tag{50}$$

In formulas (49), (50), the notation (48) is used.

We calculate the natural frequencies of the beam using the equation (50). The first three natural frequencies are 1.8891; 4.705; 7.8611 for $t = \mathbf{0.05}$ and 1.9022; 4.7563; 7.8673 for $t = \mathbf{0.1}$.

The results of the calculations are presented in the form of graphs. Figures 4-6 show the dependence of the deflection, the shear force and the bending moment on the longitudinal coordi-

nate of the beam in the vicinity of the second resonant frequency of the beam with short-circuited electrodes.

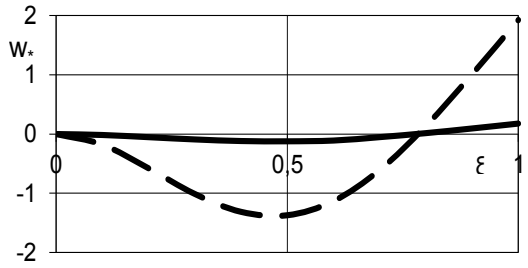

Figure 4. The deflection w_* as a function of the coordinate ξ near the second resonance of the beam at $\lambda_2 = 4.693$.

In all figures, the dashed line represents the quantities of a beam with short-circuited electrodes and the solid line represents the quantities for a beam with disconnected electrodes.

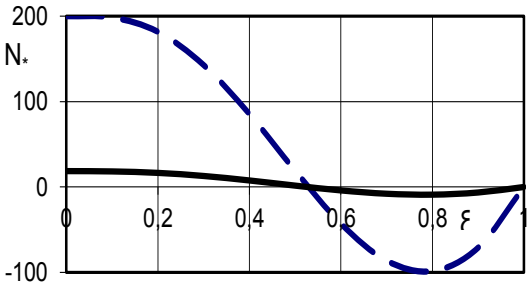

Figure 5. The shear force N_* as a function of the coordinate ξ near the second resonance of the beam at $\lambda_2 = 4.693$.

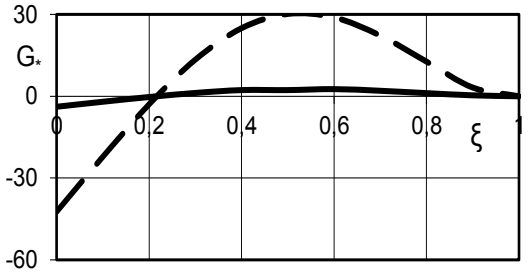

Figure 6. The moment G_* as function of the coordinate ξ near the second resonance at $\lambda_2 = 4.693$.

The performed calculations confirm that a change in the electrical conditions on the electrodes of the piezoelectric layers makes it possible to avoid resonance and, as a consequence, an increase in the amplitude values of the desired values.

CONCLUSION

A study was carried out on the new method of vibration damping of a structure at resonance using the example of a multi-layer beam. Analytical solutions of the problem of beam passive vibration suppression are obtained. Numerical calculations were performed confirming the effectiveness of using the piezoelectric effect for passive vibration control. It is shown that forcers, moments, displacements and deformations of beam in the vicinity of the natural frequency can be significantly reduced by as a result of changes in the electrical conditions on the surfaces of the piezoelectric layers.

REFERENCES

1. **Preumont A., Kazuto Seto**. Vibration Control of Active Structures. John Wiley&Sons, 2008, 295 pages.
2. **Inmah D.J.** Vibration with Control. Wiley Online Books, 2017 (IBSB: 9781119375081).
3. **Frolov K.V.** (Eds.) Vibracii v tehnike. Spravochnik. Tom 6. Zashhita ot vibracii i udarov [Vibrations in technology. Vol. 6]. Moscow, Mechanical Engineering, 1981, 456 pages (in Russian).
4. **Huertas V.V., Rohal'-Ilkiv**. Vibration suppression of a flexible structure. // *Procedia Engineering*, 2012, vol. 48, pp. 233-241.
5. **Berlincourt D.A., Curran D.R., Jaffe H.** Piezoelectric and piezomagnetic materials and their function as transducer Mason W P (Eds.) Physical Acoustics 1A (Academic Press New York), 1964, pp. 204-326.
6. IEEE Standart on Piezoelectricity ANSI-IEEE Std. 176, IEEE New York 1987.

7. **Rogacheva N.N.** The Theory of Piezoelectric Shells and Plates. Roca Braton, CRC Press, 1994, 260 pages.
8. **Rogacheva N.N.** The dynamic behaviour of piezoelectric laminated bars. // *J. of Applied Mathematics and Mechanics*, 2007, vol. 71, pp. 494-510.

СПИСОК ЛИТЕРАТУРЫ

1. **Preumont A., Kazuto Seto**. Vibration Control of Active Structures. John Wiley&Sons, 2008, 295 pages.
2. **Inmah D.J.** Vibration with Control. Wiley Online Books, 2017 (IBSB: 9781119375081).
3. **Асташев В.К., Бабицкий В.И., Быховский И.И., Вульфсон И.И., Вульфсон М.Н., Гольдштей Б.Г., Гоппен А.А., Гурецкий В.В., Гусаров А.А., Коловский М.З., Пальмов В.А., Пановко Г.Я., Пановко Я.Г., Панченко В.И., Писаренко Г.С., Потемкин Б.А., Синев А.В., Фролов К.В.** (ред.)**, Фурман Ф.А., Фурунжиев Р.И.** Вибрации в технике. Справочник. Том 6. Защита от вибрации и ударов. – М.: Машиностроение, 1981. – 456 с.
4. **Huertas V.V., Rohal'-Ilkiv**. Vibration suppression of a flexible structure. // *Procedia Engineering*, 2012, vol. 48, pp. 233-241.
5. **Berlincourt D.A., Curran D.R., Jaffe H.** Piezoelectric and piezomagnetic materials and their function as transducer Mason W P (Eds.) Physical Acoustics 1A (Academic Press New York), 1964, pp. 204-326.
6. IEEE Standart on Piezoelectricity ANSI-IEEE Std. 176, IEEE New York 1987.
7. **Rogacheva N.N.** The Theory of Piezoelectric Shells and Plates. Roca Braton, CRC Press, 1994, 260 pages.
8. **Rogacheva N.N.** The dynamic behaviour of piezoelectric laminated bars. // *J. of Applied Mathematics and Mechanics*, 2007, vol. 71, pp. 494-510.

Nelly N. Rogacheva, Dr.Sc. (Physics and Mathematics), Laureate of the State Prize of the Russian Federation in the field of science and technology, associate professor of Department of Applied Mathematics, National Research Moscow State University of Civil Engineering; 26, Yaroslavskoe Shosse, 129337, Moscow, Russia;
phone/fax: +7 (499)183-59-94;
E-mail: RogachevaNN@mgsu.ru.

Рогачева Нэлля Николаевна, доктор физико-математических наук, Лауреат Государственной премии Российской Федерации в области науки и техники, доцент кафедры прикладной математики; Национальный исследовательский Московский государственный строительный университет; 129337, Россия, г. Москва, Ярославское шоссе, д. 26;
тел./факс: +7(499)183-59-94;
E-mail: RogachevaNN@mgsu.ru.

DOI:10.22337/2587-9618-2019-15-2-135-143

COMPUTATIONAL RHEOLOGICAL MODEL OF CONCRETE

Vladimir N. Sidorov
Russian University of Transport (RUT – MIIT), Moscow, RUSSIA
Peoples' Friendship University of Russia, Moscow, RUSSIA
Perm National Research Polytechnic University, Perm, RUSSIA
Moscow Institute of Architecture (State Academy), Moscow, RUSSIA
Central Institute for Research and Design of the Ministry of Construction and Housing and Communal Services of the Russian Federation, Moscow, RUSSIA
Kielce University of Technology, Kielce, POLAND

Abstract: The substantiation of the computational rheological model of the material for use in computer calculations of concrete and reinforced concrete structures of arbitrary complexity, taking into account the creep of concrete, with possible changes in the intensity of the current load over time, is presented. The computational model is based on the Maxwell-Weichert generalized model of the viscoelastic material. The model was verified on the basis of experimental data and requirements of regulatory documents for the calculations of concrete and reinforced concrete structures, taking into account the creep of the material. Verification of the computational model and numerical calculations using the selected computational model were performed in the SIMULIA Abaqus software environment.

Keywords: creep, viscoelasticity, computational model, generalized Maxwell-Weichert model, calculation on deformed scheme

ВЫЧИСЛИТЕЛЬНАЯ РЕОЛОГИЧЕСКАЯ МОДЕЛЬ БЕТОНА

В.Н. Сидоров
Российский университет транспорта, г. Москва, РОССИЯ
Российский университет дружбы народов, г. Москва, РОССИЯ
Пермский национальный исследовательский политехнический университет, г. Пермь, РОССИЯ
Московский архитектурный институт (государственная академия), г. Москва, РОССИЯ
Центральный научно-исследовательский и проектный институт
Министерства строительства и жилищно-коммунального хозяйства, г. Москва, РОССИЯ
Свентокжыская Политехника, г. Кельце, ПОЛЬША

Аннотация: Представлено обоснование вычислительной реологической модели материала для использования в компьютерных расчётах бетонных и железобетонных конструкций произвольной сложности с учётом ползучести бетона, с возможным изменением интенсивности действующей нагрузки во времени. Вычислительная модель построена на основе обобщенной модели вязкоупругого материала Максвелла-Вайхерта. Модель верифицировалась на основе данных экспериментальных исследований и требований нормативных документов к расчётам бетонных и железобетонных конструкций с учётом ползучести материала. Верификация вычислительной модели и численные расчёты с использованием выбранной вычислительной модели выполнялись в программной среде SIMULIA Abaqus.

Ключевые слова: ползучесть, вязкоупругость, вычислительная модель, обобщенная модель Максвелла-Вайхерта, расчёт по деформированной схеме

1. INTRODUCTION

The most visible manifestations of concrete over time are creep, relaxation and shrinkage. These rheological properties of concrete as a building material are sufficiently fully investigated and formulated by thorough theories [1–5], etc., and their accounting in the calculations of building structures is quite clearly regulated in national and international normative docu-

ments [6-9]. However, the availability of proven theories and sound regulatory procedures, unfortunately, does not mean the existence of appropriate computational models that are conveniently calibrated based on the results of experimental studies and regulatory approaches, while of quite versatile, stable and flexible in calculating of complex building structures. The presented computational rheological model of concrete was verified on the basis of data from experimental studies of concrete creep, and it was also substantiated and calibrated in accordance with the requirements of regulatory documents for calculations of concrete and reinforced concrete structures, taking into account the material creep. When calculating structures that noticeably change their configuration in time due to material creep, such as flat arches and shells, attention is paid to the effect of calculating them by deformed scheme, which significantly specifies the change in the stress-strain state in time.

2. THEORETICAL FOUNDATIONS OF THE COMPUTATIONAL CREEP MODEL

The complete deformation of concrete ε is usually represented by its three components:

$$\varepsilon = \varepsilon_0 + \varepsilon_{cr} + \varepsilon_{shr}, \tag{1}$$

where ε_0 is the so-called "instantaneous" deformation which manifests itself at the moment of loading the structure, ε_{cr} is the creep deformation that develops over time, ε_{shr} is the shrinkage deformation. The key parameter characterizing the creep of concrete in EC2 [6] and PN [7] is the creep coefficient (creep factor) $\varphi(t,t_0)$ established between the moment of application of the load t_0 and the age of concrete t:

$$\varphi(t,t_0) = \frac{\varepsilon_{cr}}{\varepsilon_0}. \tag{2}$$

At the same time, the concept of creep measure $C(t,t_0)$ is also used in these regulatory documents:

$$\varphi(t,t_0) = \mathrm{E_b}(t_0) \cdot C(t,t_0), \tag{3}$$

where $\mathrm{E_b}(t_0)$ is the elasticity modulus of concrete at the time of loading t_0.
In turn, the creep measure is the initial key parameter in the NIIZhB Recommendations [8]:

$$C(t,t_0) = \frac{1}{\mathrm{E_b}(t_0)} - \frac{1}{\mathrm{E_b}(t)} + C(\infty,t_0), \tag{4}$$

where $C(\infty,t_{0\,=\,28})$ is the limit creep measure.
In this case the concept of creep characteristic (creep coefficient) $\varphi(t,t_0)$ is also used:

$$C(t,t_0) = \frac{\varphi(t,t_0)}{E(t_0)}. \tag{3a}$$

The rheological model based on the generalized model of a viscoelastic material — the generalized Maxwell model (Wiechert model) [10], [11] was chosen to study and apply to the modeling of concrete creep. Elements of the mechanical interpretation of this model is a parallel combination of n springs ($i = 1 \div n$) with "temporary" elastic moduli E_i, and n dampers with viscosity coefficients η_i connected in series with each other in pairs, as well as of an elastic element with "long-term" stiffness E_∞.
The basis of the generalized Maxwell model is the elementary model of the viscoelastic Maxwell material. Its mechanical representation is a spring with stiffness (modulus of elasticity) E, consistently coaxed with a damper having a viscosity coefficient η. According to this model, the material resistance is proportional to the speed of its strain

$$\dot{\varepsilon} = \dot{\varepsilon}_y + \dot{\varepsilon}_в, \tag{10}$$

folding from the rate of elastic strain $\dot{\varepsilon}_y$ and the rate of viscous strain $\dot{\varepsilon}_в$. In turn, the elastic strain of the material is interpreted by the strain of the elastic spring with the stiffness E:

$$\varepsilon_y = \frac{\sigma_y}{E}, \quad \text{from where} \quad \dot{\varepsilon}_y = \frac{\dot{\sigma}_y}{E}. \quad (11)$$

And the rate of viscous strain in this elementary model is represented by the properties of a damper with the coefficient of viscosity η:

$$\dot{\varepsilon}_в = \frac{\sigma_в}{\eta}. \quad (12)$$

The serial connection of the spring and damper in the Maxwell model means that the stresses σ in both its elements are the same, i.e. $\sigma = \sigma_y = \sigma_в$, but the strains in the elastic and viscous elements are different, i.e.

$$\varepsilon_y \neq \varepsilon_в \, (\varepsilon = \varepsilon_y + \varepsilon_в).$$

Thus, according to (10)-(12), the strain rate of the material, represented by the Maxwell elementary model, will vary in proportion to time t:

$$\dot{\varepsilon}(t) = \frac{\sigma(t)}{\eta} + \frac{\dot{\sigma}(t)}{E}, \quad (10a)$$

herewith at a constant stress σ_0 the strain ε will increase linearly.
In turn, the solution (10a) with respect to $\sigma(t)$:

$$\sigma(t) = \sigma_0 \cdot e^{\left(\frac{-t}{\tau}\right)} = E \cdot \varepsilon_0 \cdot e^{\left(\frac{-t}{\tau}\right)} \quad (13)$$

shows that according to the elementary Maxwell model, when the strain ε_0 is fixed, the stress $\sigma(t)$ decreases in time t according to the exponential law. It in general corresponds to the nature of the manifestation of relaxation in a deformable material, such as for example concrete. In (13)

$$\tau = \frac{\eta}{E}$$

is the so-called relaxation time.
If you move from the elementary Maxwell model (one pair of series-connected spring and a damper) to the Maxwell generalized model (n parallel-connected the pairs with an additional spring of "long-term" stiffness E_∞), dependence (13) takes the form:

$$\sigma(t) = E_\infty \cdot \varepsilon_0 + \sum_{i=1}^{n} E_i \cdot \varepsilon_0 \cdot e^{\left(\frac{-t}{\tau_i}\right)},$$

or

$$\sigma(t) = \varepsilon_0 \cdot \left[E_\infty + \sum_{i=1}^{n} E_i \cdot e^{\left(\frac{-t}{\tau_i}\right)} \right], \quad (14)$$

Where

$$\tau_i = \frac{\eta_i}{E_i}$$

is the relaxation time of the i -th damper ($i = 1 \div n$) in the generalized Maxwell model. Thus, in the generalized Maxwell model, the viscoelasticity of a material is characterized by the generalized relaxation modulus depending on time (the so-called relaxation function):

$$E_R(t) = \frac{\sigma(t)}{\varepsilon_0} = E_\infty + \sum_{i=1}^{n} E_i \cdot e^{\left(-\frac{t}{\tau_i}\right)}. \quad (15)$$

It can be seen that the relaxation function $E_R(t)$ of a material is actually represented in (14), (15) in the form of an exponential series (Prony series).

3. COMPUTATIONAL IMPLEMENTATION OF THE RHEOLOGICAL MODEL

The generalized Maxwell model of viscoelastic properties of a material is implemented in the SIMULIA Abaqus software environment with the "viscoelastic" option [12]. It is represented here by two functions, having the form of an exponential Proni series. This is the s so-called shear relaxation function:

$$G(t) = G_\infty + \sum_{i=1}^{n} G_i \cdot e^{\left(-\frac{t}{\tau_i}\right)}, \qquad (16)$$

where

$$G = \frac{E}{2 \cdot (1 + v_0)}$$

is the modulus of elasticity in shear, v_0 is the Poisson coefficient, and also the function of bulk relaxation:

$$K(t) = K_\infty + \sum_{i=1}^{n} K_i \cdot e^{\left(-\frac{t}{\tau_i}\right)}, \qquad (17)$$

where

$$K = \frac{E}{3 \cdot (1 - 2 \cdot v_0)}$$

is the coefficient of volume stiffness.
In the SIMULIA Abaqus program, the parameters of the "viscoelastic" material model are set by the dimensionless shear relaxation modulus:

$$g_R(t) = \frac{G(t)}{G_0} = 1 - \sum_{i=1}^{n} g_i \cdot \left(1 - e^{\left(-\frac{t}{\tau_i}\right)}\right) \qquad (16a)$$

where

$$G_0 = E_0/(2 \cdot (1 + v_0))$$

is the instantaneous modulus of elasticity in shear, as well as the dimensionless modulus of bulk relaxation:

$$k_R(t) = \frac{K(t)}{K_0} = 1 - \sum_{i=1}^{n} k_i \cdot \left(1 - e^{\left(-\frac{t}{\tau_i}\right)}\right), \qquad (17a)$$

where

$$K_0 = E_0/ \cdot (1 - 2 \cdot v_0)$$

is the coefficient of instantaneous volume stiffness.
Obvious complexity here can have the assignment of values of the parameters of the material G_i, K_i, τ_i, which can be obtained by static and dynamic tests of the material for creep and relaxation. However, under the condition of relatively small changes in stresses over time in the simulated structure, you can use the simple case of specifying the modules $g_r(t)$ (16*a*) and $k_r(t)$ (17*a*) with the introduction of the concept of effective modulus of elasticity [6], [8]:

$$E_{c,eff} = \frac{E_0}{1 + \varphi(t, t_0)}. \qquad (18)$$

Then the expression of the dimensionless shear relaxation modulus is considerably simplified:

$$g_r(t) = \frac{G_R(t)}{G_0} = \frac{\frac{E_0}{2 \cdot (1 + v_0) \cdot (1 + \quad (t, t_0))}}{\frac{E_0}{2(1 + v_0)}},$$

or

$$g_r(t) = \frac{1}{1 + \varphi(t, t_0)}, \qquad (16b)$$

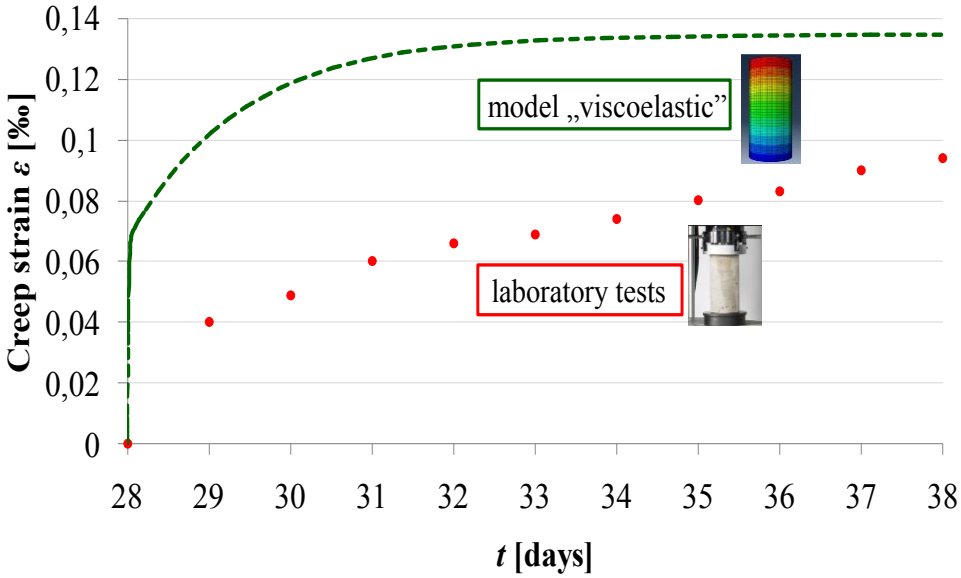

Figure 1. Comparison of the dependences of creep strain in samples of the 1-st group (t_0 = 28 days), obtained in the experiment and in numerical simulation.

where $\varphi(t,t_0)$ is the creep coefficient of the material (2). In this case, the values of the time-varying coefficient $\varphi(t,t_0)$ in the computational model of creep can be set both on the basis of the material test results, and in accordance with the regulatory recommendations [6] - [8] and others. Similarly, the view of the dimensionless bulk relaxation modulus is simplified:

$$k_r(t) = \frac{K_R(t)}{K_0} = \frac{1}{1+\varphi(t,t_0)} \qquad (17б)$$

4. VERIFICATION OF THE COMPUTATIONAL CREEP MODEL

To test the "viscoelastic" model, we used the results of experimental studies of two groups of concrete samples [11]. Each sample had the shape of a cylinder with a height of 0.3m and a diameter of 0.15m. Cylindrical samples subjected to prolonged axial compression. Samples of the 1-st group were loaded (σ_I = 10.67[MPa]) at the age of t_0 = 28 days, having on this day the modulus of elasticity $E_{(28)}$ = 36200[MPa]. Samples of the 2-nd group were loaded (σ_{II} = 2.47[MPa]) 1 day after their manufacture (t_0 = 1), having the elastic modulus $E_{(1)}$ = 22201[MPa]. When specifying the dimensionless relaxation moduli of the material using formulas (16*b*) and (17*b*) in the "viscoelastic" model, the concrete creep factor $\varphi(t, t_0)$ was calculated based on the experimental results. The figures 1 and 2 show the results of a comparison of the dependences of the creep strain in the samples obtained in the experiment and in numerical simulation using the "viscoelastic" model.
Testing the performance of the "viscoelastic" model with setting the values of the dimensionless moduli of material relaxation using formulas (16*b*) and (17*b*) with an abrupt change in load value in time gave quite satisfactory results (figure 3).

5. CONCLUSION

Accounting for material creep in the calculation of reinforced concrete structures of some types, such as flat arches and shells, can reveal a significant change in their stress-strain state over a long time. Below the difference in the results of the calculation in the traditional way and by deformed scheme of the flat reinforced concrete arch with a span of 20 m and a height of 2 m under a permanent load is shown.

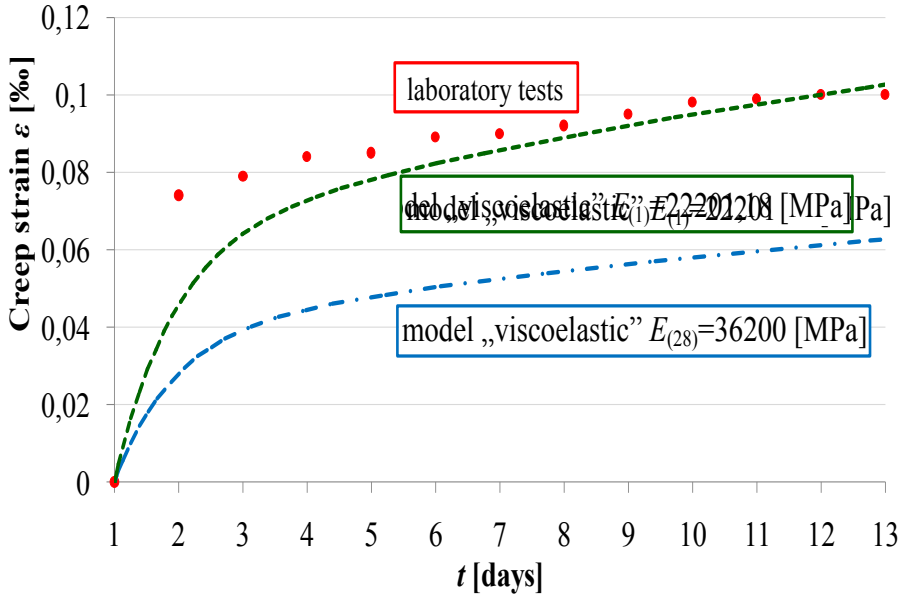

Figure 2. Comparison of the dependences of creep strain in samples of the 2-st group (t_0 = 1 day), obtained in the experiment and in numerical simulation.

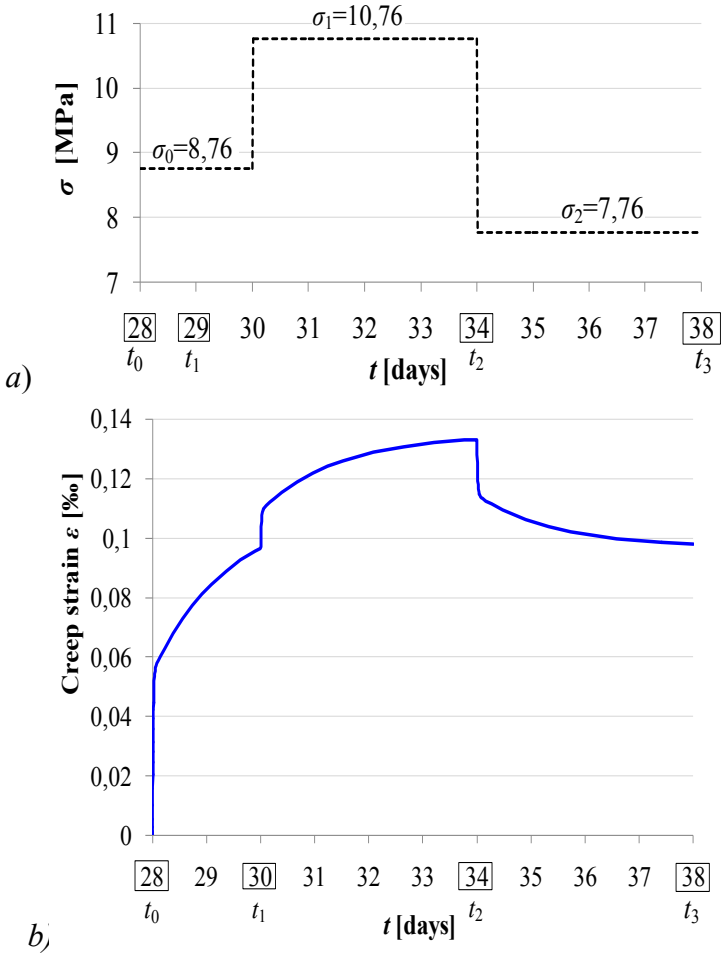

Figure 3. The change in creep strain in time with an abrupt change in load value: a) change in stress over time; b) change in creep strain in time.

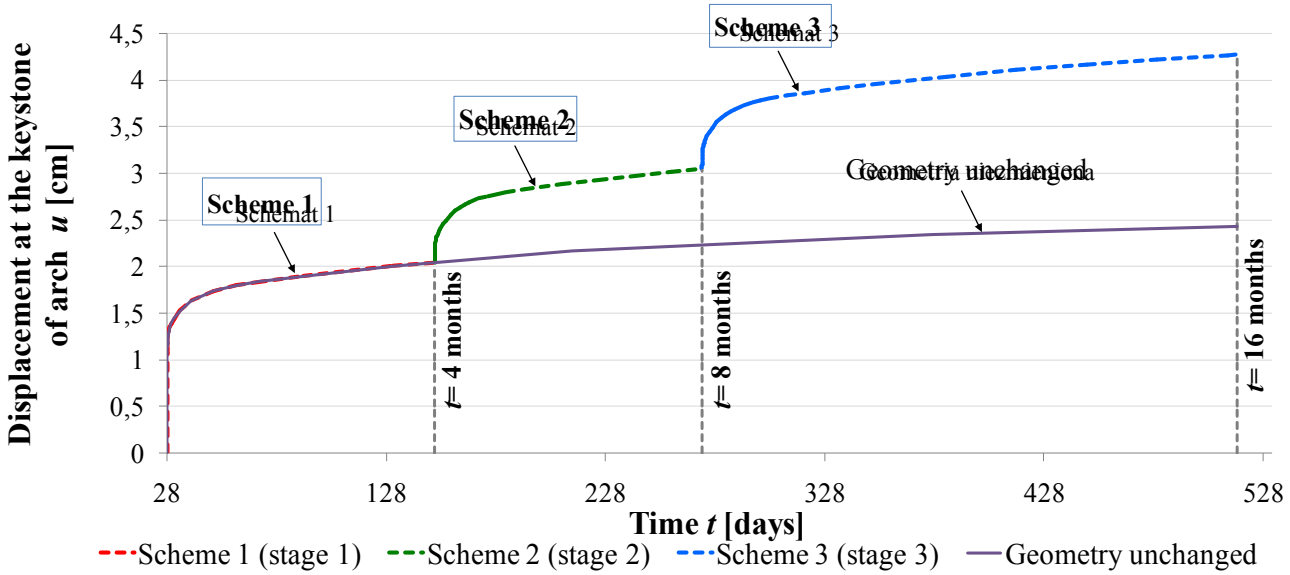

*Figure 4. The increase in the deflection of a gentle arch in the castle section **u** in time **t***
– at traditional time calculation (bottom line);
– when calculating by the deformed scheme (upper lines).

The arch was simulated in a time period of 16 months, taking into account the creep of the material. When calculating this construction, the "viscoelastic" concrete creep model calibrated in accordance with the requirements of [6] was implemented. When calculating by deformed scheme, the arch configuration was recalculated on the 4-th and 8-th month of loading. The difference in the deflections of the castle arch section obtained on the 516th day in two ways was 58 percent (figure 4).

5. FUNDING

The research was carried out at the expense of the state program of the Russian Federation "Development of science and technologies" for 2013–2020 and the Program for Fundamental Research of State Academies of Science for 2013–2020, as part of the Plan for Fundamental Scientific Research of the Ministry of Construction and Housing and Communal Services of the Russian Federation for 2018: 7.4.2 "Development and numerical implementation of methods for determining the stress-strain state of spatial slab-shell reinforced concrete structures, taking into account physical non-linearity, cracking and acquired anisotropy"; 7.4.17 "Research and development of adaptive mathematical models, numerical and numerical-analytical methods as the basis and component of monitoring systems of bearing structures of unique buildings and constructions".

REFERENCES

1. **Arutjunjan N.H.**, **Zevin A.A.** Rastchjot Elementov Stroitelnych Konstrukcji s Utchjotom Polzutchesti [Raschet Jelementov Stroitel'nyh Konstrukcij s Uchetom Polzuchesti]. Moscow, Strojizdat, 1988, 256 pages (in Russian).
2. **Aleksandrovsky S.V.** Calculation of Concrete and Reinforced Concrete Structures for Changes in Temperature and Humidity Over Time [Raschet Betonnyh i Zhelezobetonnyh Konstrukcij na Izmenenija Temperatury i Vlazhnosti vo Vremeni]. Moscow, Strojizdat, 1973 (in Russian).
3. **Bondarenko V.M.**, **Bondarenko S.V.** Engineering Methods of the Nonlinear Theory

of Reinforced Concrete [Inzhenernye Metody Nelinejnoj Teorii Zhelezobetona]. Moscow, Stroiizdat, 1982, 287 pages. (in Russian).
4. **Prokopovich I.Ye.**, **Zedgenidze V.A.** Prikladnaja Teorija Polzuchesti [Applied Theory of Creep]. Moscow, Strojizdat, 1980, 240 pages (in Russian).
5. **Bazant Z.P.** Scaling of Structural Strength. London, Elsevier, 2005.
6. EN1992-1-1. Eurocode 2: Design of concrete structures, 2008.
7. PN-B-03264: Pre-norma fib Model Code. Concrete, Reinforced Concrete and Prestressed structures. Static Calculations and Design, 2010.
8. NIIZhB. Recommendations on Concrete Creep and Shrinkage Consideration when Calculating Concrete and Reinforced Concrete Structures [Rekomendacii po Uchetu Polzuchesti i Usadki Betona pri Raschete Betonnyh i Zhelezobetonnyh Konstrukcij]. Moscow, Stroiizdat, 1988, 124 pages (in Russian).
9. SNiP 52-01-2003. Construction norms and rules of the Russian Federation. Concrete and reinforced concrete structures. Principal rules [Betonnye i Zhelezobetonnye Konstrukcii. Osnovnye Polozhenija]. Moscow, Stroyizdat, 1988 (in Russian).
10. **Schiessel H.**, **Metzler R.**, **Blumen A.**, **Nonnenmacher T.F.** Generalized Viscoelastic Models: Their Fractional Equations with Solutions. // *Journal of Physics A: Mathematical and General*, 1995, No. 28, pp. 6567-6584
11. **Sidorov V.N.**, **Nowak K.** Substantiation of the Use of Viscoelastic Material Model in Numerical Analysis the Creep of Concrete Structures. // *IDT 2017 – Proceedings of the 2017 International Conference on Information and Digital Technologies*, 2017, pp. 339-343.
12. ABAQUS – Standard, User's Manual, Theory Manual and Keywords Manual, 19.7.1. Time domain viscoelasticity. USA, Boston: Hibbitt, Karlsson and Sorensen, Inc., 1306 pages.

СПИСОК ЛИТЕРАТУРЫ

1. **Аратюнян Н.Х.**, **Зевин А.А.** Расчет элементов строительных конструкций с учетом ползучести. – М.: Стройиздат, 1988. – 256 с.
2. **Александровский С.В.** Расчет бетонных и железобетонных конструкций на изменения температуры и влажности во времени. – М.: Стройиздат, 1973.
3. **Бондаренко В.М.**, **Бондаренко С.В.** Инженерные методы нелинейной теории железобетона. – М.: Стройиздат, 1982. – 287 с.
4. **Прокопович И.Е.**, **Зедгенидзе В.А.** Прикладная теория ползучести. – М.: Стройиздат, 1980. – 240 pages.
5. **Bazant Z.P.** Scaling of Structural Strength. London, Elsevier, 2005.
6. EN1992-1-1. Eurocode 2: Design of concrete structures, 2008.
7. PN-B-03264: Pre-norma fib Model Code. Concrete, Reinforced Concrete and Prestressed structures. Static Calculations and Design, 2010.
8. НИИЖБ. Рекомендации по учету ползучести и усадки бетона при расчете бетонных и железобетонных конструкций. М., Стройиздат, 1988. – 124 с.
9. Строительные нормы и правила РФ. СНиП 52-01-2003. Бетонные и железобетонные конструкции. Основные положения. М., 2004.
10. **Schiessel H.**, **Metzler R.**, **Blumen A.**, **Nonnenmacher T.F.** Generalized Viscoelastic Models: Their Fractional Equations with Solutions. // *Journal of Physics A: Mathematical and General*, 1995, No. 28, pp. 6567-6584
11. **Sidorov V.N.**, **Nowak K.** Substantiation of the Use of Viscoelastic Material Model in Numerical Analysis the Creep of Concrete Structures. // *IDT 2017 – Proceedings of*

the 2017 International Conference on Information and Digital Technologies, 2017, pp. 339-343.
12. ABAQUS – Standard, User's Manual, Theory Manual and Keywords Manual, 19.7.1. Time domain viscoelasticity. USA, Boston: Hibbitt, Karlsson and Sorensen, Inc., 1306 pages.

Vladimir N.Sidorov, Corresponding Member of the Russian Academy of Architecture and Construction Sciences, Prof., Dr.Sc.; Professor of Department of Building structures, Buildings and Facilities, Russian University of Transport (MIIT); Professor of Department of and Construction, Peoples' Friendship University; Professor of Department of Building Structures and Computational Mechanics, Perm National Research Polytechnic University; Moscow Institute of Architecture (State Academy); Central Institute for Research and Design of the Ministry of Construction and Housing and Communal Services of the Russian Federation; Kielce University of Technology; 9b9 Obrazcova street, Moscow, 127994, Russia;
E-mail: sidorov.vladimir@gmail.com.

Сидоров Владимир Николаевич, член-корреспондент РААСН, профессор, доктор технических наук; профессор кафедры «Строительные конструкции, здания и сооружения», Российский университет транспорта (МИИТ); профессор Департамента строительства Российского университета дружбы народов; профессор кафедры строительных конструкций и вычислительной механики Пермского национального исследовательского политехнического университета; Междисциплинарный учебный центр Вечернего факультета (МУЦ ВФ), Московский архитектурный институт (государственная академия); Центральный научно-исследовательский и проектный институт Министерства строительства и жилищно-коммунального хозяйства Российской Федерации; Свентокжыская Политехника; 127994, Россия, г. Москва, ул. Образцова, 9б с. 9;
E-mail: sidorov.vladimir@gmail.com.

DOI:10.22337/2587-9618-2019-15-2-144-158

MATHEMATIC MODEL OF A BEAM PARTIALLY SUPPORTED ON ELASTIC FOUNDATION

Vladimir I. Travush [1], Vladimir A. Gordom [2], Vitaly I. Kolchunov [3], Yevgeny V. Leontiev [4]

[1] Russian Academy of Architecture and Construction Sciences, Moscow, RUSSIA
[2] Orel State University named after I.S. Turgenev, Orel, RUSSIA
[3] Southwest State University, Kursk, RUSSIA
[4] Main Department of State Expertise, Moscow, RUSSIA

Abstract: The paper presents the methodic for analytical determining of stress-strain state of a beam partially supported on elastic foundation at sudden damage of foundation structure (partial failure). Bending equation for a beam is written using dimensional parameter and solved with the initial parameters method. Such approach allows to obtain dimensional analytical solution to static and dynamic problems for universal boundary conditions of a beam since it always leads to equations' system of second order. Using numerical analysis for various values of generalized stiffness parameter of a system "beam – foundation", we established affecting of the length of failure foundation part to stress-strain state of the beam for two supporting variants: partial supporting and supporting by two ends with foundation failure in the middle part of the beam.

Keywords: system "beam – foundation", accidental impact, sudden foundation failure, forces, deflections

МАТЕМАТИЧЕСКАЯ МОДЕЛЬ БАЛКИ, ЧАСТИЧНО ОПЕРТОЙ НА УПРУГОЕ ОСНОВАНИЕ

В.И. Травуш [1], В.А. Гордон [2], В.И. Колчунов [3], Е.В. Леонтьев [4]

[1] Российская академия архитектуры и строительных наук, г. Москва, РОССИЯ
[2] Орловский государственный университет имени И.С. Тургенева, г. Орел, РОССИЯ
[3] Юго-западный Государственный университет, г. Курск, РОССИЯ
[4] Главгосэкспертиза России, г. Москва, РОССИЯ

Аннотация: Приведена методика аналитического определения усилий напряженно деформированного состояния балки частично опертой на упругое основание при внезапном дефекте основания – частичного ее разрушения. Уравнение изгиба балки записаны в безразмерных координатах и решены методов начальных параметров это позволяет получать безразмерные аналитические решения статических и динамических задач универсальными по отношению к условиям закрепления балки, поскольку всегда приводит к системе уравнений второго порядка. Численным анализам для различных значений параметра обобщенной жесткости системы «балка-основание» установлено влияние длинны утраченной части основания на напряженно деформированное состояние балки при двух вариантах опирания на упругое основание: частичное опирание и опирание по двухопорной схеме с разрушением основания в средней части пролета.

Ключевые слова: система «балка-основание», аварийное воздействие, внезапный дефект основания, усилия, перемещения

1. INTRODUCTION

Traditional approach for solving the problem of static and dynamic flexure of a beam supported on elastic foundation with discrete changes of geometric and (or) mechanical characteristics of this beam and (or) foundation along it length is representation of a system "beam – foundation" as series of rod sections supported on elastic foundation in the boundaries of which proper-

ties of the beam and foundation change it values continuously or constant [1-6]. At the same time, it leads to solving of Cauchy problem for system of ordinary differential equations with variables parameters. Besides boundary conditions, solving of these equations requires accepting continuity conditions for coefficients in the discontinuity points of the first order (conjunction of sections). For many sections, such approach is laborious since it leads to a large number *N* of equations for determining of integration constants ($N = 4n$, where *n* is sections' number). In this case, the initial parameters' method (IPM) becomes effective [7-10]. The method allows to obtain dimension less analytical solutions to static and dynamic problems. These solutions are universal for different types of boundary conditions and number of sections since it always leads to equations' system of second order. It is conveniently to apply the IPM procedure in addition with state vectors for an arbitrary cross section of a beam and matrixes of initial cross section affecting to arbitrary cross section [6, 8, 9, 11-14].

This paper presents the first part of investigation of dynamic interaction of a continuous footing with foundation under it. The continuous footing is simulated as an elastic flexible Bernoulli-Euler beam of finite length and elastic foundation under it. Despite a large number of literature to problems linked with rod systems supported on different types of foundation, there is not advanced analysis of the case, when statically loaded system during operation loss it foundation or its part. In according to Structural Mechanics, constructively nonlinear system appears un this case. This process causes appearing of additional dynamic forces in the system. While not all accidental impacts are classified and reactions of structural elements are not investigated enough. Since, the present study is actual, theoretically interesting and practically significant.

The first part of the problem for constructing and investigating of the mathematic models of dynamic transmitting processes into loaded beam at sudden foundation damage (partial failure) is analysis of stress-strain state of loaded beam at quasi-static failure of the supporting foundation part. The case of entire foundation failure is not considered because it deletes the subject of investigation.

Solutions to static problems are used further to formulate initial conditions for dynamic problems and for comparison of stress-strain state before and after appearing of a damage.

2. MATHEMATIC MODEL

2.1. Cantilever beam partially supported on Winkler foundation.

Beam of *l* length, of cross section area *A* and axial inertia moment *I*, made of material of ρdensity and with elasticity modulus *E* supports partially on elastic Winkler foundation of *k* stiffness (Figure 1.1).

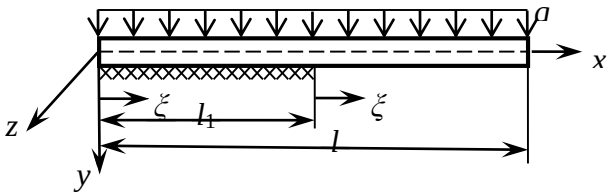

Figure 2.1. Calculational model for a beam partially supported on elastic foundation.

The length of the first section is l_1. Let us assume that beam's ends with coordinates $x = 0$ and $x = l$ are free. The beam is loaded along the span with evenly distributed load *q*. It is formulated the problem for determining of deflections and bending moments in dependence to length of the supported section. Beam is considered as a composite one after foundation failure and consists of two homogeneous sections supported on a step foundation of partially constant stiffness: $k_1 = k$ and $k_2 = 0$. We construct solution to this problem separately for each section using local coordinates x_i, y_i, z_i $(i = 1, 2)$: x_i is longitudinal axis, y_i and z_i is main central inertia axis of the cross section. When we chose the origin point at initial cross section of each section, the

continuity condition for solution to this problem means that state of the end cross section of previous section is the initial for the next one. Let us introduce dimensionless coordinates and parameters

$$\xi_i = \frac{x_i}{l},\ w_i = \frac{v_i}{l},\ (i = 1,2)$$

– deflection of the beam;

$$v = \frac{l_1}{l}$$

– relative length of the supported part of the beam;

$$\overline{q} = \frac{ql^3}{EI}$$

– external load;

$$\alpha = \sqrt[4]{\frac{kl^4}{4EI}}$$

– generalized stiffness parameter of a system "beam – foundation".

Consider the successive bending of each section.

2.2. Bending of the first section $0 \le \xi_1 \le v$.

Solution to bending equation

$$\frac{d^4 w_1}{d\xi_1^4} + 4\alpha w_1 = \overline{q}, \qquad (2.1)$$

expressed through the initial parameters of this section

$$w_{10} = w_1(0), w'_{10} = w'_1(0), w''_{10} = w''_1(0), w'''_{10} = w'''_1(0)$$

takes the form [6, 12, 13]

$$w_1(\xi_1) = \frac{\overline{q}}{4\alpha^4}(1 - K_4(\alpha\xi_1)) + w_{10}K_4(\alpha\xi_1) + w'_{10}K_3(\alpha\xi_1) + w''_{10}K_2(\alpha\xi_1) + w'''_{10}K_1(\alpha\xi_1),$$

where $K_i(\alpha\xi_1)$ is Krylov function [7, 14]:

$$K_1 = \frac{\sin\alpha\xi_1 ch\alpha\xi_1 - \cos\alpha\xi_1 sh\alpha\xi_1}{4\alpha^3}, K_2 = K'_1,$$

$$K_3 = K'_2, K_4 = K'_3, K_1 = \frac{1}{4\alpha 4}K'_4$$

State of an arbitrary cross section of the first segment of the beam can be expressed by matrix equation

$$\overline{w}_1 = V_1(\xi_1)\overline{W}_{10} + \overline{q}\,\overline{V}_{1q}(\xi_1), \qquad (2.2)$$

where $\overline{w}_1(\xi_1) = \{w_1(\xi_1)\ w'_1(\xi_1)\ w''_1(\xi_1)\ w'''_1(\xi_1)\}^T$ is state vector for an arbitrary cross section ξ_1 of the first section; $\overline{W}_{10} = \{w_{10}\ w'_{10}\ w''_{10}\ w'''_{10}\}^T$ – vector of initial parameters of the first section;

$$V_1(\xi_1)_{4\times 4} = \begin{pmatrix} K_4(\alpha\xi_1) & K_3(\alpha\xi_1) & K_2(\alpha\xi_1) & K_1(\alpha\xi_1) \\ -4\alpha^4 K_1(\alpha\xi_1) & K_4(\alpha\xi_1) & K_3(\alpha\xi_1) & K_2(\alpha\xi_1) \\ -4\alpha^4 K_2(\alpha\xi_1) & -4\alpha^4 K_1(\alpha\xi_1) & K_4(\alpha\xi_1) & K_3(\alpha\xi_1) \\ -4\alpha^4 K_3(\alpha\xi_1) & -4\alpha^4 K_2(\alpha\xi_1) & -4\alpha^4 K_1(\alpha\xi_1) & K_4(\alpha\xi_1) \end{pmatrix}$$ – matrix of initial parameters of the first section affecting to state of section ξ_1 of this section;

$$\overline{V}_{1q}(\xi_1) = \left\{\frac{1 - K_4(\alpha\xi_1)}{4\alpha^4} \quad K_2(\alpha\xi_1) \quad K_2(\alpha\xi_1) \quad K_3(\alpha\xi_1)\right\}^T$$ – vector of forces for the first section.

2.3. Bending of the second section

$0 \le \xi_2 \le 1-\nu$.

Flexure of this section can be expressed by equation

$$\frac{d^4 w_2}{d\xi_2^4} = \bar{q}, \tag{2.3}$$

general solution to which in the form of the initial parameters' method should be written as [6]

$$w_2(\xi_2) = \frac{\bar{q}\xi_2^4}{24} + w_{20} + w'_{20}\xi_2 + w''_{20}\frac{\xi_2^2}{2} + w'''_{20}\frac{\xi_2^3}{6}$$

or in the matrix form

$$\overline{w}_2(\xi_2) = V_2(\xi_2)\overline{W}_{20} + \bar{q}\,\overline{V}_{2q}, \tag{2.4}$$

where

$$\overline{w}_2(\xi_2) = \{w_2(\xi_2)\ w'_2(\xi_2)\ w''_2(\xi_2)\ w'''_2(\xi_2)\}^T$$

– state vector of an arbitrary cross section ξ_2 of the second section;

$$\overline{W}_{20} = \{w_{20}\ w'_{20}\ w''_{20}\ w'''_{20}\}^T$$

– vector of initial parameters for the second section;

$$V_{2\,4\times4}(\xi_2) = \begin{pmatrix} 1 & \xi_2 & \frac{\xi_2^2}{2} & \frac{\xi_2^3}{6} \\ 0 & 1 & \xi_2 & \frac{\xi_2^2}{2} \\ 0 & 0 & 1 & \xi_2 \\ 0 & 0 & 0 & 1 \end{pmatrix}$$

– matrix of initial parameters for second section affecting to state of a cross section ξ_2 of this segment;

$$\overline{V}_{2q}(\xi_2) = \left\{\frac{\xi_2^4}{24}\quad \frac{\xi_2^3}{6}\quad \frac{\xi_2^2}{2}\quad \xi_2\right\}^T$$

– force vector for the second segment.

2.4. Conjunction condition for segments.

Conjunction condition of segments can be expressed in matrix form as equality of vectors

$$\overline{w}_1(\nu) = \overline{w}_2(0), \tag{2.5}$$

From equation (2.2) for $\xi_1 = \nu$ it follows

$$\overline{w}_1(\nu) = V_1(\nu)\overline{W}_{10} + \bar{q}\,\overline{V}_{1q}(\nu), \tag{2.6}$$

and from equation (2.4) for $\xi_2 = 0$, we obtain

$$\overline{w}_2(0) = \overline{W}_{20} \tag{2.7}$$

since the matrix $V_2(0)$ is singular, and vector $\overline{V}_{2q}(0) = \overline{0}$. Substituting (2.6) and (2.7) into (2.5), we obtain expression of initial parameters for the second segment through initial parameters of the first segment

$$\overline{W}_{20} = V_1(\nu)\overline{W}_{10} + \bar{q}\,\overline{V}_{1q}(\nu).$$

Then from equation (2.4), it follows

$$\begin{aligned} &\overline{w}_2(\xi_2) = V_{21}(\xi_2;\nu)\overline{W}_{10} + \\ &+ \bar{q}\left(\overline{V}_{21q}(\xi_2;\nu) + \overline{V}_{2q}(\xi_2)\right), \end{aligned} \tag{2.8}$$

where

$$V_{21\,4\times4} = V_2(\xi_2)V_1(\nu)$$

– affecting matrix of initial parameters for the first segment to state of an arbitrary cross section ξ_2 of the second segment;

$$\overline{V}_{21q} = V_2(\xi_2)\overline{V}_{1q}(\nu)$$

– vector of additional loads for the second segment.

Thus, state of both segments of the beam is expressed through initial parameters of the first segment. Two parameters are known in advance from condition for the left end of the beam $(\xi_1 = 0)$. The next two unknown parameters can be determined from conditions at the right end of the beam for

$$\xi_2 = 1 - \nu.$$

2.5. Determination of unknown initial parameters.

Let us write matrix equation (2.8) in the extended form

$$\begin{pmatrix} w_2(\xi_2) \\ w_2'(\xi_2) \\ w_2''(\xi_2) \\ w_2'''(\xi_2) \end{pmatrix} = \begin{pmatrix} 1 & \xi_2 & \frac{\xi_2^2}{2} & \frac{\xi_2^3}{6} \\ 0 & 1 & \xi_2 & \frac{\xi_2^2}{2} \\ 0 & 0 & 1 & \xi_2 \\ 0 & 0 & 0 & 1 \end{pmatrix} \begin{pmatrix} K_4(\alpha\xi_1) & K_3(\alpha\xi_1) & K_2(\alpha\xi_1) & K_1(\alpha\xi_1) \\ -4\alpha^4 K_1(\alpha\xi_1) & K_4(\alpha\xi_1) & K_3(\alpha\xi_1) & K_2(\alpha\xi_1) \\ -4\alpha^4 K_2(\alpha\xi_1) & -4\alpha^4 K_1(\alpha\xi_1) & K_4(\alpha\xi_1) & K_3(\alpha\xi_1) \\ -4\alpha^4 K_3(\alpha\xi_1) & -4\alpha^4 K_2(\alpha\xi_1) & -4\alpha^4 K_1(\alpha\xi_1) & K_4(\alpha\xi_1) \end{pmatrix} \begin{pmatrix} w_{10} \\ w_{10}' \\ w_{10}'' \\ w_{10}''' \end{pmatrix} +$$

$$+ \bar{q} \left[\begin{pmatrix} 1 & \xi_2 & \frac{\xi_2^2}{2} & \frac{\xi_2^3}{6} \\ 0 & 1 & \xi_2 & \frac{\xi_2^2}{2} \\ 0 & 0 & 1 & \xi_2 \\ 0 & 0 & 0 & 1 \end{pmatrix} \begin{pmatrix} \frac{1 - K_4(\alpha\nu)}{4\alpha^4} \\ K_1(\alpha\nu) \\ K_2(\alpha\nu) \\ K_3(\alpha\nu) \end{pmatrix} + \begin{pmatrix} \frac{\xi_2^4}{24} \\ \frac{\xi_2^3}{6} \\ \frac{\xi_2^2}{2} \\ \xi_2 \end{pmatrix} \right] \tag{2.9}$$

In order to further construction, it is need to take in account restraints at the ends of the beam. Then boundary conditions take the form In order to further construction, it is need to take in account restraints at the ends of the beam. Then boundary conditions take the form

$$\begin{aligned} w_1''(0) &= w_1'''(0) = 0 \\ w_2''(1-\nu) &= w_2'''(1-\nu) = 0 \end{aligned} \tag{2.10}$$

From the first two conditions (2.10), it follows

$$w_{10}'' = w_{10}''' = 0.$$

From the second group of conditions (2.10) using equation (2.9), we obtain parameters w_{10} and w_{10}', as solutions to the system of algebraic equations

$$\begin{cases} \left(K_2(\alpha\nu) + (1-\nu)K_3(\alpha\nu)\right)w_{10} + \\ + \left(K_1(\alpha\nu) + (1-\nu)K_2(\alpha\nu)\right)w_{10}' = \\ = \dfrac{\bar{q}}{4\alpha^4}\left(K_2(\alpha\nu) + (1-\nu)K_3(\alpha\nu) + \left(\dfrac{(1-\nu)^2}{2}\right)\right) \\ K_3(\alpha\nu)w_{10} + K_2(\alpha\nu)w_{10}' = \\ = \dfrac{\bar{q}}{4\alpha^4}\left(K_3(\alpha\nu) + 1 - \nu\right) \end{cases}$$

From where we obtain

$$w_{10} = \frac{\bar{q}}{4\alpha^4}\left(1 - \frac{(1-\nu)K_1(\alpha\nu) + \dfrac{(1-\nu)^2}{2}K_2(\alpha\nu)}{K_2^2(\alpha\nu) - K_1(\alpha\nu)K_3(\alpha\nu)}\right)$$

$$w_{10}' = \frac{\bar{q}}{4\alpha^4} \cdot \frac{(1-\nu)K_2(\alpha\nu) + \dfrac{(1-\nu)^2}{2}K_3(\alpha\nu)}{K_2^2(\alpha\nu) - K_1(\alpha\nu)K_3(\alpha\nu)}$$

In accordance with matrix equation (2.2), deflections $w_1(\xi_1)$ and bending moments $w_1''(\xi_1)$ in an arbitrary section ξ_1 of the first segment are determined by functions

$$w_1(\xi_1) = K_4(\alpha\xi_1)w_{10} + K_3(\alpha\xi_1)w'_{10} + \\ + \frac{\bar{q}}{4\alpha^4}(1 - K_4(\alpha\xi_1)), \qquad (2.11)$$

$$w_1(\xi_1) = -4\alpha^4(K_2(\alpha\xi_1)w_{10} + \\ + K_1(\alpha\xi_1)w'_{10}) + \bar{q}\,K_2(\alpha\xi_1). \qquad (2.12)$$

Deflections $w_2(\xi_2)$ and bending moments $w_2''(\xi_2)$ in an arbitrary cross section ξ_2 $w_2(\xi_2)$ of the second segment are determined by functions from matrix equation (2.8)

$$w_2(\xi_2) = C_0 + C_1\xi_2 + C_2\xi_2^2 + \\ + C_3\xi_2^3 + C_4\xi_2^4, \qquad (2.13)$$

$$w_2''(\xi_2) = 2C_2 + 6C_3\xi_2 + 12C_4\xi_2^2, \qquad (2.14)$$

where

$$C_0 = K_4(\alpha v)w_{10} + K_3(\alpha v)w'_{10} + \frac{\bar{q}}{4\alpha^4}(1 - K_4(\alpha v));$$

$$C_1 = -4\alpha^4 K_1(\alpha v)w_{10} + K_4(\alpha v)w'_{10} + \bar{q}\,K_1(\alpha v);$$

$$C_2 = -2\alpha^4 K_2(\alpha v)w_{10} - 2\alpha^4 K_1(\alpha v)w'_{10} + \\ + \frac{\bar{q}}{2}K_2(\alpha v);$$

$$C_3 = -\frac{2}{3}\alpha^4 K_3(\alpha v)w_{10} - \frac{2}{3}\alpha^4 K_2(\alpha v)w'_{10} + \\ + \frac{\bar{q}}{6}K_3(\alpha v);$$

$$C_4 = \frac{\bar{q}}{24}.$$

2.6. Numerical results.

Using Maple we carried out calculation of dimension less deflections $w(\xi)$ and bending moments $w''(\xi)$ for a beam, partially supported on elastic foundation and loaded with evenly distributed load $\bar{q} = 1$. Calculations are performed for different values of generalized stiffness parameter α of a system "beam – foundation" in order to determine influence of damage value (length of failure part of foundation) to stress-strain state of the beam at increasing such damage from one of end cross sections of this beam. Figures 2.2-2.6 and Table 2.1 present such calculation results.

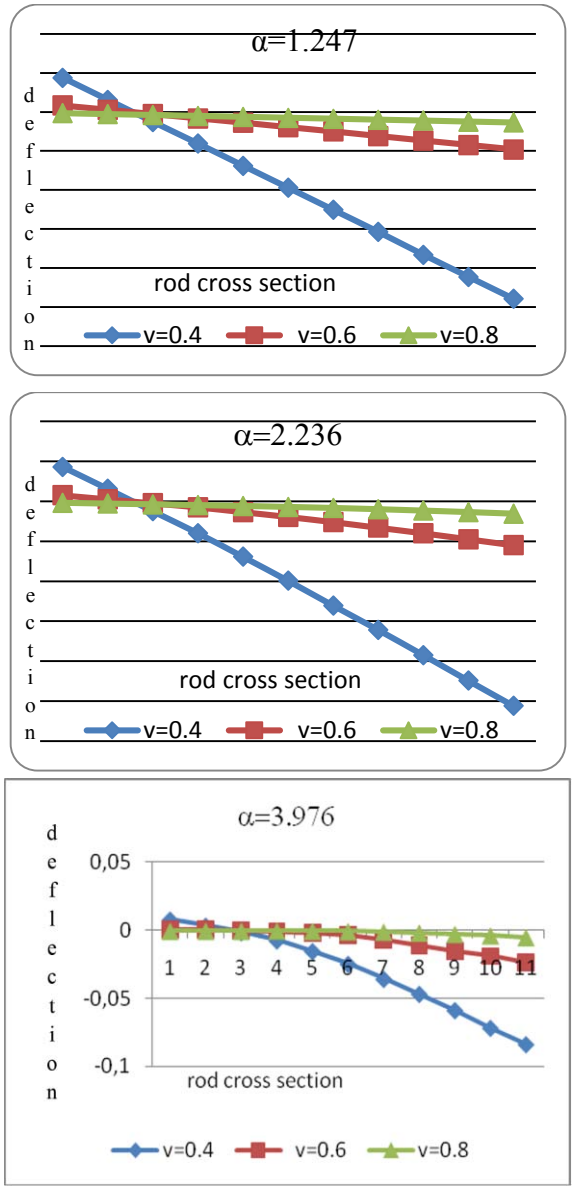

Figure 2.2. Diagrams for comparison deflections of the beam at length decreasing of supported part of the beam.

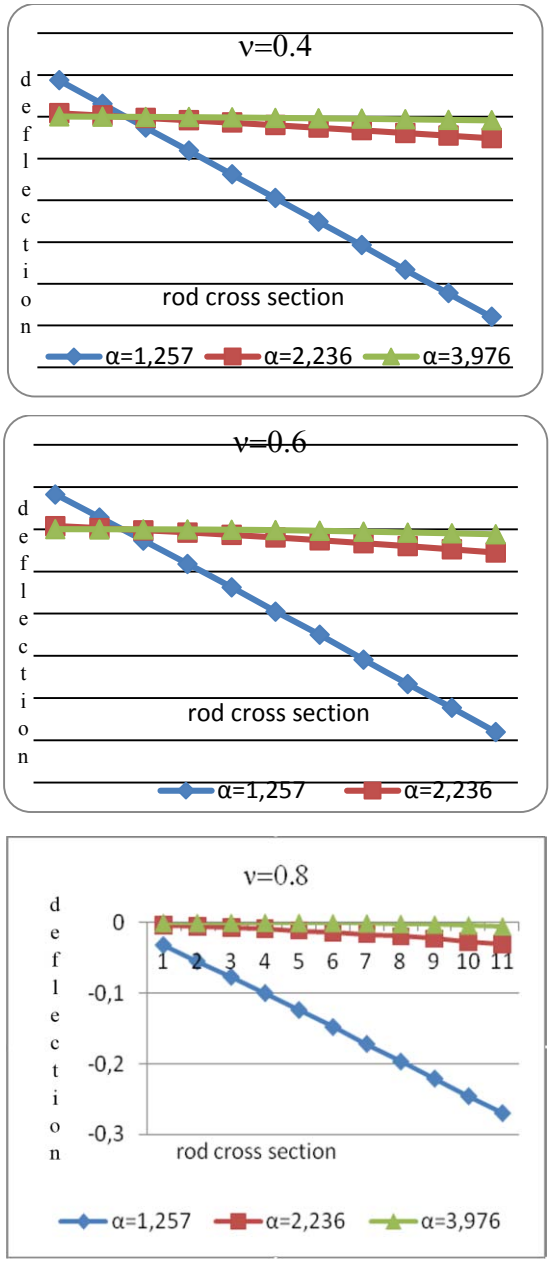

Figure 2.3. Diagrams for comparison of deflections at constant damage sizes.

Figure 2.2 shows diagrams for comparison deflections of the beam when supported part of the beam decreases for values $\nu = 0{,}8; 0{,}6; 0{,}4$ (or, respectively, damage length increases for values $1-\nu = 0{,}2; 0{,}4; 0{,}6$) for three values of α parameter of generalized stiffness of a system "beam - foundation": $\alpha = 1{,}275; 2{,}236; 3{,}976$.

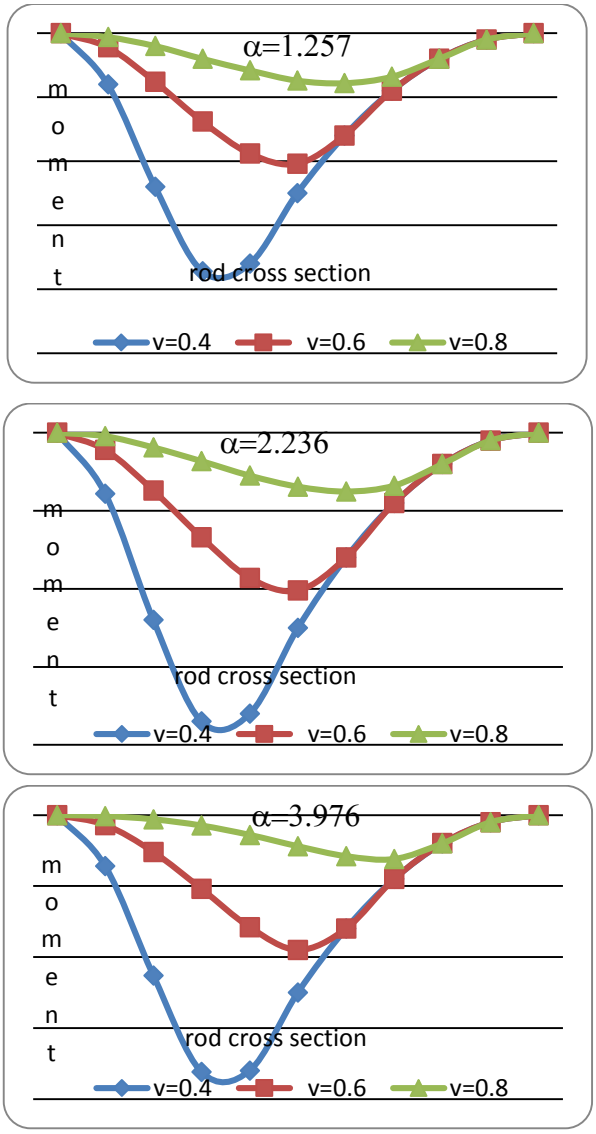

Figure 2.4. Diagrams of bending moments for different combinations of stiffness variants α.

Figure 2.3 shows comparison of diagrams of deflections at constant values of damage length $1-\nu = 0{,}2; 0{,}4; 0{,}6$ for different generalized stiffness of a system "beam – foundation": $\alpha = 1{,}275; 2{,}236; 3{,}976$. Let us note that in accordance with Winkler model, a free beam entirely supported on foundation ($\nu = 1$) and loaded with evenly distributed load $\bar{q}$, moves in parallel itself without flexure for value $\bar{q}/4\alpha^4$.

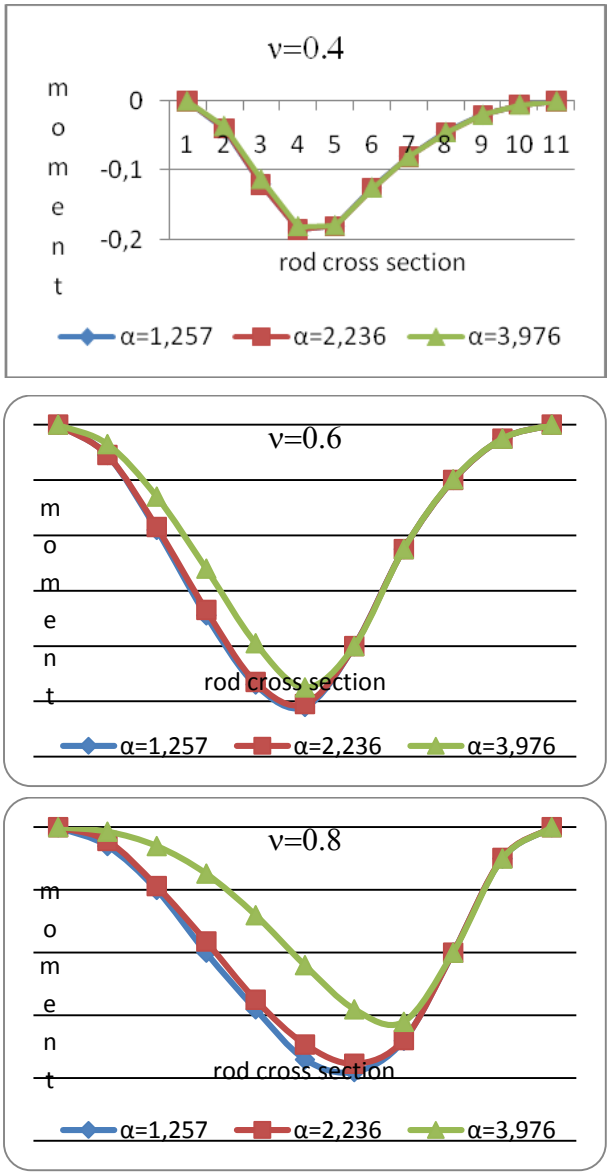

Figure 2.5. Diagrams of bending moments for different combinations of damage sizes $(1-v)$.

Diagrams' character for all variants of system stiffness α and damage sizes v is similar: maximum deflections increase with increasing length of cantilever part for constant system stiffness, and it decreases for large values of stiffness for constant length of cantilever.

Figures 2.4 and 2.5 presents diagrams of bending moments for different combinations of stiffness α and damage values $1-v$.

The maximum moment for all cases arises in the supported part of the beam and moves to the left end of the beam at damage increasing. Value of maximum moment for all stiffness variants α significantly depends on the damage value

$$(1-v): w_{\max_{1-v=0,6}} \geq w_{\max_{1-v=0,4}} \geq w_{\max_{1-v=0,2}}$$

(Figure 2.4) and does not depend on system stiffness α for constant length of damaged part $(1-v)$ (Figure 2.5).

Table 2.1 presents values of maximum deflections and bending moments for considered stiffness variants of a system "beam – foundation" and sizes of supported part of the beam v.

Let us present an example of a system "beam – foundation", the generalized stiffness of which takes the value $\alpha = 3{,}976$. It is reinforced concrete beam of l = 6.7 m length with rectangular cross section and sizes b = 0.25 m (width), h = 0.18 m (height), A = 0.045 m^2 is area of cross section. Inertia moment of cross section is $I = 1{,}215 \cdot 10^{-4}$ m^4. Elasticity modulus for beam material is $E = 3.05 \cdot 10^{10}$ N/m^2. Foundation material is gravel with modulus k_1 = 75 MPa/m. Module of subgrade reaction $k = k_1 b = 1{,}875 \cdot 10^6$ Pa. Then parameter is $\alpha = 3{,}976$. Increasing (decreasing) of th is parameter can be linked with increasing (decreasing) of foundation stiffness k_1 (for constant flexural stiffness of a beam), whether decreasing (increasing) of flexural stiffness EI of a beam (for constant foundation stiffness).

3. Partially supported beam with two supporting segments.

3.1. Formulation and solution to the problem.

Here we formulate similar problem for the beam, foundation and load as it was above. The difference is that the internal part of the beam does not support on foundation (Figure 3.1). We consider the beam as a composite structure.

Table 2.1. Maximum deflections and bending moments.

Parameter	Deflections				Bending moments			
α \ v	1	0,8	0,6	0,4	1	0,8	0,6	0,4
1,257	0,1	0,197	0,961	4,79	0	0,039	0,102	0,19
2,236	0,01	0,031	0,11	0,512	0	0,038	0,101	0,19
3,976	0,001	0,0057	0,0236	0,084	0	0,032	0,095	0,19

This one consists of three homogenous segments supported on step foundation with partially constant stiffness: $k_1 = k_3 = k,\ k_2 = 0$.

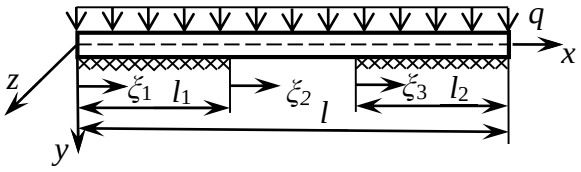

Figure 3.1. Calculation scheme of partially supported beam with two supporting segments.

Let us introduce dimensionless variables and parameters

$$\xi_i = \frac{x_i}{l};\ w_i = \frac{v_i}{l}(i = 1,2,3),\ v_1 = \frac{l_1}{l},\ v_2 = \frac{l_2}{l}$$

Deflection for the first segment $(0 \le \xi_1 \le v_1)$ and the third segment $(0 \le \xi_3 \le v_2)$ are described by solution (2.2) to equation (2.1), and state of cross sections ξ_1 and ξ_3 is described by matrix equation respectively:

$$\overline{w}_1(\xi_1) = V_1(\xi_1)\overline{W}_{10} + \overline{q}\,\overline{V}_{1q}(\xi_1), \qquad (3.1)$$

$$\overline{w}_3(\xi_3) = V_1(\xi_3)\overline{W}_{30} + \overline{q}\,\overline{V}_{1q}(\xi_3), \qquad (3.2)$$

and for the second segment $(0 \le \xi_2 \le 1 - v_1 - v_2)$ it is described by solution (2.4) to equation (2.3). State of a cross section ξ_2 of the second segment

$$\overline{w}_2(\xi_2) = V_2(\xi_2)\overline{W}_{20} + \overline{q}\,\overline{V}_{2q}(\xi_2), \qquad (3.3)$$

Using conjunction conditions for segments: first and second

$$\overline{w}_1(v_1) = \overline{w}_2(0).$$

And second with third

$$\overline{w}_2(1 - v_1 - v_2) = \overline{w}_3(0).$$

We express initial parameters of the second and third segments through the initial parameters of the first segment

$$\overline{w}_{20} = V_1(v_1)\overline{W}_{10} + \overline{q}\,\overline{V}_{1q}(v_1), \qquad (3.4)$$

and

$$\overline{w}_{30} = V_2(1 - v_1 - v_2)V_1(v_1)\overline{W}_{10} + \\ + \overline{q}\left[V_2(1 - v_1 - v_2)\overline{V}_{1q}(v_1) + \overline{V}_{2q}(1 - v_1 - v_2)\right] \qquad (3.5)$$

Substituting (3.4) and (3.5) to formulas (3.2) and (3.3) respectively, we obtain expression for state vector of all segments through the initial parameters of the first segment (two parameters are known: $w''_{10} = w'''_{10} = 0$).

$$\overline{w}_2(\xi_2) = V_2(\xi_2)V_1(v_1)\overline{W}_{10} + \\ + \overline{q}\left[V_2(\xi_2)\overline{V}_{1q}(v_1) + \overline{V}_{2q}(\xi_2)\right] \qquad (3.6)$$

$$\overline{w}_3(\xi_3) = V_1(\xi_3)V_2(1 - v_1 - v_2)V_1(v_1)\overline{W}_{10} + \\ + \overline{q}\left[V_1(\xi_3)V_2(1 - v_1 - v_2)\overline{V}_{1q}(v_1) + \right. \\ \left. + V_1(\xi_3)\overline{V}_{2q}(1 - v_1 - v_2) + \overline{V}_{1q}(\xi_3)\right]. \qquad (3.7)$$

Further, using matrix representation of state vectors for three segments (3.1), (3.6), (3.7), boundary conditions

$$w_1''(0)=w_1'''(0)=0$$
$$w_3''(v_2)=w_3'''(v_2)=0 \qquad (3.8)$$

And extended form of the equation (3.7) (similar to equation (2.9)), we obtain, satisfying to the second condition pair (3.8), system of equations for determining initial parameters w_{10} and w'_{10}:

$$\begin{cases} -4\alpha^4\left(K_2(\alpha v_2)(Z_1+Y_1+U_1)+K_1(\alpha v_2)(Z_2+Y_2+U_2)\right)+K_4(\alpha v_2)(Z_3+Y_3+U_3)+ \\ \qquad +K_3(\alpha v_2)(Z_4+Y_4+U_4)+K_2(\alpha v_2)=0 \\ -4\alpha^4\left(K_3(\alpha v_2)(Z_1+Y_1+U_1)+K_2(\alpha v_2)(Z_2+Y_2+U_2)\right)+K_1(\alpha v_2)(Z_3+Y_3+U_3)+ \\ \qquad +K_4(\alpha v_2)(Z_4+Y_4+U_4)+K_3(\alpha v_2)=0 \end{cases} \qquad (3.9)$$

Further, we determine deflection for segments

$$w_1(\xi_1)=K_4(\alpha\xi_1)w_0+K_3(\alpha\xi_1)w'_0+q\frac{1-K_4(\alpha\xi_1)}{4\alpha^4} \qquad (3.10)$$

$$w_2(\xi_2)=\left(K_4(\alpha v_1)-4\alpha^4\left(\xi_2K_1(\alpha v_1)+\frac{\xi_2^2}{2}K_2(\alpha v_1)+\frac{\xi_2^3}{6}K_3(\alpha v_1)\right)\right)w_0+$$
$$+\left(K_3(\alpha v_1)+\xi_2K_4(\alpha v_1)-4\alpha^4\left(\frac{\xi_2^2}{2}K_1(\alpha v_1)+\frac{\xi_2^3}{6}K_2(\alpha v_1)\right)\right)w'_0+ \qquad (3.11)$$
$$+\overline{q}\left(\frac{1-K_4(\alpha v_1)}{4\alpha^4}+\xi_2K_1(\alpha v_1)+\frac{\xi_2^2}{2}K_2(\alpha v_1)+\frac{\xi_2^3}{6}K_3(\alpha v_1)+\frac{\xi_2^4}{24}\right)$$

$$w_3(\xi_3)=K_4(\alpha\xi_3)Z_1+K_3(\alpha\xi_3)Z_2+K_2(\alpha\xi_3)Z_3+K_1(\alpha\xi_3)Z_4+$$
$$+\overline{q}\left(\begin{array}{l}K_4(\alpha\xi_3)Y_1+K_3(\alpha\xi_3)Y_2+K_2(\alpha\xi_3)Y_3+K_1(\alpha\xi_3)Y_4+\\ +K_4(\alpha\xi_3)U_1+K_3(\alpha\xi_3)U_2+K_2(\alpha\xi_3)U_3+K_1(\alpha\xi_3)U_4+\frac{1-K_4(\alpha\xi_3)}{4\alpha^4}\end{array}\right); \qquad (3.12)$$

where

$$Z_1=w_{10}\left(K_4(\alpha v_1)-4\alpha^4\left(U_4K_1(\alpha v_1)+U_3K_2(\alpha v_1)+U_2K_3(\alpha v_1)\right)\right)+$$
$$+w'_{10}\left(K_3(\alpha v_1)+U_4K_4(\alpha v_1)-4\alpha^4\left(U_3K_1(\alpha v_1)+U_2K_2(\alpha v_1)\right)\right);$$
$$Z_2=-4\alpha^4w_{10}\left(K_1(\alpha v_1)+U_4K_2(\alpha v_1)+U_3K_3(\alpha v_1)\right)+$$
$$+w'_{10}\left(K_4(\alpha v_1)-4\alpha^4\left(U_4K_1(\alpha v_1)+U_3K_2(\alpha v_1)\right)\right);$$
$$Z_3=-4\alpha^4\left(w_{10}\left(K_2(\alpha v_1)+U_4K_3(\alpha v_1)\right)+\right.$$
$$\left.+w'_{10}\left(K_1(\alpha v_1)+U_4K_2(\alpha v_1)\right)\right);$$
$$Z_4=-4\alpha^4\left(w_{10}K_3(\alpha v_1)+w'_{10}K_2(\alpha v_1)\right);$$

$$Y_1=\frac{1-K_4(\alpha v_1)}{4\alpha^4}+U_4K_1(\alpha v_1)+U_3K_2(\alpha v_1)+U_2K_3(\alpha v_1);$$
$$Y_2=K_1(\alpha v_1)+U_4K_2(\alpha v_1)+U_3K_3(\alpha v_1);$$
$$Y_3=K_2(\alpha v_1)+U_4K_3(\alpha v_1);$$
$$Y_4=K_3(\alpha v_1);$$

$$U_1=\frac{(1-v_1-v_2)^4}{24};U_2=\frac{(1-v_1-v_2)^3}{6};$$
$$U_3=\frac{(1-v_1-v_2)^2}{2};\ U_4=1-v_1-v_2.$$

3.2. Numerical results.

Using Maple, we provide calculations of dimension less deflections $w(\xi)$ and bending moments $w''(\xi)$ for beam supported on elastic foundation and loaded with evenly distributed static load $\overline{q}=1$ for different combinations of mechanical and geometric characteristic of a system "beam – foundation". At the same time, the middle part does not support on foundation in contrast with mentioned above case. For all cases end soft he beam are free and value of evenly distributed dimensionless load is $\overline{q}=1$. Figures 3.2 – 3.8 present calculation results as relative diagrams.

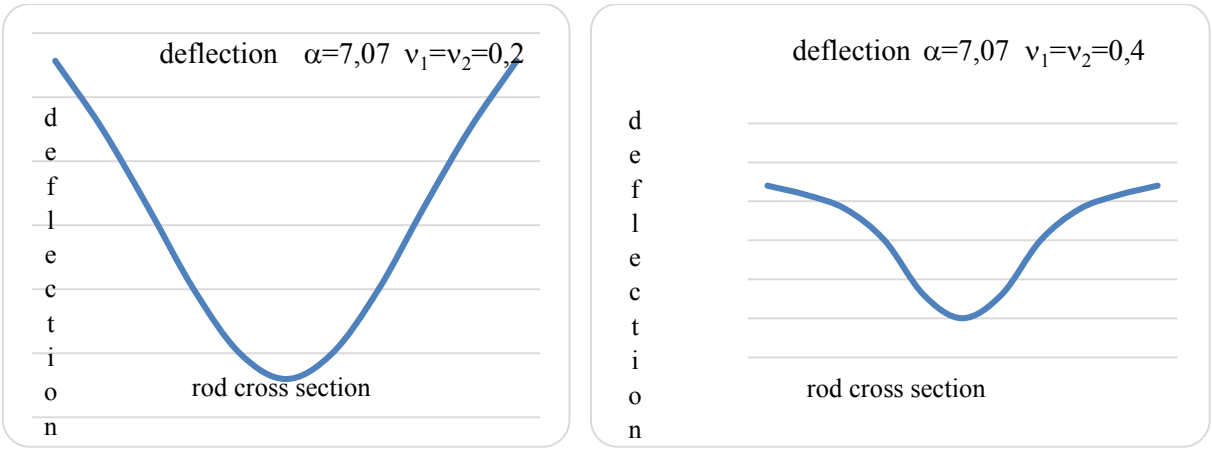

Figure 3.2. Beam deflection for system stiffness value $\alpha = 7{,}07$.

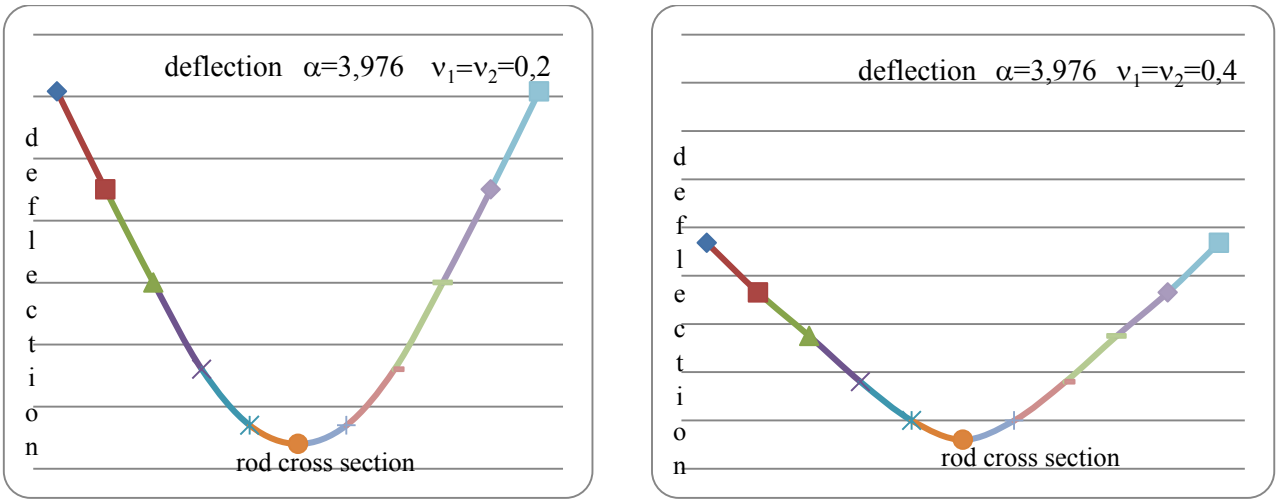

Figure 3.3. Deflections of the beam for system stiffness value $\alpha = 3{,}976$.

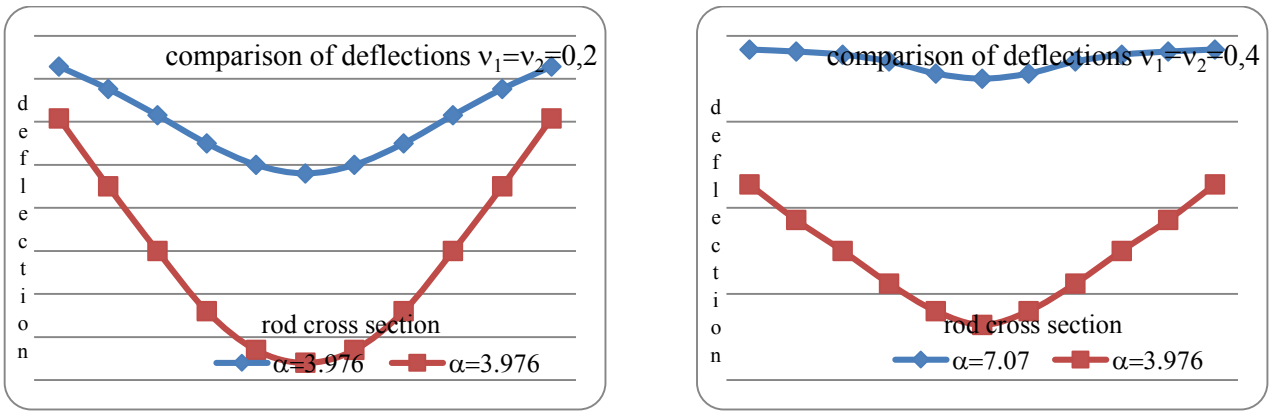

Figure 3.4. Comparison of deflections by attribute of damage length Δ.

Figures 3.2-3.4 show diagrams of beam deflections for symmetric location of supported section of equal length $(v_1 = v_2)$ and different values of free segment length simulating damage $\Delta = 1 - v_1 - v_2$ for two values of generalized stiffness of a system "beam – foundation": $\alpha = 7{,}07;\ 3{,}976$. Figure 3.2 shows diagrams of deflection for system stiffness value $\alpha = 7{,}07$.

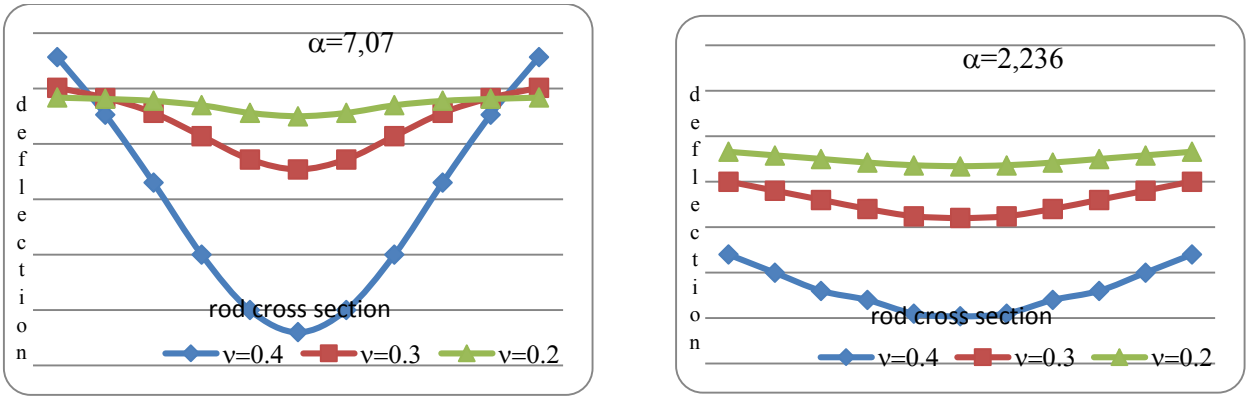

Figure 3.5. Comparison of deflections by attribute of generalized stiffness.

Let us note that relatively to parameter α of generalized stiffness of a system "beam – foundation" its value $\alpha = 7{,}07$ corresponds, for example, to reinforced concrete beam with length of $l = 6{,}7$ m, rectangular cross section with sides: width $b = 0.25$ m, height $h = 0.18$ m, inertia moment of a cross section is $I = 1{,}215 \cdot 10^{-4}\text{m}^4$, Yung modulus is $E = 3.05 \cdot 10^{10}\text{N/m}^2$. The beam supports on ballast layer of crushed stones with modulus $k_1 = 7.5$ MPa/m. Module of subgrade reaction is $k = k_1 b = 1{,}875 \cdot 10^6$ Pa. At the same time

$$\alpha = \sqrt[4]{\frac{kl^4}{4EI}} = 7{,}07 .$$

Increasing (decreasing) of parameter α value for given length of the beam may be reached, for example, at increasing (decreasing) of foundation stiffness k (for constant beam stiffness EI), whether with decreasing (increasing) of flexural stiffness of a beam EI (for constant foundation stiffness k). Figure 3.3 presents deflections of the beam for system stiffness value $\alpha = 3{,}976$.

In order to compare, Figure 3.4 presents diagrams of deflections in relation with damage length Δ for different values of system stiffness α.

In order to compare, Figure 3.5 presents diagrams of deflection for attribute of generalized system stiffness for different values of damage length Δ.

Figure 3.6 shows diagram of beam deflections for system with high generalized stiffness $\alpha = 9{,}236$ for damages section length Δ=0,4.

Figure 3.7 presents comparison of diagrams of bending moments by attribute of damaged section length for generalized stiffness $\alpha = 2{,}236$.

Figure 3.8 shows diagrams of deflections and bending moments for the case of non-symmetric sections' location and non-equal length of it.

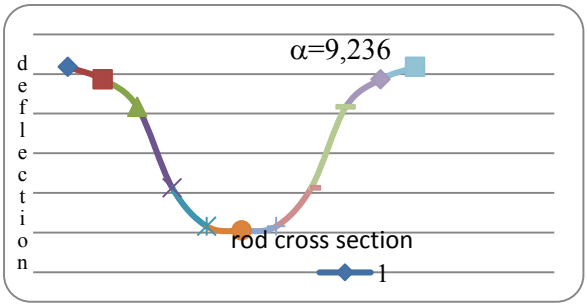

Figure 3.6. Diagram of beam deflection for high generalized stiffness $\alpha = 9{,}236$.

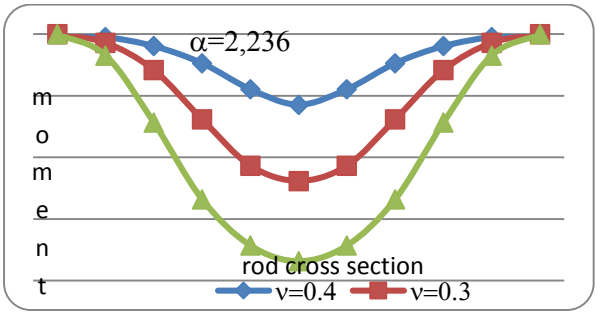

Figure 3.7. Diagrams of bending moments for $\alpha = 2{,}236$.

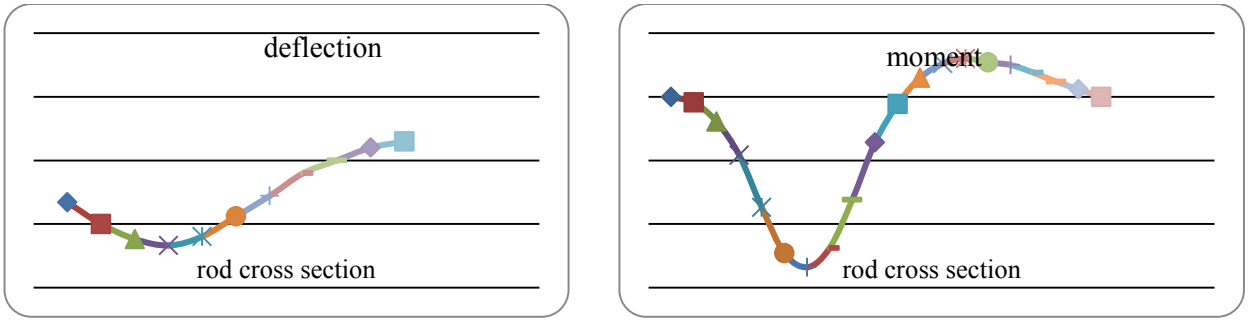

Figure 3.8. Diagrams of deflections and bending moments for $\alpha = 3{,}976$, $v_1 = 0{,}2$ *and* $v_2 = 0{,}6$ $(\Delta = 0{,}2)$.

Numerical analysis shows that character and values of deflections and bending moments for symmetrically supported beams significantly depend on damage value $\Delta = 1 - v_1 - v_2$ and generalized stiffness of system "beam foundation". For all values of stiffness from considered range $2{,}236 \le \alpha \le 7{,}07$ and damage sizes $0{,}2 \le \Delta \le 0{,}6$, deflection functions are convex (diagrams of deflections are plotted in tension zones). For high values of generalized stiffness $\alpha > 7{,}07$ and large damages $\Delta > 0{,}6$, inflections appear and deflection changes it direction. Values of maximum deflections increase for all stiffness values (Figures 3.3, 3.4). For supported segments of different length (Figure 3.8), moments change it sign (diagram in Figure 3.8,b is plotted in tension zones).

CONCLUSIONS

Suggested mathematic deformation model for beam partially supported on elastic foundation is constructed using the initial parameters' method and allows to obtain dimensionless analytical solution to quasi-static universal problems for different variant of boundary conditions at sudden appearing of foundation damage (partial foundation failure).

REFERENCES

1. **Doyle P., Pavlovich M.** Vibration of beams on partial elastic foundation. // *Earthquake Engineering and Structural Dynamics*, 1982, Volume 10, pp. 663-674.
2. **Eisenberger M., Yankelevsky Z., Adin M.A.** Vibration of beams fully or partially supported on elastic foundation. // *Earthquake Engineering and Structural Dynamics*, 1985, Volume 13, pp. 651-660.
3. **Lellep J., Sakkov E**. Buckling of stepped composite columns. // *Mechanics of Composite Materials*, 2006, Volume 42, No 1. pp. 63-72.
4. **Denisova L.M., Mironov A.N., Khalyavkin A.A.** K issledovaniyu poperechnykh kolebaniy valoprovodov sudov [To the study of transverse oscillations of vessels' shaft lines]. // *Vestnik Astrakhanskogo GTU*. Seriya: Morskaya tekhnika i tekhnologiya, 2010, No 1, pp. 95-99 (in Russian).
5. **Kurbatskiy Ye.N.** Raschet fundamentov zdaniy i sooruzheniy s dvumya uprugimi kharakteristikami osnovaniya s ispol'zovaniyem svoystv izobrazheniy Fur'ye finitnykh funktsiy [The calculation of the foundations of buildings and structures with two elastic characteristics of the base using the properties of the Fourier images of finite functions]. // *Vestnik MGSU*, 2014, No 1, pp. 41-50 (in Russian).
6. **Gordon V.A., Poturayeva T.V., Semenova G.A.** Napryazhenno-deformirovannoye sostoyaniye balki, chastichno opertoy na uprugoye osnovaniye [Stress-strain state of a beam partially supported on an elastic base] // *Fundamental'nyye i prikladnyye*

problemy tekhniki i tekhnologii, 2015, No 5-2(313), pp. 191-197(in Russian).
7. **Babakov I.M.** Teoriya kolebaniy [Theory of oscillations]. Moscow, Drofa, 2004, 591 pages (in Russian).
8. **Gryazev M.V., Zheltkov V.I., Vasin A.A., Vasina M.V.** Prikladnyye zadachi mekhaniki deformiruyemogo tverdogo tela. Chast' 1. Statika sterzhney [Applied problems of mechanics of a deformable solid. Part 1. Statics of rods]. Tula, Izd-vo TulGU, 2011, 112 pages (in Russian).
9. **Chadayev Yu.A.** Primeneniye metoda nachal'nykh parametrov k opredeleniyu dinamicheskikh sostoyaniy tsentral'noszhatykh pryamykh neodnorodnykh sterzhney [Application of the method of initial parameters to the determination of the dynamic states of centrally compressed straight inhomogeneous rods]. Diss. k.f.-m.n. Tula, 2014, 83 pages (in Russian).
10. **Brusova V.I., Gordon V.A.** Metod nachal'nykh parametrov pri issledovanii chastichnogo razrusheniya nagruzhennoy balki [The method of initial parameters in the study of partial destruction of a loaded beam] // *Sb. materialovMezhdunar. NTK "Aktual'nyye problemy stroitel'stva i stroitel'noy industrii"* [Proc. of the Intern. STC "Actual problems of construction and construction industry"]. Tula, TulGU, 2010, pp. 6-7 (in Russian).
11. **Gordon V.A., Poturaeva T.V., Semenova G.A.** Matrix of influence for rod with cross cracks [Matrix of Influence on the rod with cross cracks]. // *Fundamental'nyye i prikladnyye problemytekhniki i tekhnologii*, 2018, No. 5 (331), pp. 6-13 (in Russian).
12. **Gordon V.A., Kolchunov V.I., Trifonov V.A.** Reaktsiya sistemy «balka-uprugoye osnovaniye» na vnezapnyye izmeneniya granichnykh usloviy [Reaction of the "beam – elastic foundation" system to sudden changes in the boundary conditions] // *Stroitel'stvo i rekonstruktsiya*, 2018, No. 1, pp. 8-21 (in Russian).
13. **Gordon V., Pilipenko O.** Vibration of loaded beam initiated by fully or partially destruction of the elastic foundation. // *Proceedings of the 22 Intern. Congress on sound and vibration*. Italy, Florence, 2015.
14. **Gordon V.A., Pilipenko O.V., Trifonov V.A.** A transient dynamic process in a structurally nonlinear system «beam-elastic foundation» // *Proceedings of 6-th European Conference on Computational Mechanics (ECCM6)*. Glasgow, UK, 2018.
15. **Tolokonnikov L.A.** Mekhanika deformiruyemogo tverdogo tela [Mechanics of a deformable solid]. Moscow, Vysshaya shkola, 1979, 580 pages (in Russian).

СПИСОК ЛИТЕРАТУРЫ

1. **Doyle P., Pavlovich M.** Vibration of beams on partial elastic foundation. // *Earthquake Engineering and Structural Dynamics*, 1982, Volume 10, pp. 663-674.
2. **Eisenberger M., Yankelevsky Z., Adin M.A.** Vibration of beams fully or partially supported on elastic foundation. // *Earthquake Engineering and Structural Dynamics*, 1985, Volume 13, pp. 651-660.
3. **Lellep J., Sakkov E**. Buckling of stepped composite columns. // *Mechanics of Composite Materials*, 2006, Volume 42, No 1. pp. 63-72.
4. **Денисова Л.М., Миронов А.Н., Халявкин А.А.** К исследованию поперечных колебаний валопроводов судов. // *Вестник Астраханского ГТУ*. Серия: Морская техника и технология, 2010, №1, с. 95-99.
5. **Курбацкий Е.Н.** Расчет фундаментов зданий и сооружений с двумя упругими характеристиками основания с использованием свойств изображений Фурье финитных функций. // *Вестник МГСУ*, 2014, №1, с. 41-50.
6. **Гордон В.А., Потураева Т.В., Семенова Г.А.** Напряженно-деформиро-ванное состояние балки, частично опертой на упругое основание. // *Фундаментальные и прикладные проблемы техники и тех-*

нологии, 2015, №5-2(313), с. 191-197.
7. **Бабаков И.М.** Теория колебаний. – М.: Дрофа, 2004. – 591 с.
8. **Грязев М.В., Желтков В.И., Васин А.А., Васина М.В.** Прикладные задачи механики деформируемого твердого тела. Часть 1. Статика стержней. – Тула: Изд-во ТулГУ, 2011. – 112 с.
9. **Чадаев Ю.А.** Применение метода начальных параметров к определению динамических состояний центрально-сжатых прямых неоднородных стержней. Диссертация на соискание ученой степени кандидата физико-математических наук по специальности 01.02.04 – «Механика деформируемого твердого тела». – Тула, ТГУ, 2014. – 83 с.
10. **Брусова В.И., Гордон В.А.** Метод начальных параметров при исследовании частичного разрушения нагруженной балки // *Сб. материалов Междунар. НТК «Актуальные проблемы строительства и строительной индустрии»*. Тула: ТулГУ, 2010, С. 6-7.
11. **Gordon V.A., Poturaeva T.V., Semenova G.A.** Matrix of influence for rod with cross cracks. // *Фундаментальные и прикладные проблемы техники и технологии*, 2018, №5(331), с. 6-13.
12. **Гордон В.А., Колчунов В.И., Трифонов В.А.** Реакция системы «балка - упругое основание» на внезапные изменения граничных условий. // *Строительство и реконструкция*, 2018, №1, с. 8-21.
13. **Gordon V., Pilipenko O.** Vibration of loaded beam initiated by fully or partially destruction of the elastic foundation // *Proceedings of the 22 Intern. Congress on sound and vibration*. Italy, Florence, 2015.
14. **Gordon V.A., Pilipenko O.V., Trifonov V.A.** A transient dynamic process in a structurally nonlinear system “beam – elastic foundation”. // *Proceedings of 6-th European Conference on Computational Mechanics (ECCM6)*. UK, Glasgow, 2018.
15. **Толоконников Л.А.** Механика деформируемого твердого тела. – М.: Высшая школа, 1979, 580 с.

Vladimir I. Travush, Full Member of the Russian Academy of Architecture and Construction Sciences, Professor, Dr.Sc., Vice-President of the Russian Academy of Architecture and Construction Sciences; 107031, Moscow, st. Bolshaya Dmitrovka, 24/1;
phone/fax +7 (495) 625-79-67; e-mail: travush@mail.ru.

Vladimir A. Gordon, Advisor of the Russian Academy of Architecture and Construction Sciences, Professor, Dr.Sc., Head of the Department of Higher Mathematics; Orel State University named after I.S. Turgenev; 302026, Orel, st. Komsomolskaya, 95; phone/fax +74862419802;
E-mail: gordon@ostu.ru.

Vitaly I. Kolchunov, Full Member of the Russian Academy of Architecture and Construction Sciences, Professor, Dr.Sc., Head of Department of Unique Buildings and Structures; Southwest State University (SWSU);; 305040, Russia, Kursk, st. 50 let Oktyabrya, 94;
phone/fax +74712222461; e-mail: asiorel@mail.ru.

Evgeny V. Leontiev, Head of the Department of Constructive Reliability and Safety of Main State Expertise of Russia; 119049, Moscow, st.Bolshaya Yakimanka, 42/1-2; phone/fax +74956259595;
E-mail: e.leontyev@gge.ru.

Травуш Владимир Ильич, академик РААСН, профессор, доктор технических наук, вице-президент Российской академии архитектуры и строительных наук; 107031, Москва, ул. Большая Дмитровка, д.24, стр.1;
тел./факс +7(495)625-79-67; e-mail: travush@mail.ru.

Гордон Владимир Александрович, советник РААСН, профессор, доктор технических наук, профессор кафедры технической физики и математики Орловского государственного университета имени И.С. Тургенева; 302026, г. Орел, ул. Комсомольская, 95;
тел./факс +74862419802; e-mail: gordon@ostu.ru.

Колчунов Виталий Иванович, академик РААСН, профессор, доктор технических наук, заведующий кафедрой уникальных зданий и сооружений Юго-Западного государственного университета; 305040, Россия, г. Курск, ул. 50 лет Октября, 94;
тел./факс +74712222461; e-mail: asiorel@mail.ru.

Леонтьев Евгений Владимирович, начальник отдела конструктивной надежности и безопасности объектов Главгосэкспертизы России; 119049, г. Москва, ул. Большая Якиманка, 42, стр. 1-2;
тел./факс +74956259595; e-mail: e.leontyev@gge.ru.

DOI:10.22337/2587-9618-2019-15-2-159-164

NON-CONSERVATIVENESS OF FORMULAS AS AN OBSTACLE TO THE MOTION SIMULATION

Vladimir B. Zylev, Alexey V. Steyn, Nikita A. Grigoryev
Russian University of Transport (MIIT), Moscow, RUSSIA

Abstract: The paper considers the specifics of connection setting between deformations and stresses as applied to the problem of large non-linear oscillations, when deformations are considered arbitrarily large. It is noted that the introduction of some arbitrary physical relations in the computational model can lead to the establishment of a non-conservative system. It is shown, for example, that distribution of the ordinary Hooke's law formulas to the area of large deformations leads to the establishment of material with the non-conservative properties. The examples are given for the numerical solution of problems with the nonlinear oscillations, where an increase in the oscillation amplitudes or occurrence of unauthorized internal friction is shown. The simplest version of the material properties free from the indicated deficiencies is given. One of the paper conclusions is that when specifying the elastic properties of the material, it is necessary to ensure that the resulting system is conservative.

Keywords: membranous systems, n-step numerical method, equations of motion, large deformations, non-conservativeness

ФОРМУЛЬНАЯ НЕКОНСЕРВАТИВНОСТЬ КАК ПОМЕХА МОДЕЛИРОВАНИЯ ДВИЖЕНИЯ

В.Б. Зылев, А.В. Штейн, Н.А. Григорьев
Российский университет транспорта (МИИТ), г. Москва, РОССИЯ

Аннотация: В работе рассматриваются особенности задания связи между деформациями и напряжениями применительно к задаче больших нелинейных колебаний, когда и деформации рассматриваются произвольно большими. Отмечается, что введение некоторых произвольных физических соотношений в расчетную модель может приводить к созданию неконсервативной системы. Показывается, например, что распространение обычных формул закона Гука в область больших деформаций ведет к созданию материала с неконсервативными свойствами. Приводятся примеры численного решения задач о нелинейных колебаниях, где демонстрируется нарастание амплитуд колебаний или появление несанкционированного внутреннего трения. Приводится простейший вариант свойств материала, свободного от указанных недостатков. Один из выводов работы заключается в том, что при задании упругих свойств материала нужно следить за тем, чтобы полученная система была консервативной.

Ключевые слова: Мембранные системы, шаговый численный метод, уравнения движения, большие деформации, неконсервативность

The paper relates to the field of structural mechanics that considers the dynamics of deformable systems without any restrictions on the magnitude of displacements and deformations. In order to reduce the scope of work, it shall be limited to non-linear elasticity, isotropic material, and the plane stress condition. From the geometrical point of view, it shall be assumed that the system can be considered using a triangular finite element, the displacement field in which is given by a linear function. The object of practical application here may be the dynamics of inflatable capsules when they are filled with air [1]. The dynamic solution method in the examples given below is based on an explicit computational scheme with extrapolation according to Adams [2,3,4]. The article, however, is devoted not to the integration method of the motion

equations, but to the influence on the resulting motion of the selected physical relation system, that allow one to determine stresses and then the nodal reactions in the element using the well-known deformations. Figure 1 shows a triangular finite element before deformations (solid line) and the same element after deformations (dashed line) at some current moment of the dynamic solution. The deformed element can be combined with the initial one to calculate reactions in the local axes (Figure 1).

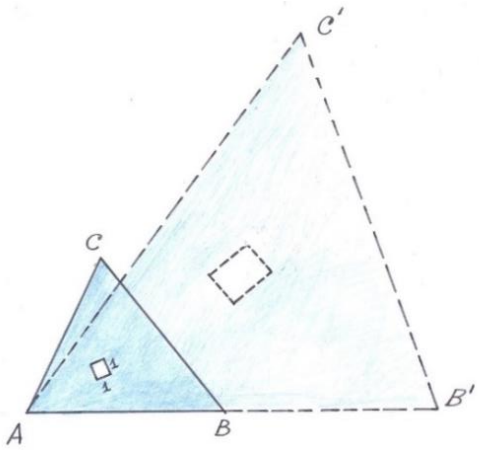

Figure 1. Trianglular finite element before and after deformations.

In the original triangular element, it is possible to select a square with ordinary sides that correspond to the main directions. After the deformations, this square will turn into a rectangle. The problem of determining the main directions with the well-known position of the element points is a fundamentally non-complicated purely geometrical problem and its solution will not be highlighted. It only shall be noted that the main directions in the original and deformed elements do not coincide, since the elementary square undergoes not only a deformation, but also a hard rotation. The current values of the main deformations ε_1 and ε_2 shall be determined since the displacement field inside the element is given. The values ε_1 and ε_2 can be determined in different ways; here the relative elongations shall mean the ratio of the segment elongation to its original length. Figure 2 shows the unit cube before and after deformations.

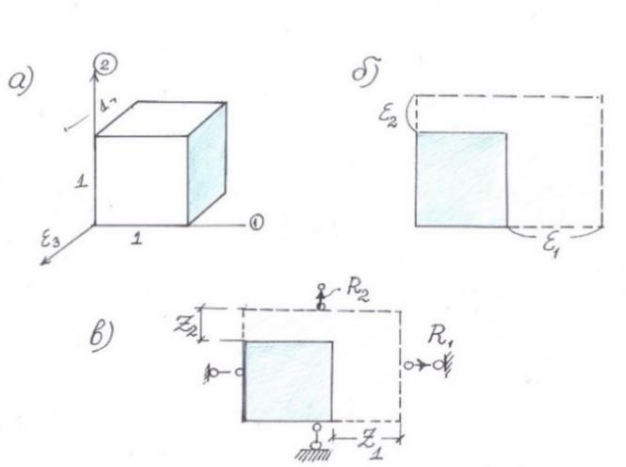

Figure 2. The unit cube before and after deformations.

Now we will discuss the issue of calculating the reactions R_1 and R_2 in the system with two displacements $z_1 = \varepsilon_1$ and $z_2 = \varepsilon_2$. We will first consider the possibility of using the usual Hooke's law formulas, in the form in which it is applied for small deformations. For the main stresses and for the main deformation in the direction of the plate thickness the formula shall be as follows:

$$\begin{aligned}
\sigma_1 &= \frac{E}{1-\mu^2}(\varepsilon_1 + \mu\varepsilon_2) \\
&= \frac{E}{1-\mu^2}(z_1 + \mu z_2) \\
\sigma_2 &= \frac{E}{1-\mu^2}(\varepsilon_2 + \mu\varepsilon_1) \\
&= \frac{E}{1-\mu^2}(z_2 + \mu z_1) \\
\varepsilon_3 &= -\frac{\mu}{E}(\sigma_1 + \sigma_2) \\
&= -\frac{\mu}{1-\mu}(z_1 + z_2)
\end{aligned} \tag{1}$$

where E is a modulus of elasticity, μ is a Poisson's ratio.

Further, it can be assumed that the obtained stresses refer to the deformed dimensions of the element, then the required reactions shall be as follows:

$$R_1 = \sigma_1(1+\varepsilon_2)\cdot(1+\varepsilon_3) = \frac{E}{1-\mu^2}(z_1+\mu z_2)\cdot(1+z_2)\cdot\left[1-\frac{\mu}{1-\mu}(z_1+z_2)\right]$$
$$R_2 = \sigma_2(1+\varepsilon_1)(1+\varepsilon_3) = \frac{E}{1-\mu^2}(z_2+\mu z_1)(1+z_1)\left[1-\frac{\mu}{1-\mu}(z_1+z_2)\right] \quad (2)$$

Having determined the partial derivatives of the reactions by displacements, we shall obtain the elements of the tangent stiffness matrix for the system shown in Figure 2.

$$r_{12} = \frac{\partial R_1}{\partial z_2} = \frac{E}{1-\mu^2}\left\{\mu + z_1 + 2\mu z_2 - \frac{\mu}{1-\mu}[(1+\mu)z_1 + {z_1}^2 + 2(1+\mu)z_1 z_2 + 2\mu z_2 + 3\mu z_2^2]\right\}$$
$$r_{21} = \frac{\partial R_2}{\partial z_1} = \frac{E}{1-\mu^2}\left\{\mu + z_2 + 2\mu z_1 - \frac{\mu}{1-\mu}[(1+\mu)z_2 + {z_2}^2 + 2(1+\mu)z_1 z_2 + 2\mu z_1 + 3\mu z_1^2]\right\} \quad (3)$$

The formulas (3) show that the tangent stiffness matrix in this case is not symmetrical to $r_{12} \neq r_{21}$ that means that the system is not conservative [4]. The special particular case is possible when $\mu = \frac{1}{3}$ but this is exactly the exception. Non-conservativeness in this case means that the use of this material model shall lead to an increase in oscillations or to occurrence of an unauthorized internal friction, that is there shall be not just an inaccurate reflection of the material properties, but a qualitatively incorrect model behavior.

We shall consider a test case. Figure 3 shows a plane computational scheme. The triangular finite element with two fixed vertices is connected to a much more massive and rigid rod element ***A B***.

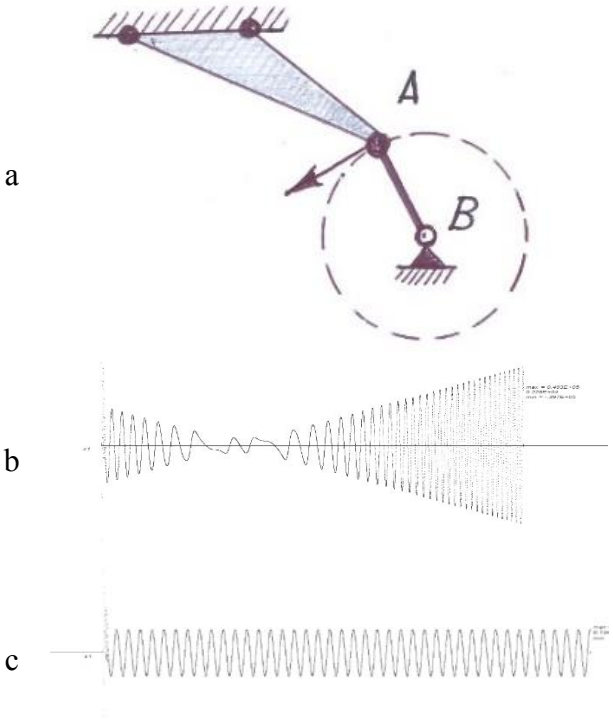

Figure 3. Computing solution of the problem of the rod rotation connected by a triangular element, the diagrams show the time dependence of the horizontal velocity component at point A: a) the computational scheme; b) an incorrect model behavior with non-conservative properties; c) the conservative model.

Point A is given with an initial velocity corresponding to its counterclockwise rotation. The rod material has a moderate Voigt-type internal friction that provides a quick transition to the motion that can be approximately described as rotation around point ***B***.

The diagram Figure 3b shows a case where the triangle material has the non-conservative properties described above. The specified initial counter-clockwise rotation of the rod ***A B*** initially slows down rapidly; the non-conservativeness is evident as an unauthorized internal friction. When the rod stops, it begins to unwind in a clockwise direction. Its angular velocity and rotation frequency are increased. The system works like a perpetual motion machine that means, of course, a qualitative error in the physical relations of the model. This article is

devoted to this negative specification. The well-formed material properties are certainly known [5]. However, the process of forming new material properties cannot be fully completed. Sometimes, the quite complex computational algorithms can be used to obtain stress values, and during their development it is possible to obtain negative results similar to those just considered.
Having returned to our formulas, it shall be noted that they can be greatly simplified and the non-conservativeness defect can be removed by assuming that the strain energy of a single element (Figure 2) is expressed through displacements as follows:

$$U = \frac{E}{2(1-\mu^2)}(z_1^2 + 2\mu z_1 z_2 + z_2^2)$$

and then the reactions shall be determined by formulas

$$R_1 = \frac{\partial U}{\partial z_1}; \quad R_2 = \frac{\partial U}{\partial z_2}.$$

In this case, the matrix symmetry shall be guaranteed. If these simplifications are introduced into the computer program, then instead of the incorrect diagram in Figure 3, b we will receive the diagram with stable rotation in Figure 3, c.
We will demonstrate the considered specifications with a more complicated example. The thin membrane in a stress-free state has a square form with the sides of 2×2 meters, thickness of 10^{-4} meters, the density of the sheath material of 10^3 kg/m^3, modulus of elasticity E=120 MPa, the Poisson's ratio of $\mu = 0{,}2$. The membrane is affected by its own weights and nine equal, suddenly exerted and single forces of 1444 N directed upwards. The forces are applied to the central points of the sheath model. The system nodes are influenced by the external resistance forces proportional to the node velocities and their weight with a friction coefficient of 5 s^{-1}. The expected motion scenario is that the membrane is elevated from a horizontal position, the damped oscillations are available for some time, after which the equilibrium position shall be established.

If we take the material properties as non-conservative, then the expected scenario shall not be implemented (see Figure 4). At first, the sheath takes a position close to the equilibrium position that can also be judged by the vertical displacement diagram in Fig. 4. Next, there are increasing fluctuations, like a flutter that lead to the time moment $t \approx 0{,}5c$ and to the computational chaos (see Figure 4).

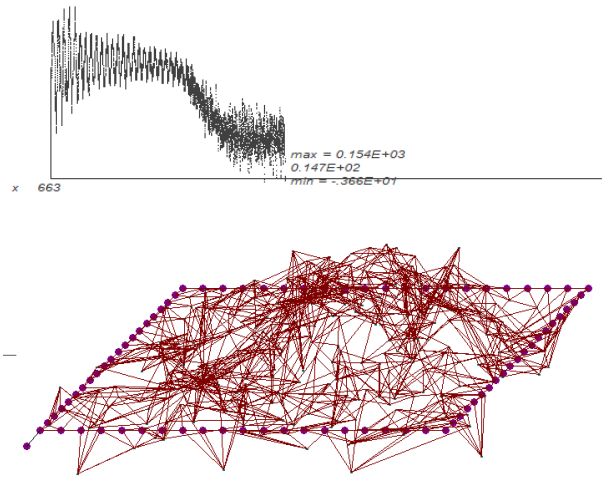

Figure 4. Attempt to calculate the membrane using the non-conservative material that leads to the computational chaos. The diagram shows the change of the center point vertical coordinate in time.

If we take the material that corresponds to the conservativeness properties, then the solution shall be relevant to the scenario described above, its result is shown in Figure 5, the system is almost in the equilibrium position by the time moment $t \approx 1c$.
It shall be noted that with a decrease in load, when the deformations are actually small, both the material models considered behave practically consistently, and the non-conservative properties are weakened so that they can be ignored. An increase in the external resistance forces also leads to the fact that the system is out of the equilibrium position, but this transition shall be surely simulated incorrectly.

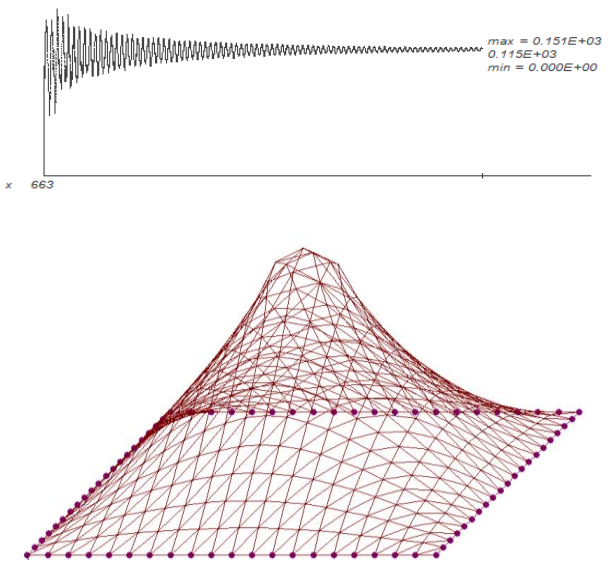

Figure 5. The equilibrium position of the system, obtained by using a material with conservative properties. The diagram shows the change of the central point vertical coordinate in time.

CONCLUSIONS

1. When the material is simulated, it is necessary to ensure that the material has conservative properties.
2. The extention of the traditional Hooke's law formulas for small deformations to the large deformations leads not only to the inaccurate physical relations, but to the qualitatively incorrect material description that leads to the energy release during nonlinear motion of the system.
3. The symmetry of tangent stiffness matrix can be used to control the non-conservativeness properties of the computational models.

REFERENCES

1. **Zylev V.B., Steyn A.V., Grigoryev N.A.** Dinamicheskoe modelirovanie vozdukhonesomoi pnevmokonstruktsii v protsesse napolneniia [Dynamic modeling of airborne pneumatic construction during filling]. *Collection of conference articles. Actual problems and prospects for the development of building structures: innovation, modernization and energy efficiency in construction*. Almaty, 2018, pp. 140-145 (in Russian).
2. **Zylev V.B.** Vychislitel'nye metody v nelineinoi mekhanike konstruktsii [Computational methods in the non-linear structural mechanics]. Moscow, Research Center “Engineer”, 144 pages (in Russian).
3. **Aleksandrov A.V., Potapov V.D., Zylev V.B.** Stroitel'naia mekhanika. Kniga 2. Dinamika i ustoichivost' uprugikh sistem [Structural mechanics. Vol.2. Dynamics and stability of elastic systems]. Moscow, Higher School, 2008, 384 pages (in Russian).
4. **Bolotin V.V.** Nekonservativnye zadachi teorii uprugoi ustoichivosti [Non-conservative problems of the elastic stability theory]. Moscow, State Publishing House of Physical and Mathematical Literature, 1961, 340 pages (in Russian).
5. **Oden J.** Konechnye elementy v nelineinoi mekhanike sploshnykh sred [Finite elements of nonlinear continua]. Moscow, Mir, 1976, 464 pages (in Russian).

СПИСОК ЛИТЕРАТУРЫ

1. **Зылев В.Б., Штейн А.В., Григорьев Н.А.** Динамическое моделирование воздухонесомой пневмоконструкции в процессе наполнения. // *Сборник статей конференции «Актуальные проблемы и перспективы развития строительных конструкций: инновации, модернизация и энергоэффективность в строительстве»*. – Алматы, 2018, с. 140-145.
2. **Зылев В.Б.** Вычислительные методы в нелинейной механике конструкций. – М.: НИЦ Инженер, 1999. – 144 с.
3. **Александров А.В., Потапов В.Д., Зылев В.Б.** Строительная механика. Книга

2. Динамика и устойчивость упругих систем. – М.: Высшая школа, 2008. – 384 с.
4. **Болотин В.В.** Неконсервативные задачи теории упругой устойчивости. – М.: «Государственное издательство физико-математической литературы», 1961. – 340 с.
5. **Оден Дж.** Конечные элементы в нелинейной механике сплошных сред. – М.: Мир, 1976. – 464 с.

Vladimir B. Zylev, Advisor of the Russian Academy of Architecture and Construction Sciences, Professor, Dr.Sc, Head of Department of Structure mechanics, Russian University of Transport (MIIT); 9, Obraztsova Street, 127994, Moscow, Russia;
E-mail: Zylevvb@yandex.ru.

Alexey V. Steyn, PhD, Assistant professor of "Department of Structure mechanics", Russian University of Transport (MIIT); 9, Obraztsova Street, 127994, Moscow, Russia; e-mail: avsh7714@yandex.ru.

Nikita A. Grigoryev, PhD, Assistant professor of "Department of Structure mechanics", Russian University of Transport (MIIT); Build. 9, 9 Obraztsova St., Moscow, Russia 127994; e-mail: Gr_Nik2003@mail.ru.

Зылев Владимир Борисович, советник Российской академии архитектуры и строительных наук, профессор, доктор технических наук, заведующий кафедрой «Строительная механика», Российский университет транспорта (МИИТ); 127994, Россия, г. Москва, ул. Образцова, д 9, стр. 9; e-mail: Zylevvb@yandex.ru.

Штейн Алексей Владимирович, кандидат технических наук; доцент кафедры «Строительная механика», Российский университет транспорта (МИИТ); 127994, Россия, г. Москва, ул Образцова, д 9, стр. 9;
E-mail: avsh7714@yandex.ru.

Григорьев Никита Алексеевич, кандидат технических наук; кандидат технических наук; доцент кафедры «Строительная механика», Российский университет транспорта (МИИТ); 127994, Россия, г. Москва, ул. Образцова, д 9, стр. 9; e-mail: Gr_Nik2003@mail.ru.